The centrality of both hippocampal-cortical structure and memory to negative symptoms after a First Episode of Psychosis

Carolina Makowski

Integrated Program in Neuroscience

Departments of Psychiatry, Neurology and Neurosurgery

McGill University, Montreal, Canada

Tuesday, June 4, 2019

A thesis submitted to McGill University in partial fulfillment of the requirements for the degree of Doctor of Philosophy

TABLE OF CONTENTS

ACKNOWLEDGMENTS **6**

ORIGINAL CONTRIBUTIONS OF THESIS **10**

PEER-REVIEWED PUBLICATIONS AND CONTRIBUTIONS OF AUTHORS **10**
OTHER RELATED LEAD-AUTHOR PUBLICATIONS **13**
OTHER RELATED CO-AUTHORED PUBLICATIONS **13**
INVITED PRESENTATIONS **14**
CONFERENCE ABSTRACTS **15**

LIST OF FIGURES **18**

LIST OF TABLES **20**

ABSTRACT **21**

RÉSUMÉ **23**

CHAPTER 1 : INTRODUCTION **25**

SPECIFIC OBJECTIVES OF THESIS. **28**

CHAPTER 2 : BACKGROUND **31**

2.1 DEFINING PSYCHOSIS **31**
2.1.1. Prevalence and diagnostic boundaries 31
2.2 PREDICTORS OF FUNCTIONAL OUTCOME AFTER A FIRST EPISODE OF PSYCHOSIS **32**
2.2.1. Negative symptoms 33
2.2.2. Verbal memory 35
2.2.3. Intersection of negative symptoms and verbal memory 36
2.3 MAGNETIC RESONANCE IMAGING (MRI) STUDIES OF PSYCHOSIS PATIENTS **38**
2.3.1. Frontal-temporal lobes are key regions of interest in psychosis 38
2.3.2. Progressive brain changes after a first episode of psychosis 40
2.3.3. White matter abnormalities 44
2.3.4. Network-based investigations 49
2.4. THEORY OF HIPPOCAMPAL CENTRALITY IN PSYCHOSIS **53**
2.4.1. Premise of hippocampal centrality theory 54
2.4.2. Hippocampal links to neocortical regions 58
2.5. MATURATIONAL TRAJECTORIES OF HIPPOCAMPUS AND CORTEX: IMPLICATIONS FOR A FEP **63**

CHAPTER 3 : NEUROIMAGING METHODS **66**

3.1. QUALITY CONTROL OF MRI DATA **67**
3.2. LIMBIC AND SUBCORTICAL STRUCTURE **72**
3.2.1. Choosing MAGeT: evaluating accuracy of subcortical segmentation. 72
3.2.2. Hippocampal-amygdalar volumetry and shape morphometry 77
3.3. MEASURES SAMPLED ALONG THE CORTICAL SURFACE **81**
3.3.1. Cortical thickness and comparison with other commonly-derived cortical metrics 81
3.3.2. Cortical White-Gray Matter Contrast (WGC) 82
3.3.3. Quantitative T1 imaging 87
3.4. GRAPH THEORY MEASURES OF CENTRALITY **90**

CHAPTER 4 : HIPPOCAMPAL-CORTICAL MATURATIONAL TRAJECTORIES DIFFERENTIATE FEP PATIENTS WITH PERSISTENT NEGATIVE SYMPTOMS 93

PREFACE 93
4.1. MATURATIONAL TRAJECTORIES OF HIPPOCAMPAL-AMYGDALAR MORPHOMETRY 95
ABSTRACT 96
INTRODUCTION 97
METHODS 100
Participants. 100
Neuroimaging component. 100
Clinical assessment and demographic data. 101
Post-processing: MAGeT-Brain. 102
Statistical analyses. 103
Neuroanatomical analyses: volume. 103
Neuroanatomical analyses: surface area. 104
Supplementary linear mixed effects models with altered covariates. 105
RESULTS 105
Socio-demographic and clinical data. 105
Hippocampal and amygdalar volumetry. 109
Hippocampal and amygdalar shape morphometry – vertex-wise results. 112
Hippocampal and amygdalar shape morphometry – post hoc region-of-interest results. 114
DISCUSSION 115
ACKNOWLEDGMENTS AND DISCLOSURES 122
4.2. MATURATIONAL TRAJECTORIES OF CORTICAL THICKNESS 123
ABSTRACT 124
INTRODUCTION 125
METHODS 128
Participants. 128
Neuroimaging component. 128
Clinical assessment and demographic data. 129
MRI acquisition. 130
Post-processing. 131
Statistical analyses. 131
Cortical thickness analyses. 132
RESULTS 134
Socio-demographic and clinical results. 134
Cortical thickness analyses. 138
Main effect of group. 138
Main effect of timepoint. 138
Group by time interaction. 139
Group by age interaction: linear effects of age. 139
Group by age interaction: quadratic effects of age. 140
DISCUSSION 142
ACKNOWLEDGMENTS AND DISCLOSURES 147

CHAPTER 5 : INTERSECTION OF NEGATIVE SYMPTOMS AND VERBAL MEMORY ON CHANGES IN CORTICAL CONTRAST AND THICKNESS AFTER A FIRST EPISODE OF PSYCHOSIS 148

PREFACE 148
ABSTRACT 151
INTRODUCTION 152

METHODS **155**
Sample. 155
Negative symptom dimensions and change over time. 157
Verbal Memory (VM) performance. 158
MRI acquisition. 158
MRI post-processing. 159
Cortical Thickness (CT). 159
White-Gray Matter Contrast (WGC). 159
Statistical analyses of behavioural and clinical data. 160
Surface-based brain analyses. 161
RESULTS **163**
Relationship between VM and Δ negative symptoms. 166
Associations between Δ negative symptoms and ΔWGC and ΔCT. 166
Interaction between VM and Δ Expressivity on ΔWGC and ΔCT. 169
DISCUSSION **172**
ACKNOWLEDGMENTS AND DISCLOSURES **179**

CHAPTER 6 : LINKING HIPPOCAMPAL CENTRALITY AND VERBAL MEMORY TO NEGATIVE SYMPTOMS AFTER A FIRST EPISODE OF PSYCHOSIS **180**

PREFACE **180**
ABSTRACT **183**
INTRODUCTION **184**
METHODS **187**
Subjects. 187
Negative symptoms and verbal memory data. 187
MRI acquisition. 188
MRI processing. 189
Hippocampal labels. 191
Sampling of the qT1 map for hippocampal labels. 192
Generation of Cortical Surfaces. 192
Sampling of qT1 maps for cortical surfaces. 193
Calculating pairwise co-occurring change in anatomy. 193
Graph theory application: participation coefficient of hippocampal parcel. 194
Box 1 195
Statistical analyses. 196
Demographic and clinical data. 196
Group differences in co-occurring change matrices. 196
Group differences in hippocampal Participation Coefficient (PC). 197
Control analysis: testing centrality of default mode and ventral attention networks. 197
Relationship between negative symptoms and verbal memory deficits. 197
Mediation analysis. 198
RESULTS **198**
Sample. 198
Verbal memory and negative symptom relationships. 200
Group differences in co-occurring change matrices. 200
Group differences in PC of the hippocampal parcel. 202
Control analysis: group differences in PC of the default mode and ventral attention networks. 204
Brain-behaviour relationships in FEP patients. 204
Control analyses: no brain-behaviour relationships with default mode and ventral attention networks 206
Mediation analysis: modeling verbal memory, negative symptoms, and hippocampal centrality. 206

DISCUSSION **207**
Conclusions. 213
ACKNOWLEDGMENTS AND DISCLOSURES **214**

CHAPTER 7 : CONCLUSIONS **215**

LIMITATIONS **217**
FUTURE DIRECTIONS **219**
Re-purposing existing treatments and interventions. 219
Prodromal stages. 221
Imaging genetics. 222
Beyond psychosis: generalizing findings to other disorders. 223

CHAPTER 8 APPENDICES – SUPPLEMENTARY MATERIAL FOR CHAPTERS 4-6 ..... **225**

APPENDIX-I: SUPPLEMENTARY MATERIAL FOR CHAPTER 4.1 (MAKOWSKI ET AL *TRANSLATIONAL PSYCHIATRY* 2017) **225**
SUPPLEMENTARY METHODS **225**
Patient exclusion from the neuroimaging study. 225
SUPPLEMENTARY TABLES **226**
SUPPLEMENTARY FIGURES **228**
APPENDIX-II: SUPPLEMENTARY MATERIAL FOR CHAPTER 4.2 (MAKOWSKI ET AL *NPJ SCHIZOPHRENIA* 2016) **230**
Additional MRI Quality Control (QC) information. 230
APPENDIX-III: SUPPLEMENTARY MATERIAL FOR CHAPTER 5 (MAKOWSKI ET AL, *PSYCHOLOGICAL MEDICINE* REVISIONS SUBMITTED 2019) **234**
SUPPLEMENTARY METHODS **234**
Neuroimaging sample details. 234
Quality Control procedures. 234
Choosing the best model for vertex-wise CT and WGC data. 235
SUPPLEMENTARY RESULTS **237**
VM at baseline 237
VM in relation to negative symptom domains at baseline. 237
Relationship between ΔVM and Δ negative symptoms. 238
SUPPLEMENTARY TABLES **239**
SUPPLEMENTARY FIGURES **243**
APPENDIX-IV: SUPPLEMENTARY MATERIAL FOR CHAPTER 6 (MAKOWSKI ET AL., IN PREPARATION *MOLECULAR PSYCHIATRY* 2019) **248**
SUPPLEMENTARY METHODS **248**
Sample after consideration of study criteria and Quality Control (QC). 248
Altered parameters in imaging protocol. 249
QC of processed images. 250
Group differences in qT1: Hippocampal circuit data. 251
Group differences in qT1: Cortical surface data. 251
SUPPLEMENTARY TABLES **252**
SUPPLEMENTARY FIGURES **254**

BIBLIOGRAPHY **256**

Acknowledgments

I have been graced with the guidance of many inspiring mentors throughout my time working in research. To my supervisors, Martin Lepage and Alan Evans: I have no idea how I ended up with not one, but two incredible mentors and lab teams that encouraged, motivated, and supported my work every step of the way. I definitely hit the doctoral jackpot. To Martin: Many thanks for unfailingly supporting my work and truly helping me to advance my career. I came to your office with wild ideas sometimes, but you always gave me the space and flexibility to pursue my project goals, while still keeping me grounded (no, I haven't solved world hunger yet!). It's been an absolute pleasure working with you and I know there will be many more collaborations to come. To Alan: Thank you for unapologetically pushing me to keep moving forward and to never lose sight of the bigger picture, regardless of the rejection letters (sprinkled with some triumphs!) colouring my inbox. You never failed to come through when I needed a lending hand. It's been an incredibly long summer since I first started in your lab, but I promise I'm only checking out temporarily (do I really have any other choice?).

To my "third" supervisor, Mallar Chakravarty: I have always admired your exceptional drive and collaborative spirit. Thank you for always being honest, critical, and supportive of my work, and never refraining from pushing me to my full potential.

To Dr. Joober: thank you for providing me with valuable feedback over the past five years. It has been incredibly refreshing to see how invested you are in furthering our understanding the neurobiology of psychiatric disease as a clinician and psychiatrist. You have always brought a translational perspective to my work that I highly respect.

To Dr. Ashok Malla, Dr. Jai Shah, and the PEPP-Montreal team: thank you for allowing me to see first-hand the challenges patients and their families face every day. The amazing work that PEPP-Montreal carries out to help improve lives is a source of true hope that we can find successful treatments for psychosis.

To various funding agencies that have funded my work over the years, including Fonds de la recherche en santé du Quebec (FRSQ), Canadian Institutes of Health Research (CIHR), and Healthy Brains for Healthy Lives (HBHL).

To my Lepage lab family, past and present: I am always amazed by the insane amount of help I have received from this group throughout the years. Karyne, you are the glue that keeps this lab together and a big reason why I have the participants that I do in my thesis! You are a master coordinator and I will miss your warmth and support. And thank you for providing the French version of my abstract. I want to thank Michael Bodnar for helping me kickstart my thesis and helping me navigate the complexities of analyzing clinical data alongside imaging – I think I took in a healthy dose of cynicism from you ☺. To Synthia Guimond, for always being my cheerleader and being there whenever I needed to vent about the challenges that come with academia. Your own path towards becoming a PI and never giving up along the way has been really inspiring and hopeful to me. I'm really proud of what you have been able to achieve. Finally a special thank you to Sophie and Jake for helping me with my work, and Danielle, for lending a supporting hand (and hug) when I most needed it.

To my MCIN lab mates: I've had the wonderful opportunity of working with both the "technology" and "scientific" sides of the lab. It would take an entire page to list all of you but I would like to give a shout out to: the LORIS team (my first contact with the neuroimaging world! I'm proud to say, I now know what a bug is); Leigh MacIntyre for being the quickest responder on the planet; Pierre Rioux & the CBRAIN team (for making computing way less daunting); my wonderful officemates PJ Toussaint and Claude Lepage (always keeping up my blood sugar levels with baked goods and secret ingredients!); and finally to my fellow North Wingers, with a special thank you to Budha for always being so encouraging, and all of the grad students in the lab.

To Samir Das, thank you for being such a big part of my journey – I have always admired your ability to stay calm and collected in moments of chaos, while still maintaining a sense of humour. I hope I will be able to carry forward all of the lessons you have taught me along the way.

A special thank you to John Lewis for your invaluable help with image processing and stimulating conversations that really helped shape this work. I really don't know where this thesis would be without you – probably a lot shorter with far more bold claims ☺ .

I would like to send a heartfelt thank you to Penelope Kostopoulos for being my first mentor and initiating me into this hectic and amazing world of neuroscience. I met you at one of the most difficult times of my life and I am forever grateful that you took a chance on me. Your unwavering guidance and confidence in me has truly shaped the researcher I am today. Ευχαριστώ!

To my Neuro girls – Rachel, Noor, Desiree, and Gloria. Rachel, missing you like crazy in New York but so happy I had the chance to meet you when I did. You exude resilience and generosity, and I know you will become the absolute best doctor. To Noor, you have encouraged me to speak up in times where I once would have regretfully stayed quiet – your strength and leadership are something I truly admire. Desiree, from high school chemistry to undergrad physics ("leeeetle charge q") to grad school – I am so grateful I got to share it all with you. You have a heart of gold and I don't know where I would be without all of our wine and music show nights. Gloria – I'm in tears now. Mentally, physically, emotionally, I don't know how I would have finished my PhD without you in my life. You ARE my family here in Montreal – you are the most vibrant, honest, and warm-hearted person I have ever known, and I know you have an equally vibrant future ahead of you. Te quiero mucho chiquita.

To Andrew V.: thank you for bringing me so much joy during every day of my thesis-writing marathon. Words cannot express how lucky I feel to have you in my corner.

Finally, to my warrior A.J.S. Makowski clan: I am not sure anyone could ever fully comprehend what you all had to sacrifice and fight for to get me to where I am today. To Andy: głowa dogóry! To Mama llama: all I can do is love you to pieces. To Sylvia: I have fully accepted that I will always be the dziecko. I am eternally grateful for the limitless support and love the three of you have given me.

Original Contributions of Thesis

Peer-reviewed publications and contributions of authors

I was the first author of four original manuscripts, included in chapters 4-6, as follows:

Chapter 4: C. Makowski, M. Bodnar, J. Shenker, A.K. Malla, R. Joober, M.M. Chakravarty, M. Lepage (2017). "Linking Persistent Negative Symptoms to Amygdala-Hippocampus Structure in First Episode Psychosis". *Translational Psychiatry*, 7, e1195; doi:10.1038/tp.2017.168

Chapter 4: C. Makowski, M. Bodnar, A. K. Malla, R. Joober, M. Lepage (2016). "Age-related cortical thickness trajectories in first episode psychosis patients presenting with early persistent negative symptoms", *npj schizophrenia*, 2, 16029.

Chapter 5: C. Makowski, J. D. Lewis, C. Lepage, A. K. Malla, R. Joober, M. Lepage, A. C. Evans. "Intersection of Verbal Memory and Changes in Expressivity on Cortical Contrast in First Episode Psychosis". *Psychological Medicine*, Revisions Submitted March 2019.

Chapter 6: C. Makowski, J. D. Lewis, B. Khundrakpam, C. L. Tardif, L. Palaniyappan, R. Joober, A. K. Malla, J. Shah, M. Bodnar, M. M. Chakravarty, A. C. Evans, M. Lepage. "Altered Hippocampal Centrality in Relation to Coordinated Changes of Intracortical Microstructure in First Episode Psychosis", In Preparation for *Molecular Psychiatry.*

For each of these manuscripts, I led the statistical design and execution of the data analysis. I wrote the first draft of these manuscripts and incorporated revisions from co-authors and peer reviewers.

My co-authors were integral to the completion of this work. From the Douglas Institute: the breakdown of the contribution of authors was as follows (in alphabetical order):

1. Michael Bodnar (now at the University of Ottawa): help with study design and interpretation of results in Chapters 4 and 6
2. M. Mallar Chakravarty: helped with image processing and interpretation of results in Chapters 4 and 6; also helped with study design and MRI acquisition of Chapter 6
3. Ridha Joober: helped with study design and oversaw clinical assessments in Chapters 4, 5, and 6; also helped with interpretation of results for Chapters 4 and 5
4. Martin Lepage: supervisor of PhD thesis
5. Ashok K. Malla: helped with study design of Chapters 4, 5, and 6; also oversaw clinical assessments and helped with interpretation of results for Chapters 4 and 5
6. Jai Shah: helped with study design of Chapter 6
7. Joseph (Jake) Shenker (now at Concordia University): helped with image processing of Chapter 4

From the Montreal Neurological Institute, these co-authors contributed in the following way:

1. Alan C. Evans: co-supervisor of PhD thesis
2. Budhachandra Khundrakpam: helped with statistical analysis and interpretation of results in Chapter 6
3. Claude Lepage: helped with image processing in Chapter 5
4. John D. Lewis: helped with image processing, statistical analysis, visualization of data/results, and interpretation of results in Chapters 5 and 6
5. Christine L. Tardif: helped with MRI acquisition and provided guidance for statistical analysis for Chapter 6

Finally, one national collaborator was included as a co-author in Chapter 6 from Western University:

1. Lena Palaniyappan: helped with statistical design and interpretation of results in Chapter 6

The original contributions to scientific knowledge of the works presented in this thesis are:

1) the longitudinal characterization of negative symptomatology and neuroanatomical changes in two independent neuroimaging samples of first episode of psychosis patients

2) the demonstration of altered hippocampal and cortical maturational trajectories after a first episode of psychosis in patients presenting with persistent negative symptoms

3) the application of a novel measure of white-gray matter cortical contrast alongside cortical thickness in first episode of psychosis

4) the demonstration that cortical thinning in the prefrontal cortex in relation to worsening negative symptoms is more strongly driven by expressivity deficits, rather than amotivation

5) the identification of significant interactions between verbal memory and expressivity deficits on language-related peri-cortical anatomy, suggesting a plausible mechanism whereby expressivity deficits may be more strongly linked to speech production, rather than general cognitive abilities

6) evidence for dynamic changes occurring in verbal memory over time after a FEP, which urges the field to re-visit the notion that neurocognitive deficits are largely stable in psychotic disorders

7) the demonstration of reduced centrality of hippocampal circuitry, driven by myelin-dense output regions of the hippocampus, in relation to co-occurring changes in intracortical microstructure after a first episode of psychosis compared to healthy controls

8) novel evidence showing that the hippocampus is central to changes in negative symptoms

9) the identification of changes in verbal memory as a mediator of the relationship between altered hippocampal centrality and changes in negative symptoms after psychosis onset

Other related lead-author publications

C. Makowski, J. D. Lewis, C. Lepage, A. K. Malla, R. Joober, M. Lepage, A. C. Evans. "Structural Associations in First Episode Psychosis Using Cortical Contrast and Cortical Thickness". *Cerebral Cortex*, In Press, https://doi.org/10.1093/cercor/bhz040

C. Makowski, M. Lepage, A. C. Evans (2019). "Head motion: The dirty little secret of neuroimaging in psychiatry". *Journal of Psychiatry and Neuroscience*, 44(1), 62-68.

C. Makowski, S. Béland, P. Kostopoulos, N. Bhagwat, G. A. Devenyi, A. K. Malla, R. Joober, M. Lepage, M. M. Chakravarty (2018). "Evaluating accuracy of striatal, pallidal, and thalamic segmentation methods: comparing automated approached to manual delineation". *NeuroImage Special Issue: Brain Segmentation and Parcellation,* 170, 182-198.

L. Buchy*, **C. Makowski***, A. K. Malla, R. Joober, M. Lepage (2018). "A longitudinal study of cognitive insight and cortical thickness in first-episode psychosis". *Schizophrenia Research,* 193**,** 251-260.
*These authors contributed equally to the manuscript.

L. Buchy*, **C. Makowski***, A. K. Malla, R. Joober, M. Lepage (2017). "Longitudinal trajectory of clinical insight and its covariation with cortical thickness in first-episode psychosis". *Journal of Psychiatric Research*, 86, 46-54.
*These authors contributed equally to the manuscript.

Other related co-authored publications

S. Béland, **C. Makowski**, S. Konsztowicz, L. Buchy, M.M. Chakravarty, M. Lepage. (2019) "Clarifying associations between cortical thickness, subcortical structures, and a comprehensive assessment of clinical insight in enduring schizophrenia". *Schizophrenia Research*, 204, 245-252.

S. Das, X.L. Boucher, C. Rogers, **C. Makowski**, F. Chouinard-Decorte, K. Klein, N. Beck, P. Rioux, S. T. Brown, Z. Mohades, C. Zweber, V. Foing, M. Forest, K. J. O'Donnell, J. Clark, M. Meaney, C. Greenwood, A.C. Evans (2018). "Integration of "omics" data and phenotypic data within a unified extensible multimodal framework". *Frontiers in Neuroinformatics*. https://doi.org/10.3389/fninf.2018.00091

G. Kiar, **C. Makowski**, J-B Poline, S. Das, A. C. Evans (2017). "The Montreal Neurological Institute Ecosystem: Enabling Reproducible Neuroscience from Collection to Analysis in the Web" In: Neuroinformatics in the Age of Big Data: Working with the Right Data and Tools. (Roskams J, Brose K, eds) pp. 51-56 Washington, DC: SfN.

L. Buchy, M. Barbato, **C. Makowski**, S. Bray, F. P. MacMaster, S. Deighton, J. Addington (2017). "Mapping structural covariance networks of facial emotion recognition in early psychosis: a pilot study". *Schizophrenia Research,* 189, 146-152.

C. Kuang, L. Buchy, M. Barbato, **C. Makowski**, F. MacMaster, S. Bray, S. Deighton, J. Addington (2017). "A pilot study of cognitive insight and structural covariance in first-episode psychosis". *Schizophrenia Research*, 179, 91-96.

M. Bodnar A. K. Malla, **C. Makowski**, R. Joober, M. Lepage (2016). "The effect of second-generation antipsychotics on hippocampal volume in first episode psychosis: longitudinal study". *British Journal of Psychiatry Open*, 2(2), 139-46.

S. Das, T. Glatard, L. C. MacIntyre, C. Madjar, C. Rogers, M.-E. Rousseau, P. Rioux, D. MacFarlane, Z. Mohaddes, R. Gnanasekaran, **C. Makowski**, P. Kostopoulos, R. Adalat, G. Niso, J. T. Moreau, A. C. Evans (2016). "The MNI data-sharing and processing ecosystem". *NeuroImage*, 124(Pt B), 1188-95.

Invited Presentations

"Altered Hippocampal Centrality in Relation to Coordinated Changes of Intracortical Microstructure in First Episode Psychosis". Schizophrenia International Research Society (SIRS), Orlando, FL, USA. April 13, 2019.

"All Paths Lead to the Hippocampus: A Framework for Understanding Negative Symptoms in Psychosis". Cerebral Imaging Centre Lecture Series, Douglas Mental Health University Institute, Verdun, QC, Canada. March 27, 2019.

"All Paths Lead to the Hippocampus: A Framework for Understanding Negative Symptoms in Psychosis". Feindel Brain Imaging Lecture. Montreal Neurological Institute, Montreal, QC, Canada. March 18, 2019.

"Hippocampal Centrality in Psychosis: A Little Structure with Big Responsibilities". Neuroimaging In Mental Health (NIMI) Seminar Series, London, Canada. May 29th, 2018.

"Deconstructing Psychosis with Structural Neuroimaging: Moving Beyond Positive Symptoms". Cognition & Circuits Seminar Series, Montreal Neurological Institute, Montreal, QC, Canada. April 18th, 2018.

"Early Intervention in Psychosis: Clinical and Neuroimaging Applications from PEPP-Montreal"**.** Lecture at FIDMAG Research Foundation, Barcelona, Spain. April 11th, 2018.

"The Hippocampus and Psychosis: Lessons from a Little Structure with Big Responsibilities". Healthy Brains for Healthy Lives (HBHL) Monthly Meeting, McGill University, Montreal, QC, Canada. January 30th, 2018.

"Cortical Gray-White Matter Contrast in First Episode Psychosis". Back to OHBM Event, CRIUGM, Montreal, QC, Canada. October 16th, 2017.

"Diving Under the Cortex in First Episode Psychosis: Characterization of Accuracy in Subcortical Volumetry and Shape Morphometry". Imaging/Modeling Journal Club, San Diego, CA, USA. May 24, 2017.

"Measuring Gray-White Matter Contrast and Cortical Thickness: A Potential New Couple in MRI?" Douglas Institute Research Blitz, Montreal, QC, Canada. February 16th, 2017.

"Structural Anatomical Trajectories in First Episode Psychosis Patients with Persistent Negative Symptoms". PEPP Research Day, Douglas Mental Health University Institute, Verdun, QC, Canada. June 13, 2016.

"Age-related cortical thickness trajectories in first episode psychosis patients presenting with persistent negative symptoms". Douglas/Psychiatry Research Day, Douglas Mental Health University Institute, Verdun, QC, Canada. June 10, 2016

"Neuroanatomical Changes After a First Episode of Psychosis: At the Intersection of Structure and Symptoms". Cerebral Imaging Centre Lecture Series, Douglas Mental Health University Institute, Verdun, QC, Canada. May 18, 2016.

"Hippocampal and Amygdalar Structural Changes Across Age in First Episode Psychosis". Society of Biological Psychiatry, Atlanta, GA, USA. May 12, 2016.

"Neural Underpinnings of Psychosis: At the Intersection of Structure, Function, and Symptoms". Feindel Brain Imaging Lecture, Montreal Neurological Institute, Montreal, QC, Canada. April 25, 2016.

"Cortical thickness changes with age in a subset of first episode psychosis patients presenting with persistent negative symptoms: a longitudinal MRI study". Schizophrenia International Research Society (SIRS), Florence, Italy. April 5, 2016.

Conference Abstracts

C. Makowski, J. D. Lewis, B. Khundrakpam, C. L. Tardif, L. Palaniyappan, R. Joober, A. K. Malla, J. Shah, M. Bodnar, M. M. Chakravarty, A. C. Evans, M. Lepage. "Altered Hippocampal Centrality in Relation to Coordinated Changes of Intracortical Microstructure in First Episode Psychosis", Montreal Neurological Institute Brain Imaging Centre Retreat, Montreal, December 2018.

G. Shafiei, R. D. Markello, A. Talpalaru, **C. Makowski**, P. Hagmann, N. R. Cashman, M. M. Chakravarty, A Dagher, B. Mišić. "Spatial patterning of brain tissue volume deformation in schizophrenia reflects network architecture", Montreal Neurological Institute Brain Imaging Centre Retreat, Montreal, December 2018.

C. Makowski, J.D. Lewis, C. Tardif, R. Joober, A.K. Malla, J. Shah, M.M. Chakravarty, A.C. Evans, M. Lepage. "Quantitative Structural Imaging Changes After a First Episode of Psychosis",

Organization for Human Brain Mapping, Singapore, June 2018.

S. Das, S. T. Brown, J.-B. Poline, T. Glatard, P. Rioux, V. Fonov, **C. Makowski**, A. C. Evans, "The MNI Open Science Ecosystem: Interoperability and APIs for sharing data and pipelines", Organization for Human Brain Mapping, Singapore, June 2018.

A. Taheri, J. Lurie, R. Abou-Haidar, S. T. Brown, S. Das, A. Doyle, N. Khalili-Mahani, G. Kiar, P. Kostopoulos, C. Lepage, L. Lewis, **C. Makowski**, C. Rogers, P.-J. Toussaint, A. C. Evans. "PIVT: A Platform Independent Visualization Tool", Organization for Human Brain Mapping, Singapore, June 2018.

C. Makowski, J.D. Lewis, C. Tardif, R. Joober, A.K. Malla, J. Shah, M.M. Chakravarty, A.C. Evans, M. Lepage. "Intracortical and Superficial White Matter Microstructural Changes After a First Episode of Psychosis", Society of Biological Psychiatry, New York, May 2018.

C. Makowski, C. Tardif, G. Devenyi, R. Amaral, G. Buck, R. Joober, A.K. Malla, J. Shah, M.M. Chakravarty, M. Lepage. "Multimodal Quantification of Memory Circuit Microstructure in First Episode Psychosis", Schizophrenia International Research Society, Florence, April 2018.

R. Rosengard, **C. Makowski**, J. Shah, A. Malla, R. Joober, M. Lepage. "Prior Subthreshold Psychotic Symptoms Associated with Thicker Right Inferior Frontal Gyrus Among Patients in a First Episode of Psychosis", Schizophrenia International Research Society, Florence, April 2018.

A. Doyle, **C. Makowski**, C. Lepage, P.J. Toussaint, A.C. Evans. "Automatic Quality Control of Human Brain T1w MRI Scans", Neural Information Processing Systems, Long Beach, December 2017.

C. Makowski, J.D. Lewis, C. Lepage, A.K. Malla, R. Joober, M. Lepage, A.C. Evans. "Cortical Gray-White Matter Contrast Underlying Negative Symptoms and Verbal Memory in First Episode Psychosis", Organization for Human Brain Mapping, Vancouver, June 2017.

C. Makowski, S. Béland, P. Kostopoulos, N. Bhagwat, G. A. Devenyi, A. K. Malla, R. Joober, M. Lepage, M. M. Chakravarty. "Evaluating accuracy of striatal, pallidal, and thalamic segmentation methods: comparing automated approached to manual delineation", *Schizophrenia Bulletin*. International Congress on Schizophrenia Research, San Diego, March 2017.

S. Guimond, S. Sarvode, **C. Makowski**, M. Chakravarty, M. Keshavan. "Altered Age-Related Subcortical Trajectories in Familial High-Risk of Schizophrenia with Transition to Psychosis", Harvard Psychiatry Research Day, Boston, March 2017.

C. Makowski, S. Béland, P. Kostopoulos, N. Bhagwat, G. A. Devenyi, A. K. Malla, R. Joober, M. Lepage, M. M. Chakravarty. "Evaluating accuracy of striatal, pallidal, and thalamic segmentation methods: comparing automated approached to manual delineation", Quebec Bio-imaging Network (QBIN), Montreal, Feb 2017.

C. Kuang, L. Buchy, M. Barbato, **C. Makowski**, F. MacMaster, S. Bray, S. Deighton, J. Addington. "A pilot study of cognitive insight and structural covariance in first-episode psychosis", Hotchkiss Brain Institute (HBI) Summer Student Symposium, Calgary, August 2016.

C. Makowski, M. Bodnar, A. K. Malla, R. Joober, A. C. Evans, M. Lepage. **"**Cortical thickness changes with age in a subset of first episode psychosis patients presenting with persistent negative symptoms: a longitudinal MRI study", Organization for Human Brain Mapping (OHBM), Geneva, June 2016.

L. C. MacIntyre, S. Das, **C. Makowski**, C. Rogers, J. Stirling, Z. Mohades, P. Kostopoulos, D. MacFarlane, C. Madjar, V. Fonov, D. L. Collins, A. C. Evans. "Quality Control Tools and Best Practices for Neuroimaging Data Management", Organization for Human Brain Mapping (OHBM), Geneva, June 2016.

C. Makowski, M. Bodnar, J. Lewis, C. Lepage, A. C. Evans, A. K Malla, R. Joober, M. Lepage. "Cortical Thinning and Structural Covariance in a Subset of First Episode Psychosis Patients Exhibiting Persistent Negative Symptoms". Integrated Program in Neuroscience (IPN) Retreat, Montreal, September 2015.

C. Makowski, M. Bodnar, J. Lewis, C. Lepage, A. C. Evans, A. K Malla, R. Joober, M. Lepage. "Cortical Thinning and Structural Covariance in a Subset of First Episode Psychosis Patients Exhibiting Persistent Negative Symptoms". Society of Biological Psychiatry Conference, Toronto, May 2015.

List of Figures

Figure 2.1. The two-factor model of negative symptoms. 34
Figure 2.2. Links between neurocognition, motivation, and functional outcomes. 37
Figure 2.3. Progression of gray matter abnormalities in schizophrenia across the cortex. 42
Figure 2.4. Distribution of white matter fibers in the human brain. 47
Figure 2.5. Affected brain hubs in schizophrenia. 51
Figure 2.6. Gross anatomy and circuitry of the medial temporal lobe. 55
Figure 2.7. Lesions in schizophrenia along the hippocampal subfield pathway. 56
Figure 2.8. Anatomy of the prefrontal cortex and medial temporal lobe. 60
Figure 3.1. Proposed quality control workflow for MRI datasets. 71
Figure 3.2. Box-whisker plots of percent volume difference between automated methods and manual segmentation. 75
Figure 3.3. Bland-Altman plots, comparing volume differences between each automated method and manually derived volumes, against manual volumes. 76
Figure 3.4. Example segmentation of bilateral hippocampus and amygdala using the MAGeT-Brain algorithm. 79
Figure 3.5. Depiction of morphological branch of MAGeT for surface area extraction. 80
Figure 3.6. Three-dimensional rendering of hippocampal subfields and output white matter. 80
Figure 3.7. MRI-based cortical thickness. 82
Figure 3.8. MRI-based white-gray contrast (WGC). 83
Figure 3.9. Top 3 components from PCA with WGC data and brain-behaviour relationships. 85
Figure 3.10. Top 3 components from PCA with CT data and brain-behaviour relationships. 86
Figure 3.11. Schematic of the magnetic resonance principles underlying the T1 relaxation time. 88
Figure 3.12. Quantitative T1 values across brain tissue types. 89
Figure 3.13. Calculation of the participation coefficient in brain networks. 91
Figure 4.1. Amygdalar and hippocampal volumes: significant group main effects and group*age interactions. 111
Figure 4.2. Significant group*age interactions in surface area of the left hemisphere. 112
Figure 4.3. Significant group*age interactions in surface area of the right hemisphere. 114
Figure 4.4. Mean curves for SAPS/SANS scores across clinical visits in FEP sub-groups. 136
Figure 4.5. Main effects of group and time. 138
Figure 4.6. Age*group interaction: linear effects of age. 140
Figure 4.7. Age^2*group interaction: quadratic effects of age. 141
Figure 5.1. ΔAmotivation and ΔExpressivity deficits associated with ΔWGC and ΔCT. 168
Figure 5.2. Interaction between baseline VM and ΔExpressivity on ΔWGC and ΔCT. 171
Figure 6.1. Image processing workflow. 190
Figure 6.2. Group differences in coordinated coupling matrices. 202
Figure 6.3. Group differences in hippocampal PC. 203
Figure 6.4. ΔVerbal memory mediates the relationship between HC centrality and Δ negative symptoms. 207
Figure 8.1. Sample distribution by group and by age. 228
Figure 8.2. Supplementary analyses of amygdalar-hippocampal surface area with additional covariates. 229
Figure 8.3. Linear age by group interaction comparing sPNS and non-PNS patients. 233
Figure 8.4. Effect of antipsychotic medication on cortical metrics. 243

Figure 8.5. Spaghetti plots of negative symptoms.....244
Figure 8.6. ΔAmotivation and ΔExpressivity deficits associated with ΔWGC and ΔCT across time, excluding mean(σ) as a covariate.....245
Figure 8.7. Interaction between baseline VM and ΔExpressivity on ΔWGC and ΔCT, excluding mean(σ) as a covariate. 246
Figure 8.8. Interaction between baseline VM and ΔExpressivity on ΔWGC and ΔCT, covarying for general cognitive ability.....247
Figure 8.9. Assignment of individual regions of interest to 8 parcels. 254
Figure 8.10. Group differences in IC and SWM qT1. 255
Figure 8.11. No group differences in PC of default mode and ventral attention networks. 255

List of Tables

Table 4.1. Demographic and clinical information for longitudinal sample. 108
Table 4.2. Amygdalar and hippocampal volumes: descriptives. 110
Table 4.3. Demographic and clinical information for longitudinal sample. 135
Table 4.4. Generalized estimating equations statistics for negative and positive symptoms..... 137
Table 5.1. Demographic and clinical information. 164
Table 6.1. Demographics and clinical information. 199
Table 6.2. Brain-behaviour analyses. 205
Table 8.1. Generalized Estimating Equations (GEE) analyses and statistics. 226
Table 8.2. Supplementary analyses of amygdalar-hippocampal volumes with additional covariates. 227
Table 8.3. Cortical thickness percent change per year 231
Table 8.4. Akaike Information Criterion (AIC) values comparing linear and quadratic models. 231
Table 8.5. Results not impacted by antipsychotic medication. 232
Table 8.6. Comparison of demographics for patients included vs. excluded in Chapter 5 239
Table 8.7. Comparing clinical and cognitive patient data by diagnosis. 240
Table 8.8. Descriptives of baseline VM data. 240
Table 8.9. General demographics for cross-sectional sample. 241
Table 8.10. DKT regions and abbreviations 252
Table 8.11. Group differences in hippocampal circuit qT1. 253

Abstract

This thesis presents a series of longitudinal studies of First Episode of Psychosis (FEP) patients, emphasizing the dynamic nature of clinical, cognitive, and neuroanatomical changes in the one to two years following psychosis onset. Chapters 1 and 2 provide a general introduction and background information on the current state of knowledge from neuroimaging studies of patients with psychosis across different stages of the disorder. They also cover critical gaps in treatment strategies, particularly for negative symptoms, that largely stem from unknown biological mechanisms. Chapter 3 introduces the neuroimaging methodology that is used throughout the dissertation to study neurobiological alterations that underlie negative symptoms after a FEP. Chapter 4 includes the first pair of published studies to investigate the trajectories of limbic-neocortical maturation shortly after a FEP, where patients are stratified by negative symptom presentation. These studies demonstrate that patients with persistent negative symptoms not only vary greatly in terms of their clinical presentation but also have significantly altered neuroanatomical trajectories with age in the amygdala, hippocampus, prefrontal and temporal cortices. Chapter 5 investigates the source of such trajectories, introducing a novel white-gray matter contrast measure alongside a more commonly used measure of cortical thickness, to better understand the influence of changes in myelin proximal to the white-gray matter boundary. Relationships with verbal memory are also explored, adding an important cognitive factor that relates to negative symptoms. Findings from this chapter suggest that verbal memory is more strongly associated with expressivity deficits than another negative symptom dimension, amotivation. The intersection of expressivity and verbal memory is related to alterations in both white-gray matter contrast and cortical thickness in language-related regions of fronto-temporal cortices. This study demonstrates the presence of neuroanatomical changes near the inner edge of

the cortex, positioning peri-cortical myelin as a key measure of interest for the final investigation in Chapter 6. This last manuscript chapter provides evidence that the coupling of intracortical and hippocampal microstructure, particularly apparent in myelin-rich hippocampal output regions, is reduced in patients with a FEP compared to healthy controls. Importantly, results from this chapter provide a biological mechanism with the hippocampus at the epicenter of neuroanatomical abnormalities associated with negative symptoms after a FEP. These symptoms also interact significantly with changes in verbal memory deficits, which is found to be a mediator of the significant relationship between hippocampal centrality and changes in negative symptoms after psychosis onset. Chapter 7 provides a final summary of these findings.

Altogether, this thesis provides evidence for dynamic changes that occur within fronto-temporo-limbic structures alongside changes in negative symptoms after a FEP. Neuroimaging measures that index myelin content were found to be sensitive in detecting such changes within a critical time window for therapeutic intervention. Specifically, Chapter 6 bridges findings from the first three investigations of this thesis and posits compromised hippocampal connectivity as a key factor underlying the course of negative symptoms after psychosis onset. Such a clear anatomical target holds promise for altering the pathophysiological course of closely related cortical targets that underlie the dysconnectivity aspect of psychotic disorders, which in turn may have an impact on clinical outcomes.

Résumé

Cette thèse présente une série d'études portant sur les patients ayant subi un premier épisode de psychose (PEP) et mettant l'emphase sur la nature dynamique des changements cliniques, cognitifs et neuroanatomiques qui surviennent suivant un PEP. Les chapitres 1 et 2 sont une introduction générale et la mise en contexte de l'état actuel des connaissances sur les études en neuroimagerie menées auprès de patients atteints de psychose à différents stades de leur maladie. Ils couvrent aussi des lacunes importantes dans les stratégies de traitement, particulièrement les symptômes négatifs qui proviennent en grande partie de mécanismes biologiques inconnus. Le chapitre 3 introduit la méthode de neuroimagerie utilisée pour étudier les altérations neurobiologiques après un PEP. Le chapitre 4 inclut une paire d'études qui explorent la trajectoire de la maturation limbique-néocorticale après un PEP, où les patients sont stratifiés selon la présentation de leurs symptômes négatifs. Ces études démontrent que les patients avec des symptômes négatifs persistants varient grandement non seulement en termes de présentation clinique, mais ont aussi des trajectoires neuroanatomiques altérées de façon significative en fonction de l'âge dans l'hippocampe et les cortex préfrontaux et temporaux. Le chapitre 5 étudie les sources de telles trajectoires, en introduisant une nouvelle mesure de contraste entre la matière blanche-grise en plus de la mesure plus commune de l'épaisseur corticale, pour mieux comprendre l'influence des changements de myéline à la frontière de la matière blanche et grise. La relation avec la mémoire verbale est aussi explorée, ajoutant un facteur cognitif important qui fait le lien avec les symptômes négatifs. Les résultats de ce chapitre suggèrent que la mémoire verbale est plus fortement associée aux déficits d'expressivité que d'une autre dimension des symptômes négatifs, l'amotivation. Le croisement de l'expressivité et de la mémoire verbale est relié à des altérations neuroanatomiques des régions reliées au langage des cortex fronto-temporaux. Cette étude démontre la présence de

changements neuroanatomiques près des bords internes du cortex, positionnant la myéline péri-corticale comme une mesure d'intérêt clé pour l'étude finale au chapitre 6. Ce chapitre apporte l'évidence que le couplage des microstructures intra-corticales et de l'hippocampe, particulièrement apparent dans les régions riches en myélines, est réduit chez les patients avec un PEP en comparaison aux contrôles sains. Plus important encore, les résultats proposent un mécanisme biologique avec l'hippocampe comme épicentre des anomalies neuroanatomiques associées aux symptômes négatifs après un PEP. Ces symptômes interagissent aussi de façon significative avec les changements dans les déficits de mémoire verbale, ce qui s'est avéré être un médiateur dans la relation significative entre la centralité de l'hippocampe et les symptômes négatifs après l'apparition de la psychose. Le chapitre 7 apporte une conclusion finale.

Dans son ensemble, cette thèse apporte l'évidence des changements dynamiques qui se produisent dans les structures temporo-limbiques en même temps que le changement des symptômes négatives après un PEP. Les mesures de neuroimagerie qui répertorient le contenu en myéline se sont avérées sensibles à détecter ces changements à l'intérieur d'une fenêtre de temps critique pour les interventions thérapeutiques. Spécifiquement, le chapitre 6 fait le pont entre les résultats des trois premières études de cette thèse et positionne la connectivité compromise de l'hippocampe comme un facteur clé sous-jacent à l'évolution des symptômes négatifs après l'apparition de la psychose. Une cible anatomique si claire est prometteuse pour altérer l'évolution pathophysiologique des cibles corticales étroitement reliées qui sous-tendent l'aspect de déconnexion des troubles psychotiques, ce qui pourrait en retour avoir un impact sur les résultats cliniques.

Chapter 1 : Introduction

> "It is our belief, or perhaps I should say fantasy, that the limbic lobe of man may not yield up the secrets of smell, or of auditory hallucinations, or of fundamental mechanisms of mental disease […]. However, continuing limbic lobe studies may bring us one blind step nearer to the location of these deeper mechanisms."
>
> William Beecher Scoville, (1954).

These words from the celebrated neurosurgeon, Dr. William B. Scoville, were trailblazing observations resulting from tissue resections initially performed in psychotic patients, and later patients with intractable epilepsy, such as the world-renowned patient H.M (Scoville 1954; Scoville and Milner 1957). Although there was no concrete evidence at the time for the functional anatomical role of the hippocampus, even for memory, Dr. Scoville's astute reflections in the early 1950s hinted at the significance of the hippocampal formation within the human brain as a binding component to biological mechanisms underlying psychiatric conditions such as psychosis, particularly of the manifestation of symptoms that moved beyond the psychosis or positive symptomatology itself.

Psychotic disorders are among the most debilitating of psychiatric conditions, largely interfering with global functioning and daily life (Eaton et al. 1995; Malla and Payne 2005). The first episode of psychosis (FEP) in particular marks a critical transition point in the life of affected individuals, often occurring at a time when adolescence meets adulthood, and self-identity and social roles are actively being shaped (Arnett et al. 2014). The impact of a FEP has thus been associated with significant cognitive, social, and neuroanatomical deficits, which often persist over time (Townsend and Norman 2004; Morgan et al. 2007; Addington and Addington 2008; Dazzan et al. 2015; Díaz-Caneja et al. 2015). Second-generation antipsychotics currently represent the most efficacious line of treatment for positive symptoms (e.g., hallucinations, delusions) (Leucht

et al. 2013), but there is a dearth of successfully established treatments for other symptom dimensions underlying psychosis, namely negative symptoms (e.g., flat affect, anhedonia) (Arango et al. 2004; Millan et al. 2014; Fusar-Poli et al. 2015; Marder and Galderisi 2017) and cognitive deficits (e.g., processing speed and verbal memory impairments) (Green and Nuechterlein 1999; Lin et al. 2014). The lack of adequate treatment for such negative symptoms and cognitive deficits has been a point of frustration for psychiatrists, patients and their families alike, and has contributed to the stagnancy of progress and innovation in treatment; a problem that psychiatry at large faces. As a clear example, the first medication treating positive symptoms of psychosis, chlorpromazine, was first introduced for psychiatric use in 1952, and is still considered to be the greatest pharmacological breakthrough not only for psychosis, but in psychiatry (López-Muñoz et al. 2005). Although the efficacy of this antipsychotic medication and advances in reducing severe side effects with atypical or "second-generation" antipsychotics have had profound effects on reducing positive symptomatology through its effects on the dopaminergic D2 receptor system, this nearly six-decade-old breakthrough is limited in use for other critical aspects of psychosis. A large problem in finding alternate biological treatment targets is the complex etiology and high degree of heterogeneity underlying the manifestation of a FEP (Knoll *et al.* 1998; Keshavan *et al.* 2011; Dickinson *et al.* 2017); disentangling key biological mechanisms underlying specific symptom and cognitive profiles thus requires longitudinal investigations across sizeable cohorts in early stages of psychosis.

From a neurobiological perspective, concerted efforts have identified the need to find reliable biomarkers to treat clinical and cognitive profiles that fall outside of traditional psychotic symptoms and beyond the reach of antipsychotic medications (Insel et al. 2010; Insel 2014; Pearlson et al. 2016). As alluded to, negative symptoms and verbal memory deficits have two-fold

importance in this biomarker search: 1) both constructs have been dubbed as significant predictors of functional outcome in patients with psychosis, and 2) they remain unmet therapeutic needs within the clinic. It is only natural then to ask how fluctuations in negative symptoms and verbal memory deficits parallel maturational changes within the cortex, including the hippocampus, and whether the intersection of these relationships carries weight to the field's understanding of the multifaceted context comprising a FEP.

The hippocampus may be ideally positioned to answer such questions and to serve as a quantifiable therapeutic target, as Dr. Scoville aptly suggested (Scoville 1954). There are multiple reasons for this:

- The hippocampus is malleable. It is one of only two known sites in the human brain that exhibit neurogenesis in adulthood (Eriksson et al. 1998; Gonçalves et al. 2016).
- The hippocampus has lower genetic heritability compared to other (sub)cortical structures, suggesting its high potential for malleability by environmental factors, or events occurring later in life (Bartsch and Wulff 2015; Walhovd, Westerhausen, et al. 2016).
- The anatomical circuitry of the hippocampus is well-defined and understood, in part due to its homology with other non-human primates and rodents (Squire et al. 2004; Clark and Squire 2013), which have allowed for the molecular characterization of specific subfields and output circuitry of the hippocampal formation, with potential applicability to humans.
- The hippocampus is characterized by an architecture that "exquisitely complements its function" (Tamminga et al. 2010), and specific lesions within different points of the circuit have been shown to lead to deficits in functionally relevant behaviours, e.g. lesions in dentate gyrus are related to deficits in pattern separation (the mechanism underlying the encoding and separation of similar events into distinct memory representations).

- The hippocampus has a protracted developmental course, which mirrors the longitudinal dynamics and extended disease process underlying psychosis (Crews et al. 2007; Marín 2016; Lockhart et al. 2018).

Multiple lines of evidence have suggested that the hippocampus may be central to positive symptoms of psychosis (Tamminga et al. 2012; Lieberman et al. 2018). However, the hippocampal formation's role amidst broader cortical networks in the progression of negative symptom severity has not been empirically tested. Further, the relationship with verbal memory within this framework is unclear; it is undeniable that the hippocampus has a clear and important role in memory formation in both healthy individuals and individuals with psychosis (Scoville and Milner 1957; Eichenbaum 2000; Bird and Burgess 2008; Tamminga et al. 2010; Wannan et al. 2018), but this has not been quantified longitudinally in early stages of psychosis. Fortunately, we now have the power to probe such questions in human patients *in vivo*, with magnetic resonance imaging (MRI) of the brain. Specifically, recent advances in MRI techniques and relevant statistical methodologies allow for the quantification of neuroanatomical structure and relationships, or "connectivity", between different brain regions, that are likely to be changing dynamically, even subtly, after a first episode of psychosis.

Specific Objectives of Thesis.

The overarching goal of this thesis is to test the contribution of cortical and hippocampal structural trajectories in patients who recently experienced a FEP to factors important for functional outcomes, namely negative symptoms and verbal memory abilities. This thesis harnesses data collection from two longitudinal neuroimaging studies: a retrospective FEP study (used in Chapters 4 and 5), for which data collection is complete, and a prospective ongoing study (used in

Chapter 6). The first retrospective study offers the advantage of a well-powered longitudinal sample to begin to explore the links between negative symptoms, verbal memory, and hippocampal-cortical structure. It should be noted that this data was collected on a 1.5T scanner, and thus, individual hippocampal subfields could not be reliably resolved. Furthermore, this study had limited longitudinal data for verbal memory. Thus, the second prospective study builds upon findings from the first, incorporating high resolution scans acquired on a 3T scanner, using multiple imaging modalities and more compact timepoints to rigorously assess and carefully follow clinical, cognitive, and neural markers following a FEP.

Specifically, the questions this thesis addresses are as follows:

1) How do hippocampal and cortical trajectories differ between FEP patients with and without persistent negative symptoms?
2) How does verbal memory relate to negative symptoms in FEP patients, and how do these prognostic indicators relate to cortical indices for both gray and white matter?
3) Are specific subfields of the hippocampus central to coordinated changes in cortical anatomy, and how does such a putative hippocampal centrality contribute to individual differences in negative symptoms and verbal memory?

This thesis is comprised of detailed background and neuroimaging methods sections, followed by four separate papers which address the research questions above. The background section introduces the reader to the clinical factors surrounding a diagnosis of a psychotic disorder, known neuroanatomical correlates and abnormalities in brain connections, as well as concrete evidence to support the pursuit of a theory of hippocampal centrality underlying negative symptoms and

verbal memory in FEP. The methods section provides an empirical foundation for the neuroimaging methods and MRI-derived metrics that are used throughout the thesis. The first two papers address the first question posed above, where alterations in neuroanatomical trajectories of limbic morphometry (published in *Translational Psychiatry*) and cortical thickness (published in *npj schizophrenia*) with age are compared between FEP patients with and without persistent negative symptoms. The third article, addressing the second aim and currently under review at *Psychological Medicine*, further examines the longitudinal tissue properties underlying fluctuations in negative symptoms and its relationship with verbal memory, using both cortical thickness and a novel metric of white-gray matter contrast. Finally, the fourth study, addressing the third aim and in preparation for *Molecular Psychiatry*, binds the first two aims together, and proposes a framework by which the hippocampus may be central to coordinated changes in cortical anatomy, which in turn may be related to negative symptom and verbal memory changes over time.

Chapter 2 : Background

2.1 Defining psychosis

2.1.1. Prevalence and diagnostic boundaries

Psychotic disorders comprise a heterogeneous set of psychiatric conditions that are bound together by the presence of psychotic or positive symptoms (e.g. hallucinations, delusions) and their significant contributions to socioeconomic burden (Goeree et al. 2005; Moreno-Küstner et al. 2018). Approximately three out of 100 individuals will have a psychotic episode at some point in their lifetime[1] (Perälä et al. 2007). Studies of individuals with psychotic disorders have primarily focused on patients with schizophrenia, a disorder defined by the presence of positive symptoms for at least 6 consecutive months in the absence of other symptoms that are more closely related to mood (e.g. depression, mania) (Tandon et al. 2013). However, it is often overlooked that schizophrenia only comprises 30% of disorders along the psychosis spectrum, with the remaining disorders vastly understudied (van Os 2016). These include other thought disorders such as schizoaffective, delusional and brief psychotic disorders, as well as affective or mood-related conditions such as bipolar disorder and depression with psychotic features. Although such labels are currently important for clinical management and for the creation of appropriate treatment plans, they have proven to be of limited use from a biological standpoint, where biology (e.g. brain structure and function, genes) does not seem to follow diagnostic boundaries (Insel et al. 2010; Owen 2018). Thus, this thesis focuses on individuals who have experienced a FEP as a whole, rather than looking at different diagnostic categories. Importantly, the work presented in this thesis aims to map individual differences in clinical profiles, regardless of the final patient diagnosis, to

[1] https://www.camh.ca/en/health-info/mental-illness-and-addiction-index/psychosis

underlying brain structural trajectories. In this manner, the knowledge gained from this thesis aims towards 'stratified psychiatry', a broad medical concept that reflects the mapping of specific characteristics within a patient population to appropriate treatments, on the basis of biomarker discovery.

Given the heterogeneity of clinical presentation of patients with a psychotic disorder, as well as the factors leading up to a first episode of psychosis, it is easy to be overwhelmed by the vast number of questions that could be asked in the investigation of brain-behaviour relationships in FEP patients. Thus, a more thorough investigation into significant predictors of functional outcomes after a FEP, situated in our knowledge of available treatments for psychosis and their efficacy, is germane to the framework presented in this thesis, and is further elaborated upon in the next section.

2.2 Predictors of functional outcome after a First Episode of Psychosis

Moving beyond the positive symptoms of psychosis, negative symptoms and cognitive deficits comprise two additional behavioural domains that have significant clinical implications, given that clear treatments for the improvement of such clinical measures have not yet been established. With respect to determinants of functional outcome after the stabilization of a FEP, many studies and reviews have consistently drawn the same conclusions: negative symptoms predict poor functional outcome more reliably than positive symptoms (Foussias et al. 2014; Remington et al. 2016; Galderisi et al. 2018), and cognitive deficits are important contributors to functional outcomes after a FEP (Malla, Norman, et al. 2002; Jordan et al. 2014).

2.2.1. Negative symptoms

Negative symptoms characterizing schizophrenia and the related psychoses are comprised of blunted affect, anhedonia, alogia, asociality and avolition (Kirkpatrick et al. 2006). These symptoms do not affect all patients equally, and efforts have been put forth to derive clinically meaningful subgroups of patients on the basis of their negative symptom presentation. Patients with persistent negative symptoms (PNS) comprise one such subgroup, which delineates a subtype of patients presenting with primary (i.e. in the absence or presence of only mild positive symptoms and other potentially confounding symptoms) or secondary (i.e. in the presence of moderate to high levels of positive, depressive, symptoms, among others) negative symptoms for at least six months after stabilization of a FEP (Hovington et al. 2012). The importance of better understanding the mechanisms giving rise to PNS was emphasized by the NIMH consensus statement on negative symptoms, highlighting that PNS represent a currently "unmet therapeutic need" and urgently require attention (Kirkpatrick et al. 2006). Although this statement was put forth over a decade ago, PNS remains an extremely difficult symptom construct to treat and is often associated with poor prognosis (Hovington et al. 2012, 2013, Galderisi et al. 2013, 2018).

Another approach to the dissection of negative symptoms that would allow for the characterization of individual differences, which the above categorical characterization of PNS precludes, is to investigate subject-specific fluctuations in negative symptoms over time. Although many studies simply report mean negative symptom scores (based on scales such as the Scale for the Assessment of Negative Symptoms [SANS] (Andreasen 1984a), Positive and Negative Syndrome Scale [PANSS] (Kay et al. 1987), Brief Psychotic Rating Scale [BPRS] (Overall and Gorham 1962), and the Clinical Assessment Interview for Negative Symptoms [CAINS] (Kring et al. 2013)), it is likely that different types of negative symptoms have different underlying

pathophysiology that would not be captured by pooling these symptoms together into a single score. Thus, a large body of work has been dedicated to addressing the heterogeneity of negative symptoms themselves, and finding clusters or different factors of negative symptoms. By and large, two different models stand out from this sea of literature: 1) a two-factor model, comprising deficits in expressivity and motivation (Messinger et al. 2011; Jang et al. 2016; Marder and Galderisi 2017), and 2) a five-factor model separating negative symptoms into alogia, anhedonia, avolition, asociality, and blunted affect (Kirkpatrick et al. 2006; Strauss et al. 2018). The two-factor model (see **Figure 2.1**) is particularly intriguing given recent evidence that these symptoms have differential longitudinal courses after a FEP; namely, expressivity deficits tend to improve in the two years following a FEP, whereas amotivation remains stable across this time period (Lutgens et al. 2019). However, reports on the neuroimaging correlates of PNS and subdomains of negative symptoms are sparse, particularly with respect to their longitudinal characterization. This will further be discussed in the introductions of Chapters 4 and 5.

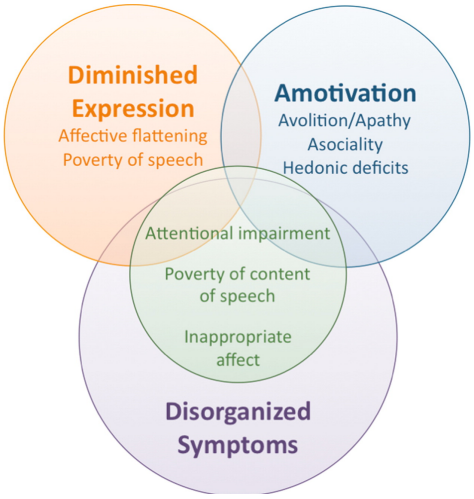

Figure 2.1. The two-factor model of negative symptoms.
This model highlights distinct dimensions for Diminished Expression (referred to as "expressivity" deficits in this thesis) and Amotivation. These factors exclude symptoms that are more closely related to disorganized thought (bottom of figure).
From: Foussias et al. (2014).

2.2.2. Verbal memory

Patients with psychotic disorders tend to exhibit deficits across all cognitive domains (e.g. executive function, speed of processing, attention); however, the verbal memory domain stands out clearly from the rest. Not only do patients with psychosis have the most pronounced deficits in verbal memory compared to other cognitive domains (Saykin et al. 1994; Aleman et al. 1999; Cirillo and Seidman 2003), but these problems are present across diagnoses (e.g. schizophrenia, bipolar) and stages (e.g. ultra-high risk, first and subsequent psychotic episodes) (Brewer et al. 2005a; Barch and Sheffield 2014; Sheffield et al. 2017). There is also a graded pattern of verbal memory deficits across stages; for instance, verbal memory deficits are milder in individuals in the ultra-high risk state (i.e. who later may transition to full-blown psychosis) and in unaffected relatives of patients with psychosis. This suggests a potential biological predisposition or genetic risk that may be shared between verbal memory capacity and psychotic disorders. However, the reasons for the disparate contribution of verbal memory to functional outcome in psychotic disorders compared to other cognitive processes remains elusive.

Certain subdomains of verbal memory are also more affected than others, which provides an avenue to dissect potential underlying neural processes. There is accumulating evidence for specific deficits in episodic verbal memory (i.e. information that needs to be explicitly recalled) as opposed to more implicit forms of verbal memory; again, the selectivity for deficits in episodic verbal memory can be found in both patients with schizophrenia and unaffected relatives (Sponheim et al. 2004). Dissecting this construct of episodic memory further, Cirillo and Seidman (2003) present evidence from multiple studies suggesting that verbal memory impairments in psychosis can largely be accounted for by the *encoding* stage of memory. That is, there does not seem to be a significant amount of information lost after a longer delay in recall when comparing

immediate and delayed recall performance. Knowledge of the source of verbal memory deficits offers a strong case for an underlying biological mechanism seated within the hippocampal formation or broader medial temporal lobe. Deficits in encoding, likely due to abnormalities within the hippocampal formation, would naturally have downstream effects on other memory-related processes, such as retention or recollection. In mapping such neuropsychological abnormalities from encoding or memory *formation* to memory *recollection*, it is feasible that abnormalities within the hippocampus and surrounding structures may then give rise to further deficits in highly connected regions known to subserve such higher cognitive functions, of which the hippocampal-prefrontal cortical network cannot be ignored. A more detailed glimpse at the literature supporting a hippocampal-prefrontal cortical network in verbal memory, with potential for extrapolation to verbal memory deficits and negative symptoms in psychosis, is included in Section 2.4.

2.2.3. Intersection of negative symptoms and verbal memory

Given the importance of negative symptomatology and verbal memory abilities in the course of illness in patients with FEP, it is natural to ask whether the relationship between these two constructs may better inform treatments. It has been suggested that negative symptoms are likely more related to verbal memory deficits compared to associations with positive symptoms (Cirillo and Seidman 2003). With respect to the PNS construct, patients with PNS exhibit even more pronounced verbal memory deficits compared to their non-PNS peers, and these cognitive deficits are maintained over time after a FEP (Hovington et al. 2013). One explanatory framework has been offered by several studies, suggesting that negative symptoms, in particular amotivation, mediate the relationship between neurocognition and functional outcome (Nakagami et al. 2008; Gard et al. 2009; Green et al. 2012; Foussias et al. 2014; Green and Harvey 2014; Jordan et al. 2014). That is, cognitive capacity may influence an individual's motivation and thus likelihood to

perform and complete tasks, which in turn has consequential effects on the individual's global functioning in everyday life (**Figure 2.2**).

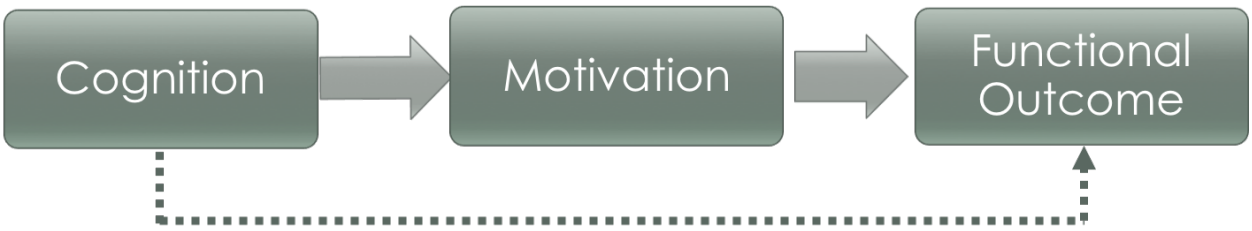

Figure 2.2. Links between neurocognition, motivation, and functional outcomes.
A framework by which motivation provides a mechanism underlying the relationship between cognition and functional outcome. Cognition may also directly influence functional outcome (dotted line). Adapted from Foussias et al. (2014).

Investigations linking individual differences in verbal memory and negative symptom severity have predominantly shown negative relationships between these two constructs; that is, patients with poor verbal memory tend to also have a high level of negative symptoms (Cirillo and Seidman 2003). However, many studies have also failed to find associations between these two clinical factors (Cirillo and Seidman 2003). This may be due in part to small sample sizes or the cross-sectional nature of many of these studies. Although few studies to date have looked at such longitudinal relationships, there is some evidence to suggest that negative symptoms can improve in the absence of any change in verbal memory performance (Nopoulos et al. 1994; Cantor-Graae et al. 1995; Hoff et al. 1999). A more careful look at the dynamic interrelationship of negative symptom fluctuations after a FEP in relation to verbal memory abilities is warranted and is further addressed in the studies presented in Chapters 5 and 6.

It should be noted that both verbal memory deficits and negative symptoms are not specific to psychosis; they are present in many disorders such as Alzheimer's Disease, Parkinson's Disease, HIV, and major affective psychiatric disorders (Brown and Pluck 2000). Both constructs also appear to have their onset much earlier than positive symptomatology. Thus, both negative symptoms and verbal memory deficits seem to have an important neurodevelopmental component that may be reflected in altered brain maturational trajectories leading up to and continuing after a first episode of psychosis (Section 2.4.4).

2.3 Magnetic Resonance Imaging (MRI) studies of psychosis patients

The advent of MRI has been met with powerful enthusiasm from clinicians, researchers, and health practitioners alike. This non-invasive technique has the capacity to acquire a substantial amount of information about brain structure in a highly efficient and rapid manner, magnifying its appeal within psychiatric research (Conlon and Trimble 1987; Mueller et al. 2012). Furthermore, the field of brain MRI has rapidly made gains since its initial acquisition several decades ago, with optimization of protocols and acquisition times to collect images with sub-millimetric in-plane resolution (Prabhakaran et al. 2012), which will be of particular importance for the study presented in Chapter 6. The sections below outline some of the key findings and themes that have been uncovered in neuroimaging studies of psychotic disorders both cross-sectionally and longitudinally, with a stronger focus on the latter.

2.3.1. Frontal-temporal lobes are key regions of interest in psychosis

The majority of neuroimaging studies in schizophrenia and the related psychoses have been conducted in cross-sectional samples. Although longitudinal studies are ideal in the pursuit of dynamic biomarkers contributing to and following a FEP, valuable information can also be gleaned

from such single-timepoint study designs. Some of the earliest brain imaging studies in schizophrenia patients revealed pronounced deficits, usually in the form of reduced gray matter volumes, within frontal and medial temporal lobes, including the hippocampus (Andreasen et al. 1986; Suddath et al. 1989; Barta et al. 1990; Bogerts et al. 1990; Turetsky et al. 1995). Some of these studies also linked cortical volume abnormalities to symptom severity. For instance, Turetsky and colleagues (1995) found that not only were frontal and temporal lobe gray matter volumes reduced in schizophrenia patients, but these abnormalities seemed to be even more pronounced in patients with enduring negative symptoms, classified as the "deficit subgroup".

Of relevance to this thesis, there has been vast interest in characterizing cortex-wide abnormalities, using automatically derived metrics such as cortical thickness and surface area across many points of the brain. These newer methods, compared to the methods employed in earlier seminal studies in the field, allow for the localization of more fine-grained changes in cortical abnormalities. In turn, introduction of automated methods to classify and define different brain regions has immensely contributed to the feasibility of including larger patient samples in a single study, enhancing power and confidence in generated findings. Using these advances in methodology, it is quite clear that cortical thickness is decreased across almost the entire cortex, with regional specificity in fronto-temporal regions highlighted in many studies (Goldman et al. 2009; van Haren et al. 2011; Cobia et al. 2012; Gong et al. 2016).

A recent landmark initiative from the Enabling Neuro-Imaging Genetics through Meta-Analysis (ENIGMA) Consortium (Thompson et al. 2014) has further solidified such findings, by pooling and meta-analyzing cortical and subcortical features from the largest sample sizes (N≈5000) of patients with schizophrenia and bipolar disorder to date, in comparison to an equally large number of healthy controls. Consistent with the above-mentioned findings, these massive

samples have indeed pinpointed widespread thinner cortex and smaller surface area in patients with schizophrenia (van Erp et al. 2018) and bipolar disorder (Hibar et al. 2018), with the largest effect sizes being found in regions of interest within the frontal and temporal lobes. Further, in ENIGMA's separate reports on subcortical and hippocampal structure in these two disorders, the hippocampus emerges as the front-runner, where volume decreases within this structure have the largest effect size when comparing cases to controls (Hibar et al. 2016; van Erp et al. 2016). These mega-analytic approaches have been fruitful in confirming previous findings and clarifying brain structural associations in disease that have previously been clouded by inconsistent findings from underpowered studies; however, they are limited in their ability to: 1) map individual differences in symptoms and cognition given the vast number of instruments compiled in such analyses; and 2) to map such associations dynamically over time. Thus, the next section discusses seminal studies investigating potential progressive brain changes after a FEP.

2.3.2. Progressive brain changes after a first episode of psychosis

Acquiring multiple MRI scans per subject facilitates the collection of valuable longitudinal datasets, which can provide indispensable information on progressive changes within clinical cohorts. Interest in studying longitudinal brain changes in schizophrenia and the related psychoses arguably stemmed from the nosology proposed by Emil Kraepelin, when he described schizophrenia as "dementia praecox" in the late 19th century (Kraepelin 1899). As this denomination suggests, schizophrenia was seen as a progressive neurodegenerative disease of brain structure, akin to dementia (Lehmann and Ban 1997; Ebert and Bär 2010). However, it became clear in later years that there were other biological processes at play with the potential for recovery that were not necessarily indicative of a purely deteriorating course. Further, many

studies later found that brain abnormalities were already present much earlier in the disease process, even before the presentation of frank psychotic symptoms. This suggested that the disease process likely stemmed from neurodevelopmental aberrations, which gave rise to the well-described neurodevelopmental hypothesis of psychotic disorders shortly thereafter (Feinberg 1982; Weinberger 1986; Keshavan et al. 1994). However, both neurodevelopmental and neurodegenerative descriptions of psychotic disorders share a common important point: there are significant neuroanatomical changes taking place throughout the disease course of psychosis that have yet to be fully characterized.

Several studies by Lynn DeLisi and colleagues provided some of the first evidence of progressive brain changes in first-episode schizophrenia patients, demonstrating increases in ventricular volume concomitant with decreases in cortical volume over the first five years after a schizophrenia onset (DeLisi et al. 1995, 1997). Since then, many extensive reviews have been carried out on this topic, all highlighting the presence of progressive brain changes at different stages within the disease course of psychosis, across nearly the entire brain (Lieberman 1999; Pantelis 2005; DeLisi 2008; Andreasen et al. 2011; Olabi et al. 2011; Cannon et al. 2015; Gong et al. 2016). Findings from the landmark Iowa Longitudinal Study (ILS) are of particular relevance for the work presented in this thesis, given their inclusion of a large sample of patients followed over multiple timepoints proximal to the emergence of a FEP (Andreasen et al. 2011). Specifically, Andreasen and colleagues (2011) were able to pinpoint that the most pronounced changes in brain structure (i.e. gray and white matter loss) were occurring during the two years following a FEP.

The schematic in **Figure 2.3** summarizes the main themes that have emerged in the investigation of progressive gray matter changes.

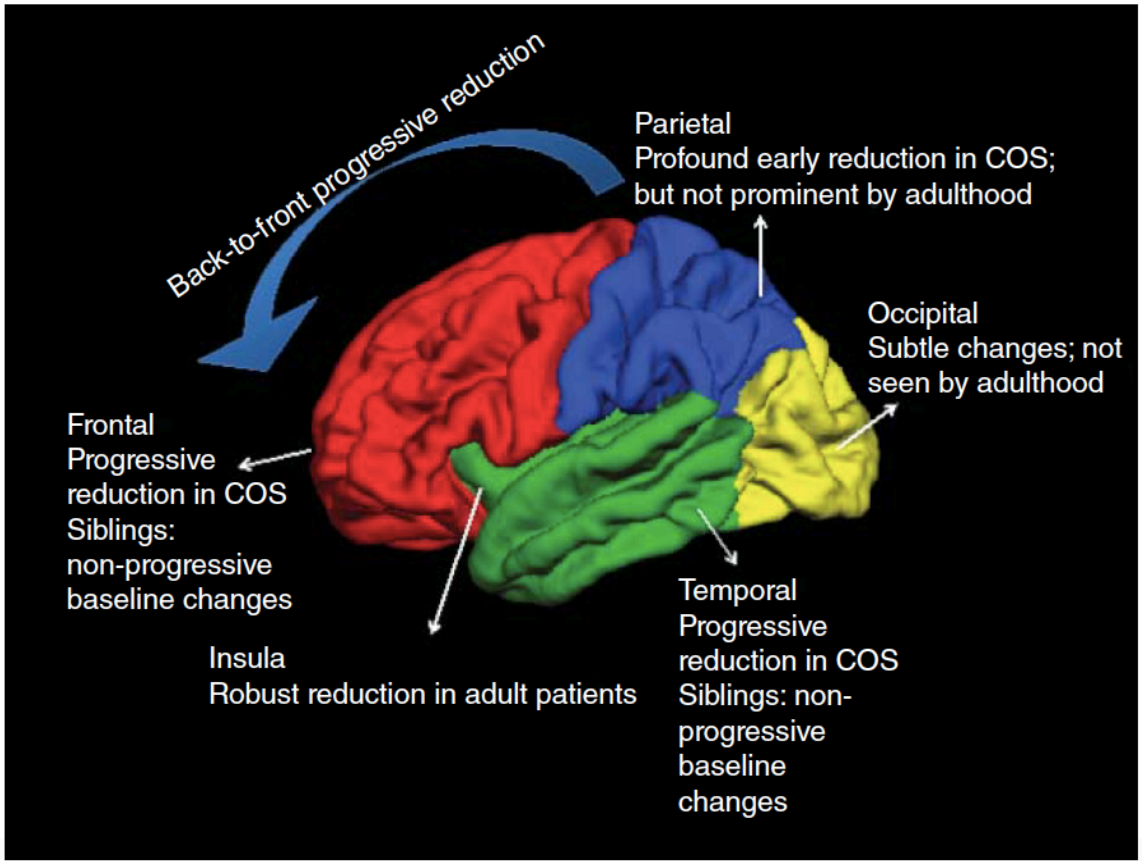

Figure 2.3. Progression of gray matter abnormalities in schizophrenia across the cortex. Abbreviation: COS: Childhood-onset schizophrenia. From: Hollis and Palaniyappan (2015).

A number of studies have also addressed these questions with surface-based measurements such as cortical thickness and surface area. These measurements are unique contributors of the gray matter volume measures included in the above-mentioned studies (and further discussed in Chapter 3), and thus might bring us one step closer to understanding the potential biological mechanisms underlying these progressive brain changes. Mirroring findings observed at the volumetric level, studies have shown pronounced cortical thinning with time in patients with schizophrenia, over and above the expected cortical thinning rate that is expected in non-clinical healthy controls (Rais et al. 2010; van Haren et al. 2011; Cobia et al. 2012). There have also been some studies investigating change over time in individuals at high risk for psychosis, who ultimately transition to psychosis (Smieskova et al. 2010; Cannon et al. 2015). One of these studies

found pronounced cortical thinning in frontal regions in 35 ultra-high risk patients who eventually transitioned to psychosis one year later (Cannon et al. 2015). However, surprisingly few studies have actually investigated changes in cortical thickness in the time period just after a FEP.

Gray matter is not restricted to the cortex, and indeed, there are reports of progressive brain changes in deeper cortical (e.g. hippocampus) and subcortical (e.g. striatum, thalamus) structures (Chakravarty et al. 2015), although these studies are not as common as investigations of neocortical gray matter changes. Focusing on limbic structures such as the hippocampus and amygdala, null findings have been reported in the two years following a FEP (Wood et al. 2001). The authors suggested that such changes may best be captured in the time period preceding psychosis onset. Along these lines, Bois and colleagues (2015) addressed such longitudinal changes in individuals at ultra-high risk for psychosis, assessing hippocampal and amygdalar volumes at baseline and two years later compared to healthy controls. That study found a significant group by time interaction effect on hippocampal volumes, such that controls showed an increase in hippocampal volumes over time, in the absence of any such change in the ultra-high risk group. It has recently been suggested that gross volumes of the hippocampus and subcortical structures may not be optimally sensitive in detecting differences across time or between groups (Chakravarty et al. 2015; Voineskos et al. 2015), and this is further addressed in Section 3.1.2.

Such null findings have also been interpreted in other ways, independently of imaging methodology; indeed, there are several studies that contest evidence for progressive brain change after a FEP altogether (Nesvåg et al. 2012; Zipursky et al. 2013; Roiz-Santiáñez et al. 2015; Haukvik et al. 2016). However, the null findings presented in those studies may be a consequence of the heterogeneity of the patient samples used. This heterogeneity could be addressed in well-powered studies by using alternative statistical approaches, such as grouping patients based on

clinically meaningful symptom dimensions, or examining individual differences in clinical and cognitive profiles to underlying neuroanatomical trajectories. Both of these approaches are employed in this thesis, where Chapter 4 stratifies patients on the basis of their negative symptom presentation, and Chapters 5 and 6 emphasize individual differences in symptomatology and cognitive performance.

It should be noted that many of the studies discussed above focus on 'gray matter-centric' measures, such as cortical/subcortical volumes or cortical thickness. However, white matter both within the cortex (i.e. intracortical myelin) and underlying the cortical mantle can yield additional information of the neurobiological correlates underlying anatomical progression in psychosis. For instance, the above-cited Iowa Longitudinal Study from Andreasen and colleagues (2011) found that white matter loss was more strongly associated with cognitive deficits than gray matter loss. The contribution of white matter abnormalities to psychotic disorders is further explored in the next section.

2.3.3. White matter abnormalities

There are multiple scales of evidence for white matter abnormalities characterizing schizophrenia and the associated psychoses; from alterations in histological measures of the proteins and cell types that characterize white matter tissue (e.g. oligodendrocytes, myelin-basic protein) (Uranova et al. 2007, 2011) to widespread brain network abnormalities (Friston 1998; van den Heuvel et al. 2013; Friston et al. 2016). The latter point has brought forth a widely-accepted theory which illustrates psychosis as a disorder of 'dysconnectivity'[2]. White matter is of particular interest in

[2] Please note the use of the prefix "dys" as opposed to "dis". The former emphasizes deviations from the norm, without imposing directionality. This is more likely to capture the nature of deviations (e.g. both positive/increased and negative/decreased effects) found in psychosis.

the study of psychotic disorders, as it has a more protracted maturational course compared to gray matter. Thus, significant changes occurring in white matter, both intracortically and within deeper brain tissue, are occurring concurrently over the time period at which psychotic disorders typically emerge (i.e. late adolescence, early adulthood) (Bartzokis 2004; Marín 2016). Furthermore, it has been proposed that tissue compartments rich in myelin (i.e. the fatty substance encasing axons) are more plastic and potentially more amenable to change (Walhovd, Westerhausen, et al. 2016; Wenger et al. 2017), providing additional justification for the investigation of white matter abnormalities in psychosis.

One of the most common ways that white matter has been quantitatively assessed *in vivo* with MRI imaging is through the use of diffusion-weighted imaging (DWI), where the coherence of bundles of axons underlying major white matter tracts can be inferred on the basis of water molecule diffusion properties in the brain. Fractional anisotropy (FA) is arguably one of the most popular measures in DWI reports comparing patients with psychosis to healthy controls, which provides a measure of the degree to which water molecule diffusion is restricted to any given direction within a particular region of the brain. The overarching theme that has emerged in the literature is that of reduced FA in patients with psychosis compared to controls. This can be interpreted as less coherent diffusion along white matter tracts and thus, potentially compromised white matter integrity in this patient population (Kubicki et al. 2005; Ellison-Wright and Bullmore 2010; Pérez-Iglesias et al. 2010; Nazeri et al. 2013; Kelly et al. 2018). A recent large-scale investigation from the above-mentioned ENIGMA consortium was conducted in over 4000 individuals with schizophrenia, indeed confirming these findings of reduced FA across most white matter tracts of interest, with the highest effect sizes found within callosal fibers joining homologous regions of the brain interhemispherically (Kelly et al. 2018). Intriguingly, lower FA

in patients with schizophrenia is more commonly reported in tracts subserving multimodal brain regions (e.g. genu of corpus callosum, joining frontal lobes), as opposed to unimodal brain regions (e.g. primary motor and sensory areas) (Kochunov et al. 2016). This would suggest that the white matter tracts that mature later in life may be more sensitive to the pathophysiology of psychosis. Indeed, recent evidence has shown that such late-maturing tracts have an accelerated age-related decline in FA in patients with schizophrenia, with early-maturing tracts relatively spared (Kochunov et al. 2016).

With respect to longitudinal studies, a handful of studies have contributed to our understanding of the trajectory of white matter changes following a FEP. One study found white matter decreases in the two to three years following a first episode of schizophrenia within inferior temporal regions, paralleled by increases in white matter within the frontoparietal junction (Whitford et al. 2007). Another found significant decreases in frontal white matter volume over a similar follow-up period in first-episode schizophrenia patients, which was also related to negative symptom severity (Ho et al. 2003). These inconsistent results from similarly designed studies are reflective of many of the studies that have been conducted on this topic (Wheeler and Voineskos 2014), further highlighting the need for more longitudinal investigations of such neuroanatomical correlates in FEP patients.

Although the majority of studies have targeted deeper white matter tracts, it is important to consider the myelin that is found near the gray-white matter boundary of the cortical mantle; that is, within superficial white matter and intracortically. There are several reasons as to why these fibers may be more vulnerable to insult, especially around the time period of psychosis onset:

1) peri-cortical myelination occurs later than myelination of deeper white matter tracts, once again highlighting a protracted maturational course (Bartzokis 2004) and an extended window of vulnerability.

2) oligodendrocytes, the glial cells that form the myelin sheath around axons, wrap around intracortical and superficial white matter fibers less times compared to deeper axons (Haroutunian et al. 2014), rendering these axons more susceptible to injury.

3) the majority of white matter fibers are found peri-cortically (Schüz and Braitenburg 2002). See **Figure 2.4**.

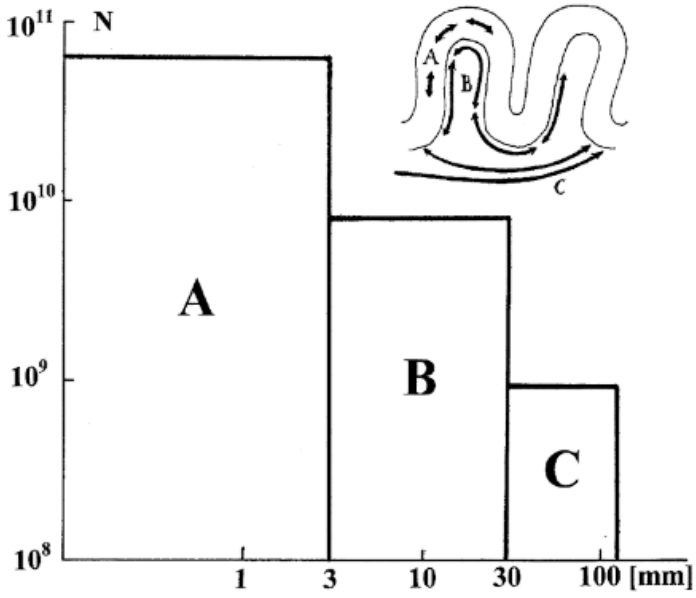

Figure 2.4. Distribution of white matter fibers in the human brain.
Class A represents intracortical fibers. Class B represents superficial white matter fibers that follow the cortical folding pattern, typically characterizing U-shaped fibers and joining proximal cortical regions. Class C represents deeper white matter fibers, typically joining more distant cortical regions. The x-axis represents the log-log range of fiber length in mm and the y-axis represents number of fibers in each class.
From Schüz and Braitenburg (2002).

Several studies have restricted their analysis of FA to superficial white matter when comparing patients with a psychotic disorder (e.g. schizophrenia, bipolar disorder) to healthy controls, mirroring the aforementioned results of widespread reductions in FA across the brain (Phillips et al. 2011; Nazeri et al. 2013; Ji et al. 2018). Intracortical myelin has also been probed using unique imaging acquisition contrasts and novel measures, which will be discussed in sections 3.3.2-3, and forms the basis of the MRI measures used in Chapters 5 and 6.

White matter myelination surrounding the hippocampus also undergoes significant transformation over the first three decades of human life (Benes et al. 1994). These regions are vastly understudied, likely because of the difficulty in accurately measuring the white matter of the Papez circuit (e.g. alveus and fimbria sitting atop the hippocampus, and the output circuitry of the fornix) with conventional structural MRI sequences. Some DWI studies have assessed integrity of the fornix in psychosis, although these studies should be interpreted with caution. Specifically, it is particularly challenging to accurately extract FA (and other diffusion tensor imaging [DTI]-based measures) from the fornix, given its close proximity to cerebrospinal fluid (CSF) within the lateral ventricles, which can significantly contaminate the signal that is being measured (Arkesteijn et al. 2017; Amaral et al. 2018).

Nevertheless, white matter regions surrounding the hippocampus remain an interesting target of study in schizophrenia. For instance, integrity of the fornix has been tightly linked to cognitive abilities in schizophrenia (Knöchel et al. 2016). A recent study in early psychosis patients from Switzerland, in the same 18-35-year age range of patients used in this thesis, investigated hippocampal volumes, white matter integrity of the fornix with DTI, and antioxidant activity (as a proxy marker of oxidative stress in the fornix) (Baumann et al. 2016). Baumann and colleagues (2016) found that lower FA and higher oxidative stress within the fornix were associated with

smaller hippocampal volumes, uniquely in the early psychosis patient group (i.e. relationships were not found in controls). Thus, studying markers of white matter microstructure within the hippocampal circuit, beyond just the hippocampal formation itself, may also prove to be fruitful in better understanding the contribution of the limbic lobe to broader white matter abnormalities across the brain.

2.3.4. Network-based investigations

Many of the studies described thus far have reported isolated anatomical changes in psychotic disorders, without addressing the relationships, or "connectivity", between distributed gray and white matter abnormalities across the brain. This idea speaks to a more network-level perspective of the brain, which is a burgeoning and active field of investigation in psychiatry. As alluded to, there is a widely cited theory of "dysconnectivity" within the brain that seems to be essential to our current understanding of psychotic disorders (Friston and Frith 1995; Friston 1998; Stephan et al. 2009; Friston et al. 2016). Intriguingly, this theory was initially posed by the prominent neurologist and anatomist, Carl Wernicke, at the turn of the 20th century (Wernicke 1906), where he theorized that psychosis stemmed from disruptions in white matter tracts joining proximal cortical regions (i.e. association fibers). Indeed, the nosology of *schizophrenia* or "split mind" coined by Eugen Bleuler shortly thereafter in and of itself reflects a dysconnection of sorts (Bleuler 1911). However, it was not until more recently within the 21st century that network-based methods evolved and were extended for use in psychiatric imaging studies. Such methods have allowed for the derivation of summary metrics that quantitatively characterize the extent of connectivity alterations found in patients with psychosis compared to controls, both in terms of brain structural and functional networks. The representation of various brain regions and the relationships or

connections between them constitutes the human brain "*connectome"* (Sporns et al. 2005). Overarching themes from studies examining the structural connectome are summarized here, given their pertinence to the work presented in this thesis (Chapter 6), although it is acknowledged that functional MRI connectome studies have also significantly contributed to our knowledge of connectivity alterations in psychosis.

The structural connectome can be measured in a variety of ways using MRI, and is not solely restricted to the white matter connections that can be measured with DWI. As a natural extension of the body of work summarized in sections 2.3.1 and 2.3.2 investigating the neuroanatomical correlates of psychotic disorders, measures such as cortical thickness or gray matter volumes can also be used to build a structural connectome. This method is known as structural covariance, with the underlying premise that regions with shared features (e.g. cytoarchitecture, genetic factors, developmental factors) will be more correlated with each other, and thus, may be part of a common structural network (Lerch et al. 2006; Alexander-Bloch et al. 2013; Evans 2013). Increases in structural covariance could also be fueled by common pathological factors, which is of relevance to the study of psychiatric disease such as psychosis (Zugman et al. 2015). Studies of structural covariance have highlighted widespread differences in pair-wise relationships between brain regions, with both increased and decreased covariance relative to healthy controls (Wheeler and Voineskos 2014; Guo et al. 2016; Palaniyappan 2017; Palaniyappan et al. 2018). However, it is acknowledged that simply looking at differences in pair-wise regional relationships between cases and controls can be difficult to interpret, and does not allow one to draw conclusions about how individual patient differences in the structural connectome are associated with clinically relevant behaviours. Thus, many studies have turned

towards the quantitative analysis of such connectomes with graph theory methods (Bullmore and Sporns 2009). Specific methods are further elaborated upon in Section 3.4.

Certain networks, or clusters of brain regions with shared structure and/or function, may also be more vulnerable to the disease process of psychosis than others. For instance, several studies have raised the idea that brain "hubs" are disproportionately affected in psychotic disorders (van den Heuvel et al. 2010; Rubinov and Bullmore 2013; Crossley et al. 2014; Klauser et al. 2017). These brain hubs can be understood in a similar manner as major geographical hubs of the world, where the "New York" and "Tokyo" equivalents in the brain are connected to many other regions in the brain, contributing largely to the transportation of various molecules/factors that are integral for quick and efficient neural communication. These brain hubs include the precuneus, cingulate cortex, and superior frontal cortex (see **Figure 2.5**), and are hypothesized to contribute to the widespread increases and decreases in structural connectivity found throughout the brain of patients with psychosis (Guo et al. 2016; Palaniyappan 2017).

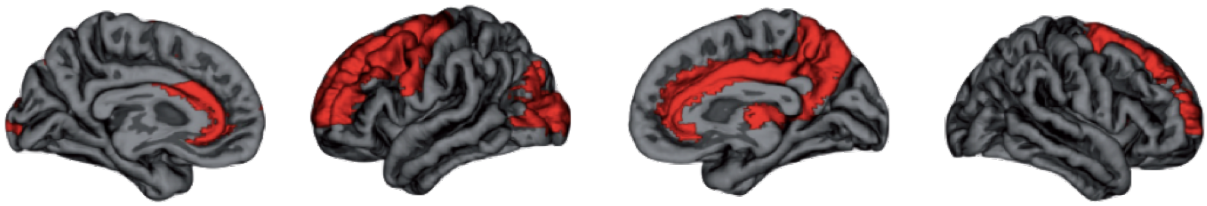

Figure 2.5. Affected brain hubs in schizophrenia.
Brain views from left to right: Left medial view, highlighting anterior cingulate cortex. Left lateral view, highlighting superior frontal and lateral occipital regions. Right medial view, highlighting cingulate cortex and precuneus. Right lateral view, highlighting superior frontal gyrus.
Figure adapted from van den Heuvel et al (2010) and Rubinov & Bullmore (2013).

Studies have begun to apply knowledge of these structural connectome abnormalities in psychotic disorders within clinically meaningful frameworks. One relevant investigation of FEP

patients examined the gyrification, or cortical folding properties, of the brain with graph theory, finding that hub regions are disproportionately affected specifically in patients who do not respond well to antipsychotic treatment (Palaniyappan, Marques, et al. 2013). These "non-responders" were also found to have more distributed, or less efficiently organized, connectivity patterns compared to FEP patients who responded to treatment and healthy controls. A follow-up study revealed that such organization of gyrification properties could also predict with 80% accuracy which individuals at clinical high-risk state for psychosis would later transition to full-blown psychosis (Das et al. 2018). There admittedly are few studies investigating structural connectomes built with cortical thickness in FEP patients, although a related investigation was carried out by Makowski et al (2019b) and will be further discussed in Chapter 3.

These studies provide compelling evidence for widespread connectome aberrations underlying patients at different stages of psychosis, which naturally asks the question: how is the structural connectome changing over time in this patient population? This is currently a highly opportune field and is directly addressed by the study presented in Chapter 6 of this thesis. The need for application of more dynamic methods to characterize connectome maturation has recently been highlighted in a review from Collin and Keshavan (2018). This insightful paper proposes an extension to the neurodevelopmental hypothesis of schizophrenia and the related psychoses, suggesting that psychosis is a disorder of altered connectome development. Thus, the characterization of maturational trajectories of brain structures pertinent to the manifestation of psychosis (e.g. fronto-temporal cortices, hippocampus) and the neuroanatomical relationships linking these regions after psychosis onset can be immensely informative in understanding the mechanisms giving rise to "difficult-to-treat" clinical indicators, such as negative symptoms and verbal memory.

It should be noted that these new approaches to connectivity alterations in psychosis do not detract from more classical studies pinpointing aberrations within the neuroanatomical structure and white matter tracts underlying fronto-temporal regions, as discussed in section 2.3.1. However, these new studies position such abnormalities within a broader framework of pathological factors that may have widespread effects on the entire brain. This idea can naturally be quite overwhelming in the search of useful and quantitative biomarkers for the treatment of psychosis; thus, finding a mechanism that may be central to these broader cortical network disruptions would yield more practical utility in the field of translational psychiatry. This brings us to the next section, which proposes the hippocampus as such a putative central marker to connectome alterations in psychosis, and resultant symptoms and cognitive deficits.

2.4. Theory of hippocampal centrality in psychosis

The hippocampus has long held the interest of scientists aiming to better understand the pathophysiology of disease. Its composition comes from the oldest cortex in the brain, i.e. *archicortex*, and has undergone significantly less evolutionary expansion compared to other cortical regions in the human brain (Ariëns-Kappers 1909). Despite its primal role in comparison to other neocortical regions, the hippocampus remains an incredibly important structure for human behavior. The famous neuropsychology studies carried out by Dr. Brenda Milner and Dr. William B. Scoville with patients that had lesions of the medial temporal lobe showed the hippocampal formation's essential role in declarative memory formation (Scoville and Milner 1957). Studies of the neuroanatomy, function, physiology and metabolism of the hippocampus have not decelerated since. The hippocampus' capacity for neurogenesis, exquisitely organized circuitry, and facilitation of neuroplastic mechanisms are just a few reasons that position the hippocampus as a

candidate target to better understand the brain in both health and disease. However, this sort of neuroplasticity comes with a tradeoff, rendering the hippocampus highly capable of adapting to new environmental stimuli but also increasing its susceptibility to insult. This realization has not escaped the notice of researchers studying psychotic disorders; indeed, the hippocampus has been pinpointed as a central structure to the manifestation of psychotic symptoms, even before the transition to a full-blown psychotic episode. However, the centrality of the hippocampus to negative symptoms and verbal memory deficits in early psychosis has not yet been explored, and could very well pose an important explanatory framework for these key prognostic indicators in FEP patients, as shown in Chapter 6 of this thesis.

2.4.1. Premise of hippocampal centrality theory

The importance of the hippocampus to the pathophysiology of positive symptoms in psychosis, such as hallucinations, delusions and disordered thought, has been described at length in many reports (Harrison 2004; Tamminga et al. 2010, 2012; Lieberman et al. 2018). Evidence from multiple scales of research were formally strung together in an influential paper by Carol Tamminga and colleagues in 2010, and further elaborated upon in a follow-up paper in 2012 by the same group (Tamminga et al. 2010, 2012).

Before summarizing the theories posited by Carol Tamminga and others, it is essential to understand some basic components of the neuroanatomy of the hippocampus and the flow of information from cortex to individual hippocampal subfields, before signals return back to the neocortex. Information from neocortical regions funnel into the parahippocampal cortex, which surrounds the hippocampus on the medial face of the brain. The parahippocampal cortex then sends

projections to cortical layers II and III of the entorhinal cortex. From here, information enters the hippocampal formation via two main circuits:

1. Circuit 1 is uniquely unidirectional, where information from the entorhinal cortex flows through perforant projections to the dentate gyrus. Information then enters the CA3 subfield via mossy fibers. CA3 projects to CA1 via Schaffer collaterals. Finally, outputs are sent to the subiculum, to be projected back to the entorhinal cortex.
2. Circuit 2 entails direct projections from the entorhinal cortex to individual subfields.

See **Figure 2.6** for a depiction of the gross anatomy of the medial temporal lobe (Panel A) and a depiction of the flow of information from entorhinal cortex through the hippocampal subfields, as described by "Circuit 1" (Panel B). It is also important to note that many of the neurochemical mechanisms underlying hippocampal function utilize the neurotransmitter glutamate, which largely supports the hippocampus' prominent role in learning and memory (Amaral and Witter 1989; Tamminga et al. 2012).

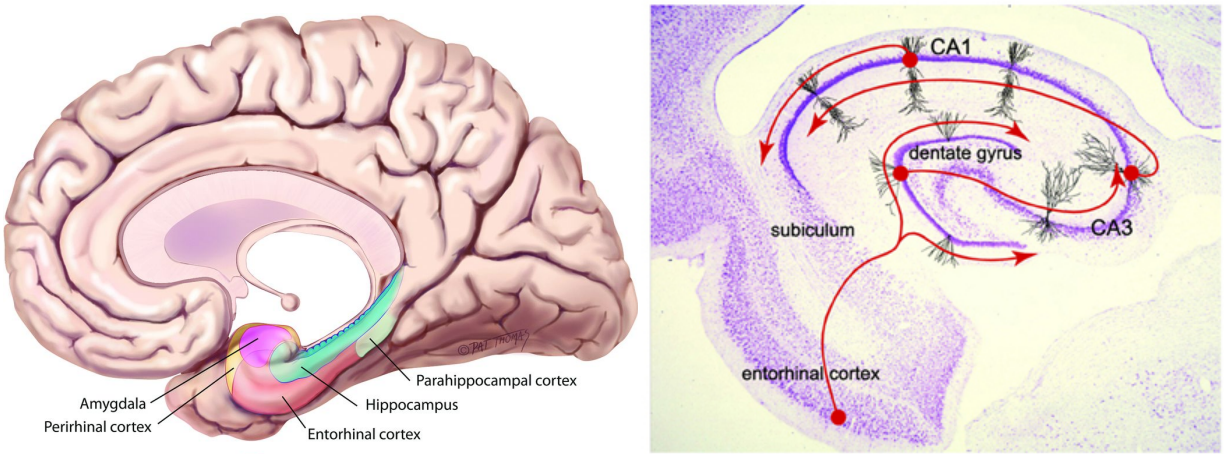

Figure 2.6. Gross anatomy and circuitry of the medial temporal lobe.
Panel A: Gross anatomy of the medial temporal lobe, shown on a medial view of the brain. Figure from (Purves et al. 2008; Raslau et al. 2015).
Panel B: Hippocampal subfields and direction of information flow. Figure from (Song et al. 2014)

How is this flow of information disrupted in psychosis? It has been posited that there are two key lesions present in patients with psychosis (depicted in **Figure 2.7**):

a. **Dentate gyrus:** Reduced glutamatergic signaling has been found within the dentate gyrus in patients with psychosis. This subfield is important for creating associations between memories, while still keeping certain memory traces distinct. In other words, the dentate gyrus is critical for "pattern separation". Thus, disruptions within this subfield may create fuzzy boundaries between distinct memories, which is then passed along to subfield CA3.

b. **CA3**: As mentioned above, in healthy hippocampal circuitry, the CA3 receives input from the dentate gyrus via the excitatory/glutamatergic-containing mossy fibers. Reduced input from dentate gyrus, as is observed in psychosis, would then disinhibit the CA3 subfield, increasing its activity. The CA3 subfield is important for "pattern completion"; thus, hyperactivity here would generate spurious associations that could potentially generate psychotic-like symptoms and be encoded in memory through long-term potentiation (LTP) mechanisms (i.e. the strengthening of synapses as a consequence of increased activity).

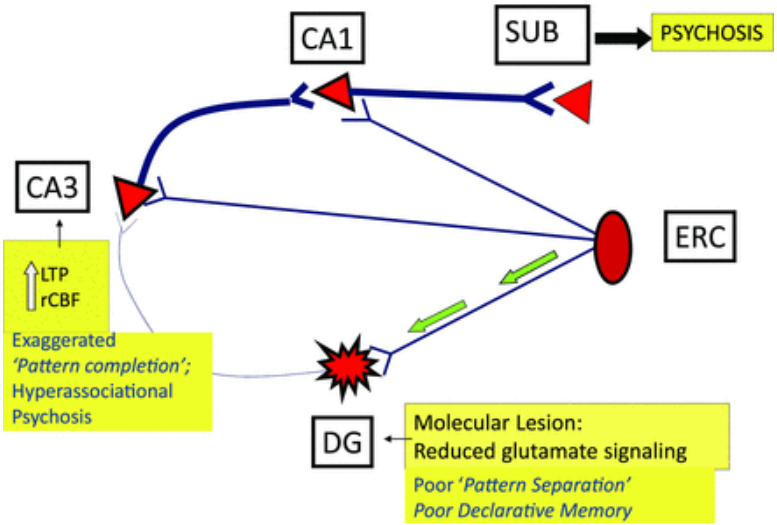

Figure 2.7. Lesions in schizophrenia along the hippocampal subfield pathway.
Abbreviations: ERC: entorhinal cortex, DG: dentate gyrus, SUB: subiculum, LTP: long-term potentiation, rCBF: regional cerebral blood flow.
From Tamminga et al. (2010).

There is strong evidence for the presence of glutamatergic dysfunction and alterations in homeostatic mechanisms of the hippocampus through preclinical, human neuroimaging and postmortem studies. Tamminga and colleagues' theories provide potential explanations as to how such alterations manifest themselves at the level of behavior in the form of psychotic symptoms. Let us investigate some of these possible mechanisms and resultant consequences of the lesions described above:

a. **Reduced glutamatergic signaling in dentate gyrus affects glutamatergic signaling in CA3**: It has been shown that there are reduced levels of mRNA transcripts (the molecular code that translates DNA into a protein) of a particular glutamatergic receptor, i.e. GluN1, within the dentate gyrus. As mentioned above, this causes decreased glutamatergic signaling through mossy fibers, depriving CA3 of excitatory inputs. The CA3 subfield tries to compensate for this reduced input by increasing its own availability of glutamatergic receptors, making it hypersensitive to any glutamatergic signaling it does receive. These increases in glutamatergic signaling may stem from genetic variations (e.g. neuregulin 1 [NRG1], disrupted in schizophrenia [DISC], dysbindin, brain-derived neurotrophic factor [BDNF], etc.).
b. **Increased signal from CA3 will increase signaling in CA1:** Hyperactivity of CA3 will result in long-term potentiation mechanisms that serve to strengthen the synapses between CA3 and its downstream subfield, CA1. This response may be graded along stages of psychosis. For instance, mildly strengthened synapses may be found in prodromal stages (i.e. before psychosis onset) resulting in subthreshold psychotic symptoms, and robustly strengthened synapses may underlie full-blown psychosis. This theory has been supported by observations of increased neuronal activity when using functional MRI. Findings of

regional increases in BDNF within CA3 have also been observed in post-mortem tissue of patients with schizophrenia.

If these lesions and functional consequences on hippocampal circuitry are already present before the onset of psychosis, it is realistic to speculate that after a FEP, more widespread alterations throughout the hippocampus may be seen a few years after psychosis onset. Indeed, this has been posited by several groups (Ho, Holt, et al. 2017; Lieberman et al. 2018; Nakahara et al. 2018), where the CA1 subfield may be initially affected, and deficits then generalize to all other subfields as psychosis progresses. These questions had eluded researchers for quite some time, as the hippocampus could only be examined in such detail in post mortem tissue, thus precluding the investigation of earlier stages of psychosis. Recently, important methodological advances have been made in neuroimaging of hippocampal subfields and associated circuitry *in vivo* and non-invasively. These methods are described in more detail in Section 3.2 and are harnessed by the study presented in Chapter 6. Such advances in hippocampal segmentation methods also facilitate exploration at the network level, where the hippocampus and connected regions may have significant implications for different symptom profiles and memory performance in FEP. Specifically, links between the hippocampus and prefrontal cortex have often been cited in the context of a supposed "memory network" (Battaglia et al. 2011); thus, hippocampal-prefrontal cortical links could also feasibly contribute to the biological framework underlying the manifestation of negative symptoms, which is described in the section below.

2.4.2. Hippocampal links to neocortical regions

The hippocampus is well-situated as a hub structure in the brain (Squire et al. 2004; Mišić et al. 2014; Moscovitch et al. 2016). Evidence suggests that the hippocampus is a key convergence

zone for information coming from multiple cortical regions (Mišić et al. 2014), where information from polysensory cortical regions are funneled into the hippocampus. In this manner, the hippocampus has been defined as the "top" structure within a hierarchy of cortical systems, where signals from the external world are processed first in primary sensory cortical regions (or unimodal regions). Processing within heteromodal regions occurs at a later stage and adds complexity to representations of external stimuli. The final binding of these features then culminates within the hippocampus (Moscovitch et al. 2016). Thus, the hippocampus has a substantial and complex role in integrating a wide array of information types, and creating a cohesive experience or memory, which is then shuffled along to other cortical regions. One of the key hippocampal-neocortical pathways that is integral to consolidation of such memories, and feasibly underlies the prognostic indicators (i.e. verbal memory, negative symptoms) of FEP central to this thesis, is that of connections between the hippocampus and prefrontal cortex (PFC). A schematic of known projections between the medial temporal lobe and PFC in healthy brain function is depicted in **Figure 2.8**.

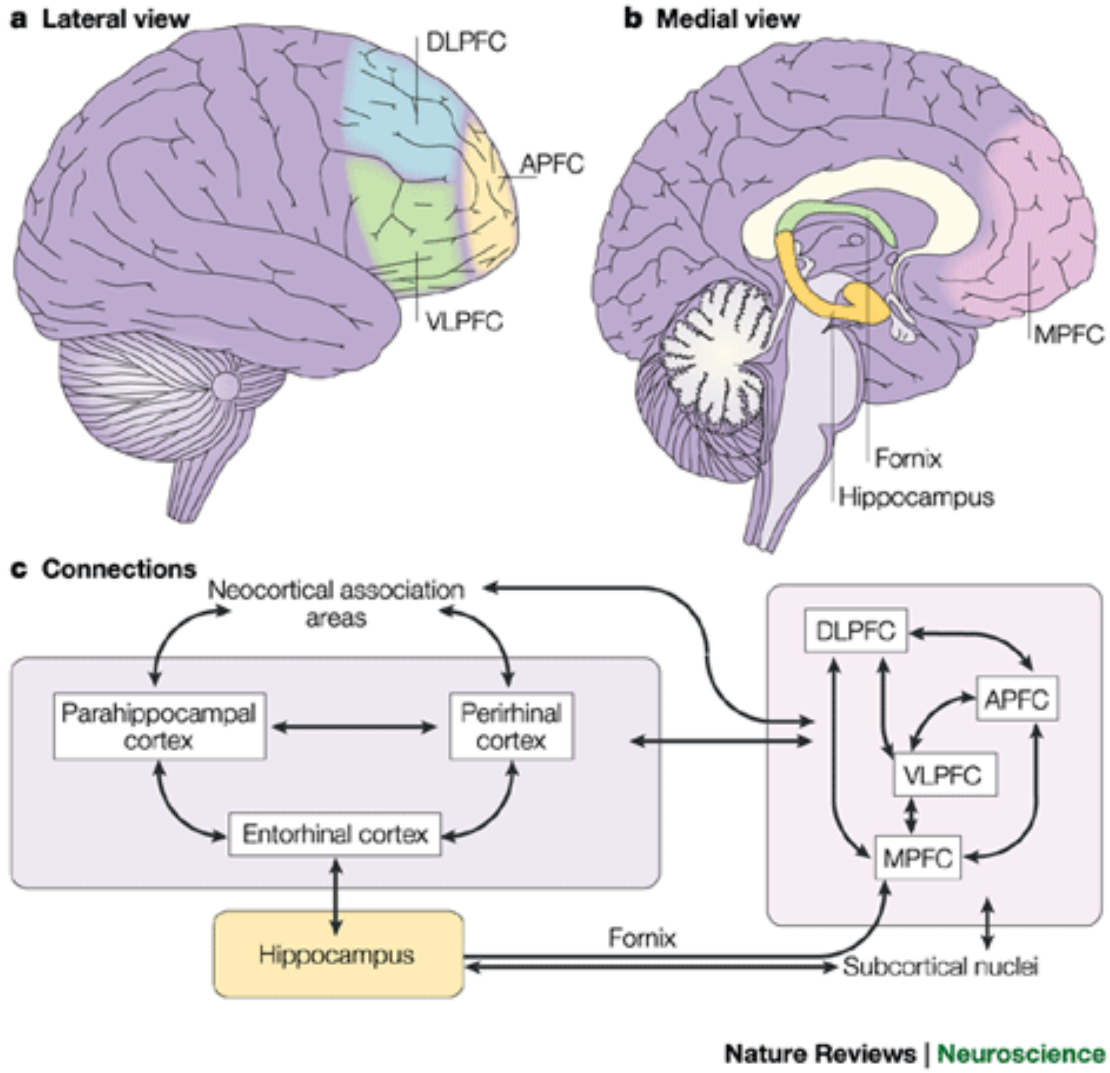

Figure 2.8. Anatomy of the prefrontal cortex and medial temporal lobe.
Abbreviations: PFC, prefrontal cortex. APFC, Anterior PFC. DLPFC, Dorsolateral PFC. MPFC, Medial PFC. VLPFC, Ventrolateral PFC.
Figure from Simons & Spiers (2003), based on work presented in Martin (1996).

The hippocampal-PFC pathway has been dubbed as the "weak link" in psychiatric disorders, and could provide valuable insight into disruptions along the path from memory encoding (within the hippocampus) to consolidation (within the PFC) (Godsil et al. 2013). Early evidence in a monozygotic twin design discordant for schizophrenia (i.e. only one twin is diagnosed with schizophrenia, whereas the other is placed at high familial risk for schizophrenia) showed that

individuals with schizophrenia had lower hippocampal volumes compared to their non-affected sibling, and these hippocampal differences are correlated with functional activation of the PFC during a working memory task (Weinberger et al. 1992). Indeed, aberrant functional coupling between the hippocampus and PFC during such higher-order cognitive tasks has since been reported in several studies of enduring schizophrenia patients (Meyer-Lindenberg et al. 2005; Wolf et al. 2009), as well as in FEP patients and at-risk individuals (Crossley et al. 2009; Schneider et al. 2017). At the structural level, anomalies in anterior hippocampus alongside cortical thinning of PFC have been related to symptom severity in schizophrenia (Qiu et al. 2013). This raises the question of whether the anatomy of the white matter connections linking these two regions is altered. Indeed, several studies have shown altered white matter integrity in schizophrenia patients compared to controls with diffusion tensor imaging in tracts linking the hippocampus-PFC (Zhou et al. 2008; Hao et al. 2009), including the fornix (Kubicki et al. 2005).

The above-mentioned associations still do not pinpoint causality, i.e. is it the hippocampus or the PFC that is the source of such neuroanatomical alterations? Understanding the flow of information in an important cognitive process such as memory may be useful in disentangling the directionality of this relationship. As alluded to, evidence from lesions studies and tract tracing studies positions the hippocampus as the source of memory, with evidence from studies of healthy individuals demonstrating that a medial temporal lobe – PFC network collectively subserves memory processes, specifically long-term memory (Simons and Spiers 2003; Öztekin et al. 2010). In this thesis, it is argued that integrity of the hippocampal-PFC pathway first stems from the hippocampus, which sets the foundation for accurate appraisal and integration of previous experience. Connections from the hippocampus to the PFC are then integral for successfully

conveying memory representations and required for individuals to successfully carry out daily cognitive tasks.

The theory of hippocampal centrality in relation to negative symptoms of psychosis has not been investigated previously, although there is strong evidence to suggest that this is a viable concept. For instance, anatomical changes of frontal and temporal lobes, including the hippocampus, have been linked to negative symptomatology in psychosis, as described in section 2.3.1. Many studies have also suggested that hypofrontality (i.e. decreased activity in the frontal cortex) is a key mechanism contributing to negative symptom severity in psychosis (Andreasen et al. 1986; Williamson 1987). Given the known dense connections between the hippocampus and PFC, and these regions' role in negative symptoms, it is intriguing to consider the possibility that the hippocampus may be central to such hypofrontality. To provide a few concrete examples, altered connections between the hippocampus and dorsolateral PFC may have functional consequences on motivation; and disruptions in tracts joining the hippocampus to the amygdala and the anterior cingulate cortex may give rise to anhedonia and expressivity deficits, given the known role of anterior cingulate cortex in reward anticipation and emotional control (Pier et al. 2016; Schulze et al. 2016).

In Section 2.4.1, we learned that alterations within specific hippocampal subfields and associated circuitry likely have propagating effects on the regions that the hippocampus directly projects to, including regions of the PFC described above, such as the anterior cingulate and dorsolateral PFC. In this manner, the pathophysiological process may start in the hippocampus and be restricted to the hippocampus in very early stages of psychosis, e.g. in prodromal stages, but then span cortical regions that are directly connected to the hippocampus in later stages, such as full-blown psychosis. With this in mind, we would also expect that hippocampal-cortical

connections are actively changing after a FEP, and this would be reflected in the patients' behaviour, for instance via changes in symptom severity or cognitive performance. Knowledge of normative maturational trajectories of the hippocampus and the rest of the cortex are outlined in the next section.

2.5. Maturational trajectories of hippocampus and cortex: implications for a FEP

The limbic lobe (including the hippocampus) and PFC both undergo pronounced developmental changes in adolescence (Crews et al. 2007). Accumulating evidence also suggests that these regions are dynamically changing and maturing even into the third and fourth decades of life, depending on the tissue type in question (for example, white matter typically has an even more protracted maturational course than gray matter, as mentioned in Section 2.3.3). These maturational changes may inform the behavioural changes happening in parallel after a FEP in late adolescence and early adulthood.

With respect to cortical thickness, a measure that has often been used to characterize maturational trajectories of the cortex over the lifespan, there is a well-described pattern of cortical thinning across nearly all cortical regions over adolescence and adulthood (Tamnes et al. 2010; Wierenga et al. 2014; Amlien et al. 2016; Walhovd, Fjell, et al. 2016). This process seems to be accelerated in schizophrenia, where studies of both childhood-onset and enduring schizophrenia patients have reported a steeper loss of gray matter with age compared to healthy controls (Rapoport and Gogtay 2011; Cropley et al. 2017). Alterations in subcortical structures have also been described in childhood-onset schizophrenia (Chakravarty et al. 2015), but surprisingly little is known about the trajectories of the hippocampus and closely linked limbic structures, such as the amygdala, in psychotic disorders. Existing studies also tend to pool all patients together in a

"case-control" manner; thus, it is unclear whether these (sub)cortical trajectories generalize to all patients, or are more pronounced in subsets of patients presenting with different types of symptoms, for instance patients with predominantly negative symptoms. This is explicitly addressed in the studies presented in Chapter 4.

Although there has been a relatively "gray-matter-centric" approach to the investigation of abnormalities in brain structural maturation in psychosis, it would be hard to deny the significant contribution of white matter, particularly myelin, when considering psychotic disorders as conditions of dysconnectivity. Gray and white matter maturational trajectories seem to be closely linked: as gray matter volumes decrease across development, white matter volumes increase. This may be due to the fact that the thickness of the myelin sheath encasing axons increases with age (Benes et al. 1994). The concurrent changes in gray and white matter volumes may also be due to myelination of intracortical fibers near the inner edge of the cortex (Salat et al. 2009; Rowley et al. 2015; Natu et al. 2018). These patterns of brain maturation exhibit heterochronicity that is important to consider in our investigation of maturational changes after a FEP; that is, different cortical regions exhibit different rates of maturation at different time periods in the human life span (Grydeland et al. 2019). This is largely due to the myeloarchitecture characterizing different brain regions; for instance, fronto-temporal regions of interest in the context of psychosis are *late-myelinating*, and tend to have thinner myelin sheaths. Thus, these regions are more vulnerable to insult in adolescence/adulthood (Bartzokis 2004), as mentioned in section 2.3.3. Myelin development also progresses in "waves" across the lifespan; a recent investigation pinpointed one particular stage where peak myelination occurred post-pubertally within cortical hub regions, i.e. association, insular and limbic cortices (Grydeland et al. 2019). This time period and set of brain regions precisely underscores the aims of this thesis, and further emphasizes the need for

integration of measures that might index the maturational trajectories of myelin. Thus, proxy measures of peri-cortical and hippocampal myelin content are incorporated into Chapters 5 and 6 to better understand potential aberrations in white matter maturation and their contributions to changes in negative symptoms.

Chapter 3 : Neuroimaging methods

We are fortunate to live in a technological era where various computational tools are available to process large amounts of data with little manual intervention. However, the integrity of our data outputs are reliant on the quality of the raw data itself. Thus, the topic of neuroimaging methods cannot be broached without first acknowledging the importance of good data and quality control procedures that can be adopted to ensure that data is prepared for subsequent processing steps. This is addressed in Section 3.1., integrating material from a commentary that was published in *Journal of Psychiatry and Neuroscience* (Makowski, Lepage, et al. 2019). In Sections 3.2 and 3.3, brief descriptions of commonly used MRI-derived metrics of the hippocampus and subcortical structures, cortex, and white matter underlying the cortical mantle are provided, emphasizing metrics that have often been employed in studies including patients with psychosis, and those that are relevant for this thesis. Section 3.2 includes a discussion on the importance of choosing the right toolbox for segmentation of subcortical structures, based on a publication in *Neuroimage* (Makowski et al. 2018). Section 3.3 introduces a novel measure of white-gray matter contrast at the inner edge of the cortex, which was compared against the oft-used measure of cortical thickness in a data-driven study using a cross-sectional sample of FEP patients, published in *Cerebral Cortex* (Makowski, Lewis, et al. 2019b). This paper serves as the precedent for the study included in Chapter 5. Finally, Section 3.4 introduces key graph theory concepts that underlie the foundation for methods presented in the last study of this thesis in Chapter 6.

3.1. Quality control of MRI data

Neuroimaging studies of psychiatric disorders often face the dilemma of how to handle patient head motion, a dilemma we are reluctant to confront. On the one hand, assembling a sufficiently large cohort for meaningful study is a painstaking process and there is a natural desire to use all data collected. On the other hand, many patient populations exhibit significantly increased motion in the scanner compared to healthy controls (Pardoe et al. 2016; Yao et al. 2017), suggesting that more scans must be excluded to obtain a clean enough sample for a significant result. Do common artefacts such as motion really make a difference in large samples and, if so, what should be done about it? Defining motion is deceivingly simple at the core but it has been surprisingly difficult for researchers to come to a consensus over the threshold of acceptable motion that can be tolerated within an MRI study. Moreover, it has become apparent that motion artefacts in neuroimaging research cannot be ignored (Havsteen et al. 2017). Both structural and functional imaging domains suffer from motion artefacts, where studies have highlighted that results obtained with the original sample, compared to a clean, quality-controlled subset of the data, yields significantly different effect sizes, and even different neuroanatomical substrates for interpretation. Recently, an editorial by Weinberger and Radulescu (2016) brought this issue to the attention of researchers in psychiatry, challenging the common interpretation of findings derived from case-control MRI studies as altered "neurobiology" in patients compared to controls. Instead, the authors urged the field to more critically and carefully acknowledge MRI-derived confounds, such as head motion, that may be clouding key findings in the literature.

Over a decade ago, Shaw and colleagues (Shaw et al. 2008) published a seminal study on the cortical thickness trajectories underlying normal development in a sample ranging from 3.5 to 33 years of age, and found predominantly non-linear relationships between cortical thickness and

age, with notable peaks within the first decade of life. However, the age window leading up to these peaks of cortical development encompasses an age group (i.e. 5-10 years of age) where children have been shown to exhibit the most movement in the MRI scanner (Greene et al. 2016). These confounds of movement provide a feasible explanation for the challenge in replicating these findings subsequently in independent samples (Lebel and Beaulieu 2011; Aubert-Broche et al. 2013; Tamnes et al. 2013; Mills and Tamnes 2014; Wierenga et al. 2014). Ducharme et al (2016) addressed such inconsistencies using a sample with similar age range as Shaw and colleagues (2008) but with the additional component of three levels of quality control: none, standard, and stringent. With increasing stringency of quality control (i.e. removal of more scans with motion), the reported non-linear cortical thickness relationships with age disappeared, and instead, predominantly linear relationships across most of the brain remained. Characterization of neurodevelopmental trajectories of white matter have also been of great interest and are similarly likely to be significantly influenced by motion. A recent investigation (Savalia et al. 2017) confirmed this sentiment, showing significant correlations between commonly reported diffusion metrics (i.e. fractional anisotropy and mean diffusivity) and age are weakened with increased motion estimates.

The above examples are convincing evidence that motion artefacts have a significant impact on structural imaging results, but why? As a simple point for comparison, motion in an MRI is akin to motion in any image taken with a camera: the higher degree of motion present, the more blurred and fuzzy the image will be. The basic physics underlying MRI data acquisition adds another layer of complexity to the effects of motion or head displacement in a resultant image. When a patient moves in the scanner, it is the spatial frequencies of the MR image, or *k-space*, that are perturbed. The errors introduced give rise to motion artefacts that are not localized but

propagate throughout the image (White et al. 2010; Havsteen et al. 2017) e.g. ghosting, ringing, blurring, etc. In both structural and functional imaging, these artefacts have downstream impact on all image-derived metrics, such as cortical thickness, regional volumes, or connectivity estimates. Further, what may be more disconcerting are the effects even subtle motion may have on image quality and subsequent interpretation of commonly used outcome measures, such as cortical thickness (Alexander-Bloch et al. 2016). Alexander-Bloch et al's (2016) work emphasized the idea that although our pipelines may have progressed to be able to handle just about anything, they do not necessarily bypass the subtle effects of "micromotion" or biased movements that ultimately may differentiate clinical populations from healthy individuals.

Cortical thinning and gray matter volume loss have been reported in many psychiatric disorders (for a relevant meta-analysis, see Goodkind et al (2015)), although it is difficult to disentangle the degree to which gray matter reductions are due to the underlying neurobiology of the disorder itself or due to motion. Yao and colleagues (2017) sought to find this answer in bipolar disorder and schizophrenia, finding that reduced surface area and cortical thickness do in fact characterize these psychotic disorders, albeit effect sizes are attenuated when taking head motion into account. One of the most comprehensive and largest investigations examining motion bias across clinical cohorts (i.e. ADHD, ASD, and schizophrenia) and different post-processing software was recently conducted by Pardoe et al (2016). This study used resting state fMRI acquisitions to inform the degree of movement present in T1-weighted images, and examined this quantitative metric of motion in the context of brain morphometry, namely cortical thickness, gray-white matter contrast, and gray matter/subcortical volumes. As expected, motion estimates were higher in all clinical populations compared to controls, and for the extreme ends of the age distribution (i.e. <20 years of age, and above 40 years). Intriguingly, cortical thickness and

measures of cortical contrast were more affected by motion than volumetry, although the latter was impacted to a greater degree by the choice of segmentation method. This paints a rather intricate and complex picture of the various levels by which motion may impact neuroimaging analyses of clinical cohorts, and underscores the importance of, at minimum, having a clear and consistent quality assurance protocol to exclude scans visibly affected by motion artefacts. Furthermore, given the manner by which different pipelines may handle motion, it is equally important to study thoroughly the processed outputs - successful runs may not always be linked to trustworthy results.

Quality control workflow

We have proposed a quality control workflow, which can serve as a framework for both prospective and retrospective datasets. This workflow is depicted in **Figure 3.1.** Details relevant to retrospectively collected structural MRI (mostly T1-weighted images) were employed for the datasets used in this thesis. Additional details can be found in Makowski et al (2019). Although there are many steps that can be taken to enhance quality of a neuroimaging dataset, sometimes a bad scan is just a bad scan, and it may be worthwhile to exercise the art of letting go in severe cases. Neuroimaging technology is developing quickly and it is reasonable to expect that better algorithms and solutions will be coming our way to handle the blurred edges in our scans. Until then, do not shy away from data cleaning; the rewards gained in validity are worth the loss of a few scans.

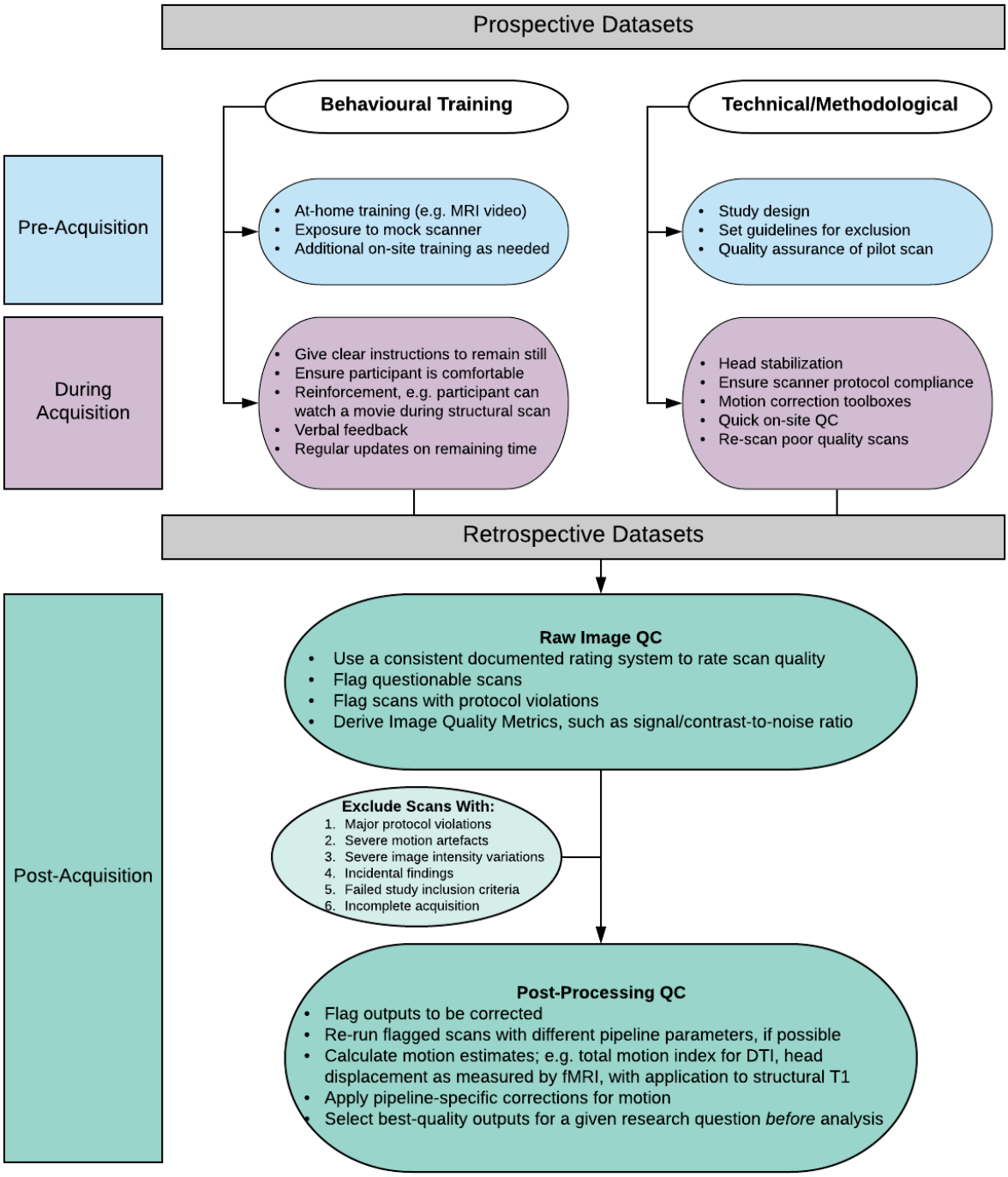

Figure 3.1. Proposed quality control workflow for MRI datasets.
Steps are proposed for both prospective and retrospective datasets. Please note this is designed as a simplified guide, and is not a comprehensive workflow for all modalities and clinical populations. Figure from Makowski et al (2019).

3.2. Limbic and subcortical structure

Accurate automated quantification of the hippocampus and other subcortical structures is a greatly pursued endeavour in neuroimaging, but poses a unique challenge due to contrast and resolution limitations in standard 1.5T and 3T T1-weighted acquisitions. While the field has observed an exponential growth of available tools to quantify brain structure with magnetic resonance imaging (MRI), and a parallel growth of collected samples and publicly available datasets (Marder 2015), manual segmentation is still considered the "gold standard" for quantifying structural volumes (Hammers et al. 2003; Prastawa et al. 2005; Gousias et al. 2012; Schoemaker et al. 2016). Many automated subcortical segmentation toolboxes exist to bypass the laborious and often infeasible efforts that manual segmentation entails. However, computer-generated results may still generate errors, both systematically and not, which need to be taken into consideration when choosing an automated segmentation toolbox. The next section includes text from a relevant investigation that was carried out, showing that the Multiple Automatically Generated Templates (MAGeT)-Brain algorithm more closely approximates manual segmentation of subcortical structures compared to two other commonly used pipelines, namely FreeSurfer and FSL. This investigation serves as the justification for using the MAGeT-Brain algorithm in subsequent chapters of the thesis (Chapters 4 and 6).

3.2.1. Choosing MAGeT: evaluating accuracy of subcortical segmentation.

As alluded to, automated methods are enthusiastically used in neuroimaging experiments. FreeSurfer (http://surfer.nmr.mgh.harvard.edu) (Fischl et al. 2002) and FSL-FIRST (http://fsl.fmrib.ox.ac.uk) (Patenaude et al. 2011) are two openly available pipelines that have been used by research groups around the globe to segment brain structures and extract subcortical

volumes. FreeSurfer uses probabilistic estimations based on Markov random fields to automatically assign a label to each voxel within an anatomical image based on a training set of previously manually delineated brains. FSL-FIRST also utilizes a probabilistic framework, and estimates boundaries of structures using information about signal intensity from the T1-weighted image, as well as applying knowledge of the expected shape of the structures. Several studies have compared FreeSurfer, FSL-FIRST and manual segmentation protocols on the same sample (Nugent et al. 2013; Pipitone et al. 2014; Grimm et al. 2015; Schoemaker et al. 2016), consistently finding that FSL and FreeSurfer tend to overestimate volumes compared to the "gold standard" of manually delineated labels. Furthermore, one study in Alzheimer's disease (Sánchez-Benavides et al. 2010) noted that methodological differences can be further exacerbated by the nature of the sample studied.

Given the wide variability in segmentation protocols and the limitations in localizing the precise location of changes within subcortical structures using volumetry, sophisticated methods have been developed to estimate surface morphometric measures of these structures (Chung et al. 2010; Raznahan et al. 2014; Sandman et al. 2014; Shaw, Sharp, et al. 2014; Chakravarty et al. 2015; Voineskos et al. 2015). These methods arguably provide complementary information alongside more conventional metrics of volumetry, and may also provide additional sensitivity in detecting finer changes between groups of interest (Chakravarty et al. 2015). Such approaches have been used in characterizing subcortical trajectories within normal development (Raznahan et al. 2014; Sussman et al. 2016), healthy ageing (Voineskos et al. 2015), neurological conditions (Miller et al. 2010; Magon et al. 2014; Caligiuri et al. 2016) and psychiatric disorders (Ballmaier et al. 2008; Ivanov et al. 2010; Shaw, Sharp, et al. 2014; Chakravarty et al. 2015). Subcortical structures (i.e. striatum, globus pallidus, and thalamus) are of particular interest in psychosis, given

their key role in the regulation of dopamine, a neurotransmitter widely disrupted in schizophrenia and psychotic disorders (Howes and Kapur 2009; Abi-Dargham and Meyer 2014). Subcortical morphometry has been explored at various stages of the disorder, including childhood-onset schizophrenia (Chakravarty et al. 2015), ultra-high risk samples (Dean et al. 2016), FEP (Mamah et al. 2012; Qiu et al. 2013), and chronic stages encompassing schizophrenia, bipolar disorder, and schizophreniform (Quigley et al. 2015; Mamah et al. 2016; Zhao et al. 2016). As morphometry is increasingly being incorporated into studies aiming to characterize biomarkers for such disorders, the field is faced with important choices regarding methodology that may have lasting impact on results.

To this end, we carried out an investigation comparing three fully-automated pipelines; namely FreeSurfer, FSL-FIRST, and MAGeT-Brain, and investigated potential differences and biases when comparing healthy controls to FEP patients (Makowski et al. 2018). Volumes of bilateral striatum, globus pallidus, and thalamus were automatically derived in a group of FEP patients and matched non-clinical controls, and compared to manual delineations. In summary, the basal ganglia and thalamus of thirty subjects (15 FEP, 15 controls) were manually defined and compared to the three automated methods. Our results suggest that all methods overestimate volumes compared to the manually derived "gold standard", with the least pronounced differences produced using MAGeT. The least between-method variability was noted for the striatum, whereas marked differences between manual segmentation and MAGeT compared to FreeSurfer and FSL emerged for the globus pallidus and thalamus. See **Figure 3.2**.

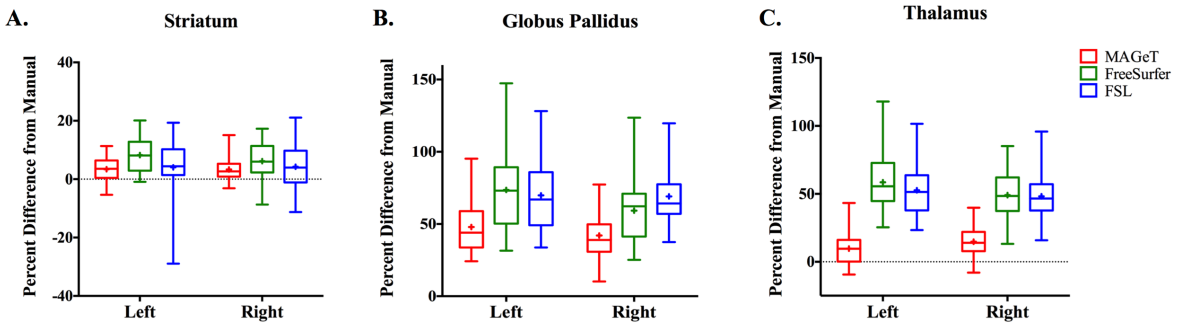

Figure 3.2. Box-whisker plots of percent volume difference between automated methods and manual segmentation.
Vertical lines of plots range from minimum to maximum values. Box plots mark 25th and 75th percentiles, with line in box marking median. The mean is marked with "+". A dotted line has been placed at y=0 for plots that have differences from manual that are negative (i.e. underestimated volumes relative to manual). A significant main effect of method was uncovered for all three panels. In Panel **A – Striatum**, FreeSurfer had significantly greater percent volume differences in relation to manual volumes compared to MAGeT and FreeSurfer ($p \leq 0.008$, corrected). In Panel **B – Globus Pallidus**, and Panel **C – Thalamus**, MAGeT had significantly smaller percent volume differences in relation to manual volumes compared to FreeSurfer and FSL ($p < 0.0001$, corrected).

Correlations between manual segmentation and automated methods were strongest for MAGeT (range: 0.51 to 0.92; $p < 0.01$, corrected), whereas FreeSurfer and FSL showed moderate to strong Pearson correlations (range 0.44-0.86; $p < 0.05$, corrected), with the exception of FreeSurfer pallidal ($r = 0.31$, $p = 0.10$) and FSL thalamic segmentations ($r = 0.37$, $p = 0.051$). Bland-Altman plots highlighted a tendency for greater volumetric differences between manual labels and automated methods at the lower end of the distribution (i.e. smaller structures), which was most prominent for bilateral thalamus across automated pipelines, and left globus pallidus for FSL (See **Figure 3.3**).

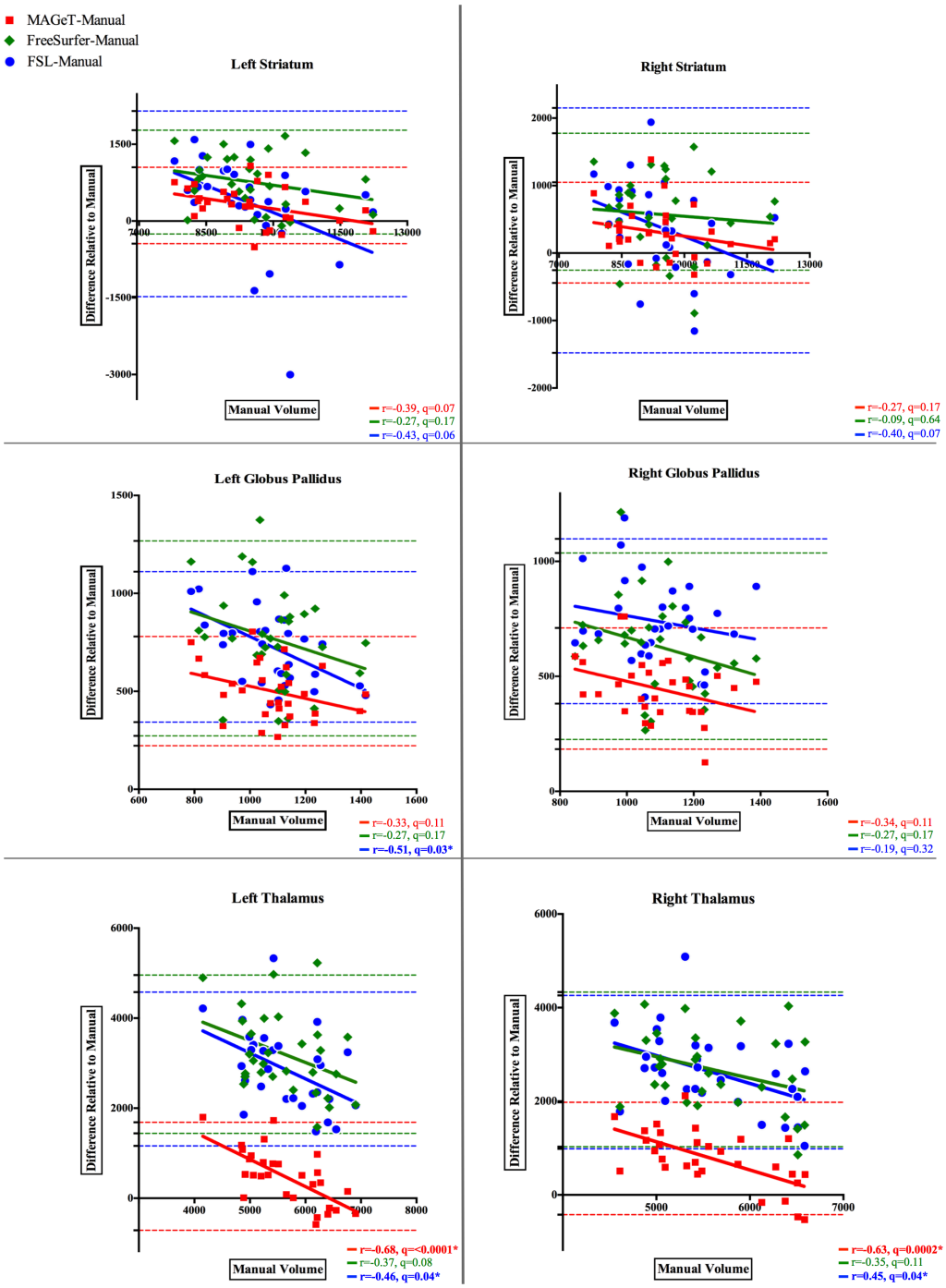

Figure 3.3. Bland-Altman plots, comparing volume differences between each automated method and manually derived volumes, against manual volumes.
Regression lines have been fit to the data for each automatic method to visualize potential biases. Confidence intervals are marked by horizontal dotted lines and colour-coded by method (Red=MAGeT, Green=FreeSurfer, Blue=FSL). Significant regression slopes after false discovery rate (FDR) correction are bolded with an asterisk.

This study provided a detailed analysis of how manual segmentations of the basal ganglia and thalamus compare against three automated segmentation pipelines, namely MAGeT, FreeSurfer, and FSL, in the clinical investigation of changes in the subcortical structures in first episode psychosis patients. Our results highlighted the closer correspondence between manual segmentations and volumes obtained with MAGeT, compared to those obtained with commonly used toolboxes provided by FreeSurfer and FSL. Our results also pinpointed inherent biases within all automated segmentation tools included in this investigation, especially for volumes skewed towards the lower end of the distribution. Similar biases have been found with FreeSurfer and FSL compared to manual segmentation when investigating hippocampal and amygdalar volumes (Schoemaker et al. 2016). With these results in mind, we felt more confident to pursue further image processing of hippocampal and subcortical structure with MAGeT-Brain, but still employed rigorous quality control procedures to ensure only good quality outputs were retained for analysis.

3.2.2. Hippocampal-amygdalar volumetry and shape morphometry

Volumetry and shape morphometry (i.e. localized measures of surface area) of the hippocampus and amygdala are utilized in Chapter 4, to better understand the maturational trajectories of these limbic structures in FEP patients with persistent negative symptoms. The entire hippocampal formation for left and right hemispheres, as opposed to individual hippocampal subfields, were considered for Chapter 4, given the limited ability to resolve hippocampal subfields with data from a 1.5T scanner. However, for Chapter 6, a sub-millimetric T2-weighted scan was acquired on a 3T scanner, allowing us to more accurately resolve hippocampal subfields and surrounding white matter. Both Chapters 4 and 6 use the same MAGeT-Brain algorithm, but with different input atlases.

The workflow for MAGeT-Brain image processing proceeds as follows. Raw T1-weighted or T2-weighted scans are submitted to the MAGeT-Brain pipeline, based on a multi-atlas segmentation approach. This technique utilizes a limited number of high-resolution atlases that have been manually segmented. For Chapter 4, atlases described previously for the amygdala (Treadway et al. 2015) and hippocampus (Winterburn et al. 2013) (https://github.com/CobraLab/atlases) are utilized and are applied to structural T1-weighted acquisitions (1mm^3). Chapter 6 utilizes sub-millimetric T2-weighted scans (0.64mm^3) and an atlas described in Amaral et al (2018), which outputs 9 structures per hemisphere: hippocampal subfields CA1, CA2/3, CA4/dentate gyrus, subiculum, and molecular layer; and output white matter regions: alveus, fimbria, fornix, and mammillary body. Segmentations are extracted from pre-defined high resolution atlases onto a library of subjects. Labels from the atlases are then propagated to a subset of 21 subjects (templates) from the neuroimaging study, a number shown to be optimal in previous work (Pipitone et al. 2014). The templates chosen for both the 1.5T and 3T datasets comprise a representative mix of eleven FEP patients and ten controls, and an approximately equal male to female ratio. Customization of atlas labels to templates is conducted using a nonlinear transformation with a version of Automatic Normalization Tools (ANTS) compatible with the minc-toolkit (https://github.com/vfonov/mincANTS). Next, a bootstrapping procedure is applied to final segmentations. Candidate labels are fused for each subject using a majority vote procedure (i.e. the label occurring most frequently at a specific location is retained) (Collins et al. 1995; Chakravarty et al. 2013).

To determine shape of limbic structures as presented in Chapter 4, surface-based representations of the amygdala and hippocampus are defined separately on the basis of the input atlas, using the marching cubes algorithm (Lorensen and Cline 1987), and morphologically

smoothed using the AMIRA software package (Visage Imaging; San Diego, CA). The resulting surfaces have approximately 1200 vertices per amygdala and 1400 vertices per hippocampus. Nonlinear transformations required to map each participant to the input template are concatenated and averaged across the 21-subject template library to increase the signal to noise ratio (Borghammer et al. 2010). Using a similar logic as was used to extract volumes, surface-based representations are warped to fit each template, and subsequently to match each participant. This yields 21 possible surface representations per participant. To ensure homology between vertices to prior MAGeT-Brain segmentations, surface vertices are redefined using a Vornoi diagram (Lyttelton et al. 2009). The median coordinate at each location/vertex of the amygdala or hippocampus are estimated to yield a single cohesive surface representation of each structure. Finally, surface area is represented as the sum of the surface area for each polygon in the surface, and all surface area values are blurred with a surface-based diffusion smoothing kernel of 5mm for both structures. See **Figure 3.4** for example segmentations of the hippocampus and amygdala for a representative candidate, and **Figure 3.5** for an overlaid mesh on the hippocampus/amygdala model (https://github.com/CobraLab/atlases) depicting the vertices used in surface area analysis. **Figure 3.6** depicts the hippocampal subfields and output white matter atlas used in Chapter 6.

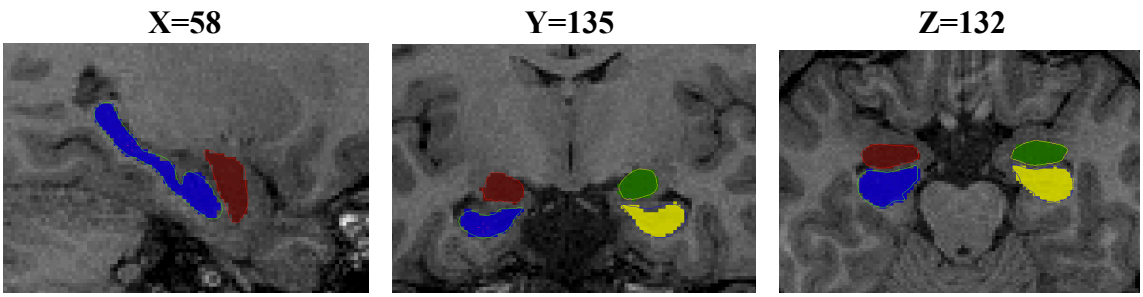

Figure 3.4. Example segmentation of bilateral hippocampus and amygdala using the MAGeT-Brain algorithm.
Legend: Blue, Left hippocampus. Yellow, Right Hippocampus. Red, Left Amygdala. Green, Right Amygdala. Corresponding surfaces are outlined around each label. X, Y, and Z coordinates listed above each image corresponding to section in sagittal, coronal, and horizontal views in MNI standard space, respectively.

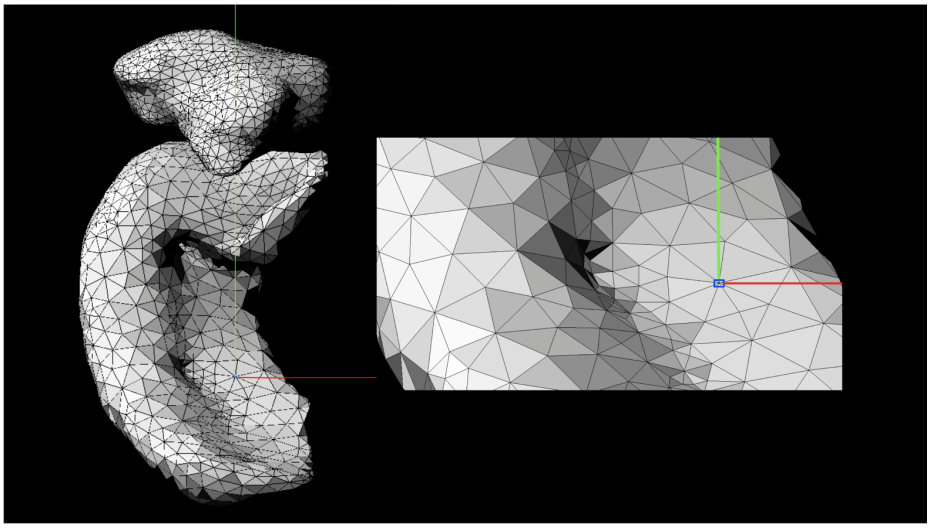

Figure 3.5. Depiction of morphological branch of MAGeT for surface area extraction.
Three-dimensional mesh overlaid on a model surface of the amygdala and hippocampus, allowing for extraction of vertex-wise surface area information. The dorsal view of the left amygdala and hippocampus is depicted on the left. The right is a magnified version to better visualize the polygons comprising one particular vertex, with the crosshairs pinpointing the same vertex in both images.

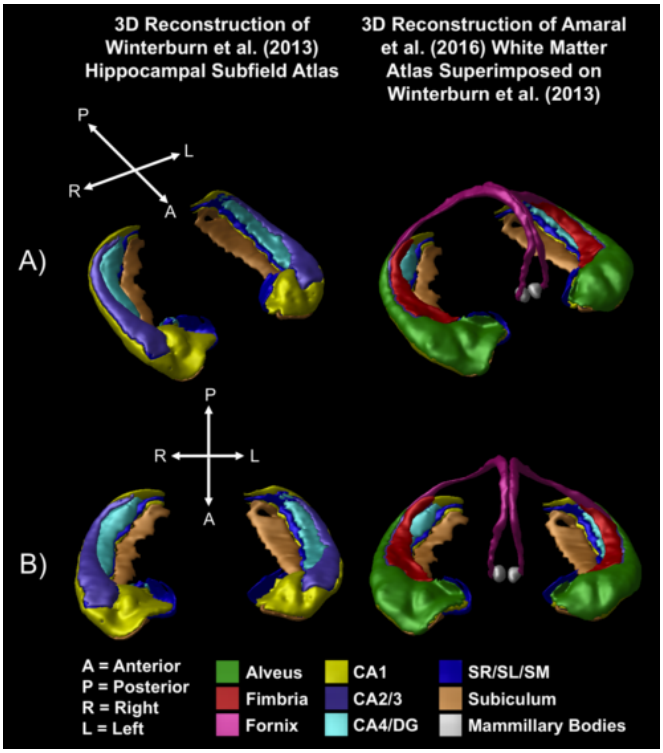

Figure 3.6. Three-dimensional rendering of hippocampal subfields and output white matter.
Abbreviations: CA, Cornu Ammonis. SR/SL/SM, stratum radiatum/lacunosum/moleculare, or the "molecular layer" of the hippocampal formation.
From: Amaral et al. (2018)

3.3. Measures sampled along the cortical surface

3.3.1. Cortical thickness and comparison with other commonly-derived cortical metrics

Cortical regions of interest can be broadly divided into gray (e.g. neuronal cell bodies or soma) and white matter (e.g. axonal tracts). As mentioned in Section 2.5, arguably more studies have focused on gray matter-centric measures in investigations of gross brain abnormalities differentiating patients from controls. Many of these early investigations used measures of gray matter volume, which was later found to be a composite measure of cortical thickness and surface area. The notion of the relative contribution of cortical thickness and surface area to cortical volume was important as it provided the potential to further dissect underlying biological mechanisms, given that cortical thickness and surface area have unique genetic contributions and maturational trajectories (Panizzon et al. 2009). Specifically, MRI-derived cortical thickness is defined as the distance between the gray-white matter boundary and the outer pial surface, and is a consequence of asymmetric division of progenitor cells from the subventricular zone in development. Surface area, on the other hand, is a result of symmetric division of these progenitor cells and seems to be more heavily genetically mediated compared to cortical thickness. Thus, cortical thickness may be more likely to change with various environmental factors through development and brain maturation, that would not be reflected in a similar fashion with surface area. This is also concordant with what we know of the hippocampus, which is also largely malleable by external/environmental factors.

Cortical thickness is of particular interest to this thesis, as it is used as a measure of interest in both chapters 4 and 5. See **Figure 3.7** for a depiction of MRI-based cortical thickness, and how it is sampled across the entire brain, using the CIVET pipeline. Cortical thickness has often been described as a composite measure of synaptic density and integrity of cell body architecture

throughout the six layers of the cortical mantle; however, newer interpretations of cortical thickness have taken into consideration the contribution of white matter to cortical thickness measures, which is further discussed below.

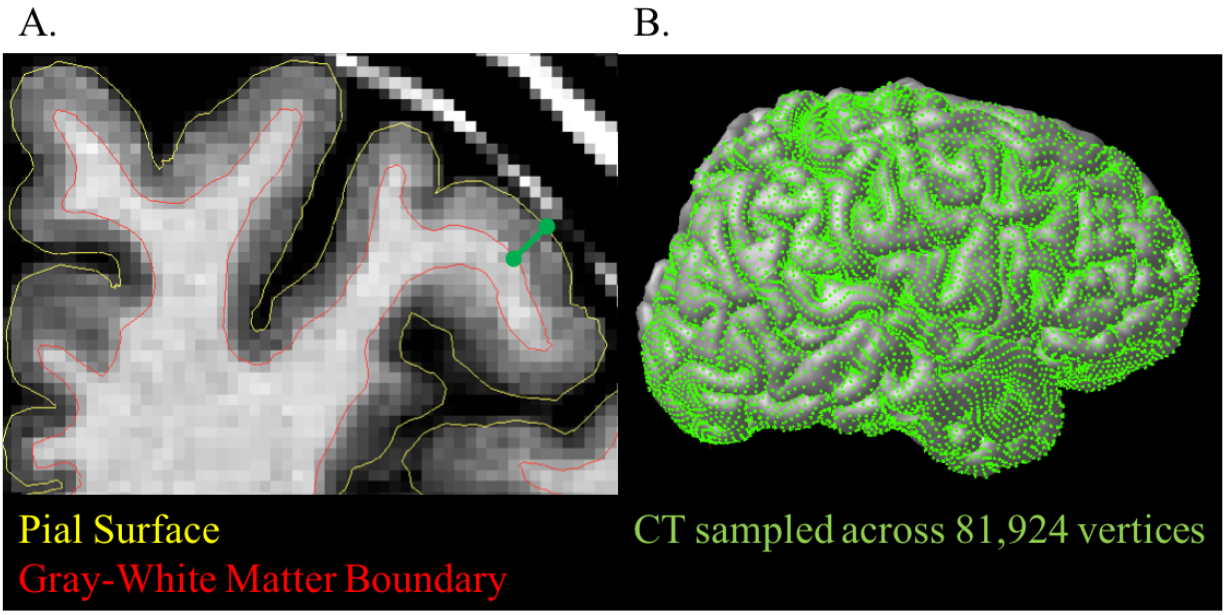

Figure 3.7. MRI-based cortical thickness.
This measure is derived from the CIVET pipeline developed at the McConnell Brain Imaging Centre of the Montreal Neurological Institute. Panel A shows a snapshot of a coronal slice on a T1-weighted MRI scan, outlining pial and gray-white matter boundary surfaces. Cortical thickness (CT) is defined as the distance between these two surfaces (green line joining surfaces in Panel A), sampled from 81,924 points or vertices across the cortical surface (green points in Panel B).

3.3.2. Cortical White-Gray Matter Contrast (WGC)

The major source of tissue contrast found in structural MRI scans comes from myelin, the fatty and protein-rich outer sheath that encases axons, and orchestrates the speed of conduction of neuronal signals throughout the brain. MRI-derived cortical thickness relies on the tissue intensity contrast between gray and white matter, and gray matter and cerebral spinal fluid in T1-weighted structural MRI. However, it has often been overlooked that the placement of the gray-white matter boundary on MRI is driven by the myeloarchitecture (that is, the patterns of myelin content) both intracortically and within superficial white matter (Rowley et al. 2015).

Obtaining a measure of white-gray matter contrast (WGC) from T1-weighted MRI may provide a meaningful marker of myelin content and other biophysical properties that may complement measures of MRI-based cortical thickness, as well as confer sensitivity in detecting subtle group differences that are relevant for the current investigation of FEP patients (Bezgin et al. 2018; Lewis et al. 2018). In Makowski et al (2019b) and in Chapter 5, additional surfaces surrounding the gray-white matter boundary were generated to estimate WGC across the same 81,924 points for which cortical thickness was estimated. See **Figure 3.8** for a depiction of this method.

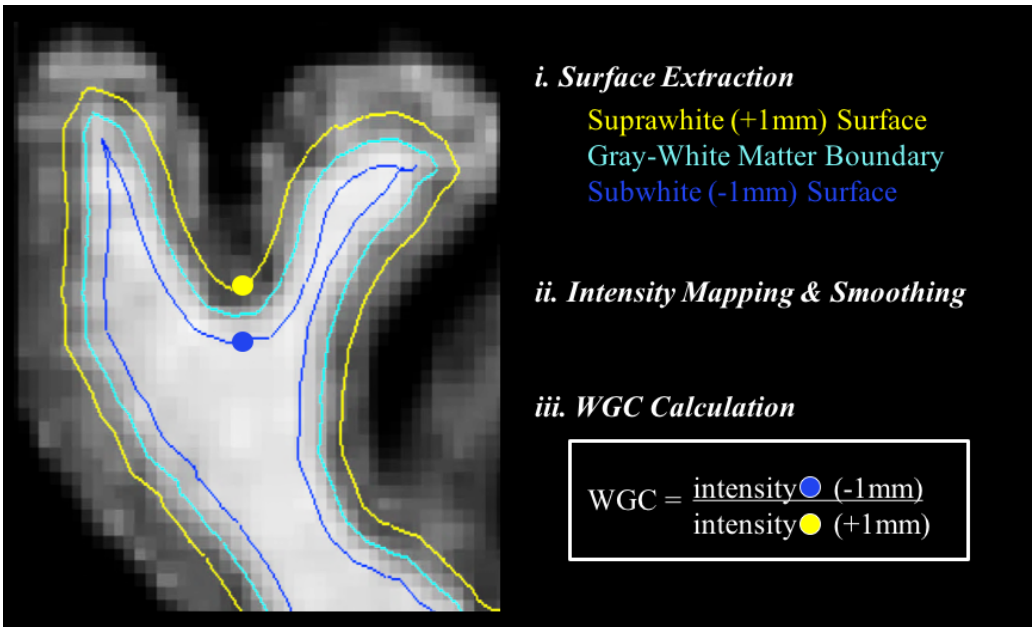

Figure 3.8. MRI-based white-gray contrast (WGC).
Illustration of 3 key steps in calculation of WGC. Method was initially presented in Lewis et al (2018) and also applied by our group recently to a cross-sectional FEP cohort (Makowski, Lewis, et al. 2019b). Left-hand panel is an example of a T1-weighted image from a participant included in this thesis, with the gray-white matter boundary and +/-1mm surfaces overlaid, as defined in Step i. Surfaces maps of the intensity of the T1-weighted MRI were then generated and smoothed with a 20mm blurring kernel (Step ii). Smoothing is done for both the -1 and +1mm surfaces before calculation of WGC (Step iii). One example vertex is identified to illustrate calculation of WGC (Step iii). Note, in some areas the surfaces do not appear to be consistently 1mm from the gray-white matter boundary; this is because a 2D visualization of the surfaces is depicted here, without taking into consideration the third dimension of the T1-weighted image.

Given that white-gray matter contrast may capture myelination properties within the cortex and superficial white matter, it is feasible that this metric may be more sensitive in capturing the extent of disruptions in the coordinated development and plasticity of cortico-cortical connections in early psychosis compared to cortical thickness. We explicitly tested this hypothesis in a recently published paper, where we showed that indeed, WGC recapitulated architectonic features of the brain and was more sensitive in detecting aberrant structural associations across the brain of FEP patients compared to cortical thickness (Makowski, Lewis, et al. 2019b).

In this investigation, we used Principal Component Analyses (PCA) to reduce dimensionality of cross-sectional WGC and CT data, and to extract patterns of features across brain regions that may share common information, without fitting a specific model *a priori.* The *SurfStatPCA* function[3] was applied to WGC and CT values for 116 FEP patients and 88 Controls at each of 81,924 vertices per subject, after regressing out age and sex. Relationships between selected component loadings and the following behavioural measures in FEP patients were assessed with Pearson correlations, and corrected for multiple comparisons with a Bonferroni correction: a) positive and negative symptoms, as assessed by the SAPS and SANS, respectively; b) general cognitive index (GCI), excluding social cognition; and c) three measures tapping into higher-order cognitive processes: verbal memory, executive function, and working memory.

In summary, we demonstrated that WGC clustered brain regions into unimodal (e.g. primary visual, somatosensory, and motor regions) and heteromodal cortices. This could indeed be driven by the differing levels of cortical myelin underlying these regions. Our results with WGC in FEP patients suggest that pericortical myelin may be a sensitive marker of abnormalities in cortico-cortical connections, even in early phases of psychotic disorders, and such network-level

[3] http://www.math.mcgill.ca/keith/surfstat/doc/SurfStat/SurfStatPCA.html

abnormalities are meaningfully related to symptom severity and cognitive ability. The same extent of significant brain-behaviour relationships was not found with cortical thickness (**Figures 3.9** and **3.10**).

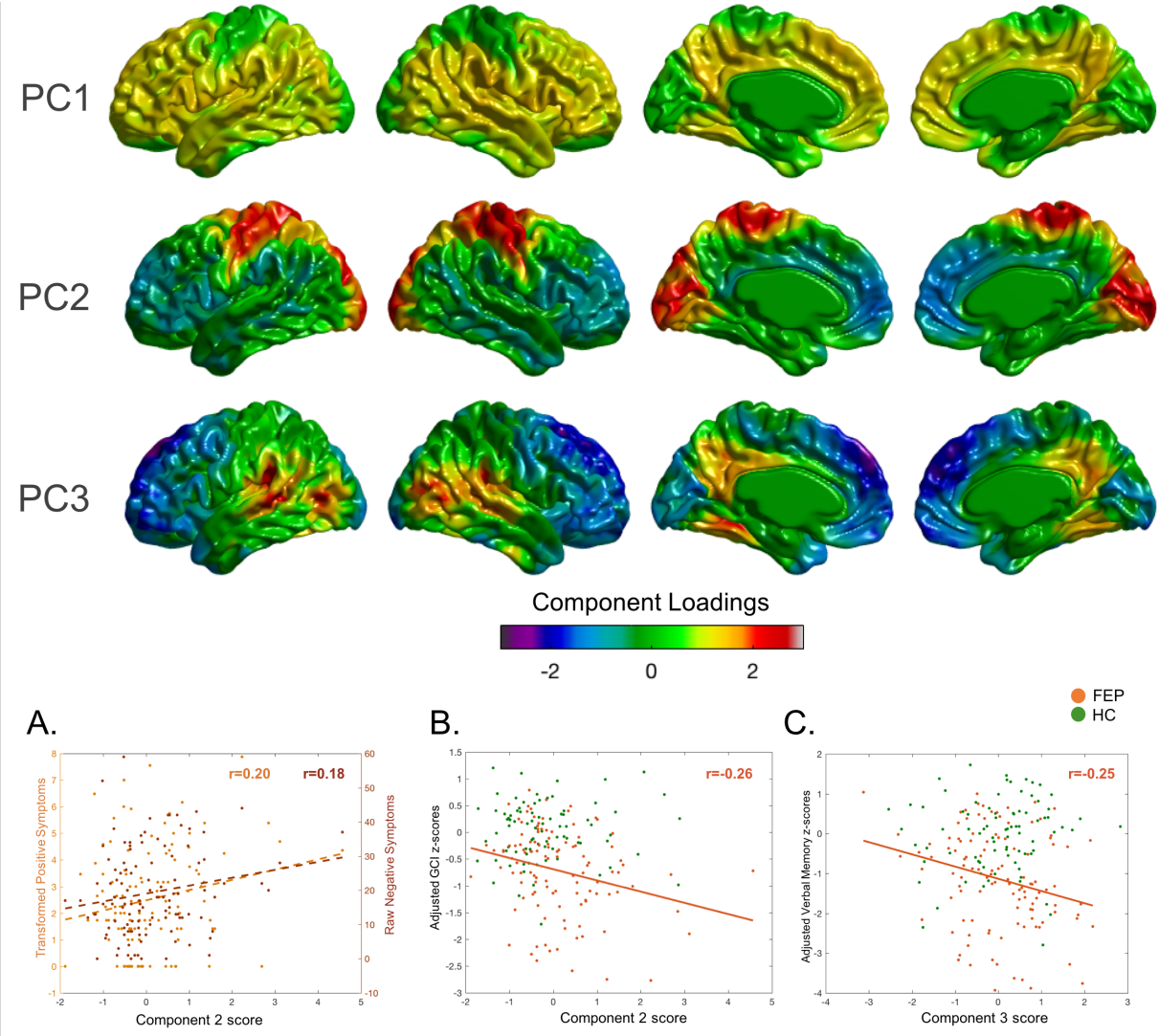

Figure 3.9. Top 3 components from PCA with WGC data and brain-behaviour relationships. Cortical surface maps reflect component loadings for each principal component (PC). PC1 reflects mean WGC signal (Makowski, Lewis, et al. 2019b). PC2 captures primary sensory and motor regions, that are associated with positive and negative symptoms (Plot A) and a general cognitive index (GCI; Plot B) in FEP patients. PC3 captures bilateral superior temporal sulci and heteromodal cortical regions, associated with verbal memory performance in FEP patients (Plot C). Association of principal component 2 with both positive and negative symptoms are presented together in Plot A, with lighter orange reflecting association with positive symptoms (note they

are square root transformed) and dark orange for negative symptoms (not transformed). For all other plots, relationships are represented in orange for patients, and compared to controls in green. A solid line is drawn for significant associations that remain significant after correction for multiple comparisons, and a dashed line represents nominally significant associations for $p<0.05$, uncorrected. The general cognitive index is significantly and negatively associated with FEP patients' component scores on principal component 2, whereas positive and negative symptoms are nominally and positively associated with this component. Finally, verbal memory is significantly and negative associated with FEP patient's component scores on principal component 3. This latter relationship also holds when covarying for antipsychotic medication ($r=-0.26$, $p=0.0056$).

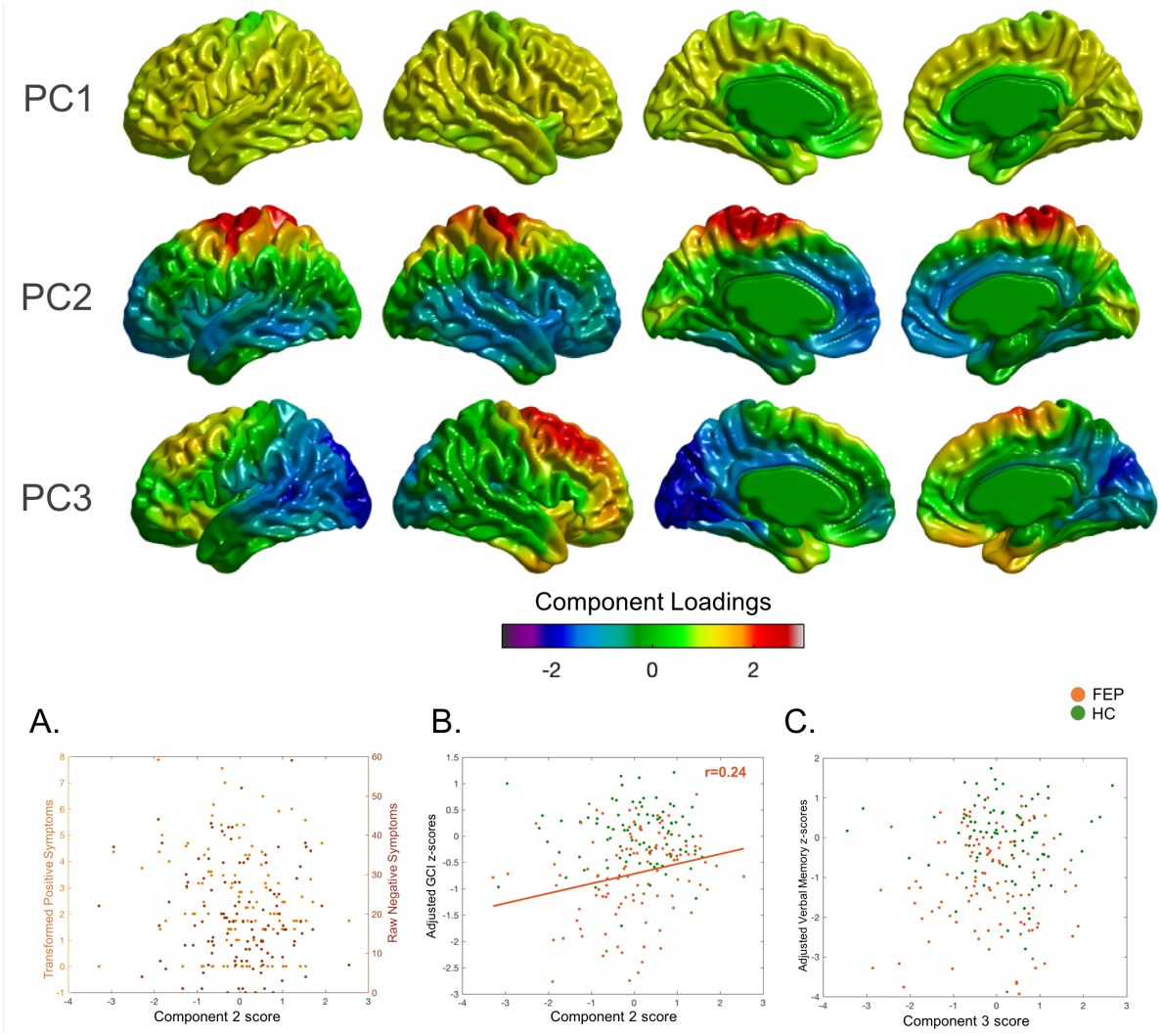

Figure 3.10. Top 3 components from PCA with CT data and brain-behaviour relationships. Cortical surface maps reflect component loadings for each principal component (PC). PC1 reflects mean CT signal (see Supplementary Figure 3). PC2 captures positive loadings on dorsal primary motor regions, and weak negative loadings in frontal-insular-temporal regions. For direct

comparison to results presented for WGC in Figure 1, we show here that positive/negative symptoms were not associated with component 2 derived from CT data (Plot A), but a nominal association was found between component loadings and a general cognitive index (GCI; Plot B) in FEP patients. PC3 captures positive loadings on right prefrontal cortex and negative loadings on occipital cortices bilaterally. Association of principal component 2 with both positive and negative symptoms are presented together in Plot A, with lighter orange reflecting association with positive symptoms (note they are square root transformed) and dark orange for negative symptoms (not transformed). For all other plots, relationships are represented in orange for patients, and compared to controls in green. A dashed line represents nominally significant associations for $p<0.05$, uncorrected. There was only a significant relationship between FEP patients' GCI and component scores on principal component 2.

This study extended the notion that psychosis is a disorder of dysconnectivity, by showing that systems-level aberrations are already present in early psychosis. WGC seems to be a promising biomarker alongside measures of cortical thickness, tapping into a compartment of tissue that may be better captured and more malleable in disorders such as psychosis. This foundational paper fueled the study presented in Chapter 5, which extends these methods to more clinically-oriented questions of the neural correlates underlying negative symptoms and verbal memory. However, it is acknowledged that our measure of WGC does not allow us to disentangle the primary source of change in white matter alterations (i.e. within intracortical layers or superficial white matter). Standard T1-weighted acquisitions suffer from strong scanner field biases, which makes it very difficult to interpret gray and white matter intensities separately. Thus, Chapter 6 extends this methodology, and uses quantitative T1 mapping to come closer to disentangling the source of microstructural changes.

3.3.3. Quantitative T1 imaging

MRI methods have quickly progressed to better resolve anatomical detail in the brain, primarily with the use of stronger magnets. This thesis captures such methodological progress, as we move from using data from a 1.5T scanner in Chapters 4 and 5, to a 3T magnet in Chapter 6. However,

the use of higher strength magnets (e.g. 3T or greater) comes with an important tradeoff: images are acquired with higher resolution but are more susceptible to bias fields; that is, more inconsistencies or inhomogeneities in tissue contrast are captured. This makes it challenging to measure any properties of brain tissue directly, and requires appropriate pre-processing steps to minimize the effects of such bias field inhomogeneities and other confounds such as proton density, which are captured with conventional T1-weighted MRI.

The use of a quantitative T1 map provides a great advantage over standard T1-weighted structural MRI acquisitions, where a precise bias-free T1 relaxation time can be extracted for every voxel in the brain (Marques et al. 2010). The T1 relaxation time is a key biophysical property that gives rise to the contrasts we see in T1-weighted images. The physical mechanisms underlying the T1 relaxation time is depicted in **Figure 3.11**. During MRI acquisition, a radio frequency (RF) excitation pulse is emitted from the scanner, which will cause hydrogen protons to spin perpendicular to the magnetic field, which causes a change in the net magnetization vector. After the RF pulse is turned off, the excited hydrogen nuclei will return to a relaxed state. The length of time that it takes the signal to reach 63% of its initial pre-excitation value is defined as the T1 relaxation time.

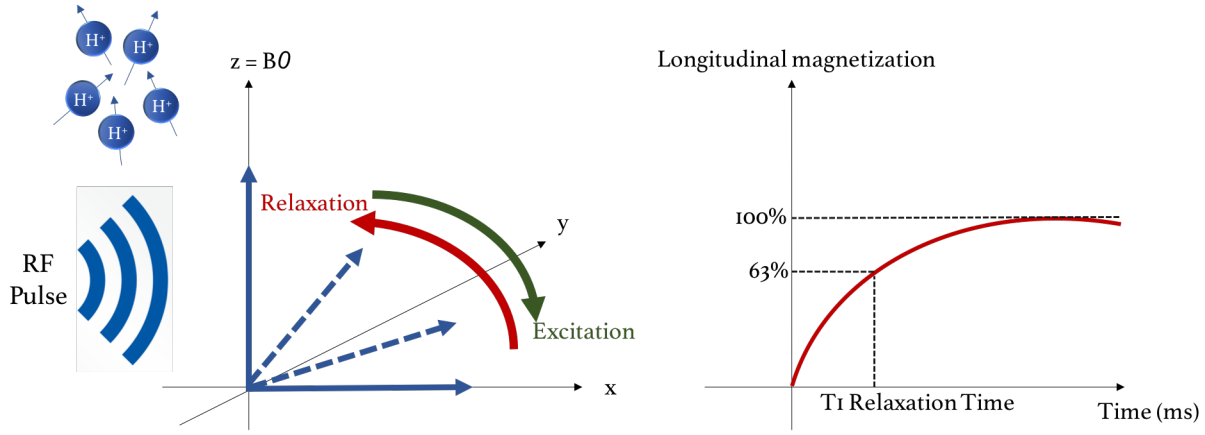

Figure 3.11. Schematic of the magnetic resonance principles underlying the T1 relaxation time.

Chapter 6 utilizes the strengths of quantitative T1 mapping from a novel MP2RAGE sequence, which acquires two different structural images at slightly different inversion times, thus producing an image free of proton density contrast and bias field inhomogeneities (Marques et al. 2010). See **Figure 3.12** for a depiction of the T1 relaxation times underlying different tissue types within the brain. The relaxation times acquired at each voxel can then be directly compared between subjects and across timepoints.

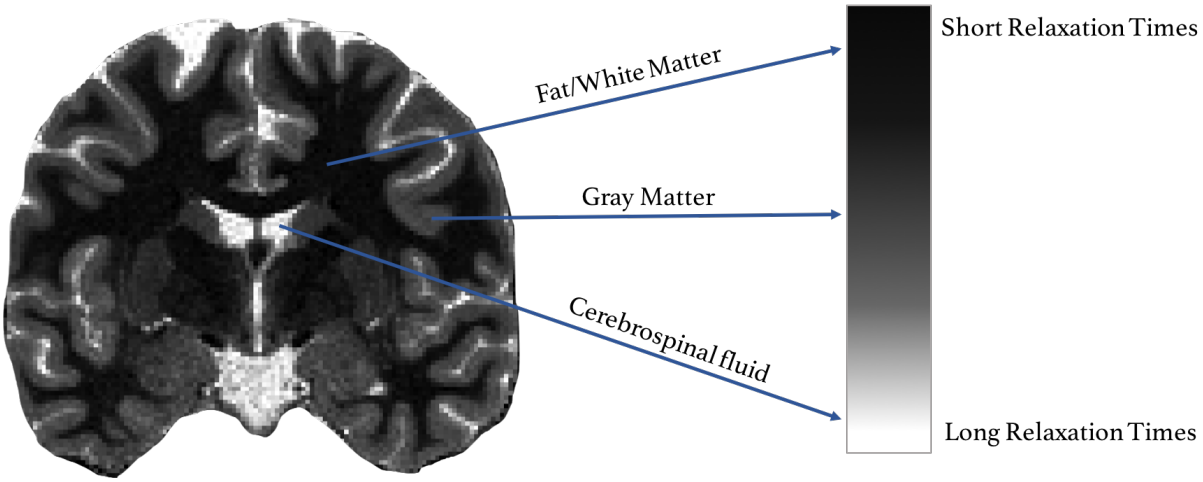

Figure 3.12. Quantitative T1 values across brain tissue types.
One coronal slice from the quantitative T1 map of an MP2RAGE sequence is depicted (Marques et al. 2010). Short relaxation times are characteristic of tissue that contain more myelin, e.g. white matter, and appear darker on the image. Gray matter appears brighter and is characterized by longer relaxation times.

Quantitative T1 mapping has been shown to be a candidate marker of myelin content and integrity (Laule et al. 2007; Deoni 2010; Dinse et al. 2015). This positions quantitative T1 mapping as an ideal MRI-based measure of microstructure for the aims of Chapter 6. Network-based measures derived from such quantitative T1 maps also have the potential to better define a microstructural connectome and its alterations in patients with psychosis. Indeed, a recent investigation of brain networks derived from intracortical quantitative T1 values supported the idea that this measure

captures connectivity information that recapitulates information carried within both structural and functional networks, over and above what cortical thickness is able to infer (Huntenburg et al. 2017). This is also supported by our recent investigation in Makowski et al. (2019b), where measures based on a putative marker of peri-cortical myelin/microstructure are better able to detect differences at the brain network level than cortical thickness.

3.4. Graph theory measures of centrality

As described in Section 2.3.4., there has been a concerted push to better understand the structural connectome of psychosis across various stages of the disorder. Recall that the connectome is a representation of different brain regions (i.e. nodes) and the relationships or connections between regions (i.e. edges) (Sporns et al. 2005). The connectome inherently captures a complicated web of relationships within the human brain. Thus, derivation of summary metrics describing the organization of such connectomes are important to better interpret differences in brain organization between patients and controls and to link individual differences in behaviour to global patterns of brain connectivity. Graph theory methods are harnessed by the study presented in Chapter 6, to specifically test the hypothesis of altered hippocampal centrality in relation to negative symptoms after a FEP. The primary measure of interest in Chapter 6 is the participation coefficient. **Figure 3.13** illustrates the measures required to calculate the participation coefficient of a node or set of nodes (i.e. module) of interest.

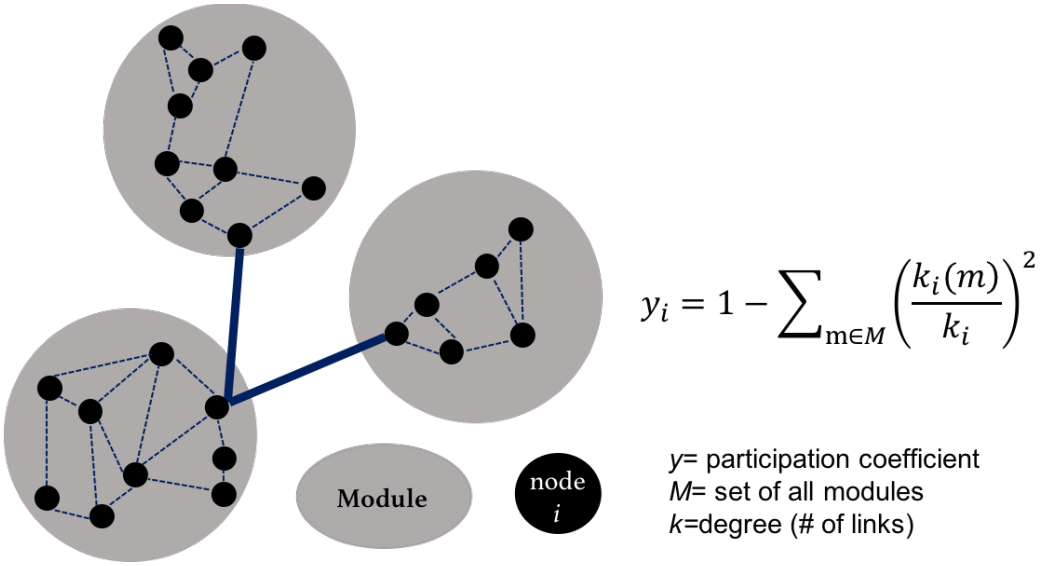

Figure 3.13. Calculation of the participation coefficient in brain networks.
Left-hand side shows a schematic of the components of a network that make up the measure of participation coefficient. Measures that can be obtained from any type of network data. For brain imaging applications, the smaller circles in the image represent individual brain regions, and the lines represent connections that describe the links between different regions (e.g. "connectivity" derived from structural covariance, diffusion weight imaging, etc.). Larger gray circles envelop brain regions within the same module. Links can be found both within communities of brain regions or "modules" (dashed lines) or between modules (solid lines). The formula and variables used to calculate participation coefficient are defined on the right-hand side of the figure.
Figure adapted from Cohen & D'Esposito (2016), and calculation of participation coefficient from Rubinov & Sporns (2010).

As can be seen from **Figure 3.13**, calculation of the participation coefficient relies on degree and the definition of modules. Degree is simply the number of connections each node has. Modules are sets of nodes that are more highly connected to each other compared to other sets of nodes. In the context of brain networks, each module may have a circumscribed role in brain function, for instance in sensory processing, and quick communication between regions within one module are critical for efficient information processing. However, such perceptual or cognitive processes rely on integration of information from other modules; thus, it is still important for each module to have one or more brain regions that facilitate inter-modular communication. This measure is of particular interest in light of the aims of this thesis, to characterize the centrality of communication

between the hippocampus and other cortical networks. This can be tapped into by the participation coefficient, which reflects the distribution of connections of brain regions within a particular module (in our case, the hippocampal circuit), in relation to brain regions of other modules (i.e. neocortical networks). A node with a high participation coefficient suggests that node has high intermodularity, i.e. it is more highly coupled or 'connected' to nodes of other modules, whereas a node with a low participation coefficient is less connected to nodes of other modules.

Chapter 4 : Hippocampal-cortical maturational trajectories differentiate FEP patients with persistent negative symptoms

PREFACE

This chapter includes the first pair of longitudinal neuroimaging studies that were published with nearly the entire sample of a study funded by the Canadian Institutes of Health Research (CIHR), which started in 2004. Specifically, this work sought to better understand the longitudinal trajectories that differentiate FEP patients with persistent negative symptoms (PNS) compared to their non-PNS peers. The categorization of patients with PNS holds clinical significance as this group of patients have a particularly challenging clinical course, and available treatments today are not effective in diminishing these symptoms, which has profound consequences on the daily functioning of affected patients. In fact, the NIMH released a statement that PNS currently represent an unmet therapeutic need, emphasizing the urgency of better understanding the biological underpinnings of these symptoms (Kirkpatrick et al. 2006). This work was a natural extension of the work done by three previous PhD students in Dr. Lepage's group: Dr. Cindy Hovington, who empirically defined PNS, and began investigating the white matter neuroanatomical correlates of patients with PNS cross-sectionally; and Dr. Audrey Benoit and Dr. Michael Bodnar, who investigated neuroanatomical gray matter correlates of PNS cross-sectionally, including volumes of the amygdala and hippocampus, and cortical thickness.

In addition to being the first series of work in the literature that examined the longitudinal progression of PNS at the neural level after a FEP, we also used novel neuroimaging techniques to more accurately map underlying neuroanatomical trajectories potentially separating PNS patients from other FEP patients. For the first manuscript investigating limbic trajectories, we used a new segmentation algorithm, MAGeT-Brain, from Dr. Chakravarty's group to investigate both

hippocampal and amygdalar volumes and shape morphometry. We opted to include the amygdala alongside the hippocampus, given its neuroanatomical proximity to the hippocampus, and well-established connections to the hippocampus and prefrontal regions, which may underlie the emotional dysregulation characteristic of negative symptoms. Although volumes of the amygdala and hippocampus have been a popular measure of choice when investigating these structures, the addition of a more fine-grained surface morphometric approach allowed us to localize potential anatomical changes along specific points of these structures, akin to what we can do with surface-based approaches of the cortex. It has also been argued that surface morphometry, such as surface area, of subcortical structures may be more indicative of neurodevelopmental or maturational processes, compared to volumes alone (Chakravarty et al. 2015). With respect to cortical thickness, we applied a newer version of the CIVET pipeline which incorporated a "marching cubes" algorithm (Lorensen and Cline 1987), to more accurately extract white matter surfaces, and ultimately, to provide us with a more accurate estimation of cortical thickness.

Another important contribution of this work was the specificity of findings to patients with primary/early PNS, as opposed to patients that present with PNS due to secondary factors. Thus, the two papers below include categories for both "early" PNS (patients who present with predominantly high levels of PNS, in the absence of other potentially confounding symptoms) and "secondary" PNS (patients who present with other potentially confounding symptoms like positive and/or depressive symptoms). This work highlights the importance of looking at age in early psychosis samples, given that a FEP occurs during a critical period of neurodevelopment (i.e. late adolescence/early adulthood), and suggests a promising avenue for future research to investigate dynamic endophenotypes of early PNS.

4.1. Maturational trajectories of hippocampal-amygdalar morphometry

Linking persistent negative symptoms to amygdala-hippocampus structure in first episode psychosis

Carolina S. Makowski[1,2], Michael Bodnar[1,3,6], Joseph (Jake) Shenker[1], Ashok K. Malla[1,4,6], Ridha Joober[1,4,6], M. Mallar Chakravarty[1,4,5], Martin Lepage[1,3,4,6]

[1]Douglas Mental Health University Institute, Verdun, Canada

[2]McGill Centre for Integrative Neuroscience, McConnell Brain Imaging Centre, Montreal Neurological Institute, Montreal, Canada

[3]Department of Psychology, McGill University, Montreal, Canada

[4]Department of Psychiatry, McGill University, Montreal, Canada

[5]Department of Biological and Biomedical Engineering, McGill University, Montreal, Canada

[6]Prevention and Early Intervention Program for Psychosis, Douglas Mental Health University Institute, McGill University, Montreal, Quebec, Canada

Published in: Translational Psychiatry. DOI: https://doi.org/10.1038/tp.2017.168

Abstract

Early persistent negative symptoms (PNS) following a first episode of psychosis(FEP) are linked to poor functional outcome. Reports of reduced amygdalar and hippocampal volumes in early psychosis have not accounted for heterogeneity of symptoms. Age is also seldom considered in this population, a factor that has the potential to uncover symptom-specific maturational biomarkers pertaining to volume and shape changes within the hippocampus and amygdala. T1-weighted volumes were acquired for early (N=21), secondary (N=30), non-(N=44) PNS patients with a FEP, and controls (N=44). Amygdalar-hippocampal volumes and surface area (SA) metrics were extracted with MAGeT-Brain. Linear mixed models were applied to test for a main effect of group, and age*group interactions. Early PNS patients had significantly reduced left amygdalar and right hippocampal volumes, as well as similarly lateralized negative age*group interactions compared to secondary PNS patients(p's<0.017, corrected). Morphometry revealed decreased SA in early PNS compared to other patient groups in left central amygdala, and in a posterior region when compared to controls. Early and secondary PNS patients had significantly decreased SA as a function of age compared to patients without such symptoms within the right hippocampal tail(p's<0.05, corrected). Significant amygdalar-hippocampal changes with age are linked to PNS after a FEP, with converging results from volumetric and morphometric analyses. Differential age trajectories suggest an aberrant maturational process within FEP patients presenting with PNS, which could represent dynamic endophenotypes setting these patients apart from their non-symptomatic peers. Studies are encouraged to parse apart such symptom constructs when examining neuroanatomical changes emerging after a FEP.

Introduction

Negative symptoms are a cluster of symptoms that represent a disabling feature for many psychiatric and neurological conditions, characterized by the absence of goal-directed behaviour, and related cognitive and emotional states underlying motivation (Andreasen 1982; Brown and Pluck 2000). It is clear that for individuals who have experienced a first episode of psychosis (FEP), the manifestation of persistent negative symptoms (PNS) underlines a significant subgroup of patients with unmet therapeutic needs (Buchanan 2007; Bodnar et al. 2014). Early persistent negative symptoms (ePNS) are defined by the presence of anhedonia-asociality, alogia, affective flattening, and/or avolition-apathy for at least six consecutive months in the absence of therapeutically significant levels of positive, extrapyramidal and/or depressive symptomatology. Patients presenting concurrently with the latter symptom cluster comprise patients with PNS due to secondary factors (sPNS), and are argued to be distinct from ePNS (Hovington et al. 2012). Evidence suggests there are pronounced cortical changes specific to ePNS compared to other FEP patients (Benoit et al. 2012; Bodnar et al. 2014; Makowski et al. 2016). Within limbic circuitry, the structure of the amygdala and hippocampus may be particularly informative given the significant level of communication between these two structures (Phelps 2004; Kensinger 2009) and external brain networks (Stein et al. 2007; Kim et al. 2011), and their crucial roles in various cognitive processes (Phelps 2004; Watson et al. 2012) thought to be compromised in PNS patients (Hovington et al. 2012, 2013).

The link between PNS and amygdalar-hippocampal (AG-HC) structure in FEP has yet to be examined longitudinally, although earlier work has examined relevant themes cross-sectionally (Buchanan et al. 1993; Benoit et al. 2012). There is a considerable amount of literature on volumetric differences in these structures, with evidence supporting lower hippocampal volumes

in chronic schizophrenia (Harrison 2004; Narr et al. 2004) albeit the strength and direction of this result is contested in earlier stages of the illness (Wood et al. 2001).

The heterogeneity among psychosis samples may contribute to such inconsistencies. Studies have addressed this by subdividing patients into subgroups according to various characteristics. For instance, previous work has pinpointed lower left hippocampal volumes localized to the tail region in first-episode schizophrenia patients who do not achieve remission after six months of treatment (Bodnar et al. 2010). In relation to negative symptoms, several studies (Gur et al. 2007; Lepage et al. 2011) have found a relationship between functional activation patterns in the amygdala and severity of affective flattening in schizophrenia. Symptom severity has also been shown to be associated with the size and shape of the amygdala in psychosis and mood disorders (Hajek et al. 2009; Qiu et al. 2013). In particular, negative symptoms may be linked to hippocampal structure, as demonstrated recently in an investigation pinpointing CA1 atrophy to worsening negative symptoms (Ho, Iglesias, et al. 2017). If these relationships hold true, one might expect that patients with ePNS may exhibit differential AG-HC structure in relation to their non-PNS peers.

In 2014, Arnett and colleagues (2014) discussed a later socio-developmental maturational period ("emerging adulthood"), encompassing the age range of 18-29 years. This has vast implications for psychosis, given the emergence of a FEP within this time frame. It is feasible that neurobiological trajectories may be altered in PNS patients showing poor functional outcome, and alterations may emerge as a function of age. There has been a great deal of literature vetting for the neurodevelopmental hypothesis of schizophrenia, but surprisingly few studies emphasizing age in these patient populations. One developmental study of emotional processing suggested longitudinal patterns of amygdalar-prefrontal (AG-PFC) connectivity with age (particularly

implicating connections to anterior cingulate and medial prefrontal cortices), where during childhood (i.e. ages 7-12), positive associations between AG-PFC connectivity strength and response to emotional faces were evident, followed by a progressive shift to negative associations in adulthood (i.e. ages 19-25) (Wu et al. 2016). This was postulated to reflect top-down inhibitory control of prefrontal regions on amygdalar function in response to emotional stimuli in normal development. The idea of aberrancies in these connections in schizophrenia being more closely related to negative symptoms is still speculative, however, previous work from our group has shown altered cortical trajectories in various prefrontal regions in ePNS with age (Makowski et al. 2016), which provides a foundation to justify further investigation of highly interconnected limbic structure. At the level of the hippocampus, a recent review proposed that the underconnectivity of AG-PFC in schizophrenia underlying emotional/sociocognitive processing deficits may be linked to hyperactivation of the hippocampus (Nakagawa and Chiba 2016). The hippocampus has been dubbed as a key anatomical region in the initiation of schizophrenia, with aberrations strongly supported by altered neurodevelopmental mechanisms (Kalmady et al. 2014). Thus, changes in structure of the amygdala and hippocampus in the early phase of psychotic disorders may provide important neurodevelopmental information differentiating subgroups of patients with different clinical profiles. Of note, differences with age might be best captured by methods aside from conventional volumetry, as demonstrated by Voineskos and colleagues (2015). Neurodevelopmental changes within subcortical structures have also been depicted by several other studies, including an investigation of a child-onset schizophrenia sample (Raznahan et al. 2014; Chakravarty et al. 2015).

The current study combines the power of a longitudinal design conducted at a single site with clinically well-characterized patients, with minimal to no prior exposure to antipsychotic

medication, to begin to address pertinent questions of differential limbic structure trajectories in subgroups of FEP. To test for specificity of results to ePNS, we also compare against a subgroup of non-PNS patients with sPNS. It is hypothesized that ePNS patients will have lower volumes within the amygdala and hippocampus compared to both sPNS and non-PNS patients and controls. Merging knowledge from amygdalar-hippocampal circuitry (Small et al. 2011; Lee, Kim, et al. 2013) and previously reported results (Bodnar et al. 2010; Mamah et al. 2012), morphometric differences within the amygdala are postulated to be localized at both lateral and medial aspects of the amygdala, involved in sensory integration and control of outputs, respectively. For the hippocampus, differences are hypothesized to be associated with the output region of the structure (e.g., subiculum; closer to the hippocampal tail), as this region has previously been pinpointed in first episode psychosis. Finally, we expect morphometric differences to vary as a function of age between ePNS and other FEP subgroups.

Methods

Participants. Ninety-five patients and 44 controls were included. See Figure 8.1 in Appendix for visualization of the sample distribution by age. All patients were recruited from the Prevention and Early Intervention Program for Psychoses (PEPP-Montréal), at the Douglas Institute, and were part of a longitudinal naturalistic outcome study. PEPP is a specialized early intervention service for individuals between the ages of 14-35 who are experiencing a FEP within a local catchment area of Southwest Montréal, Canada. Details are outlined elsewhere (Iyer et al. 2015). The program involves a comprehensive approach with intensive medical and psychosocial interventions provided within the context of a modified assertive case management model. Given the nature of the study design, no statistical methods were used to predetermine sample sizes.

Neuroimaging component. The neuroimaging study began in 2003, where patients partook in three

scheduled visits: baseline, one-year follow-up (FUP1), and two-year follow-up (FUP2). Inclusion criteria include: age above 18 years, diagnosis of affective or non-affective psychosis, IQ>70, no past antipsychotic medication treatment for more than one month before entry to PEPP, no major medical disorders, and sufficiently stable for the scanning procedure. Note, although exposure to antipsychotic medication was restricted before acceptance to PEPP, most patients were prescribed antipsychotic medication before their first scan, and thus some patients did in fact have more than one month of cumulative exposure to antipsychotic medication for the neuroimaging portion of the study. Exclusion criteria include: a history of neurological illnesses and head trauma resulting in loss of consciousness that could affect cognition, presence of neurological disorder as by medical record examination, lifetime diagnosis of substance dependence, and/or any potential contraindication for the MR scan. See supplementary methods in Appendix-I for detailed information on patients excluded from the neuroimaging study.

Non-clinical controls were recruited through advertisements within the same local catchment area. In addition to exclusion criteria listed for FEP patients, controls were excluded if they had any current/past history of Axis I disorders, and/or a first-degree relative suffering from a schizophrenia spectrum disorder. All participants provided written informed consent, and the protocol was approved by the Research Ethics Board of the Douglas Mental Health University Institute and the McGill University Faculty of Medicine.

Clinical assessment and demographic data. Diagnosis was made using the Structured Clinical Interview for DSM-IV (SCID-IV) (First et al. 1998), performed by a trained interviewer and confirmed by a research clinician psychiatrist. Depression was assessed with the Calgary Depression Scale for Schizophrenia (Addington et al. 1990). Positive and negative symptoms were

assessed with the Scale for the Assessment of Positive Symptoms (SAPS) (Andreasen 1984b) and Scale for the Assessment of Negative Symptoms (SANS) (Andreasen 1984a). Antipsychotic medication dosages were converted to chlorpromazine equivalents according to the literature (Leucht et al. 2015), and multiplied by percent medication adherence (Cassidy et al. 2010). Parental socioeconomic status (Hollingshead 1965), handedness (Oldfield 1971), and full scale IQ (Weschler 1997, 1999) were assessed for both controls and patients.

Following our previous work (Hovington et al. 2012; Makowski et al. 2016), early PNS were defined according to the following criteria: (1) global rating of moderate or more on at least one negative symptom as measured by the SANS; (2) global rating of mild or less on all positive symptoms as measured by the SAPS; (3) a total score of 4 or less on the CDSS; (4) absence of extrapyramidal symptoms requiring anticholinergic treatment; and (5) all above criteria are maintained for a period of at least six months (Buchanan 2007; Hovington et al. 2012). Patients were classified as having PNS due to secondary factors if criteria 2 , 3 and/or 4 were not met.

MRI acquisition. All scanning was carried out at the Montreal Neurological Institute on a 1.5 T Siemens Sonata scanner. T1-weighted volumes were acquired using a three-dimensional gradient echo pulse sequence with sagittal volume excitation (TR=22 ms, TE=9.2 ms, flip angle=30, 180 1-mm contiguous sagittal slices). The rectangular field of view for the images was 204 mm (SI) 256 mm (AP).

Post-processing: MAGeT-Brain. Amygdalar and hippocampal structures were extracted bilaterally using the Multiple Automatically Generated Templates (MAGeT)-Brain algorithm (Pipitone et al. 2014; Chakravarty et al. 2015; Voineskos et al. 2015)

(https://github.com/CobraLab/MAGeTbrain). This technique utilizes a limited number of high-resolution atlases that have been manually segmented as described previously: amygdala (Treadway et al. 2015); and hippocampus (Winterburn et al. 2013) (https://github.com/CobraLab/atlases). Extensive validation of MAGeT has been done previously, as shown in several references from our group (Pipitone et al. 2014; Makowski et al. 2018), which have also included subsets of the described patient sample here, with data acquired on a 1.5T scanner. Segmentations were also submitted to the shape morphometric branch of MAGeT-Brain, yielding local vertex-wise surface area maps for each subject. Information about MAGeT-Brain processing and quality control are detailed in Section 3.2.2.

Statistical analyses. Demographic and clinical variables (with a single time point) were analysed with one-way ANOVAs for continuous variables or chi-squared ratio tests for nominal variables. For IQ, an ANCOVA was used to covary for test version. SAPS/SANS sum of item scores between FEP subgroups were assessed across clinical timepoints with Generalized Estimating Equations (GEE). Antipsychotic dosages, CDSS scores, and the time period in months between scan and nearest symptom evaluation were assessed between the three patient groups at each scan-time point, using one-way ANOVAs for normally distributed variables, and Kruskall-Wallis H-tests for non-normally distributed variables. Analyses of clinical variables were conducted using PASW Statistics 21 (SPSS inc., 2009, Chicago, IL, USA) and were two-tailed with a critical p-value of 0.05.

Neuroanatomical analyses: volume. For scans that passed QC (see supplementary methods in Appendix-I), volumetric differences between FEP subgroups and controls were assessed using

linear mixed effects models applied to each structure and hemisphere separately using Matlab (2015a). Gross volumetric differences in structure were assessed with the following model:

$$Y = intercept + d_1 + \beta_1(Group) + \beta_2(Age) + \beta_3(Sex) + \beta_4(Handedness) + \beta_5(Total\ Brain\ Volume) + random(Subject) + \epsilon$$

where Y represents whole left/right amygdalar/hippocampal volume, d_1 is the random within-subjects effect, $\beta_{1\text{-}5}$ represent regression coefficients, and ε is residual error. Linear age effects were then examined separately by adding the following term to the above model: "β_6(Group*Age)". To control for multiple comparisons, the false discovery rate procedure was used with q=0.05, which limits the expected proportion of incorrectly rejected null hypotheses to 5% (Benjamini and Hochberg 1995).

Neuroanatomical analyses: surface area.

To assess differences in shape morphometry between groups, statistics were performed across all vertices of bilateral amygdalar and hippocampal surfaces using the SurfStat toolbox within Matlab (http://www.math.mcgill.ca/keith/surfstat/). Each hemisphere was assessed separately, using an equivalent mixed effects model as described in the previous section, covarying for total surface area of the structure by hemisphere in place of total brain volume ("β_5 [Total SA]"). Similarly, the main effect of group was first tested, followed by linear age*group interactions. For all analyses, statistical maps were thresholded and multiple comparisons were taken into account using random field theory (RFT) for non-isotropic images (Worsley et al. 2004), limiting the chance of reporting a false positive finding to below p=0.05.

Supplementary linear mixed effects models with altered covariates.

Four additional models were tested with altered covariates, to explore effects of different variables, in addition to the chosen covariates of sex, handedness, and total brain volume/total surface area. These four altered models were as follows: A) covarying for diagnosis, B) covarying for antipsychotic medication in the FEP patient sample only; as described above, antipsychotic dosages were converted to chlorpromazine equivalents and took into account medication adherence, C) removal of sex and handedness, and D) covarying for IQ (note two controls were excluded from this analysis, given missing IQ information). The rationale behind analyses C was motivated by the fact that our groups did not significantly differ on sex and handedness. These variables were kept in the main model presented in this manuscript, given the well-documented and clear impact of sex and handedness on neuroanatomy (Good et al. 2001; Li et al. 2014; Willems et al. 2014). However, recent evidence has not found support for the effects of handedness on cerebral anatomy (Guadalupe et al. 2014). With respect to sex differences, Pruessner and colleagues reported no sex differences in amygdalar and hippocampal volumes (Pruessner et al. 2001). Thus it is of interest to investigate how significant findings may be altered when these variables are removed from the model.

Results

Socio-demographic and clinical data. In the FEP group, baseline scans were performed on average 4.1 (SD=1.9) months after entry to PEPP. For the entire group, including controls, inter-scan intervals were approximately 13.1 (SD=1.3) months between baseline and FUP1, and 12.5 (SD=1.7) months between FUP1 and FUP2. Nine participants (6 FEP, 3 controls) were not scanned at FUP1 but were scanned at FUP2; average interscan interval was 26.7 (SD=3.1) months between baseline and FUP2.

The groups did not significantly differ in sex ratio, handedness, parental SES, or age at scanning time (see **Table 4.1**). However, controls significantly differed from all patient groups on Full-Scale IQ and years of education. Within the three patient groups, there were no significant differences in CDSS scores or time elapsed between the MRI scan and symptom evaluation. As expected, the sPNS patient subgroup had significantly higher SAPS totals compared to the ePNS and non-PNS subgroups across baseline and one-year follow-up. Also, the ePNS and sPNS subgroups had significantly higher SANS totals compared to the non-PNS subgroup across all timepoints. See Table 8.1 of Appendix-I for breakdown of SAPS/SANS scores across clinical timepoints and relevant statistics. FEP subgroups differed in distribution of diagnosis, with a higher proportion of nPNS diagnosed with affective psychotic disorders (major depression, bipolar), and higher proportions of schizophrenia/schizophreniform diagnoses in the sPNS and ePNS subgroups. Additionally, amount of antipsychotic prescribed at the second scanning timepoint was significantly higher for sPNS patients compared to non-PNS, thus diagnosis and antipsychotic medication were included as covariates in supplemental analyses (see Table 8.2 and Figure 8.2 of Appendix-I).

		FEP					
		ePNS	Non-ePNS		Controls	Statistic$_{(df)}$	*p*-value
			sPNS	Non-PNS			
General Demographics	N (+ subset with three scans)	21 (18)	30 (15)	44 (27)	44 (24)		
	Male, N (%)	15 (71.4)	21 (70.0)	31 (70.5)	25 (56.8)	$\chi^2_{(3)}$= 2.5	0.5
	Education in Years	11.1 (2.5)	11.6 (2.4)	12.7 (2.4)	14.2 (2.5)	$F_{(3,138)}$=10.4	<0.001
	Socioeconomic Status	3.4 (1.0) [16]	3.4 (1.1) [29]	3.0 (1.0) [42]	3.4 (0.9) [41]	$\chi^2_{(3)}$= 6.1	0.1
	Right Handed, N (%)	17 (81.0)	25 (83.3)	38 (86.4)	38 (86.4)	$\chi^2_{(3)}$= 0.5	0.9
	Full Scale IQ	96.9 (15.3)	97.8 (15.3)	100.3 (15.3)	111.5 (15.3) [42]	$F_{(3,136)}$=7.1	<0.0001[1]
	Diagnosis**, N(%)						
	Schizophrenia Spectrum	16 (76.2)	26 (86.7)	24 (54.5)			
	Affective Disorder	3 (14.3)	1 (3.3)	15 (34.1)		$\chi^2_{(6)}$= 13.1	0.017
	Delusional Disorder	0 (0)	1 (3.3)	2 (4.5)			
	Psychosis Not Otherwise Specified	2 (9.5)	2 (6.7)	3 (6.8)			
Scan 1	Age	23.2 (3.6)	24.5 (4.0)	4.6 (0.7)	23.8 (3.5)	$F_{(3,138)}$=1.0	0.4
	SAPS total	8.2 (10.2)	17.6 (15.3)	4.1 (5.4)		$\chi^2_{(2)}$= 24.5	<0.0001
	SANS total	25.4 (9.3)	23.5 (12.0)	14.0 (10.7)		$F_{(2,94)}$=10.8	<0.0001
	CDSS	2.4 (2.7)	3.1 (3.2)	1.7 (2.5) [43]		$\chi^2_{(2)}$= 3.4	0.2
	CPZ equivalent (in mg)	758.4 (671.3)	965.9 (844.6)	774.2 (707.9)		$\chi^2_{(2)}$=9.7	0.6
	Adherence (%)	86.6 (21.3)	87.9 (19.1)	84.6 (27.5)		$\chi^2_{(2)}$= 0.2	0.9
	Window |Scan - Symptom Eval| (months)	0.6 (0.4)	0.8 (0.5)	0.7 (0.6)		$F_{(2,94)}$=0.5	0.6
Scan 2	N	19	28	41	41		
	Age	24.3 (3.8)	25.5 (4.1)	25.6 (4.3)	24.7 (3.4)	$F_{(3,128)}$=0.7	0.5
	SAPS total	5.9 (6.2)	12.6 (9.5)	3.5 (8.7)		$\chi^2_{(2)}$= 32.9	<0.0001
	SANS total	19.9 (12.0)	21.4 (10.5)	7.5 (9.0)		$\chi^2_{(2)}$= 23.6	<0.0001
	CDSS	1.0 (1.5)	1.9 (3.0) [27]	1.4 (2.7)		$\chi^2_{(2)}$= 1.7	0.4
	CPZ equivalent (in mg)	2875.2 (2059.7)	4434.7 (3337.6)	2656.8 (2187.0)		$\chi^2_{(2)}$=10.3	0.006
	Adherence (%)	87.0 (16.0)	80.0 (19.9)	81.1 (25.5)		$\chi^2_{(2)}$=1.3	0.5
	Window |Scan - Symptom Eval| (months)	1.8 (1.5)	2.1 (1.7)	1.8 (1.2)		$\chi^2_{(2)}$= 0.3	0.9
Scan 3	N	20	17	29	27		
	Age	25.5 (3.7)	26.2 (3.7)	26.3 (4.4)	26.9 (3.5)	$F_{(3,92)}$=0.5	0.6

SAPS total	7.0 (10.3)	12.5 (17.6)	4.8 (8.1)		$\chi^2_{(2)}$= 3.5	0.2
SANS total	19.8 (11.1)	14.8 (13.2)	6.7 (8.6)		$\chi^2_{(2)}$= 18.5	<0.0001
CDSS	2.5 (3.3) [18]	2.1 (2.5)	1.6 (2.1) [28]		$\chi^2_{(2)}$= 0.7	0.7
CPZ equivalent (in mg)	4216.5 (3906.2)	6753.8 (6368.0)	5177.0 (4994.3)		$\chi^2_{(2)}$= 2.0	0.4
Adherence (%)	78.4 (26.2)	78.3 (27.9)	77.1 (28.7)		$\chi^2_{(2)}$= 0.05	0.98
Window |Scan - Symptom Eval| (months)	1.0 (1.9)	0.4 (0.5)	0.5 (0.7)		$\chi^2_{(2)}$= 0.8	0.7

Table 4.1. Demographic and clinical information for longitudinal sample.
General Demographics for whole sample are presented, followed by information corresponding to each scan. All data represented as Mean (SD), unless otherwise specified. Levene's test revealed no significant differences in variance between subgroups. Square brackets [] include adjusted sample size included in statistical analysis due to missing datapoints. All antipsychotic totals are presented as cumulative chlorpromazine equivalents in mg, as prescribed by a psychiatrist, and are reported along with corresponding medication adherence percentages. SAPS/SANS totals are presented as mean scores of the sum of item-level scores. Note that "SANS total" excludes the "attention" subscale.
[1]Post hoc comparisons showed that controls differed from all FEP patient groups in years of education (p's<0.005) and IQ (p's<0.01). IQ differences were covaried by test version. No differences existed between patient groups.
[2] IQ means and standard deviation are presented as adjusted values, covaried by test version (WAIS-III vs. WASI). There was no difference between different test versions on IQ ($F_{1,136}$=0.9, p=0.3).
[3] Assessed using Fisher's exact test of independence.
[4] Tukey's post hoc comparisons revealed significant differences in SAPS scores between sPNS and other two patient groups (p's<0.005).
[5] Tukey's post hoc comparisons revealed significant differences in SANS scores between ePNS and sPNS and remaining non-PNS patients (p<0.001) for Scans 1 and 2. For Scan 3, non-PNS still significantly differed from ePNS (p=0.001), but there was only a trend-like difference between non-PNS and sPNS (p=0.08).
[6]Post-hoc analyses indicated that sPNS patients were prescribed significantly more antipsychotic medication (in CPZ equivalent dosage) cumulatively compared to non-PNS patients at Scan 2 (p=0.02), and was still significant when taking into consideration medication adherence (multiplying CPZ equivalent by percent adherence), with $\chi^2_{(2)}$=6.2, p=0.046 (post-hoc sPNS>NonPNS p=0.03). No significant differences emerged between the ePNS group and other FEP subgroups at Scan 2.
Abbreviations: ePNS, early persistent negative symptoms. sPNS, persistent negative symptoms due to secondary factors. FUP, follow-up. SAPS/SANS, Scale for Assessment of Positive/Negative Symptoms. CPZ, chlorpromazine.

Hippocampal and amygdalar volumetry. Descriptive statistics of left/right amygdalar and hippocampal volumes adjusted for age, sex, total brain volume, and handedness are outlined in **Table 4.2**. After FDR-correction, linear mixed models revealed significant group differences for right amygdalar volumes ($F_{3,350}$=3.61, p=0.014) and hippocampal volumes ($F_{3,350}$=3.5, p=0.017). Significant effects also emerged for age*group interactions for left amygdalar volumes ($F_{3,350}$=3.73, p=0.011), as well as the right hippocampus ($F_{3,350}$=3.9, p=0.010). Post hoc tests (all p's<0.05) showed that within the left amygdala, the sPNS group had a significantly different and positive correlation with age compared to ePNS patients and controls. The non-PNS group also had a significantly different slope with age compared to ePNS patients. For the right hippocampus, the ePNS group had a significantly different negative correlation with age compared to sPNS patients and Controls. No significant group or age*group differences emerged for the right amygdala or left hippocampus (**Figure 4.1**).

			FEP			
				Non-ePNS		
Timepoint	Structure	Side	**1) ePNS**	**2) sPNS**	**3) Non-PNS**	**4) Controls**
Baseline (Scan 1)	Amygdala	L	1386.9 (22.6)	1358.7 (18.6)	1362.2 (15.4)	1377.4 (15.5)
		R	1404.5 (22.0)	1370.5 (18.1)	1381.7 (15.0)	1384.6 (15.0)
	Hippocampus	L	2488.3 (52.0)	2452.1 (42.8)	2517.4 (35.4)	2536.1 (35.5)
		R	2471.0 (52.7)	2421.4 (43.4)	2433.9 (35.9)	2490.9 (36.0)
FUP1 (Scan 2)	Amygdala	L	1384.6 (23.4)	1359.9 (19.0)	1365.7 (15.8)	1367.3 (15.8)
		R	1398.5 (22.9)	1362.9 (18.6)	1383.7 (15.4)	1395.8 (15.5)
	Hippocampus	L	2486.5 (52.2)	2485.6 (42.4)	2530.3 (35.1)	2530.8 (35.2)
		R	2446.7 (54.5)	2453.8 (44.3)	2443.2 (36.7)	2492.1 (36.8)
FUP2 (Scan 3)	Amygdala	L	1371.1 (25.7)	1363.7 (27.5)	1366.1 (20.7)	1395.2 (21.7)
		R	1394.2 (24.3)	1379.2 (26.0)	1390.4 (19.5)	1403.9 (20.5)
	Hippocampus	L	2499.5 (52.6)	2457.5 (56.3)	2557.4 (42.3)	2567.8 (44.3)
		R	2448.7 (53.2)	2453.7 (56.9)	2483.4 (42.7)	2499.3 (44.8)

Table 4.2. Amygdalar and hippocampal volumes: descriptives.
Mean hippocampal and amygdalar volumes are adjusted for total brain volume, age, sex, and handedness, with standard error in brackets. There were no differences in volumes between groups when looking at the data cross-sectionally.
Abbreviations: ePNS, early persistent negative symptoms. sPNS, persistent negative symptoms due to secondary factors. FUP, follow-up. L, Left. R, Right.

Structure	Side	Main Effect of Group			Group*Age Interaction		
		Statistic (df)	p-value	post-hoc	Statistic (df)	p-value	post-hoc
Amygdala	L	$F_{(3,350)}$=3.61	**0.014**	**1<2,4; 2<3**	$F_{(3,350)}$=3.73	**0.011**	**1<2,4; 2<3**
	R	$F_{(3,350)}$=1.9	0.1	--	$F_{(3,350)}$=1.8	0.2	--
Hippocampus	L	$F_{(3,350)}$=0.2	0.9	--	$F_{(3,350)}$=0.2	0.9	--
	R	$F_{(3,350)}$=3.5	**0.017**	**1<2**	$F_{(3,350)}$=3.9	**0.01**	**1<2, 4**

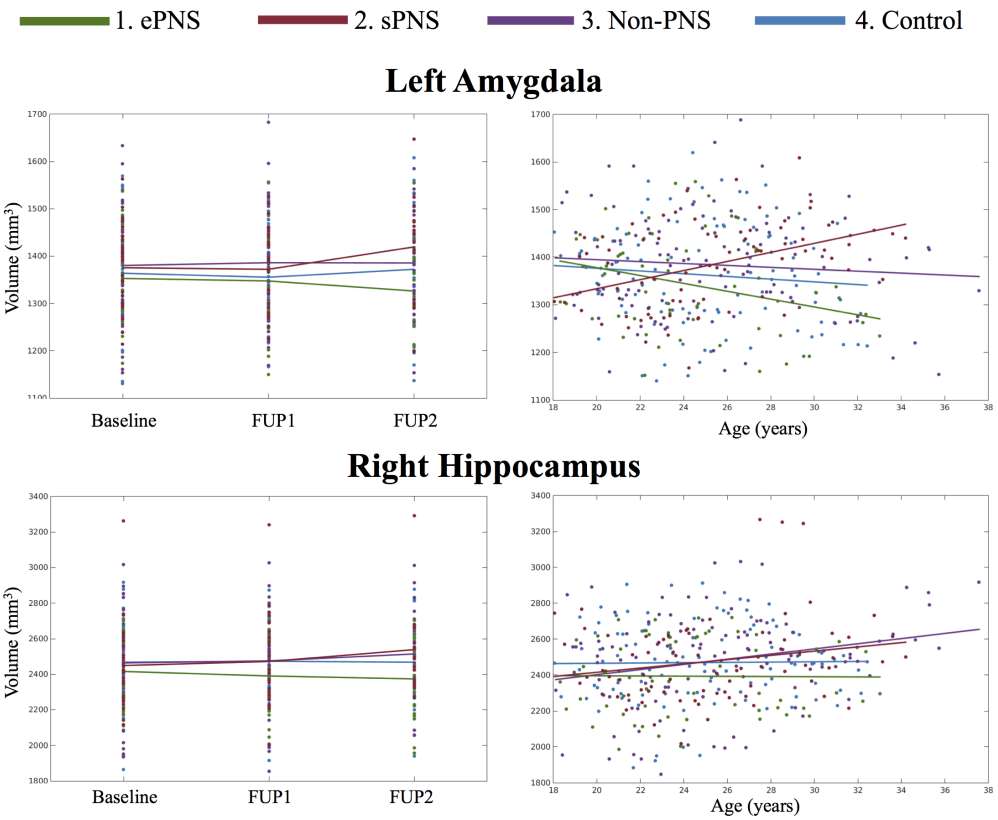

Figure 4.1. Amygdalar and hippocampal volumes: significant group main effects and group*age interactions.

Table presents statistics from linear mixed effects analyses. Significant results that survived FDR-correction for multiple comparisons are indicated in bold. Post-hoc contrasts were based on the four groups: 1) ePNS, 2) sPNS, 3) non-PNS, 4) Controls. Significant group and group*age contrasts are depicted in the corresponding graphs below the table. Abbreviations: ePNS, early persistent negative symptoms. sPNS, persistent negative symptoms due to secondary factors. FUP, follow-up.

Hippocampal and amygdalar shape morphometry – vertex-wise results. There were no significant main effects of group for either structure bilaterally. However, significant findings emerged with the age*group interaction. For the left amygdala, the following contrasts and regions had significantly different surface area trajectories with age comparing groups on vertex-wise surface area: 1) ePNS<non-PNS within a central/anterior cluster (**Figure 4.2A**), 2) ePNS<sPNS and Controls in a more dorsal central region (**Figure 4.2B**), and 3) ePNS<Controls within a posterior/centromedial portion (**Figure 4.2C**).

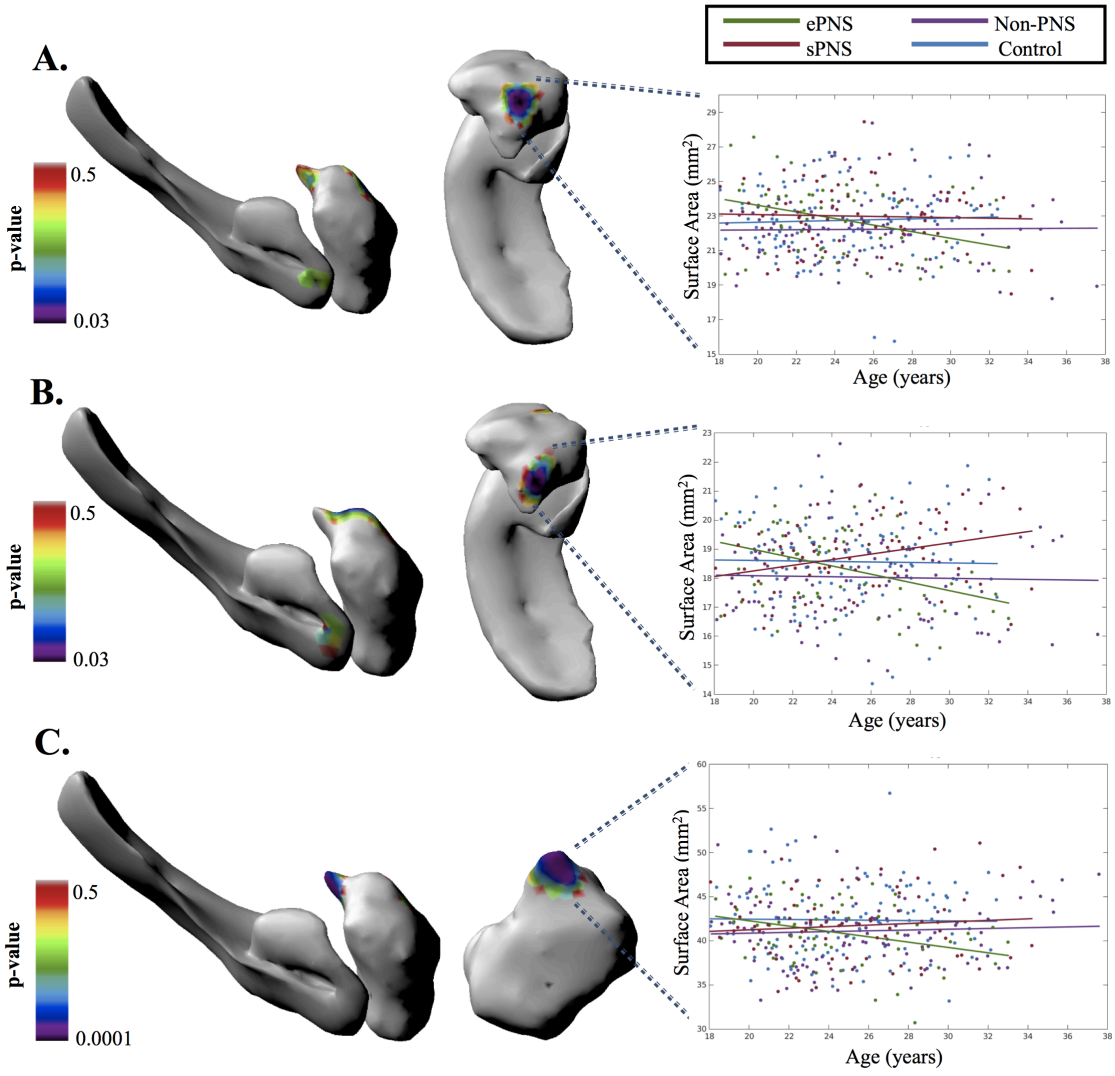

Figure 4.2. Significant group*age interactions in surface area of the left hemisphere.

Statistical maps overlaid on left hippocampal and amygdalar 3D surface renderings represent RFT-corrected p-values. Surface area metrics from clusters with a corrected p-value less than 0.05 were extracted and plotted against age for each group.
A. Significantly decreased surface area with age in the ePNS group compared to non-PNS within a central/anterior region of the left amygdala (292 df, p=0.03). Comparison of regression slopes with age reveal similar effects comparing to controls as well ($F_{(3,350)}$=5.01, p=0.002; post hoc ePNS<Controls p=0.0011).
B. Significantly decreased surface area with age in the ePNS group compared to sPNS in a more dorsal region (compared to A) of the central amygdala (292 df, p=0.03). Further comparison to other groups revealed significant differences in regression slopes with age ($F_{(3,350)}$=4.43, p=0.0045), such that the ePNS had a significantly reduced relationship between age and surface area in this cluster compared to both non-PNS and Controls (p's≤0.01).
C. Significantly decreased surface area with age in the ePNS group compared to Controls in a posterior (centromedial) portion of the amygdala (298 df, p=0.0001). Mixed effects statistics for comparison of regression slopes yielded $F_{(3,350)}$=4.19, p=0.006, where no other contrasts apart from Controls vs. ePNS were significant.
No significant interaction effects with age emerged for the left hippocampus.
Orientation: From left to right, surfaces depict left medial view, and dorsal view of the hippocampus and amygdala, with the exception of panel **C**, where the dorsal view has been replaced by a posterior view of the amygdala for better visualization of the significant cluster.
Abbreviations: ePNS, early persistent negative symptoms. sPNS, persistent negative symptoms due to secondary factors.

For the right hippocampus, a significant cluster emerged in a portion of the hippocampal tail comparing surface area trajectories with age between non-PNS patients and the other FEP subgroups; specifically, the ePNS group had a significant negative relationship with age in this cluster compared to sPNS and non-PNS subgroups, and the sPNS group also exhibited a significantly different and opposite trajectory compared to non-PNS patients and controls (p's<0.001; **Figure 4.3**). No significant age*group interactions were found for surface area across the left hippocampus or right amygdala. Controlling for diagnosis, antipsychotic medication and I.Q. did not significantly change the interpretation of results. Similarly, removing handedness and sex as covariates in the linear mixed effects model did not alter results, with the exception of one surface area cluster of the left central amygdala, which did not survive correction for multiple comparisons with RFT after removing sex and handedness as covariates, namely when comparing

age trajectories between ePNS and NonPNS patients. See Table 8.2 and Figure 8.2 of Appendix-I for results with altered covariates for volumetry and shape morphometry, respectively.

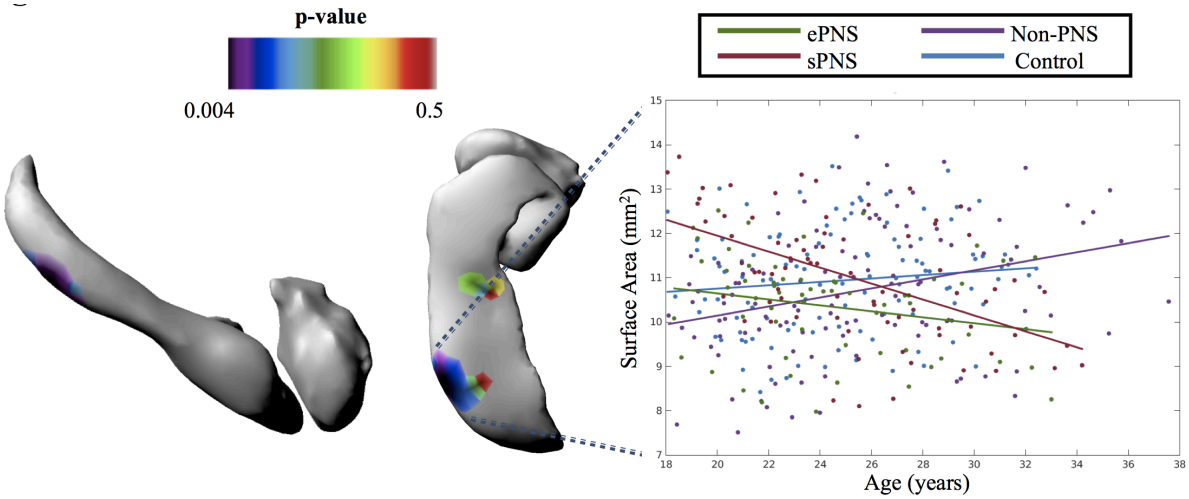

Figure 4.3. Significant group*age interactions in surface area of the right hemisphere.
Statistical maps overlaid on left hippocampal and amygdalar 3D surface rendering represent RFT-corrected p-values. Significant cluster emerged with increased surface area with age in non-PNS compared to sPNS and ePNS (p's<0.01) in a posterior/ventral portion of the hippocampus.
Further comparison to other groups revealed significant differences in regression slopes with age ($F_{(3,350)}$=7.04, p<0.001), such that the ePNS group had a significantly negative relationship between surface area in this cluster and age compared to sPNS and non-PNS (p≤0.001). In addition to sPNS differing from non-PNS, sPNS patients also had a significantly different positive slope compared to Controls (p<0.001). No significant interaction effects with age emerged for the right amygdala.
Orientation: from left to right, surfaces depict right lateral view, followed by ventral view of hippocampal and amygdalar structures.
Abbreviations: ePNS, early persistent negative symptoms. sPNS, persistent negative symptoms due to secondary factors.

Hippocampal and amygdalar shape morphometry – post hoc region-of-interest results.

For the four significant clusters that emerged through a vertex-wise investigation of surface area described above, total surface area values were extracted for each of the regions and regression slopes were calculated for each of the four groups (ePNS, sPNS, Non-PNS and Controls), to see if any other groups differed at the regional level. For the first central/anterior amygdalar cluster, in

addition to differing from non-PNS patients, the ePNS group had significantly different regression slopes from Controls (Omnibus: $F_{3,350}$=5.01, p=0.002; post hoc ePNS<Controls p=0.0011) (**Figure 4.2A**). For the second amygdalar region (dorsal to the first), ePNS had a significantly reduced relationship between age and surface area in this cluster compared to both non-PNS and Controls (Omnibus: $F_{3,350}$=4.43, p=0.0045; post hoc p's<0.01), in addition to the previously reported vertex-wise difference between ePNS and sPNS (**Figure 4.2B**). Finally, the last significant amygdalar cluster, localized more posteriorly and centromedially, did not uncover any additional significant relationships apart from the previously reported difference between ePNS and Controls (Omnibus: $F_{3,350}$=4.19, p=0.006) (**Figure 4.2C**).

For the single significant right hippocampal cluster, further post-hoc analyses of regression slopes revealed additional differences between sPNS patients and controls, (Omnibus: $F_{3,350}$=7.04, p<0.001; post hoc sPNS<Control, p<0.001) (**Figure 4.3**).

Discussion

The current study provides evidence for changes in AG-HC structural trajectories, specifically in FEP patients presenting with PNS. Volumetric findings within the left amygdala and right hippocampus indicated that ePNS patients had significantly different/decreased relationships with age compared to non-PNS patients and controls, in addition to having significantly reduced volumes within these structures. Surface area findings were similarly lateralized, where the most prominent direction of findings emerged with significant contraction with age in ePNS across several amygdalar regions and a posterior hippocampal cluster. Furthermore, the sPNS group showed significantly decreased surface area with age within the latter hippocampal region in opposition to the notable expansion with age examined in non-PNS patients and controls.

Noteworthy, non-PNS patients never differed from healthy controls. Results remained largely unaltered when covarying for IQ, diagnosis, and antipsychotic dosage, and removing sex and handedness from the model.

The differential and striking trajectories uncovered in relation to negative symptom presentation within AG-HC structure encourage further exploration of dynamic brain changes in different psychiatric samples, as others have suggested (Cropley and Pantelis 2014; Frank et al. 2015). Nacewicz and colleagues (2006) explored such age effects on the amygdala in an autistic sample, and found significantly lower amygdalar volumes in older individuals with autism, not unlike the amygdalar trajectories found within our ePNS group. Given the parallels that can be drawn between flattened affect and social impairments in autism with symptom presentation in ePNS, the amygdala represents a plausible target for future transdiagnostic work. At the level of the hippocampus, associations have been previously drawn between lower hippocampal volumes and poor functioning in FEP (Pruessner et al. 2015), lending support to our findings of decreased right hippocampal volumes in patients with ePNS and corresponding negative trajectories with age.

Notably, only age by group interactions on specific regions of AG-HC shape morphometry yielded significant results, concordant with previous claims that differences in surface area morphology may represent a dynamic and neurodevelopmental endophenotype (Raznahan et al. 2014; Shaw, De Rossi, et al. 2014; Shaw, Sharp, et al. 2014; Chakravarty et al. 2015; Shah et al. 2016). Few studies have looked at AG-HC shape morphology in psychosis, although relevant objectives were investigated in the work of Qiu et al (2013). The authors found significant surface alterations within the left hippocampal tail and right hippocampal body, with first-episode schizophrenia patients exhibiting greater inward deformations compared to first-episode mania

and controls. This is consonant with the significant inward deformations consistently seen in our ePNS group, containing a higher distribution of patients diagnosed with schizophrenia/schizophreniform (as opposed to an affective disorder). In fact, controlling for diagnosis in our analyses strengthened the statistical significance of shape deformation clusters.

The consistent lateralization of results observed across volumetric and morphometric analyses deserves discussion. Although studies in FEP and schizophrenia have uncovered differences bilaterally, many findings in psychosis have been skewed to the left hemisphere (Seidman et al. 2002; Strasser et al. 2005; Bodnar et al. 2010; Kawano et al. 2015). In contrast, our findings within the hippocampus were right-lateralized and were specific to patients with PNS. Witthaus and colleagues (2010) reported similarly lateralized findings in an investigation of patients at ultra-high risk (UHR) for psychosis and those who transitioned to having a FEP. Specifically, this study pinpointed lower volumes in a subset of UHR patients that transitioned to psychosis within the left amygdala, and lower right hippocampal volumes in FEP patients. These consistent findings at similar stages of psychosis suggest that lateralization of limbic structural volume differences may reflect an early biomarker underlying the manifestation of psychosis and subsequent negative symptomatology. The localization of deformation differences also overlapped with our initial hypotheses, where significant differences emerged in a medial region of the amygdala, a region posited to have "striatal-like" features with GABAergic-containing neural circuitry (Ehrlich et al. 2009; Lee, Kim, et al. 2013). We also observed hippocampal morphometric differences closer to the output region of the structure, in line with previous studies (Small et al. 2011; Mamah et al. 2012; Qiu et al. 2013). Although not initially hypothesized, significant differences were uncovered within central regions of the amygdala, which has an integral role in forming associations between stimuli on the basis of their motivational salience, ultimately shaping

emotional behaviours (Cardinal et al. 2002; Fernando et al. 2013). Thus, aberrancies in the development of these key regions involved in emotion and motivational behaviours may contribute to the differential expression of negative symptoms exhibited by ePNS and sPNS patients, although further work is needed to understand the mechanisms underlying the manifestation of symptoms in these two groups.

Another noteworthy point is the significantly different trajectories uncovered within the sPNS group, particularly within the hippocampus. We had initially hypothesized that the ePNS group would show the most significant changes, and we had not expected such dramatic effects in the sPNS group, meriting additional dialogue on the potential effect of positive symptoms on limbic structure, and differential changes with age. Links between hippocampal shape and positive symptomatology were recently addressed by Mamah et al (2016), where higher levels of disorganized positive symptoms were significantly correlated with surface contraction in the lateral CA1 hippocampal subregion. Depressive symptomatology also may have contributed to results within the sPNS group. For instance, previous work (Keller et al. 2008) has suggested that amygdalar volume reductions seem to be specific to the intersection of psychosis and depression. Other work has corroborated evidence for hippocampal shape changes in depression (Isıklı et al. 2013). Further longitudinal investigation of positive and depressive symptomatology in relation to amygdalar and hippocampal structure is warranted to disentangle the specific contributions of different symptom domains.

Several studies have refuted the idea of progressive structural changes in the hippocampus and amygdala after the onset of psychosis (Wood et al. 2001; Steen et al. 2006; Velakoulis et al. 2006). However, our findings suggest null findings may be a result of pooling together patients into a unitary group and simply comparing to healthy controls, which would be similarly found in

our sample if our three FEP subgroups were merged. The age window at which a FEP is experienced has large consequences for the social developmental stage of the individual, and it comes as no surprise that these effects may be manifested differentially with age at the level of limbic structure. Neurodevelopmental models of psychosis-related disorders are increasingly beginning to interlace psychosocial and biological factors into a coherent model to facilitate treatment (Murray et al. 2015), which requires further understanding of potential gene-by-environment interactions on neurobiology to help us fully understand the psychological and biological mechanisms contributing to PNS following a FEP.

It is worth discussing the chosen categorical approach, as opposed to the often-used "dimensional" approach of regressing symptom severity against neuroanatomical measures. Although meaningful information can certainly be derived by the latter approach, symptom data is often not normally distributed, and the amount of clinical information used in such brain-behaviour relationships is often limited by the imaging data. Given that the current study design had a greater number of clinical timepoints (i.e. 5+) compared to imaging timepoints (i.e. 2-3), regression analyses would have restricted the presented analysis to the available imaging data, and important dynamic information regarding the longitudinal course of symptoms across different domains would have been lost. Thus, the adopted approach capitalizes on the clinical data available in linking symptoms to neuroanatomical trajectories within the amygdala and hippocampus. Finally, our findings suggest that the resultant subgroups of patients do indeed seem to have distinct biological underpinnings in AG-HC structure, and such an approach in defining patient subgroups independent of diagnostic categories may inform and/or contribute to pending changes in diagnostic categories that have often been criticized for lacking biological validity. Although future work is certainly required to gain more confidence in the validity of the proposed subgroups,

this approach holds promise in bringing to the forefront meaningful clinical subtypes of patients who have experienced a FEP and addressing the clinical picture surrounding negative symptom presentation.

The current study offers several strengths and limitations. Recruitment strategies have been optimized for this large sample of FEP patients such that all patients were recruited from a single well-defined catchment area in the absence of other competing services. Furthermore, a wealth of longitudinal data is available for these patients, including data from structured clinical assessments to complement neuroimaging data. However, there are inherent limitations to the manner by which early and secondary PNS groups were separated. Given that the latter group exhibits treatment-resistance, and arguably, poor outcome similarly to ePNS patients, future investigations should try to incorporate additional behavioral and clinical data to disentangle neurobiological findings. It is possible that these two subgroups of patients have overlapping neuroanatomical features that were not directly addressed by this study. There was also an uneven drop-out rate among the FEP subgroups for the neuroimaging portion of the study, with the highest attrition observed in the sPNS group. Finally, imaging was acquired on a 1.5T scanner, which prevented us from reliably resolving hippocampal subfield structure, an emerging interest in the study of neuropsychiatric disorders (Wang et al. 2010; Mathew et al. 2014; de Flores et al. 2015; Haukvik et al. 2015; Kawano et al. 2015).

There have been a wide array of findings pinpointing aberrant AG-HC structure in psychotic disorders, with scant research looking at specific symptom constructs in psychosis, and further localizing changes with surface morphometry. The current study addresses these gaps in the literature and elucidates differential volumetric and shape morphometric trajectories with age within lateralized regions of the amygdala and hippocampus, in relation to persistent negative

symptoms in psychosis. These findings suggest potential neurodevelopmental aberrations that coincide with negative symptom presentation, and could represent dynamic endophenotypes underlying patient subgroups within heterogeneous first episode psychosis populations. As alluded to, current pharmacological interventions have poor efficacy on negative symptoms, and a better understanding of the biological mechanisms and anatomical/functional consequences underlying such symptom presentation may allow for better and more targeted design of future medications. In parallel with an improved description of what is occurring at the neural level, it will be important to test concrete behavioural measures, such as verbal memory, to unravel the effects of therapeutic interventions in early psychosis and other implicated neuropsychiatric conditions on potential improvement of negative symptoms. Improved models of brain-behaviour relationships alongside clinical descriptors of negative symptoms hold promise in translational research and dissipating the status of negative symptoms as a largely unmet therapeutic need in psychotic disorders, especially for more prevalent domains of negative symptoms encompassing avolition, asociality, and anhedonia.

Acknowledgments and Disclosures

The authors would like to thank Raihaan Patel, Gabriel Devenyi, and Min Tae M. Park (Cerebral Imaging Centre, Douglas Mental Health Institute, McGill University, Montreal, Canada) for helping with image processing, quality control procedures, and analysis. We also thank all PEPP-Montreal research staff for their efforts in recruitment and clinical data collection. Finally, the authors are grateful to all patients and families for participating in the study.

The study was supported by operating grants from the Canadian Institutes of Health Research (CIHR; #68961) and the Sackler Foundation to Drs. M. Lepage/A.K. Malla. Salary awards include: Fonds de la Recherche en Santé du Québec (FRSQ) (C.M., M.L., M.M.C, & R.J.), James McGill Professorship (M.L.), and Canada Research Chairs Program (A.K.M.). M. Lepage reports having received financial assistance/compensation for research and educational events from Janssen-Ortho, Eli Lilly, Roche, and Otsuka/Lundbeck Alliance. A.K. Malla reports having received financial assistance/compensation for research and educational activities from Pfizer, Janssen-Ortho, AstraZeneca, and Bristol-Myers Squibb. R. Joober reports having received consultancy honorariums from Pfizer and Janssen-Ortho. All other authors declare no competing conflicts of interest. The funding sources had no role in the design and conduct of the study; collection, management, analysis, and interpretation of the data; preparation, review, or approval of the manuscript; nor in the decision for publication.

4.2. Maturational trajectories of cortical thickness

Age-related cortical thickness trajectories in first episode psychosis patients presenting with early persistent negative symptoms

Carolina Makowski[1,2,3], Michael Bodnar [2,4], Ashok K. Malla[2,4], Ridha Joober[2,4], Martin Lepage[1,2,4]

[1]Integrated Program in Neuroscience, McGill University, Montreal, Canada

[2]Douglas Mental Health University Institute, Department of Psychiatry, McGill University, Montreal, Canada

[3]McGill Centre for Integrative Neuroscience, Montreal Neurological Institute, Montreal, Canada

[4]Prevention and Early Intervention Program for Psychosis, Douglas Mental Health University Institute, McGill University, Montreal, Quebec, Canada

Published in: *npj schizophrenia*. DOI: 10.1038/npjschz.2016.29

Abstract

Recent work has clearly established that early persistent negative symptoms (ePNS) can be observed following a first episode of psychosis (FEP), and can negatively affect functional outcome. There is also evidence for cortical changes associated with ePNS. Given that a FEP often occurs during a period of ongoing complex brain development and maturation, neuroanatomical changes may have a specific age-related component. The current study examines cortical thickness (CT) and trajectories with age using longitudinal structural imaging. Structural T1 volumes were acquired at three time points for ePNS (N=21), PNS due to secondary factors (N=31), non-PNS (N=45) patients, and Controls (N=48). Images were processed using the CIVET pipeline. Linear mixed models were applied to test for the main effects of a) group, b) time, and interactions between c) time and group membership, and d) age and group membership. Compared to the non-PNS and secondary PNS patient groups, the ePNS group showed cortical thinning over time in temporal regions and a thickening with age primarily in prefrontal areas. Early PNS patients also had significantly different linear and quadratic age relationships with CT compared to other groups within cingulate, prefrontal, and temporal cortices. The current study demonstrates that FEP patients with ePNS show significantly different CT trajectories with age. Increased CT may be indicative of disruptions in cortical maturation processes within higher-order brain regions. Individuals with ePNS underline a unique subgroup of FEP patients that are differentiated at the clinical level and who exhibit distinct neurobiological patterns compared to their non-PNS peers.

Introduction

The first episode of psychosis (FEP) marks a critical turning point in the lives of affected youth and is manifested by varying combinations of symptoms at different levels of severity. Early persistent negative symptoms (ePNS) following a FEP are of particular interest due to their high correlation with poor functional outcome (Foussias et al. 2014; Jordan et al. 2014), including low clinical insight and deteriorating premorbid adjustment (Bodnar, Joober, et al. 2016). However, ePNS has been seldom studied due to a wider focus granted to the emergence of later negative symptoms, especially in the course of schizophrenia. Such symptoms can be broadly categorized into general negative symptomatology, and primary, enduring negative symptoms (i.e. the deficit syndrome) (Buchanan 2007; Hovington et al. 2012). Persistent negative symptoms, on the other hand, arguably cover a broader scope compared to the deficit syndrome (Buchanan 2007), and allow for more flexibility in differentiating between primary and secondary negative symptoms over a shorter treatment period, as well as inclusion of less severe thresholds for negative symptom criteria (Mucci et al. 2017). It should be noted that many studies do not make this distinction between primary or secondary, or refer to these terms without acknowledging limitations of the lack of etiological basis for such symptoms in the majority of clinical practice. Thus, the principal focus of this study will rest upon the extraction of early PNS in a well-characterized clinical sample of FEP patients, including both affective and non-affective diagnoses.

From a neuroanatomical perspective, there is evidence to suggest there are gray matter abnormalities specific to patients with PNS (Bodnar et al. 2014; Galderisi et al. 2015). Although relatively fewer studies have been conducted to disentangle the neurobiological underpinnings of ePNS specifically, empirical evidence for progressive brain changes in FEP has been reported in several longitudinal studies (Andreasen et al. 2011; Cannon et al. 2015) and reviews (Olabi et al.

2011; Gong et al. 2016). However, many studies have reported inconsistent, even null findings (Nesvåg et al. 2012; Roiz-Santiáñez et al. 2015; Haukvik et al. 2016). Nesväg and colleagues (2016) commented that over a five-year period, there were no meaningful differences in cortical thickness (CT), volume, or subcortical structures in chronic schizophrenia patients compared to healthy controls. A more recent study restricted their longitudinal investigation to a three-year period, and commented that regardless of antipsychotic medication treatment, no CT changes could be observed in their sample of schizophrenia spectrum patients (Roiz-Santiáñez et al. 2015). It is clear there is still a great need to further disentangle the neural correlates of specific symptom constructs that are linked to poor prognosis and outcome, such as ePNS. Supporting this, a recent review reported disparities in reports of neurobiological changes underlying negative symptoms across different research groups (Galderisi et al. 2015). The review also encouraged future studies to distinguish between different types of negative symptoms after a FEP; for instance, comparing primary and secondary PNS (the latter having concurrent depressive, positive, and/or extrapyramidal symptomatology) (Buchanan 2007; Hovington et al. 2012).

Recent efforts have been put forth to delineate cross-sectional cortical thickness (CT) correlates of patient subgroups based on symptoms in schizophrenia or early psychosis. Nenadic and colleagues (2015) separated a sample of 87 schizophrenia patients into three groups (i.e. predominant negative, disorganized and paranoid), reporting the most extensive cortical thinning in the negative symptom group. Mørch-Johnsen et al. (2015) set their focus on persistent apathy, reporting thinner cortex within the left orbitofrontal and anterior cingulate cortices in apathetic FEP patients compared to the rest of their patient sample. Our group also reported CT findings within similar regions, in addition to elucidating patterns of cortical thinning within parahippocampal and superior temporal gyri, and the temporoparietal junction in FEP patients

presenting with ePNS, compared to their non-PNS peers (Bodnar et al. 2014). However all three of these studies were cross-sectional, thus no conclusions can be drawn about progressive changes in cortical thickness with respect to negative symptomatology.

It is important to note that many CT studies control for age within analysis, due to the well-documented normative progression of cortical thinning across age throughout adulthood (Storsve et al. 2014). However, many studies reporting on FEP incorporate samples with ages spanning from adolescence to adulthood, without inquiring how reported findings change at this critical developmental transition. One exception can be found in the work of van Haren and colleagues (2011), probing the degree of cortical thinning attributable to normative aging processes in enduring schizophrenia, based on age of onset. A recent investigation by Pina-Camacho et al. (2015) also incorporated age effects within CT analyses applied to 196 FEP patients, and revealed cortical properties specific to an onset of psychosis before 20 years of age, where significant age effects were manifested differentially in a regional and diagnostic-specific manner. Hence, age is an important factor to consider when parsing apart cortical findings within different groups of FEP patients given ongoing neurodevelopment occurring during late adolescence/early adulthood.

This study aims to address differential progression of ePNS after a FEP at the neuroanatomical level, applying whole-brain CT analyses to a large sample of longitudinally followed FEP patients. First, the main effects of group (ePNS, non-ePNS, and Controls) and scan time (Baseline, one- and two-year follow-up) were examined using linear mixed models. The effect of age on CT in ePNS and non-ePNS patients was then examined, and compared to normative cortical thinning trajectories within a healthy control group. We also assessed specificity of CT results to the ePNS group by comparing to a subset of non-ePNS patients that presented with persistent negative symptoms due to secondary factors (sPNS). We hypothesized: 1) greater

cortical thinning over time in the ePNS group compared to non-ePNS patients (including sPNS) and controls, in higher cognitive regions such as the prefrontal cortex, temporoparietal junction, and parahippocampal gyrus; 2) younger FEP patients with ePNS would show steeper rates of change in CT compared to non-ePNS patients; and 3) non-ePNS patients would show cortical thinning across age similar to healthy controls.

Methods

Participants. All patients were recruited from the Prevention and Early Intervention Program for Psychoses (PEPP-Montreal), at the Douglas Institute in Montreal, Canada, and were part of a longitudinal naturalistic outcome study. PEPP is a specialized early intervention service for individuals between the ages of 14-35 who have recently experienced a FEP within a local catchment area of Southwest Montreal. Details are outlined in Iyer et al. (2015). Briefly, the program involves a comprehensive approach with intensive medical and psychosocial interventions provided within the context of a modified assertive case management program. Inclusion criteria at PEPP include a diagnosis of affective or non-affective psychosis, an IQ above 70, and no past antipsychotic medication treatment for more than one month.

Neuroimaging component. The neuroimaging study began in 2003 and has spanned over a decade, comprising three scheduled visits: baseline, one-year follow-up (FUP1), and two-year follow-up (FUP2). Forty-two patients and forty-six controls dropped out of the study after baseline, leaving a total of 100 patients and 48 healthy controls with at least two scans. Three patients were not included in subsequent analysis due to insufficient longitudinal symptom data (2 cases) or non-compliance to the time line of the study (1 case). Only individuals ages 18 and over were

considered for the neuroimaging portion of the study, as well as clinically stable status and no major medical disorders. Exclusion criteria included a history of neurological illnesses and head trauma resulting in loss of consciousness that could affect cognition, presence of neurological disorder determined by medical record examination, lifetime diagnosis of substance dependence, and/or any potential contraindication for the MR scan.

Non-clinical healthy controls were recruited through advertisements within the same local catchment area. In addition to exclusion criteria listed for FEP patients, controls were excluded if they had any current/past history of Axis I disorders, and/or a first-degree family member suffering from schizophrenia or related schizophrenia spectrum psychosis. All participants provided written informed consent, and the research protocol was approved by the Douglas Mental Health University Institute human ethics review board.

Clinical assessment and demographic data. Diagnosis for each patient was made on the basis of structured clinical interview for DSM-IV (First et al. 1998), performed by a trained interviewer, and confirmed by at least one senior psychiatrist (RJ or AM). Depression and anxiety symptoms were assessed with the Calgary Depression Scale for Schizophrenia (CDSS) (Addington et al. 1990) and Hamilton Anxiety Rating Scale (HARS) (Hamilton 1959), respectively. Positive and negative symptoms were assessed with the Scale for the Assessment of Negative Symptoms (SANS) (Andreasen 1984a) and Scale for the Assessment of Positive Symptoms (SAPS) (Andreasen 1984b). Duration of untreated psychosis (DUP) was also assessed, referring to the period of time in weeks between onset of psychotic symptoms to adequate treatment with antipsychotics, as described elsewhere (Bodnar, Malla, et al. 2016). Antipsychotic medication dosages were converted to chlorpromazine equivalents according to the literature (Leucht et al.

2015), and multiplied by percent medication adherence (Cassidy et al. 2010). For both controls and patients, parental socioeconomic status (SES) was estimated using the Hollingshead SES Rating Scale (Hollingshead 1965), and handedness determined with the Edinburgh Handedness Inventory (Oldfield 1971). Due to a change in the neuropsychological test battery used mid-way through the study, Full Scale IQ was assessed with the Weschler Adult Intelligence Scale (WAIS-III) for a proportion of subjects, and the Weschler Abbreviated Scale of Intelligence (WASI) for the remaining sample (Weschler 1997, 1999).

Early PNS were defined according to the following criteria: (1) global rating of moderate or more on at least one negative symptom as measured by the SANS, (2) global rating of mild or less on all positive symptoms as measured by the SAPS, (3) a total score of 4 or less on the CDSS, (4) absence of extrapyramidal symptoms requiring anticholinergic treatment, and (5) all above criteria are continuously met for a period of at least six months (Hovington et al. 2012; Bodnar et al. 2014). Patients were classified as having PNS due to secondary factors, or sPNS, if criteria 2, 3 and/or 4 were not met.

MRI acquisition. All scanning was carried out at the Montreal Neurological Institute (MNI) on a 1.5 T Siemens Sonata whole body MRI system. Structural T1 volumes were acquired for each participant using a three dimensional gradient echo pulse sequence with sagittal volume excitation (repetition time=22 ms, echo time=9.2 ms, flip angle=30, 180 1 mm contiguous sagittal slices). The rectangular field of view (FOV) for the images was 204 mm (SI) 256 mm (AP). Information about quality control is detailed in Supplementary Methods in Appendix-II.

Post-processing. All raw scans that passed quality control (QC) were submitted to the CIVET pipeline (Version 2.0.0: http://www.bic.mni.mcgill.ca/ServicesSoftware/CIVET; (Zijdenbos et al. 2002; Ad-Dab'bagh et al. 2006). Detailed steps have been described by our group elsewhere (Bodnar et al. 2014) and include: 1) Registration of T1-weighted images to a standardized space and correction for non-uniformity artefacts, 2) Parcellation of gray matter, white matter, cerebral spinal fluid, and background noise, 3) Extraction of high-resolution gray and white matter surfaces comprised of 40,962 vertices within each hemisphere, 4) Non-linear registration of cortical surfaces to a high-resolution template for inter-subject correspondence of vertices, 5) Reverse transformation (initially done in step 1) to estimate CT in native space for each subject using the t-link metric and 6) smoothing the data with a 30-millimeter kernel, which has been previously shown to be an optimal level of smoothing when utilizing the t-link metric (Lerch and Evans 2005). All volumes, with the exception of one scan, passed through the pipeline and QC process, due to minimization of error within initial QC of raw scans. All CIVET outputs were quality controlled using the CBRAIN platform (Sherif et al. 2014), of which significant mask errors and/or minor pipeline errors were corrected through in-house scripts if feasible. See Appendix-II for quality control procedures.

Statistical analyses. Demographic and clinical variables (with a single time point) were analysed with one-way ANOVAs for continuous variables or Kruskall-Wallis H tests for nominal variables. For IQ, an ANCOVA was used to covary for test version. For SAPS/SANS, Generalized Estimating Equations (GEE) were used to assess differences between FEP groups across clinical time-points. Antipsychotic dosages, CDSS scores, and the time period in months between scan and nearest symptom evaluation were assessed between the three patient groups at each scan-time

point, using one-way ANOVAs for normally distributed variables (post hoc Tukey's HSD test), and Kruskall-Wallis H-tests for nonparametric variables (post hoc Mann-Whitney U-tests). Relationship between SANS totals at each scanning timepoint and DUP was estimated using Spearman's rank correlations. Analyses of clinical variables were conducted using PASW Statistics 21 (SPSS inc., 2009, Chicago, IL, USA) and were two-tailed with a critical p-value of 0.05.

Cortical thickness analyses. To assess differences in CT between ePNS, non-PNS and healthy control groups, statistics were performed across all 81,924 vertices of the cortical surface using the SurfStat toolbox within Matlab (http://www.math.mcgill.ca/keith/surfstat/). First, the main effect of group was tested using the linear mixed effects model outlined below, controlling for age, sex, handedness, and a proxy measure of Brain Volume (ProxyBV):

$$Y = intercept + d_1 + \beta_1(Group) + \beta_2(Age) + \beta_3(Sex) + \beta_4(Handedness) + \beta_5(ProxyBV) + random(Subject) + \epsilon$$

where Y represents cortical thickness, d_1 is the random within-subjects effect, $\beta_{1\text{-}5}$ represent regression coefficients, and ε is residual error. ProxyBV (subcortical gray matter + white matter + cerebrospinal fluid volume) was entered as a covariate, based on rationale provided by Karama et al (2011). Briefly, this variable excludes GM volumes, which would otherwise account for ~40% of total intracranial volume and is highly correlated with mean CT. The proxy measure of brain volume bypasses the potential of removing the effect of interest, while still controlling for important confounds associated with brain volume. To test for a main effect of time, data was

filtered to examine each group separately, and β_1(Group) was replaced with β_1(Time) in the mixed effects model. To test for the interaction between scan time (Baseline, one- and two-year follow-ups) and group, two additional terms were added: "β_6(Time)" and "β_7(Group*Time)".

Finally, we tested the interaction between age and group membership on cortical thickness. Due to the idea that cortical thickness may not change linearly over time within an individual (Raznahan, Shaw, et al. 2011; Aubert-Broche et al. 2013) linear and quadratic effects of age (i.e. age, age^2) were included in the mixed effects models. Higher-order polynomial terms were not tested. The age variable was mean-centered for all analyses. We used a forward selection approach; that is, the simplest model was tested for first (linear age effect). For linear age effects, "β_6(Group*Age)" was added to the original model outlined above. For quadratic effects of age, additional terms were incorporated: "β_7(Age^2)" and "β_8(Age^2*Group)", and tested for separately. To test whether a linear or quadratic age term provided the best fit for significant regions, parameters of each model were estimated with theoretical likelihood ratio tests. To compare different models of age directly, the Akaike Information Criterion (AIC) was applied to obtain log-likelihood values (Hamparsum 1987). The model with the best fit for the region tested has a smaller AIC value. For all analyses, statistical maps were thresholded and multiple comparisons were taken into account using random field theory (RFT) for non-isotropic images, with an uncorrected p-value of p=0.005 (Worsley et al. 2004). This procedure is implemented within SurfStat and limits the chance of reporting a false positive finding to below 0.05. Given the conservative nature of RFT, exploratory analyses were also performed using a more liberal uncorrected threshold, p=0.01. For group comparisons, analyses were initially run contrasting ePNS and all non-ePNS patients. A subsequent round of analyses then examined potential differences between sPNS, ePNS and remaining non-PNS patients. Finally, to ensure any significant results could not otherwise be

explained by exposure to antipsychotic medication, a covariate was added to all linear mixed effects models presented above to control for chlorpromazine equivalent dosages multiplied by medication adherence at each patient's scan.

Results

Socio-demographic and clinical results. In the FEP group, baseline scans were performed on average 4.0 (SD=1.9) months from entry into PEPP. For the entire group, including controls, inter-scan intervals were approximately 13.1 (SD=1.3) months between baseline and FUP1, and 12.6 (SD=1.7) months between FUP1 and FUP2. Nine participants (6 FEP, 3 controls) were not scanned at FUP1, and had an average interscan interval of 27.0 (SD=3.2) months between FUP2 and baseline. The groups did not significantly differ in sex ratio, handedness, parental SES, or age at scanning time, as seen in **Table 4.3**. However, controls significantly differed from all patient groups on Full-Scale IQ (not explained by test version) and years of education. Within the three patient groups, there were no significant differences in CDSS scores, time elapsed between the MRI scan and symptom evaluation across all scanning timepoints, nor duration of untreated psychosis/illness. Amount of antipsychotic prescribed and anxiety levels (as assessed by the HARS) were significantly higher for sPNS patients, compared to non-PNS, only at Scan 2.

		FEP						Controls		Statistic	df	*p*-value	Post-hoc
		ePNS		Non-ePNS									
				sPNS		Non-PNS							
		N	**%**	**N**	**%**	**N**	**%**	**N**	**%**				
General Demographics & Clinical Information	N (+ percent having all three scans)	**21**	86	**31**	52	**45**	58	**48**	58				
	Male	15	71	22	71	32	71	28	58	χ^2= 2.4	3	0.5	-
	Right Handed	17	81	26	84	39	87	42	88	χ^2= 0.6	3	0.9	-
	Diagnosis												
	Schizophrenia/ Schizophreniform	16	76.2	27	87.1	25	55.6						
	Affective Disorder	3	14.3	1	3.2	15	33.3						
	Delusional Disorder	0	0.0	1	3.2	2	4.4						
	Psychosis Not Otherwise Specified	2	9.5	2	6.5	3	6.7						
		Mean	**SD**	**Mean**	**SD**	**Mean**	**SD**	**Mean**	**SD**				
	Education in Years	11.1	2.5	11.7	2.4	12.6	2.4	14.2	2.5	F=10.8	3, 144	<0.0001	1, 2, 3 < 4
	Socioeconomic Status	3.4 [16]	1.0	3.3 [30]	1.2	3.0 [42]	1.0	3.3 [45]	0.9	χ^2= 5.4	3	0.1	-
	Full Scale IQ[1]	96.9	15.3	98.4	17.2	100.3	14.1	111.1 [46]	14.8	F=6.9	3, 142	<0.0001	1, 2, 3 < 4
	Duration Untreated Psychosis (weeks)	45.4 [20]	59.2	57.1	100.5	83.6 [43]	170.5			χ^2= 0.1	2	0.9	-
	Duration Untreated Illness (years)	5.3 [20]	4.4	7.8 [30]	6.5	7.2 [42]	7.1			χ^2= 1.2	2	0.6	-
Scan 1	Age	23.2	3.6	24.7	4.1	24.6	4.6	23.8	3.4	F=0.9	3, 144	0.4	-
	SANS totals	25.4	9.3	23.2	12.0	14.2	10.5			F=10.5	2, 96	<0.0001	1, 2>3
	Affective Flattening	7.5	6.1	7.7	6.0	4.4	4.8			F=4.0	2, 96	0.021	1, 2>3
	Alogia	3.2	2.7	2.1	3.4	1.0	1.9			χ^2=10.5	2	0.005	1>3
	Avolition/Apathy	6.8	2.3	5.8	3.2	3.8	2.7			χ^2=18.0	2	<0.001	1, 2>3
	Anhedonia/Asocality	7.9	2.5	7.6	4.1	4.8	3.5			F=8.3	2, 96	<0.001	1, 2>3
	SAPS totals	8.2	10.2	17.3	15.1	4.0	5.4			χ^2= 25.5	2	<0.0001	2>1, 3
	CDSS	2.4	2.7	3	3.2	1.7 [44]	2.4			χ^2= 3.2	2	0.2	-
	HARS	4.2	5.1	5.5	5.9	3.5	5.2			χ^2=5.22	2	0.074	-
	CPZ equivalent (in mg)	758.4	671.3	944.7	838.8	776.2	700			χ^2= 0.6	2	0.7	-
	Adherence (%)	86.6	21.3	86.2	20.9	84.9	27.3			χ^2= 0.4	2	0.8	-
	Window |Scan - Symptom Eval| (months)	0.6	0.4	0.8	0.5	0.7	0.6			F=0.5	2, 96	0.6	-
		N=19		**N=29**		**N=42**		**N=45**					
Scan 2	Age	24.3	3.8	25.7	4.2	25.5	4.3	24.8	3.4	F=0.7	3, 134	0.5	-
	SANS totals	13.5	10.4	22.0	10.9	8.0	9.3			F=18.2	2, 89	<0.0001	1, 2>3
	Affective Flattening	5.7	5.9	7.8	5.3	2.2	3.5			χ^2=23.6	2	<0.001	1, 2>3
	Alogia	1.7	2.2	2.4	2.7	1.0	1.9			χ^2=8.3	2	0.015	2>3
	Avolition/Apathy	5.9	3.7	4.9	4.0	1.7	2.4			F=14.2	2, 89	<0.001	1, 2>3
	Anhedonia/Asocality	6.6	4.2	6.9	4.4	3.1	3.4			F=10.0	2, 89	<0.001	1, 2>3
	SAPS totals	5.9	6.2	13.5	10.4	3.5	8.6			χ^2=24.7	2	<0.0001	2>1, 3
	CDSS	1.0	1.5	1.8 [28]	3	1.4	2.7			χ^2=1.4	2	0.5	-
	HARS	3.8	6.0	4.9 [27]	4.3	2.0	2.8			χ^2= 8.12	2	0.017	2>3
	CPZ equivalent (in mg)	2875.2	2059.7	4378.7	3291.3	2652.4	2160.4			χ^2=10.5	2	0.005[2]	-
	Adherence (%)	87.0	16.0	78.1	22	81.2	25.2			χ^2=1.9	2	0.4	-
	Window |Scan - Symptom Eval| (months)	1.8	1.5	2	1.7	1.8	1.2			χ^2= 0.2	2	0.9	-
		N=20		**N=18**		**N=30**		**N=31**					
Scan 3	Age	25.4	3.7	26.5	3.8	26.2	4.4	26.9	3.3	F=0.6	3, 98	0.6	-
	SANS totals	19.8	11.1	17.2	16.5	6.7	8.5			F=8.6	2, 67	<0.0001	1, 2>3
	Affective Flattening	5.4	5.5	6.6	6.6	1.7	3.0			F=6.4	2, 67	0.003	1, 2>3
	Alogia	2.9	3.0	2.0	3.2	1.0	1.8			χ^2=6.0	2	0.05	1>3
	Avolition/Apathy	5.2	2.9	3.7	4.2	1.6	2.2			χ^2=15.1	2	0.001	1, 2>3
	Anhedonia/Asocality	6.4	3.9	4.9	4.7	2.4	3.1			χ^2=14.4	2	0.001	1, 2>3
	SAPS totals	7.0	10.3	15.2	20.6	4.6	8.0			χ^2=4.5	2	0.09	-
	CDSS	2.5 [18]	3.3	2.3	2.6	1.5 [28]	2.1			χ^2= 1.2	2	0.6	-
	HARS	3.0 [19]	4.3	5.9	7.6	2.8 [28]	3.4			χ^2=1.98	2	0.371	-
	CPZ equivalent (in mg)	4216.5	3906.2	6540.4	6243.9	5060.3	4948.9			χ^2=1.8	2	0.4	-
	Adherence (%)	78.3	26.2	75	30.5	77.9	28.6			χ^2=0.07	2	0.97	-
	Window |Scan - Symptom Eval| (months)	1.0	1.9	0.5	0.7	0.4	0.7			χ^2= 0.7	2	0.7	-

Table 4.3. Demographic and clinical information for longitudinal sample.
General Demographics for whole sample are presented, followed by information corresponding to each scan. Scan 1 was conducted around baseline, Scan 2 represents one-year follow-up, and Scan 3 represents two-year follow-up. All data represented as Mean (SD), unless otherwise specified. Square brackets [] include adjusted sample size included in statistical analysis due to missing datapoints. Note, all antipsychotic totals are presented as cumulative chlorpromazine equivalents. SAPS/SANS totals are presented as mean scores of the sum of item-level scores from each scale; SANS totals exclude the "attention" subscale. Item-level scores for each of the four SANS subscales per timepoint are italicized. Post-hoc analyses are coded as follows: 1=ePNS; 2=sPNS; 3=Non-PNS; 4=Controls.

[1] IQ means are presented as adjusted means, covaried by test version (WAIS-III vs. WASI). There was no difference between different test versions on IQ ($F_{1,142}$=1.15, p=0.29).
[2]Post-hoc analyses indicated that sPNS patients were prescribed significantly more antipsychotic medication (in CPZ equivalent dosage) cumulatively compared to non-PNS patients at Scan 2. Further tests revealed that when taking into consideration medication adherence (multiplying CPZ equivalent by percent adherence), only a trend-like difference existed between groups ($\chi^2_{(2)}$=5.0, p=0.08). No difference between ePNS and the other two FEP subgroups at Scan 2.
Abbreviations: ePNS, early persistent negative symptoms. sPNS, persistent negative symptoms due to secondary factors. FUP, follow-up. SAPS/SANS, Scale for Assessment of Positive/Negative Symptoms. CPZ, chlorpromazine.

With respect to negative symptoms, the ePNS and sPNS groups had higher SANS scores compared to other non-PNS patients across all timepoints. The sPNS patient subgroup also had significantly higher SAPS scores compared to the other two patient groups across most clinical timepoints (with the exception of the last two-year followup assessment). See **Figure 4.4** for depiction of SAPS/SANS score for each FEP subgroup across clinical timepoints and **Table 4.4** for corresponding GEE statistics. Finally, no significant association between DUP and SANS totals pertaining to each scan timepoint was observed (Scan 1: r=-0.095, p=0.41; Scan 2: r=0.041, p=0.71; Scan 3: r=0.14, p=0.27).

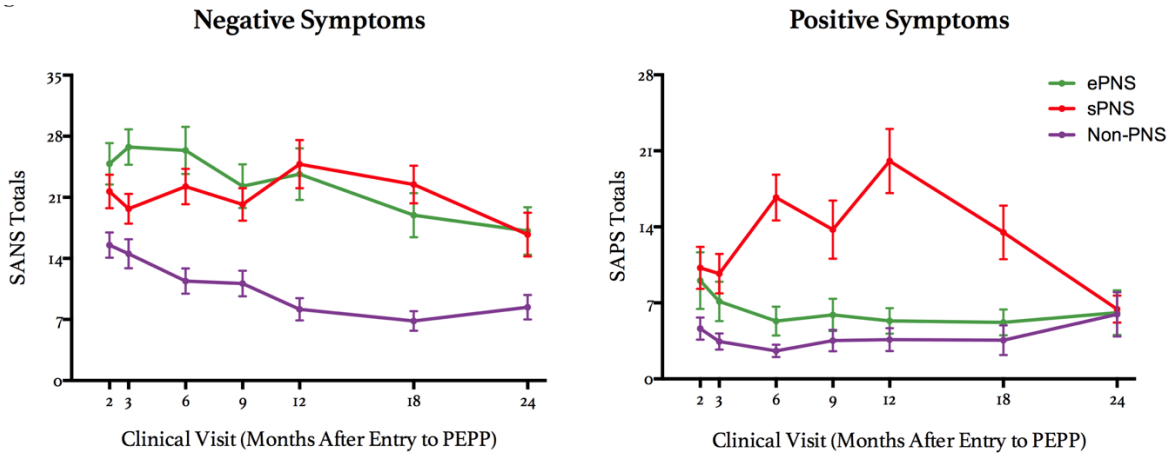

Figure 4.4. Mean curves for SAPS/SANS scores across clinical visits in FEP sub-groups. Data presented as mean ± SD. See Table 4.4 for corresponding statistics.

	ePNS		sPNS		non-PNS		Omnibus[1]		post-hoc[2]
	N	Mean (SD)	N	Mean (SD)	N	Mean (SD)	$\chi^2_{(2)}$	*p*	
2									
SANS	20	24.85 (10.58)	30	21.67 (10.62)	44	15.52 (9.59)	14.29	<0.0001	ePNS, sPNS > non-PNS
SAPS		9.05 (11.69)		10.23 (10.63)		4.64 (6.72)	8.16	0.017	sPNS > non-PNS
3									
SANS	21	26.76 (9.34)	30	19.7 (9.40)	43	14.5 (10.96)	22.36	<0.0001	ePNS > sPNS > non-PNS
SAPS		7.14 (8.34)		9.7 (9.97)		3.44 (4.92)	12.59	0.002	sPNS > non-PNS
6									
SANS	18	26.39 (11.52)	30	22.23 (11.14)	41	11.41 (9.34)	34.57	<0.0001	ePNS, sPNS > non-PNS
SAPS		5.33 (5.70)		16.7 (11.52)		2.59 (3.64)	44.98	<0.0001	sPNS > ePNS, non-PNS
9									
SANS	18	22.28 (10.62)	28	20.18 (9.84)	45	11.13 (9.87)	23.1	<0.0001	ePNS, sPNS > non-PNS
SAPS		5.89 (6.33)		13.75 (14.18)		3.53 (6.68)	13.64	0.001	sPNS > ePNS, non-PNS
12									
SANS	20	23.65 (13.24)	27	24.82 (14.46)	46	8.17 (8.68)	46.85	<0.0001	ePNS, sPNS > non-PNS
SAPS		5.35 (5.26)		20.07 (15.39)		3.61 (7.16)	28.42	<0.0001	sPNS > ePNS, non-PNS
18									
SANS	20	18.95 (11.28)	29	22.48 (11.61)	43	6.84 (7.43)	53.41	<0.0001	ePNS, sPNS > non-PNS
SAPS		5.20 (5.34)		13.48 (13.31)		3.56 (9.01)	12.92	0.002	sPNS > ePNS, non-PNS
24									
SANS	20	17.15 (12.22)	23	16.74 (12.04)	38	8.40 (8.66)	14.07	0.001	ePNS, sPNS > non-PNS
SAPS		6.1 (9.20)		6.44 (5.97)	37	5.95 (12.37)	0.052	0.98	-

Table 4.4. Generalized estimating equations statistics for negative and positive symptoms.
Negative and positive symptoms represent sum of item-level scores as assessed by the SANS and SAPS, respectively. Note, SANS total excludes the "attention" subscale. Left-hand column organizes statistics by clinical visit, relative to entry to PEPP-Montreal clinic (i.e. 2/3/6/9/12/18/24-month visits).
[1]For global omnibus tests, there was a significant main effect of group ($\chi^2_{(2)}$=65.31, p<0.001), time ($\chi^2_{(6)}$=24.02, p<0.001), and group*time interaction ($\chi^2_{(12)}$=32.20, p=0.001) on SANS scores. GEE analyses of SAPS scores also revealed a significant main effect of group ($\chi^2_{(2)}$=40.03, p<0.0001), and group*time interaction ($\chi^2_{(12)}$=34.69, p=0.001). No significant effect of time was found for SAPS scores. Omnibus results presented are "cross-sectional" per timepoint, for ease of understanding.
[2]Bonferroni corrected, p<0.025.
Abbrevations: ePNS, early persistent negative symptoms. sPNS, persistent negative symptoms due to secondary factors; SANS, Scale for the Assessment of Negative Symptoms; SAPS, Scale for the Assessment of Positive Symptoms.

Cortical thickness analyses.

Main effect of group. There was a significant cluster of cortical thinning in ePNS patients compared to the entire non-ePNS sample, within the left inferior temporal/fusiform gyrus, (Brodmann Area [BA] 37). No significant group differences between controls and FEP groups were found. See **Figure 4.5A** for details.

Main effect of timepoint. The ePNS group exhibited significant cortical thinning from Baseline to FUP2 within right middle temporal gyrus (BA 22). The non-ePNS group displayed increased CT from Baseline to FUP1 in left dorsal pre- and post-central gyri (BA 1-5), which upon further analysis, was found to be driven by the sPNS subgroup. See **Figure 4.5B-C** for details.

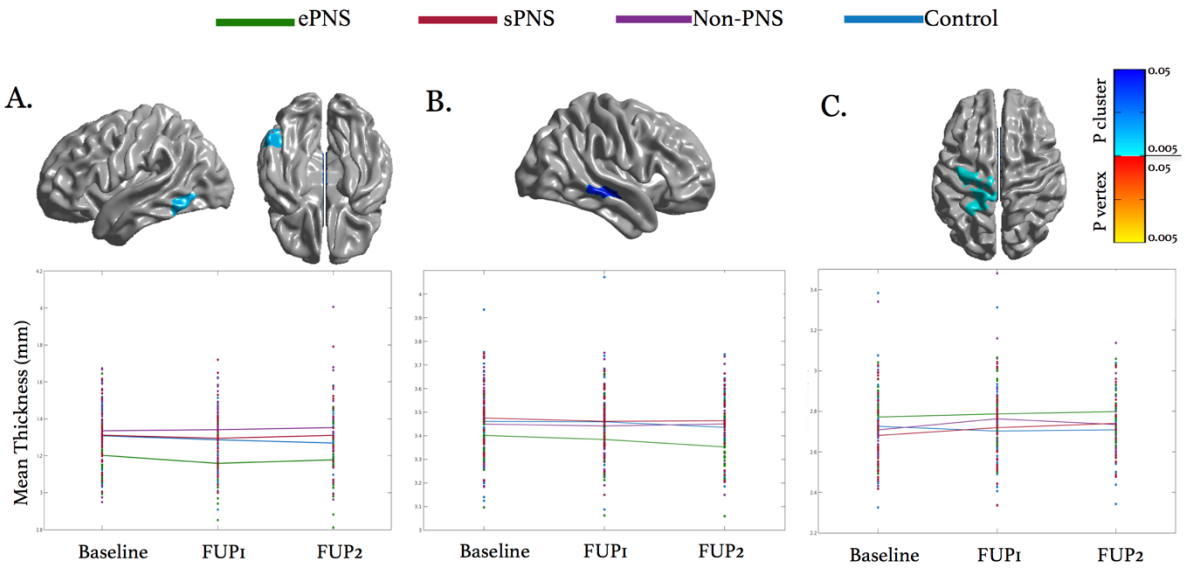

Figure 4.5. Main effects of group and time.
A. Significant cortical thinning in ePNS (main effect of group) compared to the whole non-PNS group was observed in left inferior temporal region (136 df). Plot of mean thickness of peak cluster depicted per group across three scanning timepoints. **B.** ePNS group shows significant cortical thinning from baseline to FUP2 in right middle temporal gyrus (52 df). **C.** Increases in cortical thickness from Baseline to FUP1 are seen in the Non-PNS group within the left dorsal precentral and postcentral gyri (137 df), with this increase largely driven by the sPNS subgroup. Blue colour bar represents significant RFT-thresholded clusters (no significant results at the vertex level). All statistics are projected on an average surface template generated from the analyzed sample.

Group by time interaction. No significant group*time interaction on CT was found for any contrasts comparing ePNS and non-ePNS patients and controls.

Group by age interaction: linear effects of age. Widespread frontal regions showed an interaction effect of age*group, such that the ePNS group showed a positive effect with age on CT compared to the non-ePNS sample. Further exploration using a reduced threshold of p-uncorrected=0.01 revealed significant clusters of increased CT with age within left dorsolateral prefrontal cortex (DLPFC, BA Area 9) and left inferior orbitofrontal cortex (BA 10/11) in the ePNS group compared to non-PNS. When directly comparing the ePNS and sPNS patient groups, ePNS showed a significantly different and positive relationship with age in right anterior frontal regions/orbitofrontal gyrus (BA 10/11) with p-uncorrected=0.005. Mean CT was extracted across vertices comprising 1) left DLPFC, 2) left and 3) right anterior/orbital frontal clusters. Regression slopes depicting relationship between age and mean CT for all three ROIs revealed a significantly different and positive slope for ePNS compared to sPNS, non-PNS patient groups and controls. **Figure 4.6** illustrates clusters thresholded with RFT and corresponding plots. Annual rates of change detailed in Table 8.3 of Appendix-II. No other group contrasts showed a significant linear interaction with age, with the exception of direct comparisons between sPNS and the remaining non-PNS patients, where the sPNS group showed significant CT increases with age in the left postcentral gyrus compared to remaining non-PNS patients, as depicted in Figure 8.3 of Appendix-II.

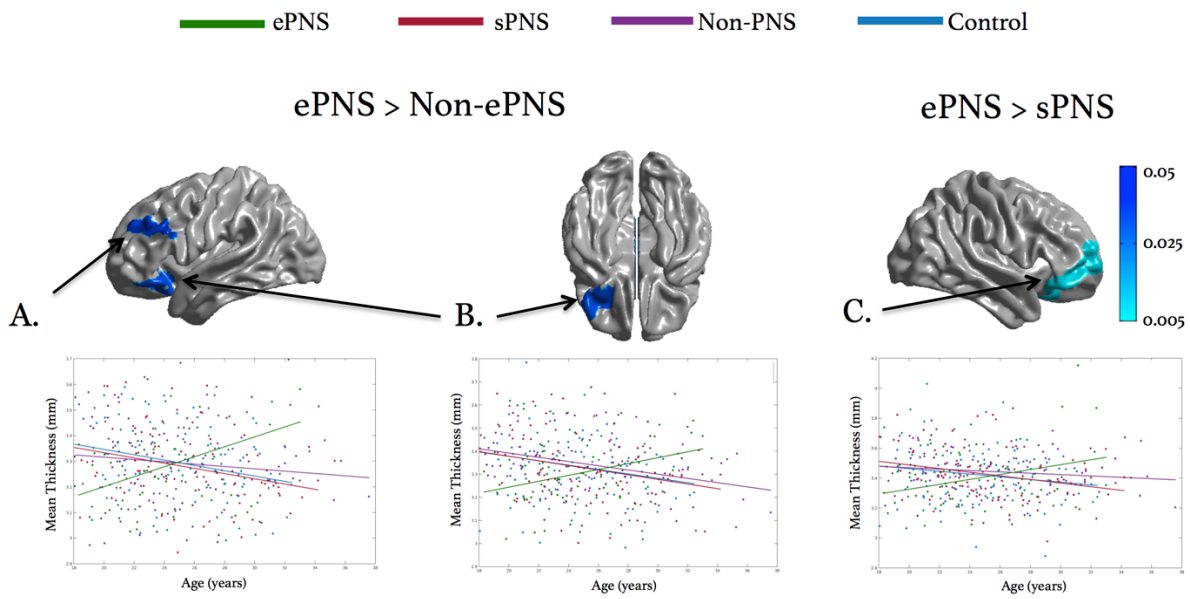

Figure 4.6. Age*group interaction: linear effects of age.
Significant prefrontal regions of interest (ROIs) extracted from examination of significant age*group interaction effect, in relation to ePNS group. ROIs "**A.**" and "**B.**" compare ePNS and entire non-PNS group, whereas "**C.**" compares ePNS and sPNS subgroups. Plots of mean cortical thickness for each ROI comparing all three patient groups and controls depicted directly below each RFT-thresholded brain map. Omnibus statistics for regions of interest are as follows: **A.** $F_{(3,371)}=9.09$, $p<0.001$; **B.** $F_{(3,371)}=6.49$, $p<0.001$; **C.** $F_{(3,371)}=5.26$, $p<0.001$. Post-hoc analyses revealed that the ePNS group had a significantly different regression slope from all other groups (controls, sPNS, and non-PNS without sPNS), with all p's ≤ 0.001. Annual rates of change after age 18 in Controls, sPNS, and Non-PNS groups amount to approximately 0.32% CT loss per year across the prefrontal ROIs. By contrast, ePNS patients showed an annual increase in CT of 0.37% per year. Blue colour bar represents significant RFT-thresholded clusters with p-corrected=0.05 (no significant results at the vertex level). All statistics are projected on an average surface template generated from the analyzed sample.

Group by age interaction: quadratic effects of age. Significant group*age^2 interactions on CT were found between the non-ePNS and ePNS patient groups, such that the ePNS group showed significantly positive quadratic effects of age within the right middle cingulate (and extending dorsomedially) with p-uncorrected=0.005 (BA 24), and a more posterior cluster of the left dorsolateral prefrontal cortex, encompassing pre-supplementary motor area (independent of the first DLPFC cluster described with predominantly linear effects of age) with p-uncorrected=0.01, in comparison to non-ePNS patients and controls. Furthermore, a significant cluster emerged

within the left inferior temporal gyrus (BA 37) with a significantly different and positive quadratic relationship of CT with age in the ePNS group compared to the sPNS group. See **Figure 4.7** for thresholded maps and plots. These three regions were all better explained by inclusion of a quadratic age term, as opposed to linear, as indicated by comparison of AIC values and significance testing with likelihood ratio tests. See Table 8.4 of Appendix-II. Furthermore, as seen in Table 8.5 of Appendix-II, significant results were not altered after covarying for antipsychotic dosage.

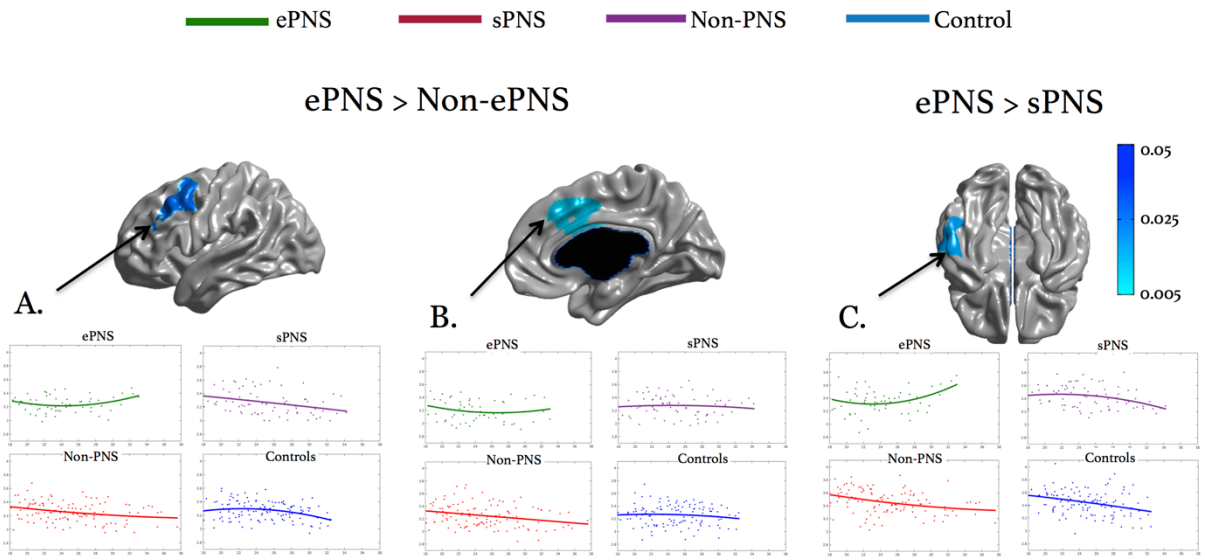

Figure 4.7. Age^2*group interaction: quadratic effects of age.
Significant prefrontal regions of interest (ROIs) extracted from examination of significant age^2*group interaction effect, in relation to ePNS group. ROIs "**A.**" and **"B.**" compare ePNS and entire non-ePNS group, whereas **"C."** compares ePNS and sPNS subgroups. Each of the three ROIs represent regions of cortical thickness with significantly different and positive quadratic relationships with age in the ePNS group only, with p-corrected<0.05. Blue colour bar represents significant RFT-thresholded clusters with p-corrected=0.05 (no significant results at the vertex level). All statistics are projected on an average surface template generated from the analyzed sample.

Discussion

The current study examined structural neuroanatomical patterns in clinically well-characterized FEP patients with ePNS between the ages of 18-35. Significant differences in CT were found at the group level across a two-year follow-up period, and longitudinally as a function of age compared to other non-ePNS patients and controls. Patients with ePNS showed significantly thinner cortex within the left inferior temporal gyrus compared to non-ePNS patients and time-specific cortical thinning over a two-year period in the right middle temporal cortex. Observed changes within bilateral temporal cortices corroborate previous studies implicating progressive brain changes within the temporal lobes in FEP (Andreasen et al. 2011; Cannon et al. 2015), and further lend support to previous findings from our research group examining the ePNS construct and its unique neuroanatomical correlates (Benoit et al. 2012; Bodnar et al. 2014; Hovington et al. 2015). On the other hand, non-ePNS patients showed a different pattern of CT change over one-year followup, with increased CT in left motor areas (i.e. dorsal pre- and post-central gyri), driven by the sPNS subgroup. This CT increase is speculated to occur as a consequence of positive symptoms, which has been supported previously by findings of a positive correlation between post-central gyri-volumes and SAPS scores (Ferro et al. 2015).

We also explored the effects of age on CT in FEP patient subgroups, motivated by the idea that neurodevelopmental processes are ongoing throughout late adolescence and early adulthood, and may be altered in patients. Linear and quadratic models of age yielded clear differential patterns of CT across age unique to ePNS, such that CT increased linearly with age in left DLPFC and bilateral orbitofrontal cortices in this group, and positive quadratic age effects were found within a second left DLPFC cluster (encompassing pre-supplementary motor area), right middle cingulate (extending dorsomedially), and left inferior temporal cortex. In a similar vein of

exploration, Ecker et al. (2014) reported significantly opposing CT trajectories with age in a sample of youth with autism spectrum disorder (ages 7-25), finding comparable linear and quadratic age*group interaction effects, with decreased thickness at younger ages, but significantly increased thickness in autistic adults.

The reported age-related CT changes in relation to ePNS in a sample of longitudinally followed FEP patients merit careful examination of potential biological markers and mechanisms underlining neurodevelopment in ePNS in future studies. The CT metric utilized in the current study underscores a biological inference of cellular gray matter composition comprising the thickness of the cortical mantle. Seminal studies of CT and gray matter volume trajectories in normative development emphasize the late maturational time course of the frontal lobes (Gogtay et al. 2004; Shaw et al. 2008); specifically, the DLPFC is under dynamic refinement for longer than was initially cited, developing well into the second decade of life (Amlien et al. 2016). Cortical maturation processes are largely steered by synaptic pruning and reorganization of synaptic connections, as well as myelination of fibers near the gray-white matter boundary (Westlye et al. 2009), which may be altered in schizophrenia (Feinberg 1982; Faludi and Mirnics 2011). Furthermore, increased CT with age may share some overlap with the early hypothesis of delayed brain maturation driving the characteristic onset of schizophrenia in adolescence (Keshavan and Hogarty 1999), albeit specific to ePNS based on our findings.

Insight into understanding the neurobiological mechanisms underlying CT changes may also be gained from the recent findings implicating neuroinflammation in schizophrenia (Gong et al. 2016; Laskaris et al. 2016). It has been proposed that at acute phases of illness, neuroinflammation may lead to global and local brain swelling (Gong et al. 2016). Although the neurobiological mechanisms underlying CT changes are difficult to elucidate using MRI, our

findings demonstrate that FEP patients with ePNS represent a clinically and neuroanatomically distinct subgroup of patients, and future studies are strongly encouraged to consider age as a significant factor when examining progressive brain changes in FEP.

At the clinical level, further support for our delineation of three separate subgroups of FEP patients was found in the significantly different longitudinal symptom profiles, namely when examining negative and positive symptoms. Relationships between negative symptoms pertaining to each scanning timepoint and duration of untreated psychosis were further explored, given previous literature indicating DUP as a potential predictor of negative symptomatology (Malla, Takhar, et al. 2002a; Perkins et al. 2005; Boonstra et al. 2012). Our own data did not uncover any differences in DUP between our FEP subgroups, nor a relationship between DUP and negative symptoms, consistent with some other studies (Craig et al. 2000; Schmitz et al. 2007), and also speaks to the potential non-linear relationship between these two variables (Boonstra et al. 2012).

The present study has several strengths and limitations. It is based on a large sample of FEP patients that were recruited from a well-defined catchment area without competing other services, thus it is likely to reflect a sample with minimal recruitment biases. Furthermore, the sample was followed longitudinally up to two years after the patient experienced a FEP, alongside reliable clinical information. However, a large proportion of patients were taking antipsychotic medication throughout the study. Although there were no differences between ePNS and other patients in antipsychotic dosage/adherence, several studies have alluded to cortical changes accompanying antipsychotic use (Ho et al. 2011; van Haren et al. 2011; Fusar-Poli et al. 2013; Ansell et al. 2015). However, an additional analyses controlling for antipsychotic medication did not diminish our significant results. It should also be noted that the ePNS group was smaller than the other patient groups, and this may have contributed to the lack of difference between our FEP

subgroups on sex, as has been reported previously in the PNS literature (Chang et al. 2013). However, it should be noted that the recruited sample already held a strong male bias, and thus it proved difficult to detect sex differences specific to PNS. For the neuroimaging analyses, to accommodate potential loss of power in the ePNS group, a slightly lower threshold was required to detect some of the significant effects reported with respect to the age*group interactions. We also did not find widespread cortical thinning comparing our ePNS and non-ePNS groups to controls, which is discordant with other reports of CT differences in FEP. In addition to heterogeneity within and across reported samples, the inconsistencies found within such investigations could be partially attributed to utilization of ROIs (which are largely dependent on the pipeline used), rather than whole-brain vertex-wise approaches, or controlling for age. This latter point deserves recognition, as the time at which a FEP occurs is highly non-trivial in both social and neurodevelopmental contexts. Although best efforts were put forward to reduce noise in the imaging data and retain only high quality scans, it is acknowledged that even subtle head motion can significantly alter cortical thickness findings, as supported by recent work (Reuter et al. 2015; Alexander-Bloch et al. 2016), which may also contribute to the explanation as to why previous studies have reported exaggerated cortical thinning in FEP samples compared to controls. Finally, caution should be exercised when interpreting the elements underlying persistent negative symptoms due to secondary factors. Our current dataset does not allow us to parse apart the etiology of symptoms, and thus we cannot say with confidence whether the persistent negative symptoms we observe are indeed primary or secondary in relation to other symptom constructs. The current sample is also limited in its definition of extrapyramidal symptoms (EPS), as patients are only identified with EPS if they are on anticholinergic medication. Thus, the sPNS sample presented in this manuscript may be an underestimate.

Progressive brain changes following a FEP are non-uniform across patients, as demonstrated by the presented findings implicating ePNS and age as significant contributing factors to underlying neuroanatomical variations in the early course of psychosis. It has not escaped our attention that ePNS patients are akin to Tim Crow's initial conception of "type II schizophrenia" in 1980 (Crow 1980), warranting further investigation due to the clear poor functional outcome associated with these symptoms (Jordan et al. 2014). The current study highlights the power of using a symptom-based classification approach as opposed to a diagnostic approach, to elucidate dynamic cortical changes across time. Such approaches may yield more fruitful results when linking biomarkers and their progression after a FEP to clinical outcome, which could further be used to inform clinical practice and psychotherapies.

Acknowledgments and Disclosures

The authors would like to thank PEPP-Montreal research staff for help with patient recruitment and carrying out clinical assessments, as well as research staff in the Lepage lab for overseeing MRI sessions and help with data coordination. The authors would also like to thank Alan C. Evans, John Lewis, and Claude Lepage for providing additional resources and guidance for statistical analysis. Finally, the authors are grateful for all participants who took part in the study.

This study was supported by operating grants from the Canadian Institutes of Health Research (CIHR; #68961) and the Sackler Foundation to Drs. M. Lepage/A.K. Malla. Salary awards include: Canada Graduate Scholarships (CGS-M) (C.M.), James McGill Professorship (M.L.), Fonds de la Recherche en Santé du Québec (FRSQ) (M.L. & R.J.), and Canada Research Chairs Program (A.K.M.). The funding sources had no role in study design; the collection, analysis nor interpretation of data; writing of the paper; nor in the decision for publication.

M. Lepage reports having received financial assistance/compensation for research and educational events from Janssen-Ortho, Eli Lilly, Roche, and Otsuka/Lundbeck Alliance. A.K. Malla reports having received financial assistance/compensation for research and educational activities from Pfizer, Janssen-Ortho, AstraZeneca, and Bristol-Myers Squibb. R. Joober reports having received consultancy honorariums from Pfizer and Janssen-Ortho. All other authors declare no competing conflicts of interest.

Chapter 5 : Intersection of negative symptoms and verbal memory on changes in cortical contrast and thickness after a First Episode of Psychosis

PREFACE

The previous chapter used a categorical approach to classify patients with negative symptoms, which did not allow us to make conclusions about individual brain-behaviour relationships. Furthermore, one of the key aims of this thesis is to better understand the biological underpinnings of both negative symptoms and verbal memory, two key predictors of functional outcome in FEP patients. Thus, this chapter investigates relationships between two dimensions of negative symptoms (expressivity deficits and amotivation) and two verbal memory processes (immediate and delayed recall) both at the level of brain and behaviour. A better understanding of such relationships can help target meaningful domains of psychosis which, thus far, have largely gone untreated.

This chapter also extends the methodology presented in Chapter 4.2, and investigates a new measure of white-gray matter contrast (WGC), alongside the often-used measure of cortical thickness (CT). As described in Chapter 3, we have previously shown that WGC may be more sensitive than CT in detecting widespread structural abnormalities in FEP compared to controls, tapping into putative network-level aberrancies that underlie individual differences in general psychopathology. Given that structural MRI is one of the most commonly used imaging techniques in psychiatric neuroimaging studies, WGC is positioned well as a potential proxy of myelin content using solely T1 images and provides both complementary and unique information alongside cortical thickness.

This chapter demonstrates distinct associations between progressive changes in negative symptoms and WGC and CT in frontal cortices early in the course of treatment for psychosis. This

work extends a key finding of cortical thinning of the prefrontal cortex in relation to negative symptoms in psychosis, although it seems such changes are specific to fluctuations in expressivity over a one to two year period after a FEP. In particular, expressivity interacts with verbal memory abilities both behaviorally and with brain regions heavily involved in language production and articulation. These findings hold when accounting for potential relationships with a general cognitive index excluding verbal memory abilities. This work proposes that deficits in articulation may be a more plausible mechanism underlying the relationship between expressivity deficits and verbal memory, rather than deficits in general cognitive ability.

Intersection of verbal memory and expressivity on cortical contrast and thickness in First Episode Psychosis

Carolina Makowski[1,2,3,4], John D. Lewis[1,2,3], Claude Lepage[1,2,3], Ashok K. Malla[4,5], Ridha Joober[4,5], Alan C. Evans[1,2,3]*, Martin Lepage[4,5]*

[1]McGill Centre for Integrative Neuroscience, McGill University, Montreal, Canada

[2]McConnell Brain Imaging Centre, Montreal Neurological Institute, Montreal, Canada

[3]Ludmer Centre for Neuroinformatics and Mental Health, Montreal, Canada

[4]Department of Psychiatry, McGill University, Verdun, Canada

[5]Prevention and Early Intervention Program for Psychosis, Douglas Mental Health University Institute, Verdun, Canada

*Authors share senior authorship.

Revisions Submitted March 2019 to *Psychological Medicine*

Abstract

Longitudinal studies of first episode of psychosis (FEP) patients are critical to understand the dynamic nature of clinical factors influencing functional outcomes; negative symptoms and verbal memory (VM) deficits are two such factors that remain a therapeutic challenge. This study uses white-gray matter contrast at the inner edge of the cortex, in addition to cortical thickness, to probe changes in microstructure and their relation with negative symptoms and possible intersections with verbal memory. T1-weighted images and clinical data were collected longitudinally for patients (N=88) over a two-year period. Cognitive data were also collected at baseline. Relationships between baseline VM (immediate/delayed recall) and rate of change in two negative symptom dimensions, Amotivation and Expressivity, were assessed at the behavioural level, as well as at the level of brain structure. VM, particularly immediate recall, was significantly and positively associated with a steeper rate of Expressivity symptom decline ($r=0.32$, $q=0.012$). Significant interaction effects between baseline delayed recall and change in expressivity were uncovered in somatomotor regions bilaterally for both white-gray matter contrast and cortical thickness. Furthermore, interaction effects between immediate recall and change in Expressivity on cortical thickness rates were uncovered across higher-order regions of the language processing network. This study shows common neural correlates of language-related brain areas underlying Expressivity and VM in FEP, suggesting deficits in these domains may be more linked to speech production rather than general cognitive capacity. Together, white-gray matter contrast and cortical thickness may optimally inform clinical investigations aiming to capture peri-cortical microstructural changes.

Introduction

Negative symptoms (e.g. amotivation, flattened affect) and cognitive impairments in individuals with psychotic disorders are strong predictors of poor functional outcome (Albert et al. 2011; Lepage et al. 2014), and are less responsive to currently available medications compared to positive symptoms (e.g. hallucinations, delusions). Verbal memory (VM) is one of the most strongly impacted of all cognitive domains in individuals with psychotic disorders (Jordan et al. 2014; Benoit et al. 2015; Guimond et al. 2016), and is linked to persistent negative symptoms (Hovington et al. 2013). There is some evidence suggesting that VM and negative symptoms, particularly deficits in communication or expressivity, may share common neural substrates. Cohen & Elvevåg (2014) have suggested that expressivity is linked to classic language areas in psychiatric disorders, although such a relationship has not been demonstrated in early stages of psychosis with non-invasive imaging techniques.

Many studies treat VM and negative symptoms as unitary constructs, although these variables are comprised of stable subdomains that are likely to be of clinical relevance; for instance, VM can be broken down into verbal learning vs. retention, and negative symptoms into amotivation and expressivity, all of which have unique environmental and biological correlates (Malla, Takhar, et al. 2002a; Leeson et al. 2009; Millan et al. 2014). For instance, different facets of VM have been differentially associated to white matter microstructure (typically assessed using metrics such as fractional anisotropy from diffusion-weighted imaging) in healthy older adults, where white matter tracts subserving left fronto-parietal regions are related to verbal working memory, whereas bilateral fronto-temporal white matter is linked to long-term episodic memory function (Charlton et al. 2013). Both gray and white matter abnormalities have been observed in

relation to amotivation symptoms (e.g. avolition, apathy) in enduring schizophrenia patients, particularly decreased cortical thickness and fractional anisotropy underlying left orbital/medial frontal cortex and cingulate cortex (Ohtani et al. 2014; Mørch-Johnsen et al. 2015, 2018). A recent study has also shown that the integrity of white matter underlying the right hemisphere homologs of these regions is related to affective flattening (Ohtani et al. 2015); however, beyond this study, very few have further investigated the structural brain correlates of expressivity deficits (Mørch-Johnsen et al. 2018), especially in first episode of psychosis (FEP) patients.

Importantly, and of relevance to the current study, longitudinal brain imaging studies of negative symptoms in FEP are scarce, although altered maturational trajectories of cortical thickness and limbic structure have been previously observed in patients with persistent negative symptoms (Makowski et al. 2016, 2017). Such longitudinal neuroimaging studies are critical to characterize the emergence of clinical, cognitive, and neuroanatomical markers that may be amenable to intervention early in the course of the disorder. Existing literature examining progressive brain changes after a FEP, irrespective of symptom profiles, have reported widespread accelerated gray matter loss (Andreasen et al. 2011; Gong et al. 2016). Various structural and functional MRI reviews of FEP patients have pinpointed progressive brain changes occurring across frontal and temporal lobes, particularly within the left hemisphere (Radua et al. 2012; Vita et al. 2012; Dazzan et al. 2015). Further, evidence suggests that the stability of medial temporal and prefrontal cortices may be essential predictors of symptomatic and functional outcomes after a first episode of schizophrenia (Dazzan et al. 2015).

White matter abnormalities have also been a key focus of studies of schizophrenia and related disorders, across different disease stages (Kubicki et al. 2005; Whitford et al. 2007, 2012; Carletti et al. 2012; Lee, Kubicki, et al. 2013; Birur et al. 2017; Klauser et al. 2017; Kelly et al.

2018). Evidence from post-mortem studies and diffusion tensor imaging suggests that white matter abnormalities, particularly within prefrontal regions, are more significantly correlated with negative symptoms compared with positive symptoms (Uranova et al. 2011; Asami et al. 2014). Other neuroimaging studies have obtained proxy measures of myelin to better understand the nature of white matter alterations in psychosis (Andreasen et al. 1991; Lang et al. 2014; Ganzetti et al. 2015; Iwatani et al. 2015). There is certainly a need to shift focus to earlier stages of psychosis, obtaining measures more proximal to a FEP, to better understand the cascade of brain structural alterations that follow.

Although measures of cortical thickness (CT) are often the choice of methodology for investigation of cortical structure in psychiatric disorders from T1-weighted MRI scans, inconsistencies have arisen in a number of studies of longitudinal cortical thickness trajectories in early psychosis, with a handful of studies contesting the evidence of progressive brain change after a FEP (Nesvåg et al. 2012; Roiz-Santiáñez et al. 2015; Haukvik et al. 2016), emphasizing the need for novel approaches to analyze structural data in clinical cohorts. Obtaining a measure of white-gray matter contrast (WGC) from T1-weighted MRI may provide a meaningful marker of myelin content and other biophysical properties that may complement measures of cortical thickness (Salat et al. 2009; Westlye et al. 2009; Andrews et al. 2017; Lewis et al. 2018). We have recently shown that WGC captures brain architectural features and putative network-level abnormalities in FEP patients more robustly than measures of cortical thickness (Makowski, Lewis, et al. 2019b). Thus, using multiple measures to assess the integrity of the cortical mantle, including a proxy measure of peri-cortical myelin, could provide a better understanding of the neurobiological correlates underlying subdomains of negative symptoms and VM, particularly in FEP patients. This is turn could be paramount in developing more effective treatments in early psychosis, and

other disorders that are characterized by similar deficits.

The aims of the current study were to i) examine the relationship between two negative symptom dimensions (Expressivity and Amotivation) and deficits in two VM processes (immediate and delayed recall), ii) relate Expressivity and Amotivation negative symptom dimensions to changes in CT and WGC across time, and iii) see how relationships in ii) interact with VM capacity. We expect Expressivity and Amotivation to be uniquely correlated with progressive changes in white-gray contrast, and to be moderated by VM abilities. Specifically, we postulate that immediate recall, a measure of verbal learning, will be more strongly correlated with Expressivity both at the levels of brain and behaviour, given that both constructs have been described as "core" traits in psychosis and less influenced by external factors (Leeson et al. 2009; Lutgens et al. 2014). On the other hand, we expect delayed recall, a measure of verbal *retention*, to be more related to Amotivation, due to these factors' higher potential to be influenced by environment.

Methods

Sample.

Patients were recruited from the Prevention and Early Intervention Program (PEPP) at the Douglas Institute in Montreal, Canada, and were part of a longitudinal naturalistic outcome study. Details are outlined elsewhere (Iyer et al. 2015). Inclusion criteria at PEPP include a diagnosis of affective (e.g. bipolar disorder, depression with psychotic features) or non-affective psychosis (e.g. schizophrenia, schizoaffective), an IQ above 70, and limited (<1month) to no previous exposure to antipsychotic medication. Patients recruited to PEPP (ages 18-35) were invited to take part in a neuroimaging study, comprising three timepoints (baseline, one/two-year follow-ups) as described in previous work (Makowski et al. 2016, 2017). Patients were recruited from February 2003 to

February 2014. The first baseline scan took place in May 2004. It should be noted that many of the initial patients recruited for the study did not meet criteria for this neuroimaging investigation, as more than 6 months passed between entry to the PEPP clinic and their baseline scan. The last two-year follow-up scan and clinical assessment for the last patient took place in April 2016.

Non-clinical healthy controls were recruited through advertisements within the same local catchment area. All participants provided written informed consent, and the research protocol was approved by the Douglas Institute human ethics review board. From 150 FEP patients recruited for the study, 88 patients (Male, N=62) were included in analysis. Data from 80 healthy controls were included for calculation of standardized VM scores, as described below. See Chapter 8 – Appendix-III for more detailed information on the final included sample. Also see Table 8.6 of Appendix-III for a comparison of patients included in the study, compared to those who were excluded.

We opted to include both affective and non-affective psychoses in our sample of FEP patients, as our group has previously shown that clinical diagnoses play a negligible role in findings related to MRI-derived metrics, including cortical thickness (Makowski et al. 2016, 2017). Further, our aims are to investigate individual clinical/cognitive profiles, rather than work within a diagnostic framework, which is being recognized as a clear setback in the field of psychiatry (Insel et al. 2010; Owen 2018; Wolfers et al. 2018). However, we also explored differences in key variables of interest, namely immediate/delayed recall, and amotivation and expressivity deficits, between patients on the schizophrenia spectrum and patients with an affective disorder. No significant differences emerged between groups as can be seen in Table 8.7 of Appendix-III.

Negative symptom dimensions and change over time.

Negative symptoms were assessed using the Scale for the Assessment of Negative Symptoms (SANS) (Andreasen 1984a), which has been shown to have good inter-rater reliability (κ=0.71) at PEPP-Montreal (Jordan et al. 2018). Item-level scores from the SANS were used to define two principal dimensions of negative symptoms: Amotivation and (lack of) Expressivity. These dimensions were based on a consistent body of literature reporting a two-factor model of negative symptoms (Malla, Takhar, et al. 2002a; Blanchard and Cohen 2006; Kirkpatrick et al. 2006; Messinger et al. 2011; Jang et al. 2016; Marder and Galderisi 2017). Items were assigned to either the Amotivation or Expressivity dimension based on a recent confirmatory factor analysis published by our group (Lutgens et al. 2019). Although other models have been proposed to categorize negative symptoms, for instance a recent investigation uncovering a 5-factor latent structure of negative symptoms in schizophrenia (Strauss et al. 2018), it is important not to dismiss a large breadth of literature that has linked motivation and expressivity dimensions of negative symptoms to functional outcomes in patients. Finally, a two-factor solution minimizes the burden of multiple comparisons and potential false positives for the purposes of our neuroimaging analysis.

Thus, based on Lutgens et al (2019), Amotivation in this study represented summed items from "Avolition-Apathy" and "Anhedonia-Asociality" domains, while the Expressivity dimension represented summed items from "Affective Flattening/Blunting" and "Alogia" domains, excluding Item 6: "Inappropriate Affect" and Item 10: "Poverty of Content of Thought", given that these items do not effectively map onto the clinical construct of Expressivity (Lutgens et al. 2019). To assess the mean rate of change in symptoms over time, a linear model was fit to each subject's longitudinal amotivation and expressivity symptom data against the participants' age over all

available timepoints for that participant. A slope was calculated and extracted for each subject to represent a single metric of change over time in symptoms.

Verbal Memory (VM) performance.

VM data were collected from a larger neuropsychological battery database for patients followed at PEPP. Due to a change in neuropsychological testing protocol, VM data were compiled from two different protocols: 1) a pen and paper format administered to patients who took part in the study from 2003 to 2010, using Logical Memory subtests of the Wechsler Memory Scale–Third Edition (WMS-III) (Wechsler 1997); and 2) the CogState Research Battery (Pietrzak et al. 2009), administered from September 2010 onwards, using the International Shopping List task. Further details of both testing protocols and tasks have been described before (Benoit et al. 2015). Z-scores were calculated for each neuropsychological test battery separately, using the mean and standard deviation of controls for immediate/delayed recall measures. Previous work from our group (Benoit et al. 2015) has shown that participants tested with the CogState Research Battery tended to perform better. Thus, in addition to using standardized scores, test version was used as a covariate in analyses using VM data. Table 8.8 of Appendix-III demonstrates there are no significant version or group*version effects on VM performance.

MRI acquisition.

Scans were collected at the Montreal Neurological Institute, all on the same 1.5-Tesla Siemens Sonata MRI scanner. Structural T1-weighted volumes were acquired for each participant using a 3D gradient echo pulse sequence with sagittal volume excitation (resolution=1mm^3, repetition

time=22ms, echo time=9.2ms, flip angle=30°, 180 1mm contiguous sagittal slices). The rectangular field of view (FOV) for the images was 256mm (AP) 204mm (SI).

MRI post-processing.

Cortical Thickness (CT). Raw T1-weighted images were submitted to the CIVET pipeline (Version 2.1.0: http://www.bic.mni.mcgill.ca/ServicesSoftware/CIVET) (June et al. 2005) for extraction of gray and white matter surfaces. Main processing steps include: 1) Registration of T1-weighted images to standardized space (Collins et al. 1994) and correction for non-uniformity artefacts (Sled et al. 1998); 2) segmentation of gray, subcortical gray and white matter, and cerebral spinal fluid (Zijdenbos et al. 2002; Tohka et al. 2004); 3) extraction of the white matter surface using a marching-cubes algorithm and extraction of the gray matter surface using the CLASP algorithm (Kim et al. 2005); 4) surface registration to a template for inter-subject correspondence (Lyttelton et al. 2007); 5) reverse transformation (initially done in step 1) to estimate CT in native space for each subject at 81,924 vertices using the t-laplace metric (Lerch and Evans 2005); and 6) smoothing the data in native space with a 20mm FWHM Gaussian kernel to diminish the impact of noise (Boucher et al. 2009). CT was estimated using the Laplacian distance between the two surfaces (Jones et al. 2000) across 81,924 vertices.

White-Gray Matter Contrast (WGC). Measures of WGC were generated as follows, similarly to what is described in Makowski et al (2019b): 1) additional surfaces were created 1mm on either side of the surface at the gray-white matter boundary (i.e. +1mm corresponds to supra-white surface, and -1mm corresponds to sub-white surface); 2) surface maps of the intensity of the T1-weighted MRI were generated and smoothed; and 3) a ratio was calculated, by dividing the

intensity of the -1mm point by the corresponding +1mm point, as defined by Lewis et al (2018). WGC values ranged from approximately 1.15 to 1.35 where lower values, closer to 1, reflect lower contrast (i.e. reduced gray-white matter distinction) whereas higher values reflect higher contrast (i.e. clearer distinction between gray and white matter). The WGC method is depicted in Chapter 3 (**Figure 3.8**). More details of quality control procedures pertinent to this study are outlined in Supplementary Methods of Appendix-III.

Statistical analyses of behavioural and clinical data.

Demographic and clinical variables were analysed with one-way ANOVAs for continuous variables or Kruskall-Wallis H tests for nominal variables. An ANCOVA was used to analyse differences in VM performance at baseline between patients and controls, covarying for test version and years of education. Additional tests to compare the effect of version on results with VM data, as well as exploratory analyses between change in negative symptoms and change in verbal memory scores for a subset of patients with longitudinal data available (N=49), are in Supplementary material. Associations between rates of change in Amotivation/Expressivity negative symptom domains and immediate/delayed recall in FEP patients were evaluated with Pearson r-correlations, adjusting verbal memory values for age, sex, and test version, and taking into account multiple comparisons with a false discovery rate (FDR) correction (Benjamini and Hochberg 1995). Analyses of behavioural and clinical variables were conducted using PASW Statistics 21 (SPSS inc., 2009, Chicago, IL, USA) and were two-tailed with a critical *p*-value of 0.05. Normality of continuous data was assessed with the Shapiro-Wilk test of normality. Non-parametric tests were used to compare demographic variables between patients and controls that were found not to be normally distributed. Demographic and clinical information was also

compared between patients included in this manuscript (N=88) and patients excluded from the study (N=47) despite meeting criteria for a FEP, due to the cross-sectional nature of their data and/or failed imaging data after QC.

Surface-based brain analyses.

Vertex-wise analysis of WGC and CT were conducted using SurfStat in Matlab (http://www.math.mcgill.ca/keith/surfstat/). As with the negative symptom data and as described in Raznahan et al (2011), a linear model was fit to each vertex for the WGC and CT data, yielding a single metric for each subject describing the rate of change in years in WGC and CT. To determine which covariates should be used for analyses, the Akaike Information Criterion (Akaike 1998) was used to determine the best model. AIC values were compared to a 'baseline' model that included centered age and sex as covariates, given the well-documented impact of age and sex on neuroanatomy, as well as their influence on the onset and progression of psychosis (Tamnes et al. 2010; Ochoa et al. 2012; Makowski et al. 2016, 2017) . Details are included in Appendix-III, including an analysis testing the effect of antipsychotic medication on WGC and CT (Figure 8.4) and justification on the exclusion of medication as a covariate.

The following model was used to assess the main effect of change in negative symptoms (η, representing either amotivation or expressivity deficits) on change in Y (representing either WGC or CT), covarying for centered age, sex, and mean σ (reflecting mean WGC or mean CT across the entire cortical surface for each participant):

$$\Delta Y = intercept + \beta_1(\Delta\eta) + \beta_2(CenteredAge) + \beta_3(Sex) + \beta_4\big(Mean(\sigma)\big) + \epsilon$$

Here, β_1 is the slope for the main effect of interest, namely, rate of change (Δ) in negative symptoms per year. Note, β_2 and β_4 reflect measures at baseline. Positive values of the rate of Y change reflect an increase in either WGC and CT per year, whereas positive values in negative symptoms reflect an increase (i.e. worsening) in symptoms per year.

The interaction between baseline VM abilities (υ, reflecting Immediate Recall or Delayed Recall) and change in negative symptoms over time (η) on rate of change in WGC and CT (ΔY) was tested with the following model:

$$\Delta Y = intercept + \beta_1(\Delta\eta) + \beta_2(\upsilon) + \beta_3(\Delta TestVersion) + \beta_4(CenteredAge) + \beta_5(Sex)$$
$$+\beta_6\big(Mean(\sigma)\big) + \beta_7(\Delta\eta * \upsilon) + \epsilon$$

where $\beta_7(\Delta\eta*\upsilon)$ represented the slope for the main predictor of interest; that is, the interaction between change in negative symptoms and baseline verbal memory. Here, β_2, β_3, β_4 and β_6 were measures taken at baseline. For visualization purposes only, patients were divided using a median split into two groups, on the basis of their verbal memory performance: "mild to moderate VM deficits" and "high VM deficits". Specific details of these groups are outlined in the Results section.

Random field theory (RFT) (Worsley et al. 2004) was used for multiple comparison correction using a stringent p-cluster threshold of p=0.001. Significant results are also presented with a more liberal cluster threshold of p=0.01 (p-corrected<0.05), to show the extent of sub-threshold results. For all significant clusters found with the more stringent cluster threshold (p=0.001), the rate of change in WGC and CT at the peak t-statistic was extracted and adjusted for centered age, sex, and Mean(σ), and used to generate scatterplots to visualize results.

Results

The final sample comprised 88 FEP patients, of which 59 patients completed all three scans, and the remainder had two scans. See **Table 5.1** for descriptive statistics and clinical information. Importantly, FEP patients had a median duration of untreated psychosis of approximately 20 weeks, highlighting the efforts that have been put forth by the PEPP-clinic to minimize patients' pathways to care within our early intervention service (Iyer et al. 2015; MacDonald et al. 2018). This also emphasizes that our FEP patients are indeed highly representative of the first-episode time period. Included patients were also compared to 47 patients that were excluded from the current study on variables collected at baseline, and these results can be found in Table 8.6 of Appendix-III. In summary, included patients did not differ largely from the excluded patients, except included patients had longer duration of untreated psychosis and untreated illness compared to excluded patients.

		FEP N=88	Controls N=80			
		N (%)		Statistic	df	p-value
	Male	62 (70)	52 (65)	χ^2=0.57	1	0.51
	Right Handed	73 (83)	73 (91)	χ^2=2.53	1	0.17
	Diagnosis					
	Schizophrenia/ Schizophreniform	63 (72)				
	Affective Disorder	16 (18)				
	Delusional Disorder	3 (3)				
	Psychosis Not Otherwise Specified	6 (7)				
		Mean (SD)		Statistic	df	p-value
General Demographics	Age at Baseline[a]	24.3 (4.1)	24.27 (3.3)	t=-0.009	164.1	0.99
	Verbal Memory - Immediate*[b,c]	-1.3 (1.4) [87]	0.03 (1)	F=23.38	1, 163	<0.001
	Verbal Memory - Delayed*[b,c]	-0.9 (1.1) [87]	0.02 (0.8)	F=16.77	1, 163	<0.001
	Education in Years*	12.0 (2.5)	14.3 (2.4)	U=1887.00		<0.001
	Socioeconomic Status	3.2 (1.1) [81]	3.0 (1.0) [76]	U=2817.00		0.34
	Performance IQ*[b]	98.7 (17.1)	106.9 (12.7)	U=2447.50		0.001
	Verbal IQ*[b]	99.8 (16.1)	110.0 (14.9)	U=2345.50		<0.001
	Cumulative CPZ equivalent (in mg)	4753.1 (4770.7)				
	Adherence (%)	80 (24)				
	Duration Untreated Psychosis (weeks)	76.4 (142.0) Median: 20.1				
	Duration Untreated Illness (years)	7.3 (6.5) Median: 6.1				
		Mean (SD)				
Baseline Symptoms (N=88)	Amotivation	11.3 (6.1)				
	Expressivity	7.1 (7.2)				
	SAPS	9.5 (12.3)				
	CDSS	2.4 (2.9)				
	Window |Scan - Symptom Eval| (months)	0.7 (0.6)				
1-year FUP Symptoms (N=80)	Amotivation	8.7 (7.0)				
	Expressivity	5.8 (6.5)				
	SAPS	7.9 (10.2)				
	CDSS	1.5 (2.7) [79]				
	Window |Scan - Symptom Eval| (months)	2.1 (2.0)				
2-year FUP Symptoms (N=65)	Amotivation	7.4 (6.8)				
	Expressivity	5.1 (6.6)				
	SAPS	7.9 (13.9)				
	CDSS	1.9 (2.6) [60]				
	Window |Scan - Symptom Eval| (months)	0.6 (1.2)				

Table 5.1. Demographic and clinical information.
General Demographics for whole sample are presented, followed by information corresponding to each scan. All data represented as Mean (SD), unless otherwise specified. Square brackets [] include adjusted sample size included in statistical analysis due to missing datapoints. All antipsychotic totals are presented as *cumulative* chlorpromazine (CPZ) equivalents in mg (i.e. a composite measure of the total amount of antipsychotic medication prescribed during the entire study), as prescribed by a psychiatrist, and are reported along with a percentage of medication

adherence. SAPS totals are presented as mean scores of the sum of item-level scores for positive symptoms. CDSS represents the Calgary Depression Scale for Schizophrenia. Duration of untreated psychosis and illness reflect length of time between onset of psychotic symptoms and onset of other psychiatric symptoms until initiation of antipsychotic medication treatment, respectively. Further details on collection of clinical data can be found in Supplementary methods of Chapter 8-Appendix III. Years of education, socioeconomic status, performance and verbal IQ were found to be non-normally distributed; thus, non-parametric tests to compare group means were used.

*FEP patients had significantly lower levels of verbal memory performance (immediate/delayed recall), lower performance and verbal IQ, and less years of education compared to HC ($p<0.05$).

[a]Degrees of freedom adjusted, as age did not meet the assumption of equal variance between groups as assessed with Levene's test.

[b]Covaried by test version. Specifically, IQ was collected with WAIS-III and WASI (more details in Appendix-III), and verbal memory was collected with a Pen and Paper neuropsychological test battery, and CogState Research Battery.

[c]Note, Mean and Standard Deviation of verbal memory in Controls does not equate to exactly 0 and 1, respectively, as the norms for verbal memory were calculated before exclusion of a subset of controls for this study due to imaging quality control.

Summary statistics for rate of change in negative symptoms domains for 88 FEP patients with longitudinal data were as follows: Mean ΔAmotivation=-1.80 (SD=4.22 Range=-11.72 – 13.61), Mean ΔExpressivity=-1.22 (SD=5.19 Range=-19.63 – 14.66). For amotivation symptoms, 5 patients had the same level (or absence) of symptoms over time (Mean Δ=–0.0038, SD=0.0086), 25 patients had worsening symptoms (Mean Δ= 3.12, SD=2.91), and 58 patients improved (Mean Δ= –4.08, SD=2.72). For expressivity symptoms, 16 patients had the same level (or absence) of symptoms over time (Mean Δ=0, SD=0), 22 patients had worsening symptoms (Mean Δ= 4.64, SD=4.02), and 50 patients improved (Mean Δ= –4.18, SD=4.01). See Figure 8.5 of Appendix-III for spread of longitudinal Amotivation and Expressivity negative symptom data.

Relationship between VM and Δ negative symptoms.

Cross-sectional relationships between VM and negative symptoms at baseline are reported in Supplementary material, where significant negative associations between baseline expressivity and immediate recall (r=-0.35, q<0.001) and delayed recall (r=-0.28, q=0.036) were found; no relationships were found with amotivation. The relationship between VM (i.e. z-scores of immediate and delayed recall) at baseline and Δnegative symptoms was assessed in 87 patients (degrees of freedom=82), for which baseline VM and longitudinal negative symptom data were available, using Pearson r correlations, adjusting verbal memory data for age, sex, and test battery. The only significant finding that survived FDR correction for multiple comparisons was a positive relationship between immediate recall at baseline and ΔExpressivity (r=0.32, q=0.012). In other words, better VM (i.e. less severe deficits) at baseline was associated with *worsening* Expressivity deficits over time. A trend-like association in the same direction was also found between delayed recall and ΔExpressivity (r=0.19, p-uncorrected=0.083). No significant associations were found with either immediate or delayed recall and ΔAmotivation (Immediate: r=0.079, q=0.476; Delayed: r=0.077, q=0.486). Finally, we assessed the relationship between change in VM and change in negative symptoms over the first year after a FEP for a subset of patients (N=49) for which data were available. No significant relationships were found, as reported in Appendix-III.

Associations between Δ negative symptoms and ΔWGC and ΔCT.

Worsening of Amotivation symptoms was associated with greater increases in WGC over time within the left superior parietal lobule and right dorsal primary motor cortex and paracentral lobule. Overlapping findings were found with respect to ΔExpressivity, with additional peaks in the left dorsal precentral gyrus and right cuneus. With respect to CT, ΔExpressivity was negatively

associated with ΔCT (i.e. cortical thinning with worsening symptoms) within left frontal regions. ΔAmotivation was not found to be significantly associated with changes in CT. Results are shown in **Figure 5.1**, along with the brain regions that survived correction for multiple comparisons with a relaxed p-cluster threshold of p=0.01**.** Plots were generated for regions that survived correction for multiple comparison with a stringent threshold of $p<0.001$.

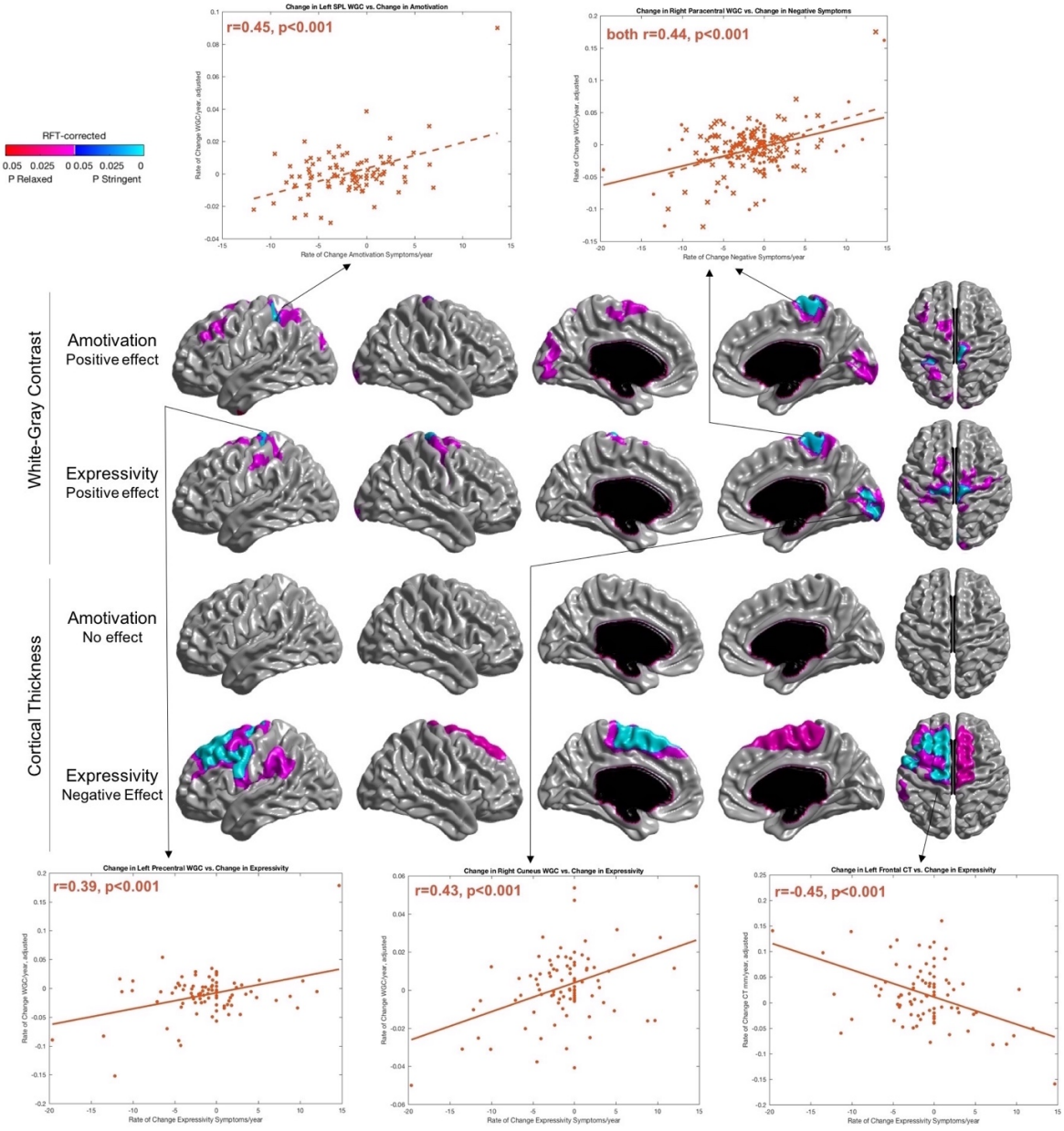

Figure 5.1. ΔAmotivation and ΔExpressivity deficits associated with ΔWGC and ΔCT.
Results are RFT-corrected, where blue colours represent significant results cluster-thresholded at a "stringent" threshold of p=0.001, whereas red/pink colour represent significant results at a "relaxed" threshold of p=0.01. Selected regions for scatterplots are those that survived multiple comparisons with the more stringent cluster threshold of p=0.001. Plots with Amotivation are plotted with a dotted line and crosses, whereas Expressivity data are plotted with a solid line and circular markers. For overlapping cluster within right paracentral gyrus of the effect of negative symptoms on WGC (top two rows), a common peak was selected where amotivation and expressivity are included on the same plot.
Abbreviations: SPL, Superior Parietal Lobule.
Orientation: Surfaces from left to right: left lateral, right lateral, left medial, right medial, dorsal.

Interaction between VM and Δ Expressivity on ΔWGC and ΔCT.

Given that no significant associations were found between verbal memory and ΔAmotivation at the behavioural level, we did not explore this contrast. No significant regions survived the stringent threshold for WGC, however results with a relaxed threshold are in **Figure 5.2.** For CT, both immediate and delayed recall interacted significantly and uniquely with changes in Expressivity. The interaction between immediate recall and ΔExpressivity was significantly associated with changes in thickness along the left hemisphere ventrally, including the left orbital and medial frontal, insular, temporal pole, and middle temporal regions. The interaction term between delayed recall and ΔExpressivity showed significant effects on the right cuneus/primary visual cortex. Results are shown in **Figure 5.2**, along with brain regions that survived correction for multiple comparisons with a relaxed p-cluster threshold of p=0.01**.** Plots were generated for regions that survived correction for multiple comparison with a stringent threshold of $p<0.001$. Even though no results survived correction for multiple comparisons with WGC with our stringent threshold, we also generated two additional plots with WGC data for right retrosplenial cortex and left central sulcus, to compare the nature of the associations against CT data.

To better visualize the direction of results, patients were divided into two groups based on their verbal memory performance using a median split, as described in the methods. Specifically, the groups were broken down as follows: "mild to moderate VM deficits" (N=43; for immediate recall patients had a z-score higher than -1.15; for delayed recall, patients had a z-score higher than -0.91) and "high VM deficit" (N=44; for immediate recall, patients had a z-score lower than or equal to -1.15; for delayed recall, patients had a z-score lower than or equal to -0.91). Note, one patient had missing verbal memory data at baseline, thus 87 patients were included in this analysis. Visualization of these groups generally revealed that patients with mild to moderate VM deficits

(i.e. more preserved VM ability) at baseline drove the *positive* association between changes in expressivity symptoms and changes in WGC. For CT, patients with mild to moderate VM deficits at baseline predominantly drove the *negative* association between changes in expressivity and changes in thickness (**Figure 5.2**).

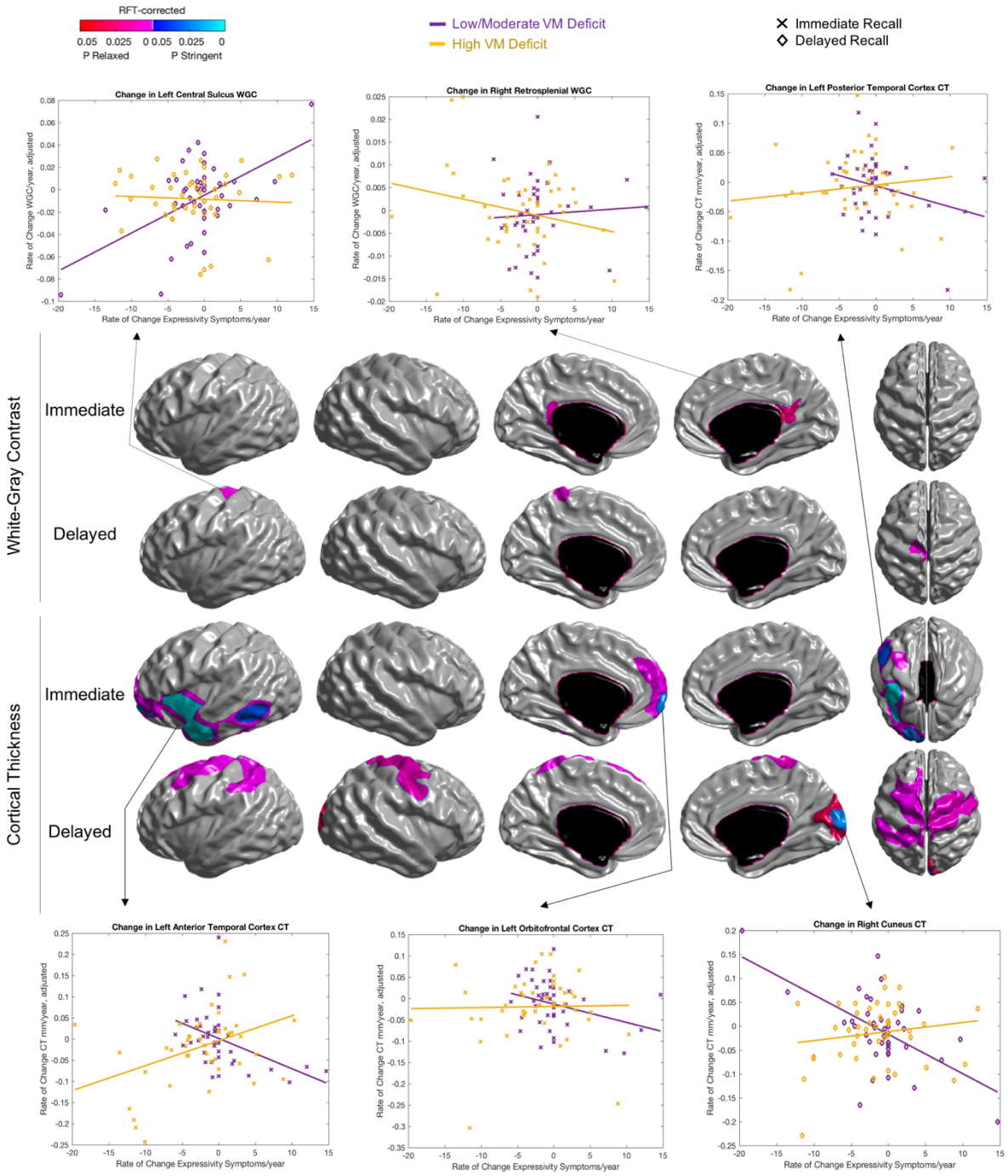

Figure 5.2. Interaction between baseline VM and ΔExpressivity on ΔWGC and ΔCT.
Results are RFT-corrected, where blue colours represent significant results cluster-thresholded at "original" stringent threshold of p=0.001, whereas red/pink colour represent significant results at a "relaxed" threshold of p=0.01. "Immediate" and "Delayed" labels of left-hand side panel refer to immediate and delayed recall of verbal memory domain, respectively. Inflated brain is presented to better visualize results within cortical folds. Selected regions for scatterplots are those that survived multiple comparisons with the more stringent cluster threshold of p=0.001 for cortical

thickness data. Although nothing survived correction after stringent correction for WGC analyses, peaks within left central sulcus and right retrosplenial cortex were plotted to explore the direction of results with WGC. To better visualize the interaction effect of two continuous variables (rate of change in expressivity and baseline VM), patients were divided based on low/moderate VM deficit (purple) and high VM deficit (yellow). Plots separating patients on the basis of immediate recall are depicted with crosses, and delayed recall with diamonds. Orientation: Surfaces from left to right: left lateral, right lateral, left medial, right medial, dorsal (with the exception of the third row, where the last surface is a ventral view).

Results were also generated *excluding* mean(σ) as a covariate; results were largely similar (Figure 8.6 of Appendix-III). To ensure results in the final analysis were specific to verbal memory, a general cognitive index was calculated across five domains (i.e. attention, executive function, speed of processing, working memory, visual memory) and controlled for in analyses, yielding similar results (Figure 8.7 of Appendix-III). Additional methods pertaining to cognitive data can be found in captions of Figure 8.7/Table 8.8 of Appendix-III.

Discussion

These results provide insight into the relationship between surface-based brain metrics and two behavioural domains that contribute strongly to outcome in FEP patients, namely negative symptoms and VM. Two novel findings emerged: 1) rate of change in expressivity and amotivation negative symptoms over the two-year period following a FEP are associated with both overlapping and distinct changes in WGC, and are also associated with changes in left prefrontal regions in relation to CT; and 2) links between baseline VM and change in expressivity deficits are found both at the behavioural and neuroanatomical level, where significant interactions on rate of change over time in neuroanatomy were uncovered, most pronounced with CT.

We also extend a key finding of cortical thinning of the prefrontal cortex in relation to negative symptoms in psychosis (Galderisi et al. 2015; Walton et al. 2017), a finding that supports

long-standing evidence that the frontal lobes are key contributors underlying negative symptom severity (Turetsky et al. 1995; Wible et al. 2001). Importantly, our findings suggest thinning is more specific to changes in Expressivity over a one to two year period. However, no associations were uncovered in the prefrontal cortex when examining WGC and negative symptom progression, suggesting these cortical thinning patterns may be due to neuroanatomical changes within more superficial layers. This idea is supported by several studies that cortical thinning of superficial layers as a key biological mechanism underlying altered neuroanatomy of the prefrontal cortex in schizophrenia (Wagstyl et al. 2016; Lake et al. 2017). Significant associations still emerged between expressivity deficits and WGC, but within primary sensory and motor regions. Similar patterns were uncovered with amotivation. We have previously shown that WGC of primary sensory and motor regions is related to general psychopathology in FEP patients (Makowski, Lewis, et al. 2019b), and may be related to alterations within the high levels of intracortical myelin that typically characterize these regions (Glasser and Van Essen 2011). It is possible that the association between contrast changes in primary sensory and motor regions and negative symptom severity is not specific to negative symptoms, but could also be related to general positive symptoms and cognitive deficits more generally. Although there are few studies that have looked at the neural correlates of expressivity and amotivation separately, one of the key regions that has emerged in several investigations is that of the association between avolition and activation of the striatum (Galderisi et al. 2015). Given our conjecture of WGC as a proxy measure of peri-cortical myelin, putatively tapping into integrity of cortico-cortical and cortico-subcortical connections, it is interesting to consider this finding in light of potential aberrancies between cortico-striatal circuitry (Haber 2016).

A key discovery in our behavioural findings was the stronger association between VM specifically with Expressivity, as opposed to both negative symptom dimensions. Consistent with previous literature, we uncovered a negative association between VM performance and negative symptoms in psychosis cross-sectionally (Hartmann-Riemer et al., 2015). However, when assessing baseline VM performance against rate of change in symptoms, we identified a relationship that, at first glance, runs counter to intuition. Namely, it was found that patients with *better* VM at baseline (i.e. a mild level of VM deficits, particularly with immediate recall) had *worsening* of Expressivity symptoms, a relationship that has largely been unexplored longitudinally in psychosis. Our results suggest that having less striking VM deficits at intake does not necessarily protect against progressive changes in Expressivity. Other key cognitive factors, such as insight, may also contribute to this relationship. Based on previously identified positive relationships between cognitive insight and VM (Lysaker et al. 2005; Lepage et al. 2008), we can consider that patients with a better ability to recall stored information are also likely to have lower self-certainty and more self-reflectiveness (a profile that characterizes high levels of cognitive insight), which could set the stage for a trajectory of worsening Expressivity as the patient internalizes their mental illness. It is also important to note that many of the patients included in this study had an improving course of negative symptoms after the first two years after a FEP, consistent with a previous study (Lutgens et al. 2019). In this context, several studies have suggested that negative symptoms can improve in the absence of any change in verbal memory performance (Nopoulos et al. 1994; Cantor-Graae et al. 1995; Hoff et al. 1999). In a related vein, we also conducted a supplementary analysis exploring the potential relationship between change in verbal memory and change in negative symptoms over the first year after a FEP, for a subset of patients (N=49) for which data were available. No significant association was found, consistent

with the studies cited above, but it is still possible that more timepoints would be needed to elucidate such longitudinal relationships. Many studies have suggested that cognition, including verbal memory, is a set of static traits, as suggested by evidence showing stability of cognitive performance from the clinical high risk state to transition to psychosis (Green and Harvey 2014; Carrión et al. 2015). However, future studies are encouraged to further investigate longitudinal cognition-symptom relationships after psychosis onset; a future direction that our group is currently investigating as well.

It is also worth discussing the granularity of results with respect to immediate vs. delayed recall in relation to Expressivity. It has been shown that immediate recall is highly related to performance on other measures of cognition in schizophrenia (Leeson et al. 2009). Immediate recall may also have a stronger biological and/or genetic predisposition; deficits in immediate recall predict conversion to psychosis (Lindgren et al. 2017) and are present in non-affected siblings of schizophrenia twins (Goldberg et al. 1993). Together, this suggests that immediate recall may be a more "hard-coded" feature of psychosis compared to retention of information (i.e. delayed recall), with stronger biological and genetic influences. Further, Expressivity has also been recently posited to be a more primary negative symptom domain, and less influenced by environmental factors, such as community resources, compared to Amotivation (Lutgens et al. 2019). Our data present a feasible model whereby Expressivity and immediate recall or *verbal learning* may share common etiology and a potential endophenotype of interest for future studies.

More preserved immediate recall abilities contributed to the relationship between worsening of Expressivity deficits and cortical thinning across higher order language processing areas in ventral frontal areas and middle/inferior temporal gyri of the left hemisphere, which contributes to the semantic encoding of language (Saur et al. 2008) and for keeping verbal

information active in working memory (Smith and Jonides 1999). These areas are subserved by white matter tracts such as the uncinate and superior longitudinal fasciculi (Friederici 2011), which have been shown to be disrupted in schizophrenia patients with predominant negative symptoms (Sigmundsson et al. 2001). With WGC, an interesting relationship also emerged between expressivity deficits and increases in contrast between patients with different levels of immediate recall performance within the retrosplenial cortex bilaterally. Although these results were only significant with a relaxed threshold when correcting for multiple comparisons, the retrosplenial cortex is interesting to consider in this context as it is a region that has been strongly linked to memory function (Vann et al. 2009), as well as more recently, to the reinforcement of salient behavioural cues (Smith et al. 2012, 2018), which is likely to contribute during immediate learning phases of memory. A previous study has also shown that white matter volume abnormalities exist within the retrosplenial cortex in schizophrenia patients (Mitelman et al. 2005).

Meanwhile, the interaction between delayed recall and expressivity uncovered regions of the dorsal language processing stream, namely superior parietal lobule, dorsal primary somato-motor and premotor areas, which relates more to language production (Saur et al. 2008). Disruptions in these cortical regions could plausibly support a mechanistic explanation of the lowered rate of speech production and/or increased psychomotor retardation observed in patients with expressivity deficits (Cohen et al. 2014; Marder and Galderisi 2017), as well as the necessity for preserved structure/function of the left posterior dorsolateral prefrontal cortex in delayed retrieval (Alexander et al. 2003). Our results also did not change when accounting for a general cognitive index that comprised five cognitive domains. Together, these results suggest that the relationship between Expressivity deficits and VM may be more closely linked to speech articulation or language production mechanisms, as opposed to general cognitive abilities.

It is worth noting that WGC and CT are related metrics, but they also tap into different neurobiological properties (Westlye et al. 2009). WGC may take myelination patterns into account more strongly than CT, and may shed light on a compartment of the cortex that may be more amenable to short-term changes (Wenger et al. 2017), which in turn may be a more viable biomarker target in FEP patient samples as measured on MRI.

Several limitations should be considered. Our model did not capture patients who had a consistently high or low level of negative symptoms, as well as the distinction between primary and secondary negative symptoms. These individual patterns of negative symptoms have been touched upon by some of our previous work (Makowski et al. 2016, 2017), but future investigations are encouraged to parse apart such trajectories in myelin and/or other microstructural compartments. The rates of change in both cortical metrics and negative symptoms should also be interpreted as a proxy measure of negative symptom/cortical change, as subtle non-linear fluctuations over time are not captured by the measures presented in this manuscript. Limitations in accurately and objectively assessing negative symptoms should also be considered, where rater bias may preclude the treatment of Amotivation and Expressivity as completely independent domains. Automated unbiased assessments of negative symptoms, such as software that has been developed to assess communication deficits and natural language in patients with schizophrenia (Cohen and Elvevåg 2014), may provide data with higher construct validity in this respect. It should also be noted that many patients ultimately showed an improvement in negative symptoms; although this improvement has been reported before in the first two years after a FEP (Lutgens et al. 2019), we cannot rule out that patients with improvement in negative symptoms ultimately comprise a subset of patients that are more motivated to participate in longitudinal studies such as the one described here. With respect to cognitive data, we collected VM from two

batteries, although examination of the tests and standardization of our data suggests test version likely did not significantly impact our findings. Our VM data was also limited by the fact that it was largely cross-sectional; as mentioned, future studies would benefit from studying potential temporal changes in such cognitive performance after a FEP. Finally, although our patient sample was largely antipsychotic-naïve at the beginning of the study, many of these patients were prescribed antipsychotic medications. Our exploration of antipsychotic medication on rate of change in WGC and CT showed no notable effect, however individual medication classes could have differential effects on gray/white matter (Bartzokis et al. 2009; Szeszko et al. 2014; Abramovic et al. 2016).

Although further work is needed to clarify the longitudinal relationships between cognition and negative symptoms, this avenue is promising in understanding domains of psychosis which have largely gone untreated. These findings may also hold implications for other neurological and psychiatric disorders characterized by negative symptom presentation and verbal memory deficits. Given that structural MRI is one of the most commonly used imaging techniques in psychiatric neuroimaging studies, extracting WGC and CT together may be fruitful in the broader search for a valid and easy-to-measure biomarker in psychiatry.

Acknowledgments and Disclosures

We would like to thank PEPP-Montreal and Lepage Lab research staff for their efforts in recruitment and clinical data collection. We are also grateful to all patients and families for participating in the study. The study was supported by operating grants from the Canadian Institutes of Health Research (CIHR, 68961, MCT-94189); the Fonds de Recherche du Quebec – Santé (FRSQ); Sackler Foundation; and by grant ANRP-MIRI13-3388 from the Azrieli Neurodevelopmental Research Program in partnership with the Brain Canada Multi-Investigator Research Initiative (to A.C.E.). It also benefited from computational resources provided by Compute Canada (www.computecanada.ca) and Calcul Quebec (www.calculquebec.ca). Salary awards include: Canadian Institutes for Health Research (CIHR; C.M., R.J., M.L., A.C.E.), Fonds de la Recherche en Santé du Québec (FRSQ; C.M., M.L., and R.J.), funding from the Canada First Research Excellence Fund, awarded to McGill University for the Healthy Brains for Healthy Lives Initiative (C.M., A.C.E.), James McGill Professorship (M.L., A.C.E.) and Canada Research Chairs Programme (A.K.M.). A.C.E. has received consulting fees from Biospective. M.L. reports grants from Otsuka Lundbeck Alliance, personal fees from Otsuka Canada, personal fees from Lundbeck Canada, grants and personal fees from Janssen, and personal fees from MedAvante-Prophase, outside the submitted work. R.J. reports receipt of grants, speaker's fees, or honoraria from AstraZeneca, BMS, Janssen, Lundbeck, Otsuka, Pfizer Canada, Shire, and Sunovion and royalties from Henry Stewart Talks. A.M. reports receipt of grants, fees, or honoraria from BMS, Lundbeck, and Otsuka. The authors have no other competing interests to disclose. The funding organizations had no role in the design and conduct of the study; collection, management, analysis, and interpretation of the data; preparation, review, or approval of the manuscript; and decision to submit the manuscript for publication.

Chapter 6 : Linking hippocampal centrality and verbal memory to negative symptoms after a First Episode of Psychosis

PREFACE

The previous manuscript-based chapters have collectively shown that changes within limbic structure (including the hippocampus) and fronto-temporal cortical structure are associated with negative symptom presentation. It is clear that many regions within the brain are changing over time after a FEP and contributing to the prognostic indicators that are of interest in this thesis. This final manuscript-based chapter builds upon the work presented thus far and investigates the interplay between hippocampal circuitry and cortical structure using more of a "network-based" approach, and links with both verbal memory and negative symptom fluctuations after a FEP.

Several methodological advances are presented in this chapter, which address some of the limitations discussed in Chapters 4 and 5:

1) Longitudinal clinical *and* cognitive measures were collected, to better understand the dynamic relationship between changes in negative symptoms and verbal memory.
2) The study design included more closely spaced timepoints and one additional imaging timepoint to detect subtle changes that may be occurring shortly after a FEP. Thus, instead of having an interscan interval of ~1 year, as was the case for data in Chapters 4 and 5, the first interscan interval is only 3 months, followed by 6 month interscan intervals.
3) Multi-modal imaging acquisitions were integrated, collected on a 3-Tesla MRI scanner. The imaging protocol includes a) a high-resolution sub-millimetric T2-weighted scan was collected, specifically designed to resolve hippocampal subfields and white matter structures surrounding the hippocampus, such as the fornix, and b) a quantitative T1 map, allowing us to disentangle whether microstructural changes in and around the cortex are

occurring below (i.e. within superficial white matter) or above the gray-white matter boundary (i.e. intracortically).

The hippocampus has been speculated to be a central component of positive symptoms; however, its centrality to negative symptoms has not yet been addressed in the field. This chapter proposes a novel framework by which the hippocampus and associated circuitry is central to the manifestation of negative symptoms. This work also shows that changes in verbal memory play an important role in explaining this relationship. This last component provides an additional layer of novelty, as cognition has often been argued to be a stable component of psychosis; a conjecture that this chapter urges researchers in the field to re-visit. This work shows that the progressive nature of brain changes after a FEP affects hippocampal microstructure predominantly, which then has propagating effects on other cortical networks, and in turn, clinical and cognitive profiles.

Altered hippocampal centrality and co-occurring changes of intracortical microstructure in First Episode Psychosis

Carolina Makowski[1,2], John D. Lewis[2], Budhachandra Khundrakpam[2], Christine L. Tardif[3], Lena Palaniyappan[4], Ridha Joober[1,5], Ashok Malla[1,5], Jai L. Shah[1,5], Michael Bodnar[6], M. Mallar Chakravarty[1,3,5], Alan C. Evans[2,3], Martin Lepage[1,5]

[1] Douglas Mental Health University Institute, Verdun, QC, Canada

[2] McGill Centre for Integrative Neuroscience, McGill University, Montreal, QC, Canada

[3] Department of Biomedical Engineering, McGill University, Montreal, QC, Canada

[4] Robarts Research Institute, University of Western Ontario, London, ON, Canada

[5] Department of Psychiatry, McGill University, Montréal, QC, Canada

[6] Royal Ottawa Mental Health Centre, Ottawa, ON, Canada

Manuscript in preparation for *Molecular Psychiatry*

Abstract

The hippocampus and associated circuitry have been posited to be fundamental to positive symptoms in psychosis, but the hippocampus' contributions to other factors important for outcome remains unclear. We test the hypothesis that longitudinal changes in the hippocampal circuit in relation to co-occurring changes of peri-cortical microstructure are altered in first episode psychosis (FEP) patients compared to controls, and that such changes are associated with negative symptoms and verbal memory. Longitudinal brain scans (2-4 visits over 3-15 months) were acquired for 27 FEP and 29 age-matched healthy controls. Quantitative T1 maps, sensitive to myelin content, were used to sample the microstructure of the hippocampal subfields and output circuitry (fimbria, alveus, fornix, mammillary bodies), intracortical (IC) and superficial white matter (SWM) regions. Co-occurring changes in pair-wise regional trajectories were calculated for each subject, and graph theory was used to calculate the participation coefficient (PC) to quantify the similarity/divergence between hippocampal and peri-cortical microstructure. The mean PC of the hippocampal parcel was significantly reduced in FEP patients compared to controls in the hippocampal-IC network, driven by differences in output hippocampal regions. Importantly, lower PC of the hippocampal circuit was associated with worsening negative symptoms, a relationship that was mediated by changes in verbal memory ability. This study provides evidence for reduced hippocampal centrality in FEP in relation to co-occurring changes in IC anatomy. The myelin-rich output regions of the hippocampus may serve as an important therapeutic target in early psychosis, with cascading effects on broader cortical networks and resultant clinical profiles.

Introduction

The hippocampus and associated circuitry have been consistently implicated in the emergence of psychosis (Tamminga et al. 2010, 2012; Samudra et al. 2015). Recent evidence suggests the hippocampus is positioned as a key convergence zone for cortical regions in the human brain (Mišić et al. 2014). A better understanding of the role of the hippocampus within broader neocortical networks in psychosis may shed light on the highly replicated finding and robust effect size of hippocampal structural abnormalities across the psychosis spectrum compared to healthy controls (Harrison 2004; Narr et al. 2004; Mathew et al. 2014; Hibar et al. 2016; van Erp et al. 2016).

Beyond positive symptoms, the dense connections of the hippocampus and output circuitry (forming the Papez circuit (Papez 1937)) to other cortical regions suggest a plausible role of the hippocampus in the manifestation of other functionally important clinical symptoms that have a paucity of effective treatments in early stages of psychosis, namely verbal memory deficits and negative symptoms (Hovington et al. 2013; Jordan et al. 2014). Our group and others have previously shown cross-sectional associations between negative symptoms and verbal memory (Cirillo and Seidman 2003; Makowski, Lewis, et al. 2019a), but the dynamic interrelationship between these two variables remains unclear. Several authors have proposed a model in which impaired cognition, including verbal memory deficits, may give rise to negative symptoms; specifically, it has been proposed that cognition equips individuals with the capacity for task performance, and motivation (impaired in patients with negative symptoms) impacts an individual's willingness to carry out such tasks. In turn, impairments in both of these domains contribute to patient functional outcome (Foussias et al. 2014; Jordan et al. 2014).

The presentation of negative symptoms and verbal memory deficits may be subserved by the connections of the hippocampus to the cortex both proximally, i.e. to the medial temporal lobe (Bird and Burgess 2008), and more distally, i.e. to the prefrontal cortex (PFC) (Godsil et al. 2013). Corroborating this, relationships between negative symptoms and hippocampal-cortical anatomy have previously been reported (Takayanagi et al. 2013; Bernasconi et al. 2015). Investigating the microstructure between neocortical regions and fine-grained structures of the hippocampus (e.g. subfields) may elucidate some of these mechanisms. Recent advances in magnetic resonance imaging (MRI) have allowed for quantitative measurement of such meso-structures *in vivo* (Pipitone et al. 2014; Ho, Holt, et al. 2017; Amaral et al. 2018; Baglivo et al. 2018; Tardif et al. 2018), offering an unprecedented opportunity to investigate the contribution of individual hippocampal components that may be dysfunctional around psychosis onset.

Applications of graph theory to brain imaging have allowed researchers to derive summary metrics of the inter-relationships between brain regions, i.e. the connectome, and thereby provide a novel perspective on brain organization in psychotic disorders (Rubinov and Sporns 2010; van den Heuvel et al. 2010; Palaniyappan et al. 2016; Das et al. 2018). Of relevance to the current investigation, a recent study probed the organization of networks of the anterior/posterior hippocampus derived from resting-state functional MRI in schizophrenia in relation to cortical regions subserving memory function (Avery et al. 2018). That study found that patients had significantly more sparse, or less modular, organization of the hippocampus compared to healthy controls, and this was related to relational memory function. However, to our knowledge, there are no studies using graph theoretical applications using longitudinal neuroimaging data in the early phases of psychosis, which has recently been encouraged in the field (Collin and Keshavan 2018).

In our previous work with first episode of psychosis (FEP) patients, we have described

changes in cortical white-gray matter contrast, a putative marker of peri-cortical myelin, underlying verbal memory deficits and negative symptoms (Makowski, Lewis, et al. 2019a, 2019b). In this study, we aim to bridge these findings to better understand the similarity or divergence in hippocampal microstructure to cortical anatomy. We adapt a previous method from our group, namely co-occurring anatomical changes (Khundrakpam et al. 2017), to investigate whether co-occurring microstructural changes between the hippocampal circuit and the cortex are altered in FEP patients compared to controls. To do so, we use a graph measure of centrality, namely the participation coefficient (Rubinov and Sporns 2010), to assess the degree of co-occurring anatomical changes between hippocampal and peri-cortical microstructure. We hypothesize that patients will have reduced coupling between the hippocampal circuit and cortex, particularly driven by output hippocampal structures, such as subfield CA1 and fornix. At the behavioural level, we aim to extend previous cross-sectional findings and better elucidate the dynamic inter-relationship between negative symptoms and verbal memory deficits shortly after a FEP. If such a relationship exists, we hypothesize that hippocampal centrality will act as a mediator between verbal memory deficits and negative symptom severity. This would offer a meaningful biological mechanism for the proposed framework of cognitive deficits influencing negative symptoms.

Methods

Subjects.

Patients were recruited from the Prevention and Early Intervention Program for Psychosis (PEPP-Montréal) at the Douglas Institute in Montreal, Canada, and were part of an ongoing longitudinal naturalistic outcome study. Details of PEPP-Montréal are outlined elsewhere (Iyer et al. 2015). Inclusion criteria at PEPP include a diagnosis of non-affective (e.g. schizophrenia, schizoaffective) and affective (e.g. bipolar, depression with psychotic features) psychosis, IQ>70, and limited (maximum 1 month) to no previous exposure to antipsychotic medication. Patients recruited to PEPP (ages 18-35) were invited to take part in a neuroimaging study, comprising four timepoints (baseline, 3/9/15-month follow-ups), with clinical and cognitive data collected concurrently. Non-clinical age-matched healthy controls were recruited through advertisements within the same local catchment area under the same four-timepoint protocol. All participants provided written informed consent, and the research protocol was approved by the Douglas Institute human ethics review board. Twenty-seven patients (Male, N=18) and 29 healthy controls (Male, N=12) had at least two usable scans and were included in this study.

Negative symptoms and verbal memory data.

The relationship between negative symptoms and verbal memory was assessed longitudinally. Two patients were missing clinical/cognitive data, leaving N=25 for this analysis. Negative symptoms were assessed using the Scale for the Assessment of Negative Symptoms (SANS) (Andreasen 1984a), which has been shown to have good inter-rater reliability (κ=0.71) at PEPP-Montreal (Jordan et al. 2018). Item-level scores, excluding the Attention subdomain (Peralta and Cuesta 1999; Malla, Takhar, et al. 2002b), were summed for each patient per timepoint. To assess

rate of change in symptoms over time, a linear model was fit to each subject's longitudinal SANS data, where the slope represented a single metric of change over time in symptoms. Verbal memory was assessed for both FEP patients and healthy controls with the Logical Memory subtests of the Wechsler Memory Scale–Fourth Edition (WMS-IV) (Wechsler 1997; Weschler 2009). Scaled scores for immediate recall (Logical Memory I) and delayed recall (Logical Memory II) were averaged to obtain a global score of memory recall performance. Similarly as with negative symptoms, a single longitudinal score was derived for each participant, by calculating the rate of change in verbal memory performance over available timepoints.

MRI acquisition.

All participants underwent MRI scanning on a 3T Siemens Magnetom Trio scanner at the Brain Imaging Center at the Douglas Institute. Anatomical MRI acquisitions are comprised of a T1-weighted MPRAGE sequence (repetition time [TR] = 2300ms, echo time [TE] = 2.98ms, field of view [FOV] = 256mm, voxel size = $1mm^3$, 192 slices, flip angle = 9°, scan time ~5 minutes), a high-resolution T2-weighted image to capture detailed hippocampal subfield information (TR = 2500ms, TE = 198ms, FOV = 206mm, voxel size = $0.64mm^3$, 320 slices, scan time ~10 minutes), and an MP2RAGE sequence (Marques et al. 2010), which includes a quantitative T1 (qT1) map, serving as a proxy measure of myelin content (TR=5000ms, TE=2.01ms, first T1=700ms, second T1=2500mm, first flip angle=4°, second flip angle=5°, FOV 256mm, voxel size $1mm^3$, 176 slices, scan time ~9 minutes). The MP2RAGE acquisition combines two different images acquired with slightly different inversion times, to diminish the spatial inhomogeneities typically caused by the transmit B_1 field, and allows for quantification of bias-free T1 relaxation times (Marques et al. 2010). Slight deviations to this protocol were acquired in a subset of scans included in the analysis,

which are detailed in Appendix-IV.

MRI processing.

Please see **Figure 6.1** for a visualization of the image processing and analysis workflow, which are described in detail in the sections below.

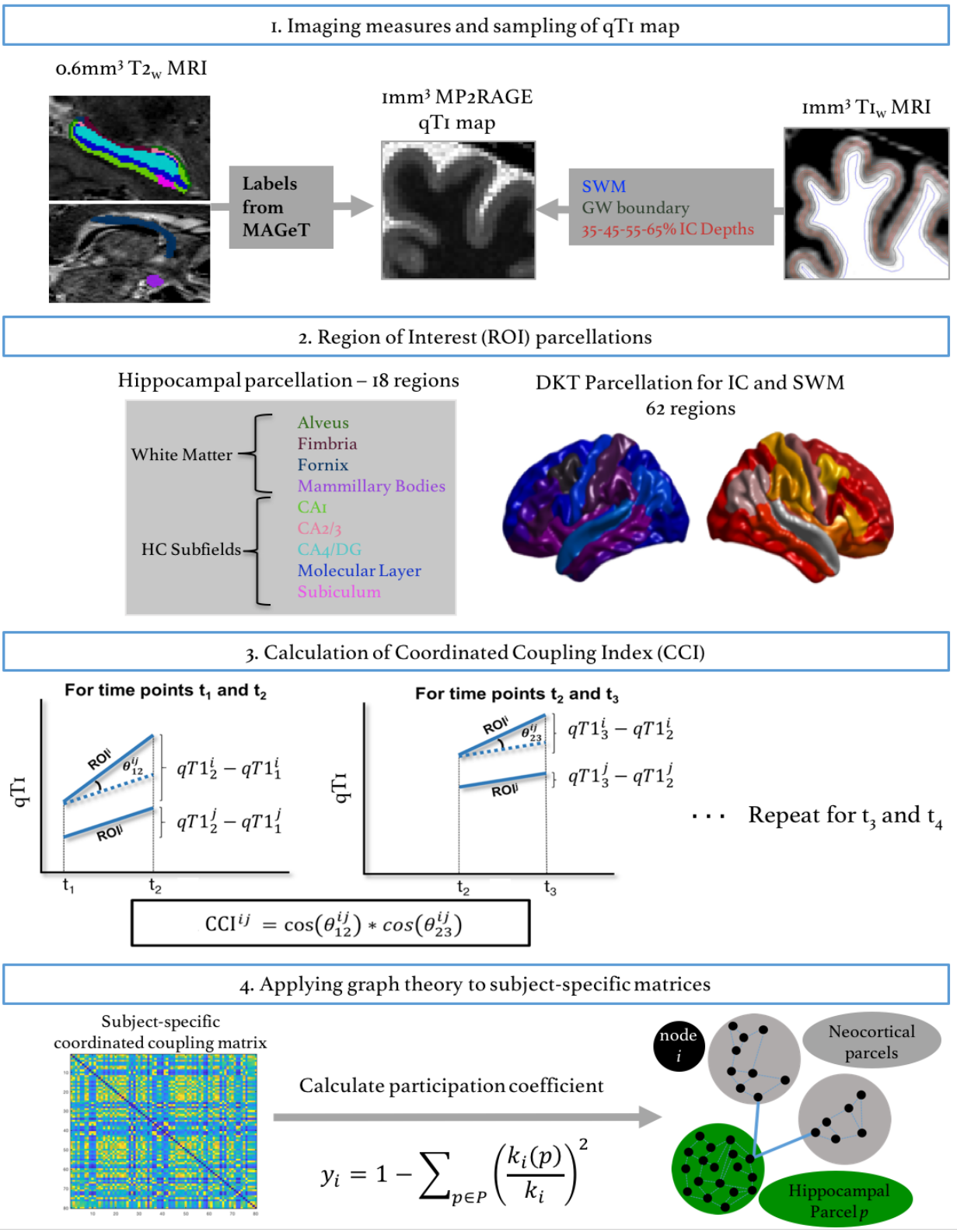

Figure 6.1. Image processing workflow.

Step 1: Sampling of qT1 map of MP2RAGE sequence for hippocampal-white matter circuit labels from MAGeT (left) and cortical surfaces (4 intracortical [IC] + 1 superficial white matter [SWM]; right). For the hippocampal-white matter regions of interest (ROIs), a mean qT1 value was obtained for each label. For cortical surfaces, a qT1 value was sampled at each of 81 924 points/vertices along the surface. For intracortical microstructure, qT1 was then averaged at 35-45-55-65% cortical depths across linked vertices.
Step 2: Definition of individual ROIs: 18 regions of hippocampal-white matter circuit, and 62 DKT regions for cortical surfaces. Colours of text of 18 hippocampal-white matter regions correspond to colour of labels used in left-hand side image of Step 1.
Step 3: Calculation of Coordinated Coupling Index (CCI), adapted from Khundrakpam et al (2017). Note, each subject has two different matrices: one includes hippocampal-white matter and IC qT1 coordinated coupling indices; another includes hippocampal-white matter and SWM qT1 coordinated coupling indices. In this schematic, *i* and *j* represent two different ROIs, and the numbers reflect timepoints. First, the slope or rate of change in qT1 between timepoint t_1 and t_2 is calculated. The same is done for region *j*. The cosine of the theta (θ) angle defining the difference between these two slopes is then calculated, representing the CCI for participants that contributed two timepoints only. For participants with more than two timepoints available (i.e. t_2 and t_3, and t_3 and t_4), this calculation is repeated and the product of the cosine of the θ angle of change between consecutive timepoints defines the CCI.
Step 4: Graph theory was applied to each individual's CCI matrix. Specifically, participation coefficient was calculated for each ROI, using the Brain Connectivity Toolbox (Rubinov & Sporns, 2010). The equation for participation coefficient is depicted in step 4, where y_i is the participation coefficient for each node *i*, contained within a particular parcel *p*. *P* represents the entire set of parcels, and k_i represents the degree or number of links for each node *i*. Parcels were defined *a priori*; one parcel included the 18 ROIS of the hippocampal-white matter circuit, and the 7 other parcels were based on functional networks (Rubinov & Sporns, 2010) defined by Yeo et al (2011). These 8 parcels are shown in Figure 8.9 of Appendix-IV. For this manuscript, the participation coefficient of the hippocampal-white matter circuit was the primary parcel of interest and is represented by the green parcel in the bottom-right hand side of the figure.

Hippocampal labels. Pre-processing of T1- and T2-weighted images was carried out using the *minc bpipe* library (https://github.com/CobraLab/minc-bpipe-library). First, high-resolution T2-weighted images were N4 bias field corrected (Tustison et al. 2010). Next, T1-weighted images were linearly registered to MNI space and cropped. The resultant bounding box of the T1-weighted image was then applied to the T2-weighted image. Pre-processed T2-weighted images were submitted to the Multiple Automatically Generated Templates (MAGeT)-Brain algorithm (https://github.com/CobraLab/MAGeTbrain) (Chakravarty et al. 2013; Winterburn et al. 2013;

Pipitone et al. 2014; Amaral et al. 2018) to extract hippocampal subfields (cornu ammonis [CA] 1, CA2/3, CA4/dentate gyrus [DG], subiculum, and molecular layer) and surrounding white matter structures (alveus, fimbria, fornix, mammillary bodies). This technique utilizes five high-resolution atlases from healthy adults that have been manually segmented (https://github.com/CobraLab/atlases/hippocampus-whitematter/). Extensive validation of MAGeT has been done previously (Pipitone et al. 2014; Makowski et al. 2018). As listed above, this atlas yields 18 hippocampal-white matter labels (9 per hemisphere) per subject.

Sampling of the qT1 map for hippocampal labels. T2-weighted images were affinely registered to MP2RAGE UNI scans ($1mm^3$), and the transforms were applied to the hippocampal labels. Mean qT1 values for each hippocampal subfield and white matter label were then sampled for each participant from the MP2RAGE qT1 map. See step 1 of **Figure 6.1**.

Generation of Cortical Surfaces. Raw T1-weighted images were submitted to the CIVET pipeline (Version 2.1.0: http://www.bic.mni.mcgill.ca/ServicesSoftware/CIVET) for extraction of gray and white matter surfaces. Main processing steps include: 1) Registration of T1-weighted images to standardized space (Collins et al. 1994), upsampling images to 0.5x0.5x0.5mm, and correction for non-uniformity artefacts (Sled et al. 1998); 2) segmentation of gray, subcortical gray and white matter, and cerebral spinal fluid (Zijdenbos et al. 2002; Tohka et al. 2004); 3) extraction of the white matter surface using a marching-cubes algorithm and extraction of the gray matter surface using the CLASP algorithm (Kim et al. 2005); and 4) surface registration to a template for inter-subject correspondence (Lyttelton et al. 2007). For a subset of subjects, an in-house blood vessel mask was used, for cases where blood vessels significantly impacted the quality of gray and white

matter surfaces output by CIVET. As described previously (Lewis et al. 2018), a distance map relative to the white surface provided by CIVET was created at 0.25x0.25x0.25mm resolution, smoothed with a 0.5mm FWHM Gaussian kernel, and used to create a gradient vector field of the distance map. Down-sampling and smoothing was done prior to creation of the vector field, due to the fact that at low resolution, some regions (particularly at the tips of gyri) have very thin white matter. From here, five additional surfaces were generated: one was moved 1mm inward along this gradient vector field to produce a superficial white matter (SWM) surface, and the others were generated at 35-45-55-65% cortical depths between the pial and white matter surfaces, comprising intracortical (IC) surfaces. Surfaces below 35% or over 65% cortical depths were not considered to avoid partial volume effects (Nürnberger et al. 2017).

Sampling of qT1 maps for cortical surfaces. The MP2RAGE qT1 map was upsampled to 0.5x0.5x0.5mm and registered to stereotaxic space. Finally, the qT1 map was sampled along 81,924 vertices for each of the five surfaces described above (1 SWM, 4 IC). See step 1 of **Figure 6.1**. The resulting surface maps were smoothed with a 20mm FWHM Gaussian kernel and qT1 values at linked vertices across the four IC depths were averaged to mitigate the effects of noise, yielding one value per vertex to summarize IC microstructure. See Appendix-IV for quality control methods for hippocampal labels and cortical surfaces.

Calculating pairwise co-occurring change in anatomy. The Desikan Killiany-Tourville (DKT) atlas was used to parcellate the brain into 62 regions (Klein and Tourville 2012). DKT regions are listed in Table 8.10 of Appendix-IV and a schematic is included in step 2 of **Figure 6.1**. Subject-specific matrices based on co-occurring changes in anatomy were created, based on methods

presented in Khundrakpam et al (2017). To create these matrices, the theta (θ) angle of separation was calculated between the qT1 rates of change of any two brain regions between each pair of timepoints. The cosine of the θ angle was then calculated to normalize values between 0 and 1. For participants with more than one consecutive pair of timepoints, the cosine of the pair-wise θ angle was multiplied. Thus, subject-specific matrices reflected the coordinated change between all possible pairs of regions, based on pairwise cosine similarity values derived from the slopes of linear changes in qT1 in an 80x80 matrix. Finally, a cumulative distribution function (CDF) kernel was applied to enhance the contrast between real and spurious links for each matrix, as described in Khundrakpam et al (2017). The final co-occurring change matrices were generated for both hippocampal-IC and hippocampal-SWM measures, hereafter referred to as HC-IC and HC-SWM networks, respectively. Please see step 3 of **Figure 6.1**.

Graph theory application: participation coefficient of hippocampal parcel. To determine whether the hippocampal circuit has altered centrality in relation to other cortical parcels in FEP patients, we labeled the 62 DKT regions into 7 functional networks based on Yeo et al. (2011). This approach was motivated by recent methods presented by Baum et al. (2017) in a neurodevelopmental cohort. It has also been shown that these 7 functional networks show high modularity and provide a strong fit to structural connectivity data (Baum et al. 2017). Hippocampal subfields and output white matter were then defined as a separate parcel. See Figure 8.9 of Appendix-IV for a visualization of node assignment. The Brain Connectivity Toolbox (brain-connectivity-toolbox.net) in Matlab was used to calculate the participation coefficient of each parcel (Rubinov and Sporns 2010). The participation coefficient reflects the distribution of co-occurring changes between a particular set of nodes in a given parcel and nodes of other parcels.

In other words, a node with a high participation coefficient suggests that node has higher between-parcel than within-parcel covariance. See step 4 of **Figure 6.1**. A participation coefficient was derived for each of the 80 nodes, as well as an average participation coefficient for each of the eight parcels.

See Box 1 for a summary of key neuroimaging and graph theory terms used in this paper.

Box 1.

Co-occurring change index (CCI): cosine similarity of longitudinal changes in qT1 values between pairs of regions. Indices are obtained for each possible pair of regions to form a subject-specific matrix of co-occurring change

HC-IC network: co-occurring change matrices including pair-wise relationships between qT1 values of the hippocampus (HC) and intracortical (IC) regions

HC-SWM network: co-occurring change matrices including pair-wise relationships between qT1 values of the hippocampus (HC) and superficial white matter (SWM) regions

Hippocampal centrality: participation coefficient based on the cosine similarity of longitudinal changes in qT1 values

Hippocampal parcel: a parcel comprising 9 regions per hemisphere of the hippocampal-white matter circuit (i.e. CA1, CA2/3, CA4/DG, subiculum, molecular layer, alveus, fimbria, fornix, mammillary bodies)

Neocortical parcels: 7 non-overlapping parcels comprising regions within the following networks: limbic, frontoparietal control, default mode, somatomotor, dorsal attention, ventral attention, and visual

Node: a brain region within a graph

Parcel: a set of brain regions within a graph, sometimes referred to as a "module" in the literature

Participation Coefficient (PC): a graph measure reflecting the distribution of co-occurring changes between a particular set of nodes in a given parcel and nodes of other parcels

Statistical analyses.

Demographic and clinical data. Demographic and clinical variables were analysed with independent sample t-tests and Mann-Whitney U tests for normally and non-normally distributed data, respectively. We tested for associations between rates of change in negative symptoms and logical memory scores in FEP patients with Pearson correlation coefficients. Given that the scaled scores of the logical memory score are already adjusted for age and sex, we did not covary for these variables in our behavioural analysis. Analyses of behavioural and clinical variables were conducted using PASW Statistics 21 (SPSS inc., 2009, Chicago, IL, USA) and were two-tailed with a critical *p*-value of 0.05.

Group differences in co-occurring change matrices. The mean of subject-specific co-occurring change matrices were derived for each group (i.e. FEP patients and healthy controls) to compare whether there were group differences in coordinated coupling of qT1 values across the brain, for both HC-IC and HC-SWM networks. Co-occurring change matrices were compared between groups by converting coupling metrics (i.e. the cosine similarity score, in the range of 0 to 1) to z-scores using a Fisher transformation and comparing the differences to a normal distribution to obtain p-values. P-values were thresholded using a two-stage false discovery rate (FDR) correction, which limits the false-positive rate for a family of hypothesis tests below 0.05 (Benjamini et al. 2006). This approach was used over the traditional FDR correction (Benjamini and Hochberg 1995), as it has been shown to better account for both independent and positively dependent correlations. Only the lower triangle of the thresholded matrices (i.e. non-duplicate pairs of regions) were considered when reporting significant pairwise correlations. Therefore, for the hippocampal and DKT parcellations, a total of 3160 (80x79/2) tests were conducted. Results were

visualized with BrainNet Viewer (Xia et al. 2013). Supplementary analyses were also conducted to assess group differences in qT1 values of the hippocampal circuit and within SWM and IC regions across the cortical surface.

Group differences in hippocampal Participation Coefficient (PC). Mean PC values of the hippocampal parcel across hippocampal nodes were derived per subject for both HC-IC and HC-SWM networks, and adjusted for age and sex. Possible relationships with mean antipsychotic medication dosage and PC were tested, to see whether medication should be covaried for. Average antipsychotic medication exposure was found to be non-normally distributed; thus a square root transform was applied to the data. The p-value threshold of significance was Bonferroni-corrected with p=0.05/2. Post-hoc tests were conducted to identify the hippocampal subregion that contributed to significant group differences.

Control analysis: testing centrality of default mode and ventral attention networks. To ensure that our results were specific to centrality of the hippocampal parcel, and not to another parcel, the same analyses were conducted testing group differences in PC and relationships with changes in verbal memory/negative symptoms of the default mode and ventral attention networks. Both of these networks have been shown to be robustly altered in patients with psychosis (Bluhm et al. 2007; Palaniyappan, Simmonite, et al. 2013).

Relationship between negative symptoms and verbal memory deficits. The interaction of changes in negative symptoms and verbal memory on mean hippocampal PC was tested, contingent on whether results were significant in the behavioural analysis above. Relationships between changes

in these two variables and mean hippocampal PC of HC-IC and HC-SWM networks were tested separately with Pearson correlations. The p-value threshold of significance was Bonferroni-corrected with p=0.05/2. Post-hoc tests were conducted to determine which node within the hippocampal parcel contributed to significant group differences. To test whether results were specific to negative symptoms, associations with change in positive symptoms (measured by the SAPS) were also tested.

Mediation analysis. A mediation analysis using the causal steps strategy (Baron and Kenny 1986; Preacher and Hayes 2008) was employed to test whether HC centrality, as measured by the mean PC of the hippocampal parcel in HC-IC and HC-SWM networks, mediates the relationship between rate of change in verbal memory and rate of change in negative symptoms. Another model was also explored whereby changes in verbal memory served as the potential mediator between HC centrality and changes in negative symptoms, if the first did not meet criteria for the causal steps strategy.

Results

Sample.

Demographic and clinical/cognitive data can be found in **Table 6.1**. The final sample comprised 27 FEP patients (Male, 18) and 29 healthy controls (Male, 12) with longitudinal neuroimaging data. For patients, 15 contributed two timepoints, 6 contributed three, and 6 contributed four timepoints. For controls, 9 contributed two, 7 contributed three, and 13 contributed four timepoints. As can be seen in **Table 6.1**, there was a trend for males to be more represented in the FEP group; sex was thus covaried for in all group analyses. Patients had significantly less years of education, lower performance IQ and lower scores on logical memory (defined as the average

between immediate and delayed recall scaled scores). Patients and controls did not differ in age or verbal IQ, or rate of change in logical memory scores. For patients, baseline scans were acquired approximately 2.2 months (standard deviation: 0.9 months) after entry to the PEPP clinic. Mean interscan intervals were as follows: 4.00 months (SD=0.76) between baseline and second scan, 6.04 (SD=0.62) between second and third scans, and 6.09 (SD=0.35) between third and fourth scans. Additional information on the final sample and excluded participants can be found in Appendix-IV.

		FEP N=27		Controls N=29				
		N	**%**	**N**	**%**	**Statistic**	**df**	***p*-value**
General Measures	Male	18	66.7	12	41.4	χ^2= 3.6	2	0.06
	Right Handed	22	81.5	29	100			
	Diagnosis[1]							
	Schizophrenia Spectrum	10	37.0					
	Affective Disorder	10	37.0					
	Psychosis Not Otherwise Specified	6	22.2					
		Mean	**SD**	**Mean**	**SD**	**Statistic**	**df**	**p-value**
	Age at Baseline	23.4	3.5	25.1	4.1	t=1.6	54	0.1
	Education in Years*	12.70	2.60	14.2	1.90	t=2.6	54	0.01
	Socioeconomic Status	2.9 [25]	1.00	3.3	1.10	U=277.5		0.1
	Performance IQ*	102.50	14.10	111.3	7.8	t=2.8	39.9	0.007
	Verbal IQ	101.40	13.00	105.6	10.9	t=1.3	54	0.2
	Logical Memory*	6.8	2.9	10.4	2.7	t=4.8	54	<0.001
	SANS	12.2 [26]	9.00					
	SAPS	18.3 [26]	17.10					
	Duration Untreated Psychosis (weeks)[2]	19.8 [25] Median: 2.4	31.50					
	Duration Untreated Illness (years)	401.8 [25] Median: 399.6	313.60					
	Baseline scan past clinic entry (months)	2.2	0.90					
		Mean	**SD**	**Mean**	**SD**	**Statistic**	**df**	**p-value**
Longitudinal Measures	ΔLogical Memory	2.7 [26]	5.30	2.5	4.0	t=-0.2	53	0.9
	ΔSANS	-12.7 [25]	17.0					
	ΔSAPS	-24.5 [25]	38.4					
	Avg CPZ equivalents (daily dose in mg)	192.6	194.5					

Table 6.1. Demographics and clinical information.

For patients, 15 contributed two timepoints, 6 contributed three, and 6 contributed four timepoints. For controls, 9 contributed two timepoints, 7 contributed three, and 13 contributed four timepoints. General Information reflects measures at baseline. All variables present for both FEP patients and healthy controls were compared with an independent sample t-test, except for socioeconomic status (SES), where the non-parametric Mann Whitney U test was used. Adjusted degrees of freedom are presented for performance IQ, as the two groups did not have equal variance. Variables with significant group differences ($p<0.05$) are bolded with an asterisk. Square brackets reflect altered sample size for cases where individual patient data was missing. Note that for ΔSANS/SAPS (measuring negative and positive symptoms, respectively), a mean negative score indicates that patients' symptoms generally improved. A mean positive score for ΔLogical Memory (indexing average change in immediate and delayed recall) indicates a general improvement.

[1] One patient missing diagnosis.

[2] One patient initiated antipsychotic medication use 9 weeks prior to their FEP, thus their DUP is technically "-9 weeks". This value influences the median quite markedly in this dataset. Removing this participant yields a mean DUP of 21.0 weeks and a median of 4.5 weeks.

Verbal memory and negative symptom relationships.

Generally, patients had an improving course of negative symptoms (Mean=-12.7, SD=9.0) and verbal memory performance (Mean=2.7, SD=5.3) over the 4 to 16-month time window investigated. Rates of change in immediate and delayed recall were significantly and positively correlated with each other ($r=0.92$, $p<0.001$). Thus, verbal memory performance in this manuscript refers to the average scaled score of immediate and delayed recall from the logical memory subtest of the WMS-IV. We found a significant relationship between rate of change in verbal memory and change in negative symptoms, whereby greater improvement in verbal memory performance (average of immediate and delayed recall) was associated with improvement in negative symptom severity ($r=-0.59$, $p=0.018$).

Group differences in co-occurring change matrices.

Two sets of co-occurring change matrices were compared between patients and controls. For HC-IC, 280 pair-wise regions out of 3160 possible pairwise comparisons (FDR-corrected, $p<0.05$) had

significantly different co-occurring change indices in patients compared to controls (**Figure 6.2**). For HC-SWM, significant pairwise differences were found for 192/3160 pairwise comparisons (FDR-corrected, $p<0.05$) (**Figure 6.2**). For both sets of results, patients showed both increased and decreased coupling between regions compared to controls across widespread brain regions, both within and across hemispheres. There were also notable patterns of altered coupling within the hippocampal circuit, as can be seen by the dense pattern of differences in the bottom right of the matrices shown in **Figure 6.2**. See Appendix-IV for group differences in qT1 values of the above-mentioned measures. In summary, higher qT1 was found in FEP patients compared to controls within the alveus and fornix bilaterally, and left CA4/DG and molecular layer (uncorrected $p<0.05$), although these findings did not survive correction for multiple comparisons (Table 8.11 of Appendix-IV). Increases in qT1 were also found along the cortical surface, particularly in SWM underlying the left insula and temporal lobes bilaterally (Figure 8.10 of Appendix-IV).

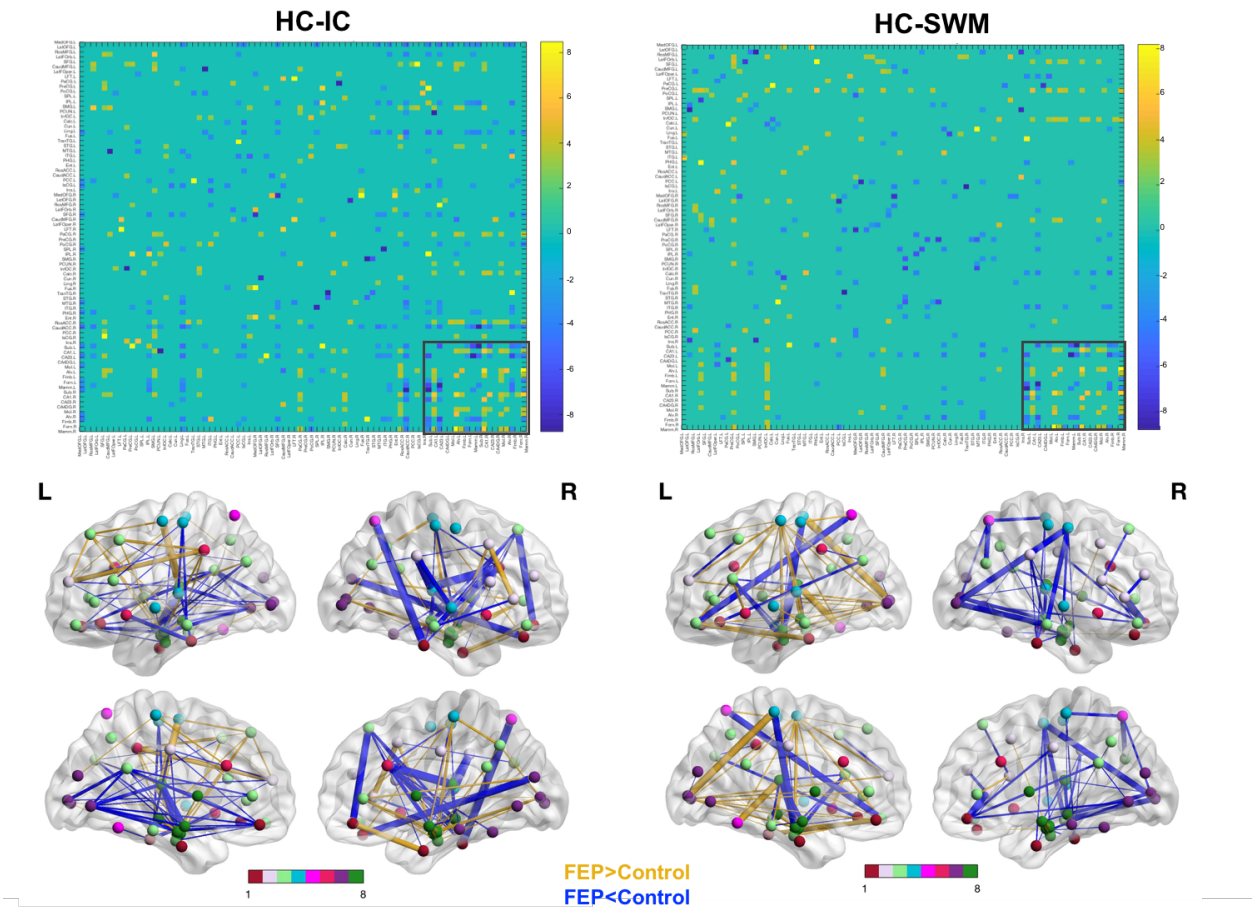

Figure 6.2. Group differences in coordinated coupling matrices.

Left-hand side, Group differences in Hippocampal-Intracortical (HC-IC) network. *Right-hand side*, Group differences in Hippocampal-Superficial White Matter (HC-SWM) network. *Top panel,* FDR-corrected matrices, of significant pair-wise group differences in coordinated coupling between regions. Dark gray square surrounds regions of the hippocampal circuit. *Bottom panel,* visualization of significant results portrayed in matrices with BrainNet Viewer. Nodes are coloured by network (hippocampal circuit + 7 functional networks). Width of lines reflect strength of pair-wise group difference. Warm colours/yellow reflects pair-wise differences that show increased coupling in FEP compared to controls. Cool colours/blue reflects pair-wise differences that show decreased coupling in FEP compared to controls.

Group differences in PC of the hippocampal parcel.

The mean PC of the 18 regions included in the hippocampal parcel was compared between groups.

Patients had significantly lower PC compared to controls in the HC-IC network ($F_{1,52}$=9.92,

p=0.003), and nominally lower PC compared to controls in the HC-SWM network ($F_{1,52}$=5.12, p=0.028). All analyses hereafter will thus only consider the PC values extracted from the HC-IC network. Post-hoc tests were then applied to individual hippocampal regions to determine which node(s) within the hippocampal parcel contributed to the lower PC in patients compared to controls. Ten of the 18 regions were found to be significant (p<0.05): CA1, alveus and fornix bilaterally; left CA2/3, subiculum and mammillary body; and right fimbria. See **Figure 6.3**.

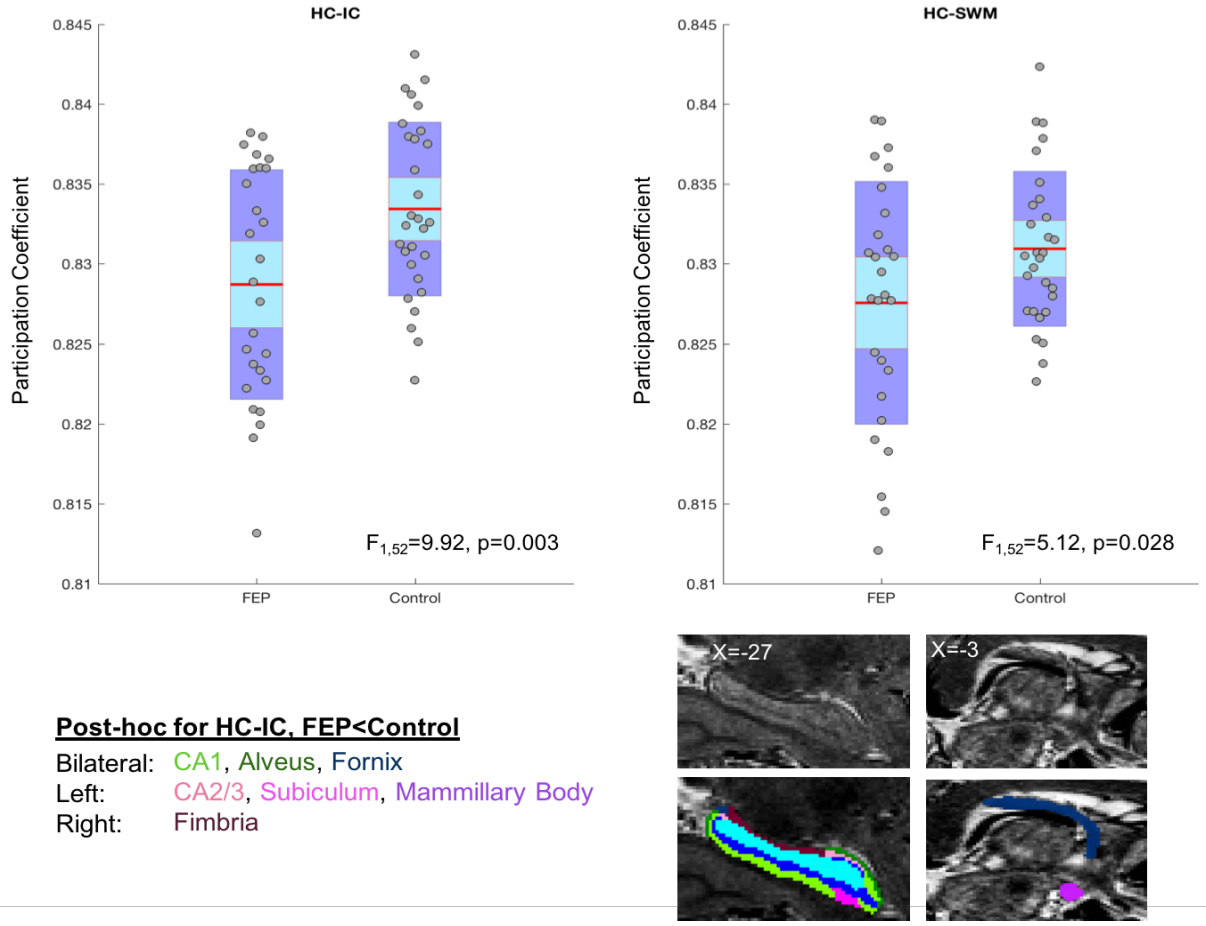

Figure 6.3. Group differences in hippocampal PC.
Top panel shows boxplots overlaid on a scatterplot of the data. For the boxplots, the red line denotes the mean, light blue boxes are the 95% confidence intervals, dark blue boxes represent 1 standard deviation, and gray dots are individual data points. The group differences in PC of the hippocampal circuit derived from the HC-SWM network did not survive correction for multiple comparisons. Bottom panel shows results of post-hoc tests applied to the PC of individual regions

making up hippocampal circuit within the HC-IC network. Ten of the 18 regions were found to have significantly lower PC in patients compared to controls ($p<0.05$). Significant regions are listed at the bottom left, and the colour of the text matches the colour of the region in the MRI-visualization of regions making up the hippocampal circuit. MRI labels on left hemisphere taken from a control included in the study.

Control analysis: group differences in PC of the default mode and ventral attention networks.

No significant group differences in mean PC of the default mode network in relation to coordinated coupling within the HC-IC network ($F_{1,52}=0.58$, $p=0.45$), nor the HC-SWM network ($F_{1,52}=0.25$, $p=0.62$) were found. Similarly, no group differences were found in the PC of the ventral attention network (HC-IC: $F_{1,52}=0.44$, $p=0.61$; HC-SWM: $F_{1,52}=1.21$, $p=0.28$). See Figure 8.10 of Appendix-IV.

Brain-behaviour relationships in FEP patients.

Associations between the PC of the hippocampal parcel from the HC-IC network and rates of changes in negative symptoms and verbal memory were evaluated. First, given the significant association between rate of change in negative symptoms and verbal memory as reported above, the interaction between these two variables was assessed against the mean PC of the hippocampal parcel. The overall model, including age and sex as covariates, was not significant ($F_{1,19}=1.56$, $p=0.22$); the interaction term was also not significant ($t=0.49$, $p=0.63$). We did not covary for antipsychotic medication[4] in this analysis as we found no association between the hippocampal PC from the HC-IC network and medication ($r=-0.0087$, $p=0.97$).

Next, rate of change in negative symptoms and verbal memory were assessed separately against hippocampal PC. For rate of change in negative symptoms, a significant negative

[4] Calculated as average daily dose across the study time period in chlorpromazine equivalents, multiplied by medication adherence

association emerged (r=-0.44, p=0.029), such that improvement in negative symptoms was associated with a higher mean hippocampal PC. For verbal memory, a significant positive association emerged (r=0.40, p=0.045), such that a more positive slope of verbal learning was associated with a higher mean hippocampal PC. No significant association was found between the hippocampal PC and change in positive symptoms (r=-0.022, p=0.92).

Post-hoc tests were then applied to assess the relationship between change in negative symptoms and change in verbal memory against individual hippocampal regions, restricting analyses to the regions that were uncovered above with significant group differences. These results are displayed in **Table 6.2**. With respect to change in negative symptoms, significant negative associations were found with the PC of the right fimbria and left mammillary body (p's<0.05). For change in verbal memory, significant positive associations were found with the PC of the left alveus and right fimbria (p's<0.05).

	Δ Negative Symptoms		Δ Verbal Memory	
HC Node	Left	Right	Left	Right
CA1	-0.1	-0.21	0.26	0.29
CA2/3	-0.24		0.2	
CA4/DG				
Subiculum	-0.21		0.29	
Molecular layer				
Alveus	-0.38	-0.27	**0.46**	0.34
Fimbria		**-0.44**		0.34
Fornix	0.073	-0.34	-0.17	**0.41**
Mamm Body	**-0.53**		0.37	

Table 6.2. Brain-behaviour analyses.
Correlations between participation coefficient of the hippocampal-white matter parcel (adjusted for age and sex) in the HC-IC network and changes in negative symptoms and verbal memory. Analyses were restricted to hippocampal nodes that showed significant post-hoc group differences. Statistics in the table are Pearson r-correlations, and significant relationships with p<0.05 are bolded in the table.

Control analyses: no brain-behaviour relationships with default mode and ventral attention networks.

The above relationships were not found between the PC of the default mode network of the HC-IC network and rate of change in negative symptoms (r=-0.21, p=0.32), nor rate of change in verbal memory (r=-0.086, p=0.72). Similarly for the ventral attention network, no associations were found between this network's PC in the HC-IC network and rate of change in negative symptoms (r=-0.046, p=0.83), nor rate of change in verbal memory (p=-0.025, p=0.91).

Mediation analysis: modeling verbal memory, negative symptoms, and hippocampal centrality.

Given that rate of change in negative symptoms, rate of change in verbal memory, and hippocampal PC in the HC-IC network (i.e. "HC centrality") were all significantly related to each other, a mediation analysis was carried out to better understand how these variables interact and predict rate of change in negative symptoms. Negative symptoms were chosen as the dependent variable as opposed to verbal memory, given past evidence that suggests verbal memory is more stable across psychosis stages, i.e. verbal memory deficits are already present prior to psychosis onset, whereas symptom severity tends to fluctuate more. The first model we tested placed HC centrality as the mediating variable between change in verbal memory and negative symptoms, but this model did not meet criteria for the causal steps strategy of mediation analysis (Baron and Kenny 1986; Preacher and Hayes 2008). Instead, our mediation analysis suggested that verbal memory serves as the mediator between HC centrality and rate of change in negative symptoms. See **Figure 6.4** for a schematic of this model with relevant statistics.

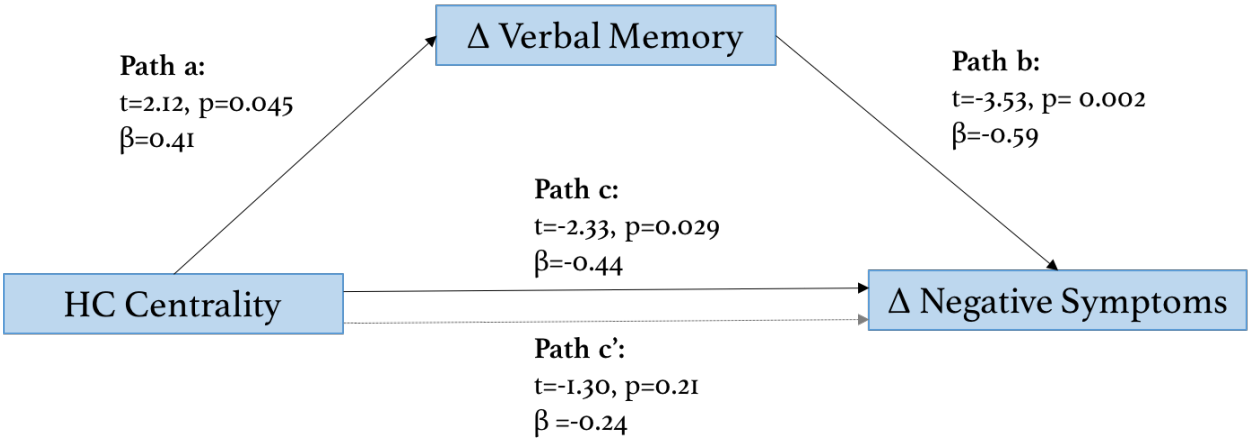

Figure 6.4. ΔVerbal memory mediates the relationship between HC centrality and Δ negative symptoms.

Path b remains significant when controlling for HC centrality (r=-0.506, p=0.012; df 22). There are two statistics shown for Path c, denoting the relationship between HC centrality and Δ negative symptoms. Path c shows a significant relationship between HC centrality and change in negative symptoms, *not* accounting for impact of verbal memory. Path c' between HC centrality and change in negative symptoms is no longer significant when taking into account Δ verbal memory, indicating that Δ verbal memory statistically mediates the relationship between hippocampal centrality and Δ negative symptoms. Note that hippocampal centrality denotes the mean PC of the hippocampal parcel in the HC-IC network, adjusted for age and sex.

Discussion

The current investigation provides novel evidence for reduced longitudinal coupling between microstructure of the hippocampus and broader cortical regions after psychosis onset. Our results demonstrate the important role of the hippocampal circuit (i.e. subfields and surrounding white matter) underlying the trajectory of negative symptoms after a FEP; a relationship which is mediated by changes in verbal memory. Our results suggest that changes in putative myelin content within the hippocampus relate to changes in microstructure intracortically in healthy controls (as observed by higher PC); the lower PC observed in FEP, which we have interpreted as decreased hippocampal centrality, suggests increased divergence of the hippocampal circuit from other cortical regions, particularly in patients with a worsening course of negative symptoms and verbal memory.

Our results suggest some degree of tissue specificity, where reduced hippocampal centrality in FEP patients compared to controls was more pronounced when examining coordinated coupling between the hippocampus and IC microstructure, rather than SWM. Our findings suggest that alterations in coordinated coupling between the hippocampus and cortical microstructure may be most strongly reflected by the myelin composition of white matter fibers terminating within the cortex. It should be noted that nominal group differences with networks including SWM were found; thus these microstructural alterations can be captured at other points along white matter fibers, including their passage through SWM before reaching their terminus within the cortex. Examining IC and SWM microstructure separately also allows us to contextualize recent findings examining white-gray matter contrast changes FEP patients and enduring schizophrenia, a method that did not allow for such localization of putative changes in peri-cortical myelin content (Jorgensen et al. 2016; Makowski, Lewis, et al. 2019a, 2019b).

Our results also show network specificity: we did not find reduced centrality or relationships with negative symptoms and verbal memory deficits when examining the participation coefficient of the default mode network, nor the ventral attention network (also referred to as the salience network). These networks were tested as they have both been found to be robustly altered in patients with schizophrenia and associated psychoses (Bluhm et al. 2007; Karbasforoushan and Woodward 2012; Gradin et al. 2013; Hu et al. 2017; Wang et al. 2017). It is possible that the well-documented alterations in these networks may stem from alterations within the hippocampus; a conjecture that needs further corroboration in the future.

The notion of the hippocampus being a central component of psychosis pathophysiology has been proposed previously (Tamminga et al. 2010; Lieberman et al. 2018). However, this study adds a novel perspective on this theory, suggesting that reduced hippocampal centrality may also

give rise to negative symptoms. Further, we uncover an explanatory framework for this relationship, whereby verbal memory mediates the association between altered co-occurring changes in hippocampal-intracortical microstructure and negative symptoms. Although our methodological approach did not allow us to define the precise neocortical regions that drive this relationship of altered centrality, it may be relevant to consider links between the hippocampal cortex and fronto-temporal regions for several reasons: i) there is evidence for progressive brain changes in fronto-temporal cortices in at least a subset of patients with psychosis, including the transition to psychosis (Cannon et al. 2015) and after a FEP, that is unlikely to be confounded by medication (Lieberman 1999; Pantelis 2005; DeLisi 2008; Andreasen et al. 2011; Olabi et al. 2011; Gong et al. 2016); ii) there is empirical evidence for direct connectivity between the hippocampus and medial temporal lobe, as well as between the hippocampus and prefrontal cortex (Martin 1996; Simons and Spiers 2003); iii) altered intracortical myelin has been noted in patients with enduring schizophrenia and other psychotic disorders within the prefrontal cortex (Lake et al. 2017; Wei et al. 2017; Tishler et al. 2018);and iv) HC-medial temporal lobe and hippocampus-PFC subserve memory, emotional expression and motivational behaviours (Squire et al. 2004; Pier et al. 2016; Schulze et al. 2016), which underlie verbal memory deficits and negative symptoms. Indeed, altered frontal connectivity has previously been linked to negative symptom severity in our group (Luck et al. 2011). Testing these specific pathways and subdividing negative symptoms into amotivation and expressivity domains would be a necessary next step to better understand the precise mechanisms underlying the altered hippocampal centrality we uncovered in this study.

Initially, we had hypothesized that the hippocampus would play an important role with regards to changes in both verbal memory and negative symptoms, given the known links between the hippocampus and prefrontal cortical regions that subserve both of these constructs and

prognostic indicators. However, our results suggest that despite being associated with each other, verbal memory deficits may not initially stem from abnormalities within the hippocampus and linked circuitry. Indeed, it is known that verbal memory deficits exist before the onset of psychotic symptoms, and are also present in non-affected relatives of patients (Cornblatt et al. 1999; Sheffield et al. 2018) and individuals with sub-threshold symptoms (Brewer et al. 2005b; Bonnín et al. 2012). It has also been proposed that the biological risk for verbal memory deficits is distinct from the risk for psychosis and associated symptoms (Cirillo and Seidman 2003) and can predict conversion to psychosis in the clinical high-risk state (Brewer et al. 2005b; Cannon et al. 2016; Seidman et al. 2016). Further work is required to understand the biological mechanism underlying the verbal memory deficits seen in patients with psychosis, but the hippocampus may play a key role across stages of the disorder, and may also contribute to the maintenance and/or exacerbation of these deficits.

This work also contributes to our knowledge of the interplay between verbal memory and negative symptoms using data collected at multiple timepoints shortly after the onset of a FEP. Our group has previously shown that verbal memory deficits are stable across time in patients with persistent negative symptoms (Hovington et al. 2013), and that baseline verbal memory deficits are associated with higher levels of negative symptom severity cross-sectionally (Makowski, Lewis, et al. 2019a), which has also been supported by several other groups (Cirillo and Seidman 2003; Hartmann-Riemer et al. 2015). However, there is a need to study these complex clinical factors in a more dynamic fashion; we have reported that worsening of negative symptoms over time is associated with intact verbal memory at baseline in FEP patients sectionally (Makowski, Lewis, et al. 2019a). We had proposed two scenarios, whereby either negative symptoms were changing independently of verbal memory abilities, or that intact verbal memory abilities at

baseline are not necessarily indicative of stability over time, which we were not able to fully test in our last investigation. In the current study, we found a robust association between worsening verbal memory and increased negative symptom severity in the 4 to 16 month period after a FEP. This finding highlights the importance of studying longitudinal relationships not only at the level of the brain structural 'connectome', but also at the level of behaviour; and particularly for neurocognitive deficits which may not always be as stable as previously thought (Green and Harvey 2014; Carrión et al. 2015).

Finally, we also tested the contribution of individual hippocampal subregions to the uncovered reduced centrality of the hippocampal circuit. We found that regions closer to the output of the hippocampal formation (i.e. subfield CA1, alveus, fimbria, fornix, mammillary body) were driving this effect, and similarly were influencing the uncovered brain-behaviour relationships with negative symptoms and verbal memory. Indeed, other studies have also pinpointed structural alterations within the CA1 subfield and the fornix in FEP (Baumann et al. 2016; Baglivo et al. 2018). Given the position of these regions in the hippocampal circuit, and their high myelin content, it is likely that these are putative hubs of the hippocampal circuit, and thus important for transferring neural signals integrated within the hippocampus to broader cortical regions. Over adolescence and early adulthood, there is increased communication between such hub regions and "non-hubs" (Cao et al. 2014; Gu et al. 2015), as well as more extensive interactions between regions that are distal to each other (Fair et al. 2009). Our results examining coordinated coupling of hippocampal and peri-cortical microstructure show altered communication of the hippocampus and neocortical networks in FEP patients, potentially due to altered myelin integrity within hippocampal hub regions. A relevant study showed that over 14-24 years of age, cortical hub regions (i.e. association areas including prefrontal and temporal regions) are characterized by a

steep rate of intracortical myelination (Whitaker et al. 2016). Intriguingly, these regions were also enriched for genes associated with risk for schizophrenia. Our work suggests that previously reported alterations in intracortical myelination of higher-order association areas in psychotic disorders (Rowley et al. 2015; Lake et al. 2017; Wei et al. 2017; Tishler et al. 2018) may be influenced by altered covariation with hippocampal microstructure, driven by hippocampal output regions or "hubs", and this may underlie the noted observations with negative symptoms and verbal memory.

This study extends structural covariance methods used in neurodevelopment (Khundrakpam et al. 2017) to assess changes after a FEP, and addresses a critical need in the field to better assess changes of the brain structural connectome in psychotic disorders with longitudinal methods (Collin and Keshavan 2018). However, several limitations remain. Firstly, we have largely interpreted signal from quantitative T1 as a marker of myelin, based on previous work (Deoni 2010; Tardif et al. 2018) and convincing evidence for the existence of myelin and microstructural alterations in psychotic disorders. However, alterations in T1 can be due to other factors, such as inflammation, reduced water content or altered iron content (Deoni 2010). We also parcellated our structural imaging data using functional networks defined by Yeo et al (2011). This was done for ease of interpretability, but it is acknowledged that a robust network-based parcellation based on microstructure and/or myeloarchitecture is lacking in the field. However, several studies have shown that networks based on microstructure have good correspondence with networks defined by resting-state functional connectivity (Baum et al. 2017; Bajada et al. 2019). It is also acknowledged that for patients and controls who only contributed two timepoints, our ability to map longitudinal changes was limited compared to participants with more timepoints. Data collection for this study is ongoing and future work from our group aims to increase the

current sample size and number of timepoints available. At the behavioural level, one might suspect that changes in verbal memory scores might be confounded by practice effects, given that the same test was used for each timepoint. One study has shown that such practice effects with the Weschler Memory Scale become much weaker after longer periods between testing (i.e. up to ~3 months) (Holdnack et al. 2013). Given that our shortest interscan interval is approximately 3 months, practice effects are likely not playing a major role in our verbal memory measure; we can also interpret any residual practice effects as a verbal learning process, which is still of interest to the current work. We also hope to extend this model with a larger sample size to better understand different negative symptom domains, namely amotivation and expressivity deficits, as we have done in previous work (Makowski, Lewis, et al. 2019a). Finally, it should be noted that our approach of measuring changes in negative symptoms linearly may be limited in capturing the true extent of fluctuations in this symptom dimension and may also be influenced by changes in positive symptoms; however, we found no relationship with hippocampal centrality and changes in positive symptoms, suggesting our results are more specific to negative symptoms.

Conclusions. The results of the current investigation suggest that the hippocampus serves as a catalyst in the dysconnectivity characterizing psychosis. Importantly, the hippocampus is a structure with high potential for plasticity; thus, treatments that can effectively ameliorate hippocampal structure and/or function may also have downstream impact on negative symptomatology. Trajectories in verbal memory may also be an important behavioural marker paralleling the changes occurring in hippocampal microstructure and negative symptoms.

Acknowledgments and Disclosures

We would like to thank PEPP-Montreal and Lepage Lab research staff for their efforts in recruitment and clinical data collection. We are also grateful to all patients and families for participating in the study. We would also like to thank Gabriel Devenyi for help with image processing, and Gabriella Buck, Gabrielle Pochiet, and Rachel Rosengard for help with imaging quality control. The study was supported by grants from the Canadian Institutes of Health Research and the Otsuka/Lundbeck Alliance. It also benefited from computational resources provided by Compute Canada (www.computecanada.ca) and Scinet high performance computing (https://www.scinethpc.ca/niagara/). Salary awards include: Canadian Institutes for Health Research (CIHR; C.M., R.J., M.M.C., A.C.E., M.L.), Fonds de la Recherche en Santé du Québec (FRSQ; M.M.C., M.L., J.L.S., and R.J.), funding from the Canada First Research Excellence Fund, awarded to McGill University for the Healthy Brains for Healthy Lives Initiative (C.M., A.C.E.), James McGill Professorship (M.L., A.C.E.) and Canada Research Chairs Programme (A.K.M.). M.L. reports grants from Otsuka Lundbeck Alliance, personal fees from Otsuka Canada, personal fees from Lundbeck Canada, grants and personal fees from Janssen, and personal fees from MedAvante-Prophase, outside the submitted work. R.J. reports receipt of grants, speaker's fees, or honoraria from AstraZeneca, BMS, Janssen, Lundbeck, Otsuka, Pfizer Canada, Shire, and Sunovion and royalties from Henry Stewart Talks. A.M. reports receipt of grants, fees, or honoraria from Lundbeck and Otsuka. A.C.E. has received consulting fees from Biospective. L.P. reports personal fees from Otsuka, Janssen, SPMM Course Limited, UK, Canadian Psychiatric Association; book royalties from Oxford University Press; investigator-initiated educational grants from Janssen, Sunovion and Otsuka outside the submitted work.

Chapter 7 : Conclusions

The first episode of psychosis is a complex manifestation of symptoms that can significantly alter an individual's global functioning. Clinicians are not yet equipped with the necessary tools and therapies to effectively treat prominent deficits arising after psychosis, namely negative symptoms and abnormal cognition. Psychotic disorders have a protracted clinical course, where vulnerability may be initiated prenatally, with accumulation of risk factors throughout childhood, adolescence and even into early adulthood for the majority of cases. This prolonged sequence of events reflects both an extended vulnerability for mental health difficulties, as well as a promising opportunity for successful intervention (Collin and Keshavan 2018). The first episode of psychosis offers a peak opportunity for early intervention and improved prognosis, if a clear and measurable treatment target is defined. This thesis sought to find such a target, through a series of longitudinal neuroimaging studies of FEP patients followed at the PEPP-Montreal clinic, mapping neuroanatomical trajectories to clinical and cognitive profiles in the one to two years after a FEP. Specifically, this work offered several biological mechanisms that underlie verbal memory deficits and negative symptoms, two dimensions that are critical for functional outcome in patients with psychosis.

Chapter 4 began exploring these mechanisms by investigating the link between maturation of limbic and neocortical regions in patients with persistent negative symptoms (PNS). We demonstrated that FEP patients with such symptoms largely differ from their non-PNS peers both at the clinical and neurobiological level over time. Specifically, patients with PNS showed altered maturation of both amygdalar-hippocampal volumes and surface area, and prefrontal cortical thickness with age, compared to patients without such symptoms and healthy controls. Further, we stratified patients based on "early" or "primary" PNS and "secondary" PNS (i.e. presenting with

other symptoms such as positive/depressive symptoms, etc), finding that limbic and neocortical maturation also differed between these two groups. Our work highlights divergent biological trajectories that may yield meaningful clues for prognosis in subsets of patients with a poor clinical course; findings that we would otherwise not be able to uncover if we pooled all FEP patients together.

Chapter 5 extended the methods presented in Chapter 4, and further delved into the magnetic resonance signal contributing to our measurement of peri-cortical anatomy. It is acknowledged that often-used measures of cortical thickness are largely reliant on the contrast between gray and white matter. Thus, we incorporated a measure of cortical contrast to better understand whether changes in anatomy underlying negative symptoms are driven by putative changes in myelin around the gray-white matter boundary. We also assessed the interplay between verbal memory performance and changes in negative symptoms. We found that these two important prognostic indicators interacted at the level of both brain and behaviour. Namely, verbal memory was associated more strongly with expressivity deficits rather than amotivation, and both variables were associated with changes in peri-cortical anatomy of language-related regions.

Finally, Chapter 6 addressed how co-occurring changes within the hippocampus and neocortex relate to changes in both verbal memory and negative symptoms in FEP patients. We clarified previous associations between cross-sectional verbal measures and longitudinal symptoms, showing that improvements in verbal memory are also associated with amelioration of negative symptoms. This behavioural finding showcases the dynamic nature of cognition, particularly verbal memory, after a FEP and sheds new light on what has previously been believed about cognition as a stable trait in psychotic disorders. Further, this chapter showed that microstructural changes within hippocampal circuitry are de-coupled from intracortical

microstructural changes in FEP patients, which we have interpreted as decreased hippocampal centrality. This in turn was shown to be associated with worsening negative symptoms, and mediated by changes in verbal memory.

In summary, this thesis proposes that the hippocampus is a candidate target, not only in impacting positive symptoms as has been previously described (Tamminga et al. 2010, 2012; Lieberman et al. 2018), but for potential amelioration of negative symptoms. The observed alterations in hippocampal microstructure may be related to co-occurring changes in microstructure of the cortex, particularly around the gray-white matter boundary. Given the evidence that verbal memory is related to negative symptoms, and even helps to explain the relationship between hippocampal-cortical links and negative symptoms, interventions to improve verbal memory may also be a key component in the treatment of negative symptoms.

Limitations

This work needs to be considered in the context of a few limitations. The majority of the work presented in this thesis was based on the assumption of largely linear relationships; i.e. between verbal memory and negative symptoms, assessing symptoms over time, between symptoms and cortical structure, etc. As we continue data collection for the study presented in Chapter 6, it will be possible to investigate non-linear relationships in behavioural variables and brain-behaviour relationships with participants that complete all four timepoints. We also addressed the possibility of non-linear relationships in cortical structure in Chapter 4, where we investigated quadratic changes in cortical thickness with age in patients with persistent negative symptoms.

It is also acknowledged that there are inherent limitations in the assessment of negative symptoms; these symptoms can be much more difficult to detect than positive symptoms, and

negative symptom assessments oftentimes rely on the subjective judgment of clinicians and symptom raters. The PEPP-Montreal clinic has achieved good inter-rater reliability on the scale used throughout this thesis to assess negative symptoms (i.e. SANS, κ=0.71) (Jordan et al. 2018), but further efforts are needed to improve reliability and enhance objectivity of such assessments.

There are many potentially confounding factors that are difficult to control for in analysis of clinical samples. One variable of particular interest in the field is the impact of pharmacological treatment, such as antipsychotic medication, on progressive brain changes in psychosis. We are fortunate to be working with an early intervention service, where inclusion criteria include minimal (i.e. less than one month) exposure to antipsychotic medication prior to entry. PEPP-Montreal also closely monitors and records the medication that is prescribed to patients after their FEP, which we have strived to incorporate in our analyses. However, we cannot rule out potential nonlinear effects of antipsychotic medication on brain structure in our analysis, or the effects of other medications that we were not able to control for in our analysis (e.g. lithium in patients diagnosed with bipolar disorder, antidepressant medication in patients with affective disorders, anticholinergic medication in those with extrapyramidal symptoms, etc). However, given that we studied a relatively acute period after a FEP, we remain confident that our FEP sample largely diminishes the influence of confounding factors that are prevalent in the investigation of more enduring psychosis samples.

Emphasis has also been placed by funding agencies to better understand sex differences in the brain. We controlled for sex in our analyses but it is known that males with psychosis tend to be affected disproportionately and have a poorer clinical course (e.g. higher negative symptoms, earlier age of onset, poorer functioning) compared to females (Cotton et al. 2009; Ochoa et al. 2012). One graduate student in Dr. Lepage's laboratory is actively investigating sex differences in

relation to verbal memory performance and hippocampal-cortical anatomy. Future work will also investigate such sex differences in patients with predominant negative symptoms.

On the imaging front, we have largely interpreted white-gray matter contrast (Chapter 5) and T1 relaxation times (Chapter 6) as proxy measures of myelin content. It would be highly beneficial to supplement these analyses with other white matter measures in the future, for instance with diffusion tensor imaging. Indeed, a graduate student is currently analyzing diffusion tensor imaging from the 1.5T imaging study (Chapters 4 and 5), and comparisons between quantitative T1 values and measures extracted from multi-shell diffusion tensor imaging with the newer 3T dataset (Chapter 6) will be conducted in the future. It is also high priority to replicate some of the findings presented in this thesis in an independent sample. To this end, we are collaborating with a "sister" PEPP-clinic in London, Ontario to replicate findings of hippocampal-cortical microstructure underlying negative symptoms in first episode of psychosis patients.

Future directions

There is no limit to the number of research questions that can be asked in the context of psychosis and underlying neurobiology. However, the direct applications of neuroimaging findings within the clinic relies on the ability to ask the most relevant questions for the benefit of translational psychiatry. This thesis aimed to do so with theoretically-driven approaches, but several future directions remain and are proposed below.

Re-purposing existing treatments and interventions.

Findings of the hippocampus being central to negative symptoms and verbal memory deficits offers a new therapeutic avenue, either through the use of pharmacological and/or

cognitive interventions known to impact the hippocampus. The advantage of targeting this structure is that we may not need to re-invent the wheel in finding a treatment that promotes hippocampal health. One promising pharmacological agent may be aripiprazole, an atypical antipsychotic medication that acts as a partial agonist at both the dopaminergic D2 and serotonergic $5HT_{1A}$ receptors (Zhang et al. 2006). Aripiprazole's unique pharmacological profile in comparison to other antipsychotic medications may contribute to its demonstrated potential to improve cognition (Nagai et al. 2009) and to elicit neurogenesis in the hippocampus (Park et al. 2009; Nowakowska et al. 2014). Further, our group has shown that an increase in hippocampal volume can be observed over a one-year treatment period specifically in FEP patients taking aripiprazole (Bodnar, Malla, et al. 2016). Our group is actively working on replicating and better understanding this finding through a study funded by the Canadian Institutes of Health Research (CIHR), which contributed to the data presented in Chapter 6. Aripiprazole has also been linked to improved verbal memory in patients with schizophrenia in several case reports (Mucci et al. 2008; Umene-Nakano et al. 2013) and open-label studies (Kern et al. 2006; Riedel et al. 2010; Bervoets et al. 2012). Given the framework proposed in this thesis, a natural next step would be to assess whether aripiprazole's putative effects on hippocampal anatomy and verbal memory might also repair cortical connectivity and in turn, ameliorate negative symptoms.

Behavioural interventions could also provide promising avenues. Of interest, there is extant literature on the effects of physical exercise on the hippocampus. Exercise has been shown to increase hippocampal volume in older adults (Erickson et al. 2011), compared to the hippocampal volume loss that is characteristic of ageing. The authors also showed that hippocampal volume increases were accompanied by increases in levels of brain-derived neurotrophic factor (BDNF, a marker for neurogenesis and neuronal growth) and improvements in memory functioning. This

sort of hippocampal plasticity in response to exercise, co-occurring with short-term verbal memory improvements, has also been demonstrated in patients with schizophrenia (Pajonk et al. 2010). Provided this evidence, again it would be intriguing to test whether such physical exercise protocols may also have an impact on negative symptoms and more globally, patient functioning.

Prodromal stages.

The onset of full-blown psychosis is a milestone event in the course of a psychotic disorder, but it is acknowledged that psychotic-like experiences and related symptoms begin much earlier in many individuals who transition to psychosis. This "prodromal" period is of utmost interest for the characterization of risk factors that might later trigger a full-blown psychotic episode. Of relevance to this thesis, there is evidence for verbal memory deficits, poor premorbid functioning, and hippocampal abnormalities prior to the onset of psychosis and in individuals at risk for psychosis (Cannon et al. 1997; Cirillo and Seidman 2003; Lieberman et al. 2018; Sheffield et al. 2018). Chapters 4-6 provided evidence for progressive brain changes occurring *after* a FEP. However, it is feasible that the described peri-cortical and hippocampal changes have already been set in motion much earlier. Study designs capturing prodromal stages are inherently difficult to acquire, and require colossal sample sizes followed over time to capture individuals who actually transition to psychosis. The North American Prodrome Longitudinal Study (NAPLS) (Addington et al. 2012) has put forth excellent efforts to make this a reality, but admittedly still has a relatively small sample of individuals with neuroimaging data who actually transitioned to psychosis (i.e. N=35 based on the largest neuroimaging sample published from this consortium to date) (Cannon et al. 2015). Another initiative that holds promise in better understanding biological risk for psychiatric disorders, including psychosis, is the Adolescent Brain Cognitive Development (ABCD) Study (abcdstudy.org) (Volkow et al. 2017). This NIH-funded longitudinal population-based study in the

United States aims to track 11,500+ children aged 9-10 years over a decade to richly characterize developmental trajectories. Notably, the ABCD Study will follow children into early adulthood, where approximately 850 participants (7.5% of the sample) are expected to have psychotic symptoms in adolescence (Kelleher et al. 2012). In this manner, phenotypic, genetic and brain imaging data can be used to better characterize the behavioural and biological risk associated with early stages of psychosis. Such discoveries could have groundbreaking implications for the detection and treatment of psychotic disorders.

Imaging genetics.

As alluded to, understanding the genetic risk contributing to the manifestation of psychotic disorders is another critical piece in our understanding of the biological mechanisms that underlie psychosis. Indeed, genetics are the foundation for brain development, and thus likely hold important information about the neuroanatomical alterations described in this thesis, which in turn may give rise to alterations in behavior (e.g. cognitive deficits, clinical symptoms, etc). Furthermore, we know that psychotic disorders have a heritable component. For instance, monozygotic twins have a 50% concordance rate for schizophrenia; that is, if one twin has schizophrenia, the other twin has a 50% chance of acquiring the disorder (Fischer 1971). Genome-wide association studies (GWAS) have pinpointed a wide array of genetic variants underlying psychotic disorders such as schizophrenia and bipolar disorder (Ripke et al. 2014; Stahl et al. 2017). We are also gaining a better understanding of the genetic architecture underlying cortical anatomy, including cortical thickness (Panizzon et al. 2009; Rimol et al. 2010; Chen et al. 2013) and white-gray matter contrast (Panizzon et al. 2012), and hippocampal subfields (Patel et al. 2017; van der Meer et al. 2018). Situating the findings from this thesis in an imaging-genetics framework

would be a valuable next step. For instance, Carol Tamminga and colleagues proposed that psychotic symptoms stemming from lesions within the dentate gyrus/CA3 may be driven at least in part by genetic variants resulting in reduced BDNF expression (Tamminga et al. 2010, 2012), or by alterations in genes important for neurogenesis in the hippocampus, such as *disrupted in schizophrenia 1* (DISC1) gene (Duan et al. 2007; Brandon and Sawa 2011) or *neuregulin 1* (NRG1) (Harrison and Law 2006; Li et al. 2007). It is possible that variations in these candidate genes contribute to this thesis' proposal of alterations in hippocampal-cortical trajectories in FEP. There is also a great deal of work to be done to better understand the genetic architecture of white matter microstructure in psychiatric disorders, which may interact with certain patterns of genetic variation within the hippocampus and thus increase risk for psychosis. It is becoming much more realistic to answer these pressing questions with the emergence of large open datasets, such as the UK Biobank (Alfaro-Almagro et al. 2018), IMAGEN (Schumann et al. 2010), and the ABCD Study described above (Volkow et al. 2017; Hagler et al. 2018).

Beyond psychosis: generalizing findings to other disorders.

Several themes described in this thesis are not unique to psychosis. From a clinical standpoint, verbal memory deficits and negative symptoms are found in many other neurological and psychiatric disorders (Brown and Pluck 2000). Negative symptoms, particularly those which impact goal-directed behavior, can be found in human immunodeficiency viruses (HIV), Alzheimer's disease, Parkinson's disease, melancholic depression, and multiple sclerosis, to name a few (Brown and Pluck 2000). Verbal memory deficits are also present in obsessive compulsive disorder, post-traumatic stress disorder, and various neurodevelopmental disorders (Nichols et al. 2004; Gunstad et al. 2006; Wild and Gur 2008; Kikul et al. 2012; Kavanaugh et al. 2016). The

hippocampus has also been posited to be an important pathophysiological component for many of these disorders. In major depressive disorder, the hippocampus has been proposed as a potential biological target, and examination of individual subfields has revealed progressive volume loss in subfield CA1 (Roddy et al. 2019; Sheline et al. 2019), a myelin-rich output structure of the hippocampus that was highlighted in our findings in Chapter 6. Another example comes from epilepsy, where seizures in patients with temporal lobe epilepsy are often initiated in the hippocampus (Saling 2009). These patients also show sustained verbal memory deficits after hippocampal tissue resection. Indeed, more studies are beginning to address the biological overlap between various classes of disorders (Cross-Disorder Group of the Psychiatric Genomics Consortium 2013; Crossley et al. 2014; Lange et al. 2018; Xia et al. 2018), moving away from the limitations of classical diagnostic frameworks, and opening up a future where brain disorders are treated in a more mechanistic and dimensional manner.

Chapter 8 Appendices – Supplementary Material for Chapters 4-6

Appendix-I: Supplementary Material for Chapter 4.1 (Makowski et al *Translational Psychiatry* 2017)

Supplementary Methods

Patient exclusion from the neuroimaging study. Forty-two patients and forty-six controls were no longer part of the neuroimaging study after baseline, due to attrition, incidental findings, substance-induced psychosis, and for other diagnostic reasons that no longer met criteria for inclusion in PEPP. This left a total of 100 patients and 48 healthy controls with at least two scans. Three patients were not included in subsequent analysis due to insufficient longitudinal symptom data (2 cases) or non-compliance to the time line of the study (1 case). For post-processing quality control, six participants (4 controls [12 scans total], 2 FEP patients [5 scans total]) were excluded entirely, and one follow-up scan belonging to a FEP patient was dropped from analysis, due to significant errors in resultant segmentations (largely due to motion and poor tissue contrast), or due to incidental findings.

Supplementary Tables

Omnibus

		Group		Time		Group*Time	
	N	Statistic$_{(df)}$	p	Statistic$_{(df)}$	p	Statistic$_{(df)}$	p
SANS	616 observations	$\chi^2_{(2)}$= 91.68	<0.0001	$\chi^2_{(6)}$= 37.62	<0.0001	$\chi^2_{(12)}$= 38.19	<0.0001
SAPS		$\chi^2_{(2)}$=48.70	<0.0001	$\chi^2_{(6)}$= 7.18	0.305	$\chi^2_{(12)}$= 30.47	0.002

Descriptives and Post-Hoc

	1) ePNS		2) sPNS		3) non-PNS		post-hoc*
	N	Mean (+SD)	N	Mean (+SD)	N	Mean (+SD)	
2							
SANS	20	9.55 (3.33)	29	8.45 (3.22)	42	6.38 (3.21)	1, 2 > 3
SAPS		3.70 (3.98)		4.52 (3.10)		2.69 (2.88)	2 > 3
3							
SANS	21	10.24 (3.02)	29	8.10 (3.37)	42	6.07 (3.55)	1 > 2 > 3
SAPS		3.24 (3.19)		4.90 (3.36)		1.86 (2.32)	2 > 3
6							
SANS	18	10.22 (2.88)	29	8.86 (3.01)	39	4.77 (2.98)	1, 2 > 3
SAPS		2.89 (2.99)		6.45 (3.69)		1.64 (1.89)	2 > 1, 3
9							
SANS	18	8.72 (3.06)	27	8.11 (2.95)	43	4.60 (3.11)	1, 2 > 3
SAPS		2.83 (2.90)		5.59 (4.42)		1.88 (2.70)	2 > 1, 3
12							
SANS	20	9.35 (3.10)	26	9.42 (3.84)	44	3.61 (2.98)	1, 2 > 3
SAPS		2.50 (2.21)		7.35 (4.36)		1.86 (2.89)	2 > 1, 3
18							
SANS	20	7.65 (3.48)	28	8.04 (3.47)	42	3.12 (2.89)	1, 2 > 3
SAPS		2.50 (2.35)		5.36 (4.10)		1.50 (2.77)	2 > 1, 3
24							
SANS	20	6.55 (3.93)	22	6.32 (3.09)	37	3.76 (3.20)	1, 2 > 3
SAPS		2.45 (2.52)		3.68 (3.39)		2.65 (4.32)	not significant

Table 8.1. Generalized Estimating Equations (GEE) analyses and statistics.
Omnibus results for SAPS and SANS global scores are presented in the top panel, with Bonferroni-corrected p=0.025. Descriptives and post-hoc analyses are presented per clinical timepoint (outlined in left-hand column, 2/3/6/9/12/18/24-months after entry to clinic). Post-hoc analyses were considered significant at p<0.05.
Abbreviations: SANS/SAPS, Scales for the Assessment of Negative/Positive Symptoms. 1, early persistent negative symptoms (ePNS). 2, PNS due to secondary factors (sPNS). 3, Non-PNS.

Structure	Side	Main Effect of Group			Group*Age Interaction		
		Statistic$_{(df)}$	*q*-value	post-hoc	Statistic$_{(df)}$	*q*-value	post-hoc
		A. Covaried by Diagnosis					
Amygdala	L	$F_{(2,237)}$=5.13	**0.013**	1,3<2	$F_{(2,237)}$=5.02	**0.015**	1,3<2
	R	$F_{(2,237)}$=2.51	0.11	-	$F_{(2,237)}$=2.28	0.13	-
Hippocampus	L	$F_{(2,237)}$=0.27	0.77	-	$F_{(2,237)}$=0.12	0.89	-
	R	$F_{(2,237)}$=5.12	**0.013**	1<2	$F_{(2,237)}$=5.69	**0.015**	1<2
		B. Covaried by Antipsychotic Dosage					
Amygdala	L	$F_{(2,239)}$=5.16	**0.013**	1,3 <2	$F_{(2,239)}$=5.16	**0.013**	1,3<2
	R	$F_{(2,239)}$=2.61	0.1	-	$F_{(2,239)}$=2.39	0.13	-
Hippocampus	L	$F_{(2,239)}$=0.49	0.61	-	$F_{(2,239)}$=0.32	0.73	-
	R	$F_{(2,239)}$=5.15	**0.013**	1<2	$F_{(2,239)}$=5.84	**0.013**	1<2
		C. Removing Sex and Handedness as Covariates					
Amygdala	L	$F_{(3,352)}$=3.49	**0.04**	1<2,4; 2<3	$F_{(3,352)}$=3.54	**0.03**	1<2,4; 2<3
	R	$F_{(3,352)}$=1.58	0.25	-	$F_{(3,352)}$=1.47	0.29	-
Hippocampus	L	$F_{(3,352)}$=0.29	0.83	-	$F_{(3,352)}$=0.18	0.91	
	R	$F_{(3,352)}$=3.31	**0.04**	1<2	$F_{(3,352)}$=3.64	**0.03**	1<2,4
		D. Covaried by IQ*					
Amygdala	L	$F_{(3,344)}$=3.21	**0.046**	1<2,4; 2<3	$F_{(3,344)}$=3.26	**0.044**	1<2,4; 2<3
	R	$F_{(3,344)}$=1.59	0.25	-	$F_{(3,344)}$=1.46	0.31	-
Hippocampus	L	$F_{(3,344)}$=0.16	0.92	-	$F_{(3,344)}$=0.10	0.96	
	R	$F_{(3,344)}$=3.23	**0.046**	1<2	$F_{(3,344)}$=3.64	**0.044**	1<2,4

Table 8.2. Supplementary analyses of amygdalar-hippocampal volumes with additional covariates.

Linear mixed effects analyses comparing FEP patient subgroups, including different covariates in addition to covariates presented in main manuscript: i.e. sex, handedness, and total brain volume (and age for main effect of group). Antipsychotic dosage was calculated as cumulative antipsychotic medication prescribed (converted to chlorpromazine equivalent dosage in mg), and multiplied by medication adherence. Medication adherence [0=never (0%), 1=very infrequently (1% to 25%), 2=sometimes (26% to 50%), 3=quite often (51% to 75%), 4=fully (76% to 100%)] was determined using a validated protocol based on composite information obtained from the patient, family members, and treating team and has been shown to be as efficacious as pill-counting (Cassidy et al. 2010). Note, controls were not included in analyses A and B, as controls do not have diagnostic/antipsychotic medication information. Analyses C and D include controls. An FDR correction for multiple comparisons was applied, with significant q-values<0.05 bolded. All post-hoc analyses correspond to p<0.05.

Abbreviations: L, Left. R, Right. 1, early persistent negative symptoms (ePNS). 2, PNS due to secondary factors (sPNS). 3, Non-PNS. 4, Controls.

* Note for analyses D (controlling for IQ), IQ information is missing for two controls, and thus they were excluded from this particular analysis.

Supplementary Figures

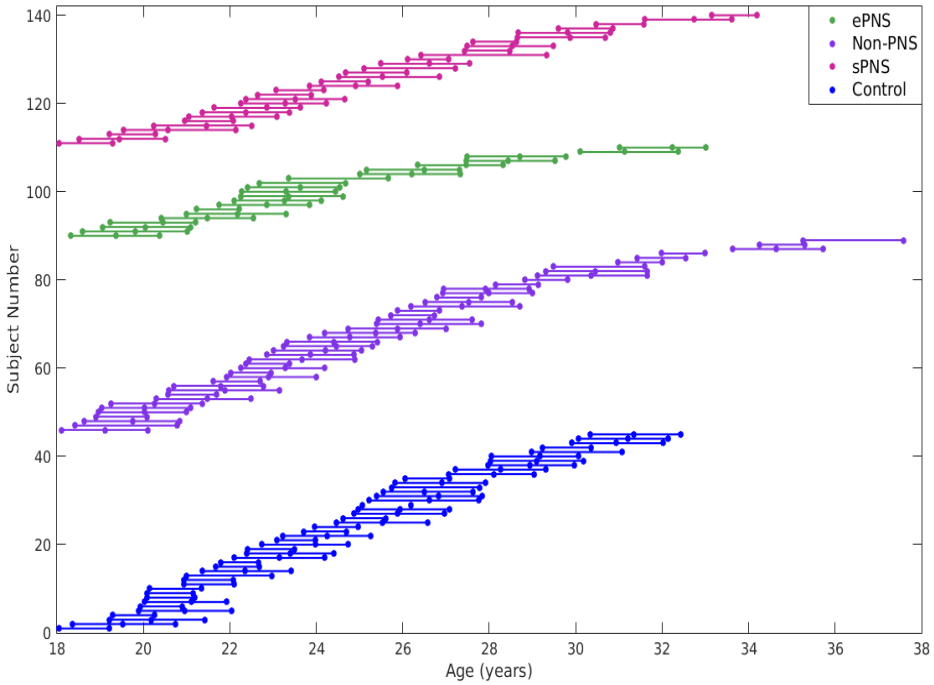

Figure 8.1. Sample distribution by group and by age.
Each horizontal line represents a subject, with each point corresponding to a single scan.
Abbreviations: 1, early persistent negative symptoms (ePNS). 2, PNS due to secondary factors (sPNS). 3, Non-PNS. 4, Controls.

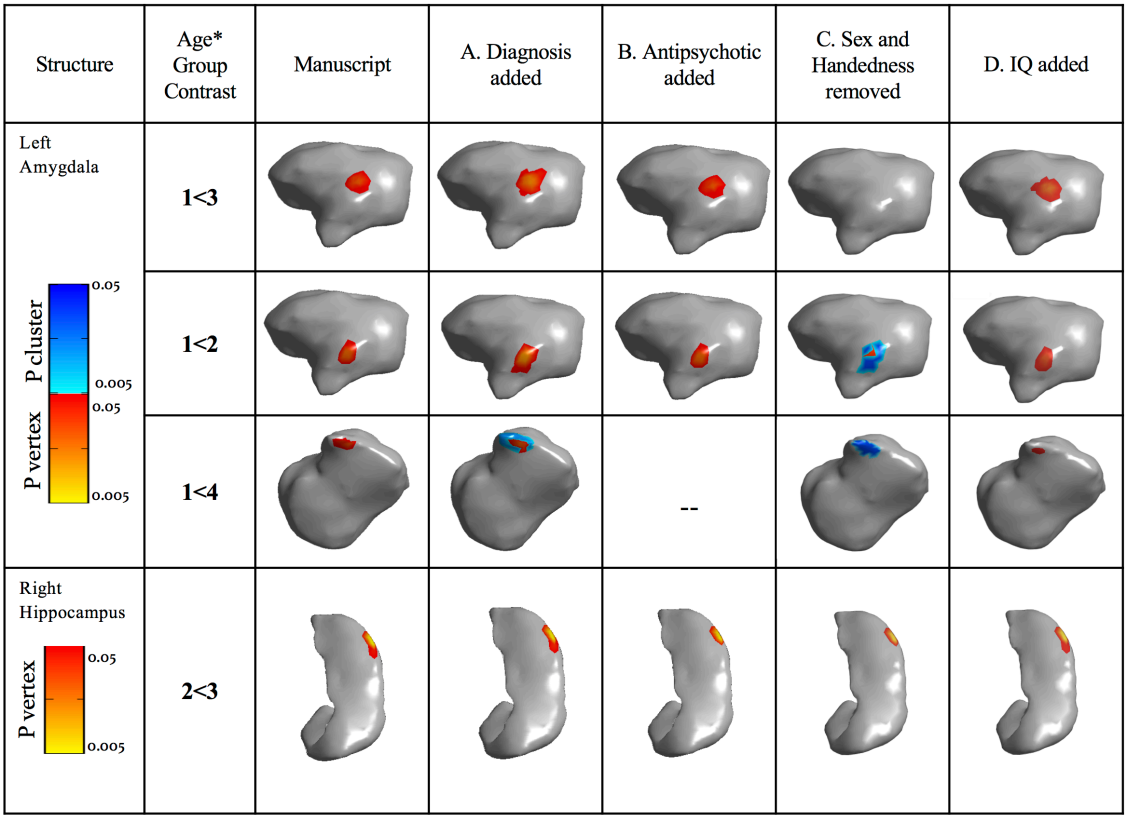

Figure 8.2. Supplementary analyses of amygdalar-hippocampal surface area with additional covariates.

Linear mixed effects analyses of surface area differences for age*group interaction, including different covariates in addition to covariates presented in main manuscript: i.e. sex, handedness, and total surface area of each structure examined (with the exception of **analyses C** where sex and handedness are removed). Antipsychotic dosage was calculated as cumulative chlorpromazine equivalent dosage in mg, multiple by percent medication adherence. Contrast for controls vs. ePNS (1<4) covarying for antipsychotic dosage was not included given that controls do not take medication. First two rows depict dorsal view of left amygdala, third row depicts posterior view of left amygdala, and bottom fourth row depicts ventral view of right hippocampus. Statistical maps are thresholded with random field theory (RFT). Note, one cluster did not survive correction for multiple comparisons with RFT after removing sex and handedness as covariates, namely when comparing age trajectories between ePNS and NonPNS patients in the left central amygdala, although this cluster nearly reached statistical significance.

Abbreviations: 1, early persistent negative symptoms (ePNS). 2, PNS due to secondary factors (sPNS). 3, Non-PNS. 4, Controls.

Appendix-II: Supplementary material for Chapter 4.2 (Makowski et al *npj schizophrenia* 2016)

Additional MRI Quality Control (QC) information.

All raw T1-weighted scans were visually inspected and quality controlled by three independent raters and scans were excluded if they exhibited excessive movement within the scanner, or the scan contained incidental findings. Scans that passed initial raw QC were then submitted to the CIVET pipeline. All CIVET outputs were quality controlled using the CBRAIN platform (Sherif et al. 2014) of which significant mask errors and/or minor pipeline errors were corrected through in-house scripts, if feasible. Specifically, inaccurate brain extractions (impacting 18 scans, corresponding to 10 FEP patients and 4 controls) were corrected by creating a new brain mask with *mincbet* within the minc-toolkit (http://www.bic.mni.mcgill.ca/ServicesSoftware/ServicesSoftwareMincToolKit), and applying this altered brain mask in subsequent stages of the CIVET pipeline. Inaccurate extraction of gray/white matter surfaces in close proximity to the posterior horn of the lateral ventricle due to a gradient error were corrected via in-house scripts (21 scans total, belonging to 13 FEP patients and 1 control). Surfaces were then re-run through specific stages of CIVET corresponding to the stage at which the error was found. Four scans did not pass through post-processing QC and corrections due to failure through the CIVET pipeline (1), and incidental findings (3 scans, belonging to one control).

Effect	Cortical Region	Manuscript Figure	ePNS	sPNS	Non-PNS	Controls
Scan Time (age controlled)	R Middle Temporal	Figure 4.5B	-0.71	-0.20	0.00	-0.38
	L Pre/Post-Central	Figure 4.5C	0.47	1.14	0.59	-0.36
Age*Group (Linear)	L DLPFC	Figure 4.6A	0.50	-0.38	-0.24	-0.29
	L OFC	Figure 4.6B	0.30	-0.39	-0.30	-0.30
	R Anterior Frontal	Figure 4.6C	0.30	-0.40	-0.30	-0.30

Table 8.3. Cortical thickness percent change per year.
Regions of interest showing linear change over time, as detailed in main manuscript in Chapter 4.2. Top half of table compares percent change per year over the two-year follow-up period for regions showing significant time effects (Figure 4.5 of main manuscript), and controlling for age. Bottom half of table quantifies percent change per year for regions showing linear effects of age (Figure 4.6 of main manuscript). Negative values represent percent cortical thinning per year, whereas positive values represent increased cortical thickness. **Abbreviations**: L, Left; R, Right; DLPFC, dorsolateral prefrontal cortex; OFC, orbitofrontal cortex; ePNS, early persistent negative symptoms. sPNS, persistent negative symptoms due to secondary factors.

Cortical Region	Manuscript Figure	Significant Term	Linear Age Term	Quadratic Age Term
L DLPFC	Figure 4.6A	Age*Group (Linear)	-256.53	-253.16
L OFC	Figure 4.6B	Age*Group (Linear)	-279.7	-275.9
R Anterior Frontal	Figure 4.6C	Age*Group (Linear)	-196.88	-193.6
L DLPFC/pre-SMA	Figure 4.7A	Age^2*Group (Quadratic)	-589.52	**-592.47**
R Middle Cingulate	Figure 4.7B	Age^2*Group (Quadratic)	-545.9	**-549.76**
L Inferior Temporal	Figure 4.7C	Age^2*Group (Quadratic)	-411.8	**-417.59**

Table 8.4. Akaike Information Criterion (AIC) values comparing linear and quadratic models. Significant likelihood ratio tests are bolded, indicating more complex quadratic term was a better fit to the data. Otherwise, a more simplistic (linear) model was used. Note, the Linear Age Term includes "Age" and "Symptoms*Age"**.** The Quadratic Age Term includes "Age", "Age^2", "Symptoms*Age", and "Symptoms*Age^2". **Abbreviations:** L, Left; R, Right; DLPFC, dorsolateral prefrontal cortex; OFC, orbitofrontal cortex; pre-SMA, pre-Supplementary Motor Area.

			Original Statistics			Controlling for Antipsychotic Medication			
Cortical Region	**Manuscript Figure**	**Significant Term**	**F-statistic**	**df**	**p-value**	**F-statistic**	**df**	**p-value**	**post-hoc**
L Inferior Temporal	Figure 4.5A	Group	6.89	1, 248	0.0012	6.91	1, 247	0.0012	ePNS<sPNS, non-PNS
R Middle Temporal	Figure 4.5B	Scan Time, ePNS	7.40	2, 53	0.0015	6.95	2, 52	0.0021	Baseline>FUP 2
L Pre/Post-Central	Figure 4.5C	Scan Time, Non-PNS	8.74	2, 188	0.00023	8.88	2, 187	0.00021	Baseline<FUP 1> FUP2
L DLPFC	Figure 4.6A	Age*Group (Linear)	5.92	2, 246	0.0031	5.91	2, 245	0.0031	ePNS>sPNS
L OFC[1]	Figure 4.6B	Age*Group (Linear)	5.33	2, 246	0.0054	5.70	2, 245	0.0038	ePNS>sPNS
R Anterior Frontal	Figure 4.6C	Age*Group (Linear)	4.78	2, 246	0.0092	4.96	2, 245	0.0077	ePNS>sPNS
L DLPFC/ pre-SMA	Figure 4.7A	Age^2*Group (Quadratic)	4.51	2, 243	0.033	4.65	2, 242	0.010	ePNS>sPNS
R Middle Cingulate	Figure 4.7B	Age^2*Group (Quadratic)	4.02	2, 243	0.019	4.03	2, 242	0.019	ePNS<sPNS, non-PNS
L Inferior Temporal	Figure 4.7C	Age^2*Group (Quadratic)	6.57	2, 243	0.0017	6.68	2, 242	0.0015	ePNS>sPNS

Table 8.5. Results not impacted by antipsychotic medication.
Mixed effects models applied to mean cortical thickness of each significant cortical region uncovered by initial vertex-wise analyses, comparing initial model presented in manuscript, and a similar model including antipsychotic medication as a covariate. All analyses controlled for gender, handedness and proxy BV as specified in main manuscript (and age when this was not a main effect of interest). Antipsychotic medication represented as cumulative chlorpromazine equivalent, multiplied by medication adherence. Given that Controls do not take such medication, controls were not included in the models presented above.
[1]Antipsychotic medication had a significant effect on cortical thickness within left OFC for linear age effect, but symptoms*age interaction remained significant even after controlling for medication. **Abbreviations.** L, Left; R, Right; DLPFC, dorsolateral prefrontal cortex; OFC, orbitofrontal cortex; pre-SMA, pre- Supplementary Motor Area; ePNS, early persistent negative symptoms. sPNS, persistent negative symptoms due to secondary factors; FUP1/2=Follow-Up Year 1/2.

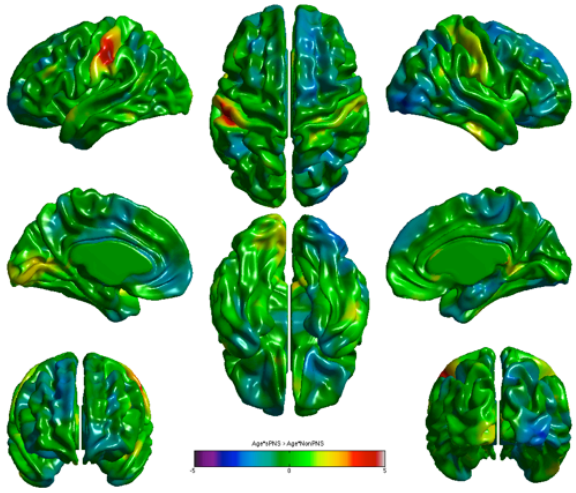

Figure 8.3. Linear age by group interaction comparing sPNS and non-PNS patients.
This was not tested in initial round of analyses as it was outside of the scope of our aims. However, we did find that cortical thickness within the left post central gyrus had a significantly different and positive age effect in sPNS compared to non-PNS, as shown by the red region of the t-statistic map above (surviving correction with RFT, $p<0.05$).

Appendix-III: Supplementary material for Chapter 5 (Makowski et al, *Psychological Medicine* Revisions Submitted 2019)

Supplementary methods

Neuroimaging sample details.

The neuroimaging study began in 2003 and spanned over a decade, comprising three scheduled visits: baseline, one-year follow-up (FUP1), and two-year follow-up (FUP2). All scans were acquired on the same 1.5T scanner. In total 150 patients and 95 controls were recruited for the study. From this sample, 142 patients and 94 controls completed a baseline scan. At this point, 7 patients and 4 controls were excluded from analysis based on the exclusion criteria for the study (e.g., incidental findings, substance-induced psychosis, low IQ). Forty-two patients and forty-five controls dropped out of the study after baseline, leaving 100 patients and 47 healthy controls with longitudinal data. In the FEP group, baseline scans were performed on average 4.1 (SD=1.9) months from entry into PEPP. For the entire group, including controls, inter-scan intervals were approximately 13.1 (SD=1.3) months between baseline and FUP1, and 12.5 (SD=1.7) months between FUP1 and FUP2. Nine participants (6 FEP, 3 controls) were not scanned at FUP1, and had an average interscan interval of 27.0 (SD=3.2) months between FUP2 and baseline. Sex ratios did not differ between the included cross-sectional sample (70% Male in FEP group, 65% Male in HC group) and the longitudinal sample (71% Male in FEP group, 65% Male in HC group), thus participant attrition did not affect the proportion of males:females in this study.

Quality Control procedures.

One rater (C.M.) manually rated all of the CIVET outputs, using a quality control module built in-house, where snapshots of the mask and surfaces overlaid on the T1-weighted image, gray and white matter surface renderings, surface-surface intersections, and surface extraction convergence

plots were created. These features were examined to ensure that a) the brain was extracted accurately, b) the surfaces generally followed the anatomy, c) no visible abnormalities (i.e. visibly jagged surfaces, or surfaces jutting out inaccurately) in gray and white matter surfaces could be detected, and d) complete convergence of the surface extraction process. For any questionable areas or outputs, the surfaces were overlaid on the T1 image and viewed slice by slice using Display software (https://mcin-cnim.ca/technology/visualization/display/). A three-point rating system was adopted: 2 for good quality surfaces (minimal error), 1 for satisfactory surfaces (mild to moderate error), and 0 for failed outputs. For the "questionable" outputs that were rated as a "1", a second rater independently rated the outputs, and a consensus was reached as to the inclusion/exclusion of the scan.

Three control scans (all follow-up scans) and 7 FEP scans (5 baseline and 2 follow-up), all belonging to unique subjects, failed the CIVET processing pipeline. From that point, 3 control scans (belonging to two participants) and 25 FEP scans (belonging to 17 patients) did not pass QC after inspection of outputs. 116 FEP patients remained after this step. From there, FEP patients with cross-sectional data only were removed for the analysis. The final sample with usable longitudinal data comprised 88 FEP patients, and a sample of 80 controls that had verbal memory data available, in addition to passing QC.

Choosing the best model for vertex-wise CT and WGC data.

To determine which covariates should be used for analyses, the Akaike Information Criterion (AIC) (Akaike 1998) was used to determine the best model for the data at hand. The method uses a likelihood function to reward goodness of fit, while including a penalty that is an increasing function of the number of estimated parameters. The baseline model was a general linear model,

which included parameters for group, centered age, and sex, as follows:

$$\Delta Y = \text{intercept} + \beta_1(\text{Centered Age}) + \beta_2(\text{Sex}) + \varepsilon$$

where Y represents vertex-wise *rate of change* in WGC or CT, $\beta_{1\text{-}2}$ represent regression coefficients and ε is residual error. From here, the model was tested with the addition of a third covariate, β_3, from the following variables: handedness, years of education, total brain volume (TBV), and mean WGC (for WGC data) and mean CT (for CT data). The best fit for the WGC data (with the smallest AIC value) included mean WGC as a covariate, in addition to centered age and sex. A similar model was selected for the CT data, including mean CT as a covariate. It should be noted that TBV also modestly improved the AIC fit, but did not reduce the AIC value to the same extent and as consistently as mean CT across all models. For consistency, only results covarying for mean WGC and mean CT and not TBV are presented in both manuscripts. Results remain largely the same when removing mean WGC and mean CT as a covariate. See Figures 8.6 and 8.7 below.

Given that both gray and white matter have been found to be affected by cumulative dosage of antipsychotic medication in patients with psychosis (Bartzokis et al. 2009; Roiz-Santiáñez et al. 2012; Vita et al. 2015), a separate analysis was included to observe potential effects of antipsychotic medication on the calculated rate of change of WGC and CT. Antipsychotic medication was defined as cumulative chlorpromazine equivalents, multiplied by adherence, as measured at the end of the neuroimaging study (i.e. this measure was taken from each patients' last scanning timepoint, and is a cumulative measure of antipsychotic medication exposure measured monthly at PEPP-Montreal). Antipsychotic medication was regressed against ΔY (i.e.

change in CT or WGC), controlling for age, sex, and Mean WGC or Mean CT (denoted as Mean(σ) in the main manuscript). No significant effects of antipsychotic medication on rate of change in WGC or CT were observed (see Figure 8.4), and this variable did not lower the AIC score when added to the above-described models. Thus we felt justified in leaving out medication as a covariate.

Supplementary Results

*VM at baseline***.**

As reported in Table 5.1 of the main manuscript, FEP patients had significantly lower VM performance (immediate and delayed recall) compared to healthy controls, when controlling for neuropsychological test battery version ($F_{1,163} \geq 16.77$, $p<0.0001$). This held true for the full cross-sectional sample as well, included in Table 8.9. Descriptive statistics of VM performance by group and version, and other relevant statistics, are included in Table 8.8. No significant group by version interaction term or main effect of version was found on VM performance. Also, no significant difference was observed within the FEP group comparing pen and paper vs. computerized test battery data, confirming that the data from the two different test batteries are comparable, and thus could be pooled in our analysis.

VM in relation to negative symptom domains at baseline.

The relationship between VM (i.e. z-scores of immediate and delayed recall) and negative symptom domains (i.e. log-transformed scores for Amotivation and Expressivity) at baseline were assessed in 115 FEP patients with Pearson r-correlations, adjusting verbal memory scores for age, sex, and test battery version. Expressivity was found to be significantly negatively associated with

both immediate (r=-0.35, q<0.001) and delayed recall (r=-0.28, q=0.036). Only a trend-like significant negative association was noted between Amotivation and immediate recall (r=-0.17, p-uncorrected=0.067), and no relationship was found between Amotivation and delayed recall (r=-0.12, q=0.215).

Relationship between ΔVM and Δ negative symptoms.

A subset of patients included in the study (N=49 from 88 patients) had verbal memory assessed at one-year follow-up. Thus, we conducted an exploratory analysis to see if there was a relationship between change in verbal memory and change in negative symptoms over this one-year period, using Pearson r correlations, adjusting VM scores by age, sex, and test battery version. For the included 49 FEP patients, we found no relationship between Δimmediate recall and ΔAmotivation (r=-0.096, p=0.51), nor Δ immediate recall and ΔExpressivity (r=-0.085, p=0.55). Similarly for Δ delayed recall, we found no relationship with ΔAmotivation (r=-0.19, p=0.18) or ΔExpressivity (r=-0.13, p=0.39). Note, a negative r value denotes that a worsening of negative symptoms is associated with a worsening of verbal memory performance (given that a negative change value reflects improvement in negative symptoms but worsening of VM).

Supplementary Tables

	Included Patients (N=88)	Excluded Patients (N=47)	Statistics Comparing Groups		
	N (%)		**Statistic**	**df**	**p-value**
Male	62 (70)	35 (74)	χ^2=0.2	1	0.6
Right Handed	73 (83)	41 (87)	χ^2=0.4	1	0.5
Diagnosis[a]					
Schizophrenia/ Schizophreniform	63 (72)	28 (60)			
Affective Disorder	16 (18)	12 (26)			
Delusional Disorder	3 (3)	0 (0)			
Psychosis Not Otherwise Specified	6 (7)	6 (13)			
	Mean (SD)		**Statistic**	**df**	**p-value**
Age	24.3 (4.1)	23.7 (4.0)	U=1893.5		0.4
Verbal Memory – Immediate[b]	-1.3 (1.4) [87]	-1.3 (1.3)	F=0.1	1,130	0.8
Verbal Memory – Delayed[b]	-0.9 (1.1) [87]	-0.9 (1.0)	F=0.02	1,130	0.9
Education in Years	12.0 (2.5)	11.8 (2.6)	t=0.4	133	0.67
Socioeconomic Status	3.2 (1.1) [81]	3.2 (1.1) [41]	U=1588.5		0.7
Performance IQ[b]	98.7 (17.1)	94.3 (14.2)	F=1.2	1,131	0.3
Verbal IQ[b]	99.8 (16.1)	97.7 (14.7)	F=0.6	1,131	0.4
CPZ equivalent (in mg) with adherence	747.9 (720.8)	818.4 (911.4)	U=2021.0		0.8
Duration Untreated Psychosis (weeks)*	76.4 (142.0)	36.9 (64.1) [44]	U=1423.5		0.05
Duration Untreated Illness (years)*	7.3 (6.5)	4.4 (4.1) [44]	U=1346.0		0.012
Amotivation	11.3 (6.1)	11.4 (7.8)	t=-0.09	133	0.9
Expressivity	7.1 (7.2)	7.4 (7.5)	U=2023.0		0.8

Table 8.6. Comparison of demographics for patients included vs. excluded in Chapter 5.
Patients were excluded (N=47) due to presence of cross-sectional data only, and exclusion on the basis of failed image quality control (QC). All data represented as Mean (SD), unless otherwise specified. Square brackets [] include adjusted sample size included in statistical analysis due to missing datapoints. A Mann Whitney U non-parametric test was used for variables that were not normally distributed. ***Bolded variables with an asterisk** reflect significant differences between Included and excluded patients. Specifically, included patients had longer duration of untreated psychosis and untreated illness compared to excluded patients. The two patient groups did not differ on any other variable. Age, socioeconomic status, chlorpromazine (CPZ) equivalents, duration of untreated psychosis/illness, and expressivity data were non-normally distributed, thus non-parametric tests were used to assess group differences.
[a]Diagnosis missing for one excluded patient.
[b]Covaried by test version. Specifically, IQ was collected with WAIS-III (Weschler 1997) and WASI (Weschler 1999) and verbal memory was collected with a Pen and Paper neuropsychological test battery, and CogState Research Battery (Pietrzak et al. 2009).

	SSZ (N=64)	AFF (N=15)	Statistics Comparing Groups		
	Mean (SD)		**Statistic**	**df**	**p-value**
Verbal Memory - Immediate[a,b]	-1.5 (1.3) [63]	-0.9 (1.3)	F=2.6	1, 74	0.1
Verbal Memory - Delayed[a,b]	-1.0 (0.9) [63]	-0.5 (1.2)	F=3.2	1, 74	0.08
Baseline Amotivation	11.8 (6.1)	9.5 (5.6)	t=1.3	77	0.2
Baseline Expressivity[c]	8.8 (8.2)	4.4 (4.5)	U=335		0.07
Δ Amotivation	-1.6 (4.6)	-2.3 (3.2)	t=0.6	77	0.6
Δ Expressivity	-1.4 (5.9)	-1.0 (2.5)	t=-0.3	77	0.78

Table 8.7. Comparing clinical and cognitive patient data by diagnosis.
Patients were categorized by Schizophrenia Spectrum (SSZ) (e.g. schizophrenia, schizoaffective) and Affective (AFF) (e.g. bipolar disorder, major depressive disorder with psychotic features) diagnoses. No significant differences emerged between diagnoses, although there was a trend-like difference for delayed recall and baseline expressivity scores, where SSZ patients tended to have worse delayed recall performance and a higher level of expressivity deficits.
[a]Verbal memory missing for one SSZ patient. Adjusted sample size is included in square brackets.
[b]Covaried by test version (Pen and Paper neuropsychological test battery vs. and CogState Research Battery (Pietrzak et al. 2009)).
[c]Non-normally distributed, thus a Mann White U non-parametric test was used to test for group differences.

Test Battery Version	**Verbal Memory Metric**	**FEP**		**Control**	
		N	**Mean (SD)**	**N**	**Mean (SD)**
Pen and Paper	Immediate	76	-1.2 (1.2)	65	0.04 (1.0)
	Delayed		-0.8 (0.9)		0.02 (0.8)
CogState	Immediate	39	-1.4 (1.7)	15	0.0 (1.0)
	Delayed		-1.0 (1.3)		0.0 (1.0)

Table 8.8. Descriptives of baseline VM data.
This analyses used a larger cross-sectional sample of 116 patients that passed quality control and 80 controls (see **Table 8.6** for demographic/clinical characterization of this sample). One-way ANOVAs were used to test an interaction effect between group and test version on verbal memory performance. There were no significant interaction effects of group by test version on either immediate ($F_{1,191}$=0.179, p=0.67) or delayed ($F_{1,191}$=0.50, p=0.48) recall. Further, there was no significant main effect of version on either immediate ($F_{1,191}$=0.38, p=0.54) or delayed ($F_{1,191}$=0.72, p=0.40) recall. As reported in the main manuscript, there is a significant main effect of group for both verbal memory metrics ($F_{1,191}\geq$28.71, p<0.001). Note, the F-statistics reported in the main manuscript are slightly different as the main effect of group is controlling for test version, and only included FEP patients with longitudinal data included in the main manuscript. Finally, independent t-tests found no significant differences in verbal memory performance within the FEP group when comparing data from pen and paper vs. computerized test battery versions ($t_{58.9}$=0.75, p=0.46 and $t_{57.9}$=1.15, p=0.25 for immediate and delayed recall, respectively; degrees of freedom adjusted for unequal variance, as assessed by Levene's test for Equality of Variances).

	FEP N=115	Controls N=80
	N (%)	
Male	82 (71)	52 (65)
Right Handed	95 (83)	73 (91)
Diagnosis[a]		
Schizophrenia/ Schizophreniform	79 (69)	
Affective Disorder	22 (19)	
Delusional Disorder	3 (3)	
Psychosis Not Otherwise Specified	10 (9)	
	Mean (SD)	
Age at Baseline	24.1 (3.9)	24.3 (3.3)
Education in Years*	11.8 (2.6)	14.3 (2.4)
Socioeconomic Status	3.2 (1.1) [105]	3.0 (1.0) [76]
Performance IQ*[b]	98.4 (16.4)	106.9 (12.7)
Verbal IQ*[b]	99.8 (15.8)	110.0 (14.9)
Cognition[b,c]		
Verbal Memory - Immediate*	-1.3 (1.4)	0.03 (1.0)
Verbal Memory - Delayed*	-0.8 (1.0)	0.02 (0.8)
Attention*	-0.8 (1.2)	0.06 (1.0)
Executive Function*	-0.7 (1.1)	0.05 (0.7)
Speed of Processing	-0.4 (1.1)	0.03 (0.8)
Working Memory*	-0.6 (0.9)	-.01 (0.8)
Visual Memory*	-0.7 (1.2)	0.09 (0.7)
General Cognitive Index*	-0.6 (0.8)	0.04 (0.6)
Clinical Information		
Cumulative CPZ equivalent (in mg)	803.5 (737.6)	
Adherence (%)	83.0 (27)	
Duration Untreated Psychosis (weeks)	70.9 (130.8) [106]	
Duration Untreated Illness (years)	7.0 (6.1) [109]	
Amotivation	11.4 (6.7)	
Expressivity	7.1 (7.3)	
SAPS	10.0 (12.5)	
CDSS	2.4 (3.1)	
Window |Scan - Symptom Eval| (months)	0.7 (0.5)	

Table 8.9. General demographics for cross-sectional sample.
This sample was used for cross-sectional analyses of the relationship between VM and negative symptom dimensions, presented above in Supplementary methods/results for Chapter 5. All data represented as Mean (SD), unless otherwise specified. Square brackets [] include adjusted sample size included in statistical analysis due to missing datapoints. Immediate and delayed verbal memory scores were obtained as described in the methods of the main manuscript. Five other cognitive domains are presented here, and merged to form a "general cognitive index", which was used as a covariate in **Figure 8.8**. Z-scores of general cognitive ability comparing FEP patients against healthy controls were calculated based on five domains of cognition: attention, executive function, speed of processing, visual memory, and working memory. A composite cognitive index was calculated by averaging the scores obtained for the five cognitive domains. Similar to the verbal memory scores, cognition was assessed with two different batteries (i.e. pen and paper, and the computerized CogState battery). Additional information on the tests comprising each cognitive domain for each battery can be found in Benoit et al (2015). All antipsychotic totals are presented

as chlorpromazine equivalents in mg, as prescribed by a psychiatrist, and are reported along with a percentage of medication adherence. SAPS totals are presented as mean scores of the sum of item-level scores. ***Bolded variables with asterisk** reflect significant differences between FEP patients and controls. Similar to the longitudinal sample presented in the main manuscript, FEP patients had significantly lower verbal memory performance, IQ, and levels of education compared to HC ($p<0.05$). FEP patients had significantly lower performance on all cognitive subdomains and the general cognitive index ($p<0.001$), with the exception of speed of processing, which showed a trend-like group difference ($p=0.06$).

[a]One patient did not have enough clinical data to reliably define a diagnosis.

[b]Covaried by test version. Specifically, IQ was collected with WAIS-III (Weschler 1997) and WASI (Weschler 1999) and verbal memory was collected with a Pen and Paper neuropsychological test battery, and CogState Research Battery (Pietrzak et al. 2009).

[c]Note, Mean and Standard Deviation of cognitive domains in Controls does not equate to exactly 0 and 1, respectively, as the norms for cognitive domains were calculated before exclusion of a subset of controls for this study due to imaging quality control.

Abbreviations: CDSS, Calgary Depression Scale for Schizophrenia. CPZ, chlorpromazine. FEP, First episode of psychosis. SAPS, Scale for Assessment of Positive Symptoms.

Supplementary Figures

i. White-Gray Contrast **ii. Cortical Thickness**

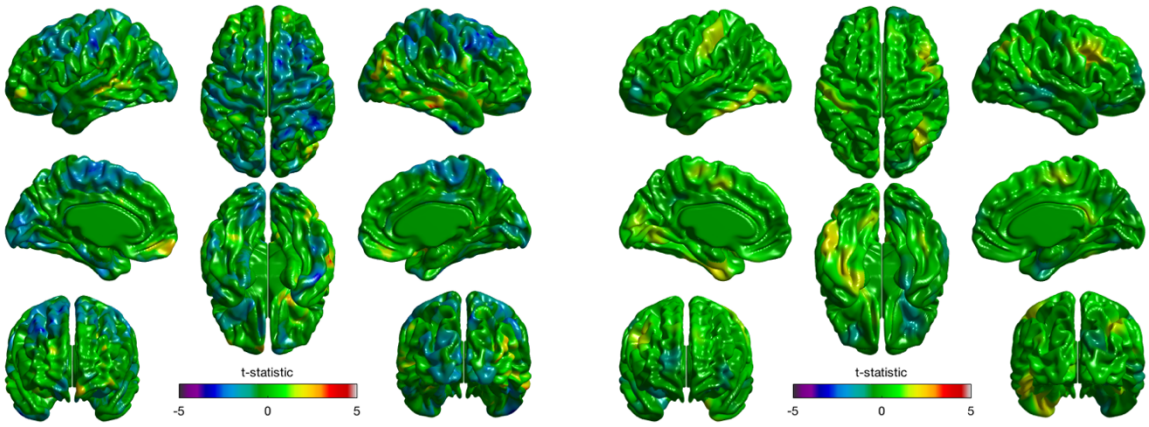

Figure 8.4. Effect of antipsychotic medication on cortical metrics.
T-statistic maps (df=83) showing main effect of antipsychotic medication on change in i) WGC and ii) CT, controlling for centered age, sex, and mean WGC for i), and mean CT for ii). Antipsychotic medication is defined as cumulative chlorpromazine equivalents, as measured at each patients' last scanning timepoint, multiplied by adherence. A positive t-statistic (warm colours) reflects a positive effect of antipsychotic medication on brain structure, and a negative t-statistic (cool colours) reflects a negative effect of antipsychotic medication. Nothing was found to be significant after RFT correction. It should be noted that there was also no significant relationships between mean baseline σ and chlorpromazine equivalents at baseline ($p's \geq 0.30$), or between mean ΔY and cumulative chlorpromazine equivalents ($p's \geq 0.16$).

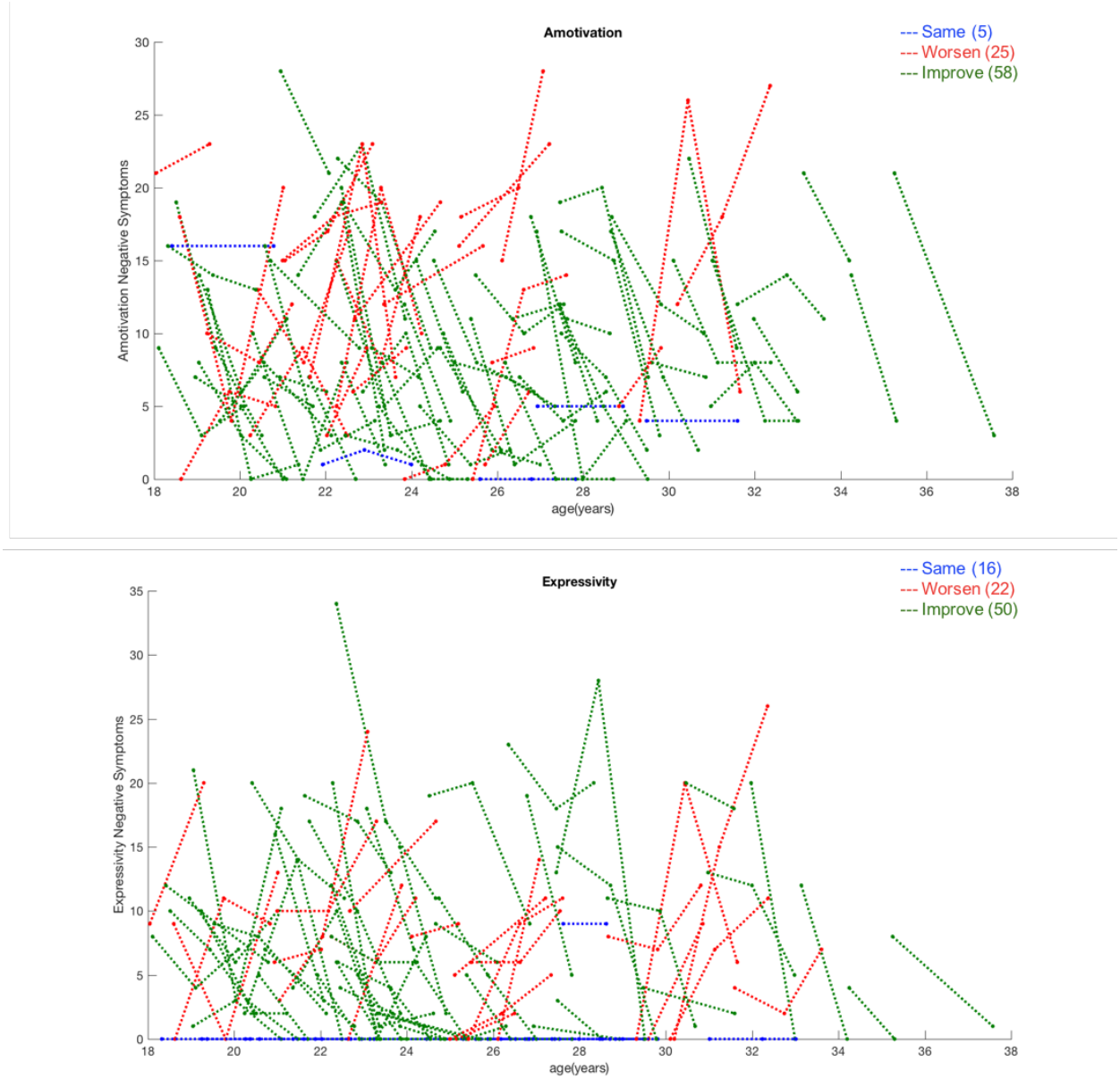

Figure 8.5. Spaghetti plots of negative symptoms.
Plots show change over time in Amotivation (top panel) and Expressivity Symptoms (bottom panel) in FEP patients. Each line joins timepoints from the same subject, and is colour-coded based on the slope of change, such that blue represents no change in symptoms (slope = 0), green represents improvement of symptoms (slope < 0) and red represents worsening of symptoms (slope > 0). The proportion of patients comprising each category are included in brackets in the legend. For amotivation symptoms, 5 patients had the same level (or absence) of symptoms over time (Mean Δ=–0.0038, SD=0.0086), 25 patients had worsening symptoms (Mean Δ= 3.12, SD=2.91) and 58 patients improved (Mean Δ= –4.08, SD=2.72). For expressivity symptoms, 16 patients had the same level (or absence) of symptoms over time (Mean Δ=0, SD=0), 22 patients had worsening symptoms (Mean Δ= 4.64, SD=4.02), and 50 patients improved (Mean Δ= –4.18, SD=4.01).

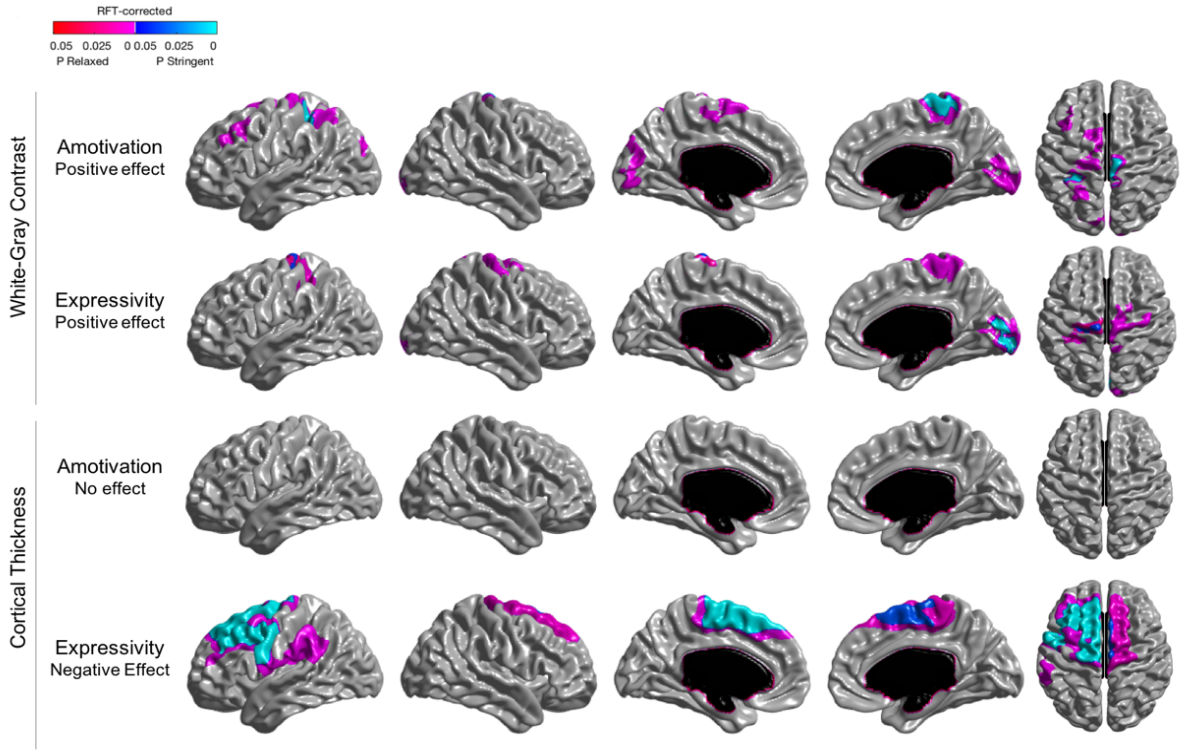

Figure 8.6. ΔAmotivation and ΔExpressivity deficits associated with ΔWGC and ΔCT across time, excluding mean(σ) as a covariate.
Results are RFT-corrected, where blue colours represent significant results cluster-thresholded at a "stringent" threshold of p=0.001, whereas red/pink colour represent significant results at a "relaxed" threshold of p=0.01. Results remain relatively unchanged from those presented in the main manuscript.
Orientation: Surfaces from left to right in each row: left lateral, right lateral, left medial, right medial, dorsal.

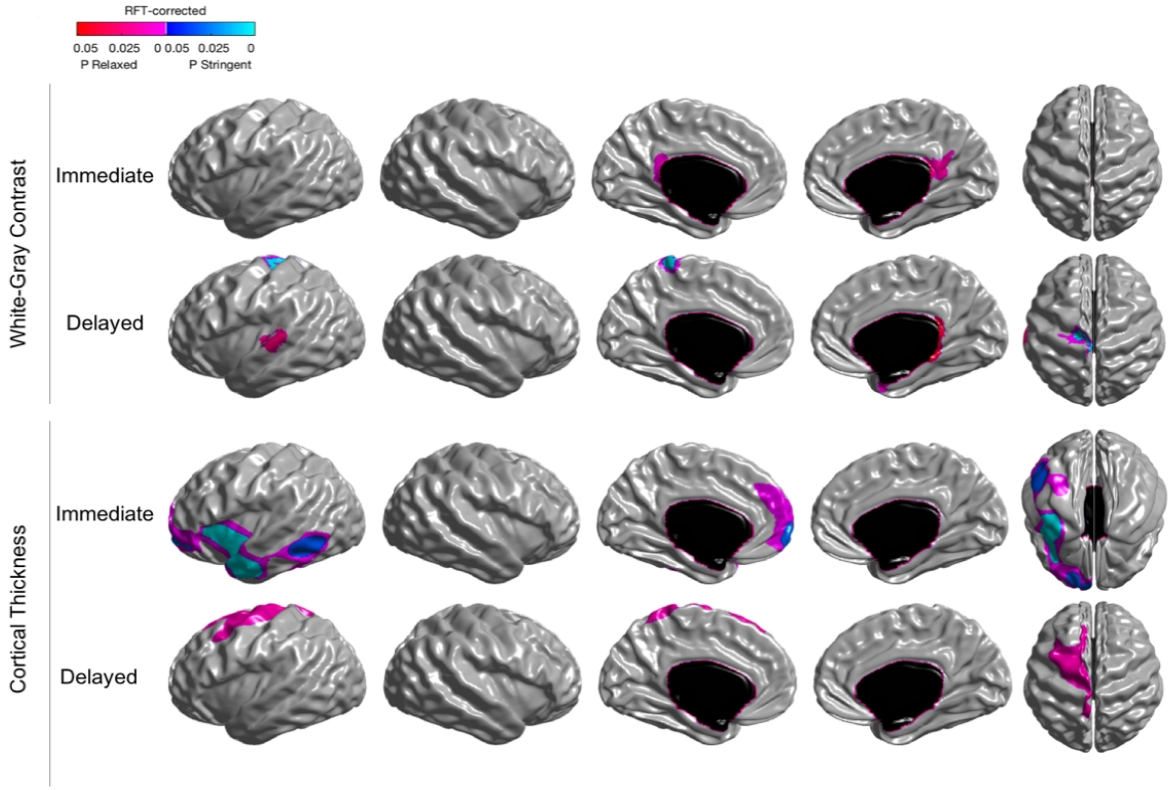

Figure 8.7. Interaction between baseline VM and ΔExpressivity on ΔWGC and ΔCT, excluding mean(σ) as a covariate.
"Immediate" and "Delayed" labels in left-hand side panel refer to immediate and delayed recall of verbal memory domain, respectively. Inflated brain is presented to better visualize results within cortical folds. Results are RFT-corrected, where blue colours represent significant results cluster-thresholded at "original" stringent threshold of p=0.001, whereas red/pink colour represent significant results at a "relaxed" threshold of p=0.01. Results remain relatively unchanged from those presented in the main manuscript, with the largest change reflected in a weaker extent of results for the interaction between delayed recall and change in expressivity on changes in CT.
Orientation: Surfaces from left to right in each row: left lateral, right lateral, left medial, right medial, dorsal (with the exception of the third row, where the right-most surface is a ventral view).

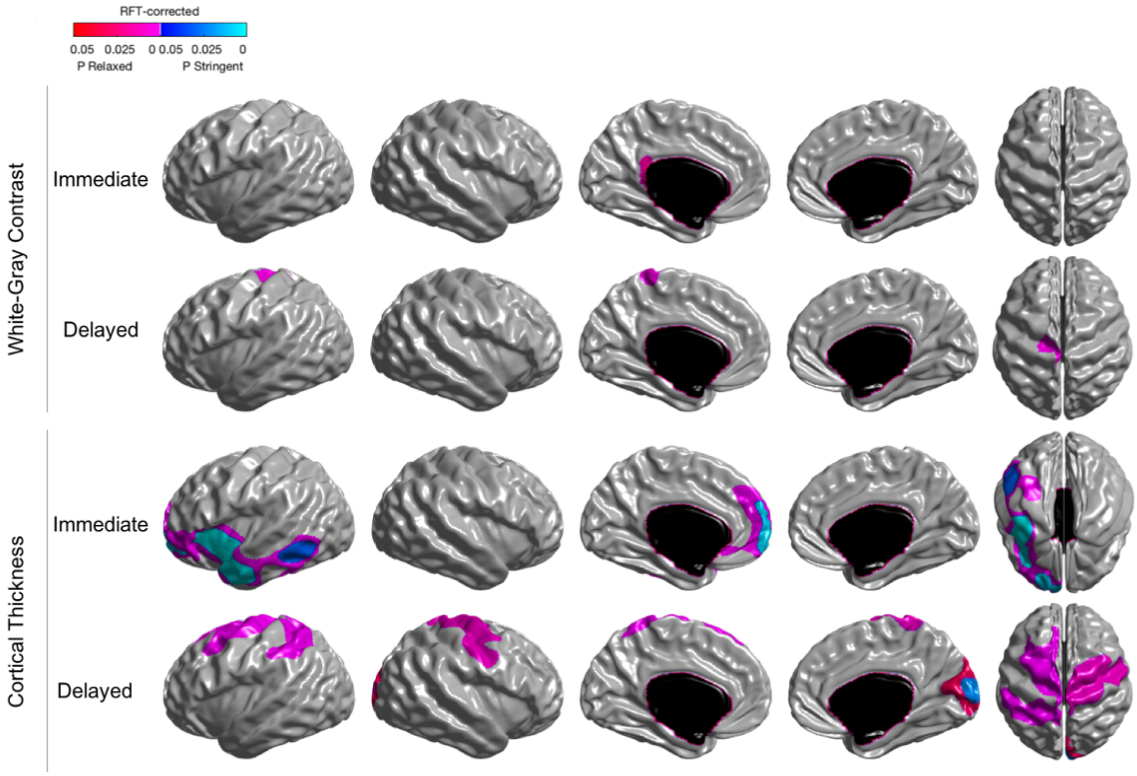

Figure 8.8. Interaction between baseline VM and ΔExpressivity on ΔWGC and ΔCT, covarying for general cognitive ability.

This analyses also included covariates that were included in Chapter 5. Z-scores of general cognitive ability comparing FEP patients against healthy controls were calculated based on five domains of cognition: speed of processing, attention, executive function, visual memory, and executive function. A composite cognitive index was calculated by averaging the scores obtained for the five cognitive domains. Similar to the verbal memory scores, cognition was assessed with two different batteries (i.e. pen and paper, and the computerized CogState battery). Additional information on the tests comprising each cognitive domain for each battery can be found in Benoit et al (2015). Within the figure, "Immediate" and "Delayed" labels in left-hand side panel refer to immediate and delayed recall of verbal memory domain, respectively. Inflated brain is presented to better visualize results within cortical folds. Results are RFT-corrected, where blue colours represent significant results cluster-thresholded at "original" stringent threshold of p=0.001, whereas red/pink colour represent significant results at a "relaxed" threshold of p=0.01. Results remain relatively unchanged from those presented in the main manuscript, suggesting that results are specific to verbal memory, and cannot be explained by general cognitive ability.

Orientation: Surfaces from left to right in each row: left lateral, right lateral, left medial, right medial, dorsal (with the exception of the third row, where the right-most surface is a ventral view).

Appendix-IV: Supplementary material for Chapter 6 (Makowski et al., In Preparation *Molecular Psychiatry* 2019)

Supplementary Methods

Sample after consideration of study criteria and Quality Control (QC).

Recruitment for this CIHR-funded longitudinal naturalistic outcome study is outcome. Scans included in analysis were acquired from December 2016 to August 2018. We chose this as the cut-off point because the 3T MRI Siemens scanner at the Douglas Institute underwent a Prisma upgrade after this time, thus we opted to only include scans pre-upgrade for this analysis. At the time of analysis, 34 FEP patients and 32 healthy controls were recruited for the study. From this sample, 4 patients were excluded (2 did not complete baseline scan, 3 dropped out after baseline, and 1 had an incidental finding), and 3 controls were excluded (2 met exclusionary criteria participation in study, and 1 dropped out after baseline). This left us with 28 FEP patients and 29 healthy controls. A few other scans failed image QC either due to failure in cortical surface QC, or significant errors in hippocampal/white-matter segmentation, as follows :

Image QC	FEP	Healthy Control
Scan 1 Baseline	2 – one due to both hippocampal labels and cortical QC, another due to cortical QC[5]	0
Scan 2 4-month follow-up	2 – one due to both hippocampal labels and cortical QC, another due to hippocampal labels only	1 – due to hippocampal labels
Scan 3 10-month follow-up	1 – due to hippocampal labels	1 – due to hippocampal labels
Scan 4 16-month follow-up	1 - due to hippocampal labels	0

[5] For one FEP scan at baseline that failed cortical QC, the patient was still included in analysis as the second scan was acquired 6 months after entry to the clinic. Thus, the second scan was still close enough to their FEP that the follow-up scans could be used in analysis.

Finally, the sample included in the main manuscript was 27 FEP patients and 29 healthy controls, contributing at least two usable scans. Please see section below on quality control procedures.

Altered parameters in imaging protocol.

A few minor alterations were made to the parameters used to acquire mp2rage, T1- and T2-weighted sequences for a handful of subjects, compared to the set protocol that is reported in the methods of the main manuscript in Chapter 6. For the MP2RAGE protocol (Marques et al. 2010), 6 FEP scans (4 baseline scans, one 4-month-follow-up, and one 10-month follow-up) were acquired with an increased echo time (TE) ranging from 2.94-2.95s, compared to the set protocol of 2.91s. For controls, 4 scans (3 baseline, and one 4-month follow-up) were acquired with an increased TE ranging from 2.94-2.97s. For the T2-weighted scan (0.64mm isotropic), three scans included in analysis had altered acquisition parameters: one 4-month follow-up scan from a control was acquired with an increased repetition time (TR) from 31s to 38s, one 4-month follow-up scan from a patient was acquired with an altered field of view (FOV) from 206 to 226 mm, and one 16-month follow-up scan from a patient was acquired with an altered TE from 2.91 to 2.97s. For the T1-weighted scan, which was only used to acquire total brain volume and to crop the T2-weighted imaging data to be less computationally intensive when processed through MAGeT, only one scan was acquired with altered acquisition parameters: this scan belonged to the 10-month follow-up scan of a patient, where the scan was acquired with an altered TE from 2.91s to 2.95s.

QC of processed images.

One rater (C.M.) manually rated all of the CIVET outputs, emphasizing accurate extraction of pial and white matter surfaces. A quality control module built in-house was used, where snapshots of the mask and surfaces overlaid on the T1-weighted image, gray and white matter surface renderings, surface-surface intersections, and surface extraction convergence plots were created. These features were examined to ensure that a) the brain was extracted accurately, b) the surfaces generally followed the anatomy, c) no visible abnormalities (i.e. visibly jagged surfaces, or surfaces jutting out inaccurately) in gray and white matter surfaces could be detected, and d) complete convergence of the surface extraction process. For any questionable areas or outputs, the surfaces were overlaid on the T1 image and viewed slice by slice using Display software (https://mcin-cnim.ca/technology/visualization/display/). A three-point rating system was adopted: 2 for good quality surfaces (minimal error), 1 for satisfactory surfaces (mild to moderate error), and 0 for failed outputs. For the "questionable" outputs that were rated as a "1", a second rater independently rated the outputs, and a consensus was reached as to the inclusion/exclusion of the scan. From here, additional intracortical (at 35-45-55-65% cortical depths) and superficial white matter (1mm below gray-white matter boundary) surfaces were extracted, as described in the main manuscript. The same three-point rating system was used for hippocampal-white matter labels. Accurate registration of these five additional surfaces and the hippocampal-white matter labels to the quantitative T1 map of the MP2RAGE sequence was also examined.

Group differences in qT1: Hippocampal circuit data.

Differences in qT1 relaxation times were compared between FEP patients and controls using linear mixed effects models in Matlab (Version 2017a), with the following model:

$Y=\text{intercept}+d_{1+}\beta_1(\text{Group})+\beta_2(\text{Centered Age})+\beta_3(\text{Sex})+\text{random(Subject)}+e$

where Y represents qT1 for each hippocampal circuit subregion (9 regions per hemisphere), d_1 is the random within-subjects effect, $\beta_{1\text{-}3}$ represent regression coefficients, and ε is residual error. A Bonferroni correction for multiple comparisons was applied (p=0.05/18=0.0028). Results are shown in Table 8.11.

Group differences in qT1: Cortical surface data.

Vertex-wise analysis of IC and SWM qT1 data were conducted using SurfStat in Matlab (http://www.math.mcgill.ca/keith/surfstat/), across 81,924 cortical vertices. Group differences (FEP vs. control) in IC and SWM qT1 values were assessed along the cortical surface with a similar linear mixed effects model as above. The key difference is that "Y" in this case represents the average qT1 value across linked vertices at 35-45-55-65% cortical depths (intracortical qT1) or the qT1 value 1mm below the gray-white matter boundary (SWM qT1). Random field theory (RFT) (Worsley et al. 2004)was used for multiple comparison correction. Given our modest sample size and the exploratory nature of this analysis, we used a slightly more relaxed p-cluster threshold of p=0.01. Results are shown in Figure 8.10.

Supplementary Tables

Lobe	Label	Abbrev	Description	Lobe	Label	Abbrev	Description
	14	MedOFG.L	MedialOrbitofrontal.L		114	MedOFG.R	MedialOrbitofrontal.R
	8	LatOFG.L	LateralOrbitofrontal.L		108	LatOFG.LR	LateralOrbitofrontal.R
	17	RosMFG.L	RostralMiddleFrontal.L		117	RosMFG.R	RostralMiddleFrontal.R
	9	LatFOrb.L	LateralFrontalOrbitalis.L		109	LatFOrb.R	LateralFrontalOrbitalis.R
	26	SFG.L	SuperiorFrontalGyrus.L		126	SFG.R	SuperiorFrontalGyrus.R
Left Frontal	1	CaudMFG.L	CaudalMiddleFrontal.L	**Right Frontal**	101	CaudMFG.R	CaudalMiddleFrontal.R
	23	LatFOper.L	LateralFrontalOpercularis.L		123	LatFOper.R	LateralFrontalOpercularis.R
	4	LFT.L	LateralFrontalTriangularis.L		104	LFT.R	LateralFrontalTriangularis.R
	13	PaCG.L	ParacentralGyrus.L		113	PaCG.R	ParacentralGyrus.R
	29	PreCG.L	PrecentralGyrus.L		129	PreCG.R	PrecentralGyrus.R
	3	PoCG.L	PostcentralGyrus.L		103	PoCG.R	PostcentralGyrus.R
	22	SPL.L	SuperiorParietal.L		122	SPL.R	SuperiorParietal.R
Left Parietal	30	IPL.L	InferiorParietal.L	**Right Parietal**	130	IPL.R	InferiorParietal.R
	5	SMG.L	SupramarginalGyrus.L		105	SMG.R	SupramarginalGyrus.R
	27	PCUN.L	Precuneus.L		127	PCUN.R	Precuneus.R
	20	InfOC.L	InferiorOccipitalCortex.L		120	InfOC.R	InferiorOccipitalCortex.R
Left Occipital	11	Calc.L	Pericalcarine.L	**Right Occipital**	111	Calc.R	Pericalcarine.R
	15	Cun.L	Cuneus.L		115	Cun.R	Cuneus.R
	21	Ling.L	LingualGyrus.L		121	Ling.R	LingualGyrus.R
	24	Fus.L	FusiformGyrus.L		124	Fus.R	FusiformGyrus.R
	28	TranTG.L	TransverseTemporal.L		128	TranTG.R	TransverseTemporal.R
Left Temporal	32	STG.L	SuperiorTemporal.L	**Right Temporal**	132	STG.R	SuperiorTemporal.R
	10	MTG.L	MiddleTemporal.L		110	MTG.R	MiddleTemporal.R
	16	ITG.L	InferiorTemporal.L		116	ITG.R	InferiorTemporal.R
	12	PHG.L	Parahippocampal.L		112	PHG.R	Parahippocampal.R
	2	Ent.L	EntorhinalCortex.L		102	Ent.R	EntorhinalCortex.R
	18	RosACC.L	RostralAnteriorCingulate.L		118	RosACC.R	RostralAnteriorCingulate.R
Left Limbic	25	CaudACC.L	CaudalAnteriorCingulate.L	**Right Limbic**	125	CaudACC.R	CaudalAnteriorCingulate.R
	31	PCC.L	PosteriorCingulate.L		131	PCC.R	PosteriorCingulate.R
	19	IsCG.L	IsthmusCingulateGyrus.L		119	IsCG.R	IsthmusCingulateGyrus.R
	7	Ins.L	Insula.L		107	Ins.R	Insula.R

Table 8.10. DKT regions and abbreviations.

Hemisphere	Structure	F-statistic df=1,159	p-value	Mean Difference (FEP-Control)	95% Confidence Interval (Lower, Upper)
Left	CA1	2.16	0.143	22.75	-7.81, 53.30
	CA2/3	2.49	0.116	30.17	-7.57, 67.90
	*CA4/DG**	*7.17*	*0.008*	*18.63*	*4.89, 32.37*
	*Molecular layer**	*6.17*	*0.014*	*22.11*	*4.53, 39.69*
	Subiculum	1.98	0.161	27.35	-11.03, 65.73
	*Alveus**	*8.47*	*0.004*	*66.15*	*21.26, 111.04*
	Fimbria	3.59	0.060	47.59	-2.04, 97.21
	*Fornix**	*4.99*	*0.027*	*41.73*	*4.85, 78.60*
	Mammillary Bodies	1.66	0.199	31.06	-16.52, 78.65
Right	CA1	0.36	0.550	8.27	-19.02, 35.57
	CA2/3	0.32	0.570	8.1	-20.03, 36.23
	CA4/DG	0.45	0.502	5.77	-11.17, 22.72
	Molecular layer	3.48	0.064	15.1	-0.88, 31.09
	Subiculum	0.41	0.522	11.15	-23.18, 45.48
	*Alveus**	*5.63*	*0.019*	*44.82*	*7.53, 82.11*
	Fimbria	0.079	0.780	7.16	-43.3, 57.63
	*Fornix**	*4.97*	*0.027*	*49.44*	*5.65, 93.23*
	Mammillary Bodies	2.76	0.099	35.07	-6.65, 76.80

Table 8.11. Group differences in hippocampal circuit qT1.
No results survived correction for multiple comparisons with a Bonferroni-threshold of p=0.0028. Structures with p-uncorrected<0.05 are italicized with an asterisk(*).

Supplementary Figures

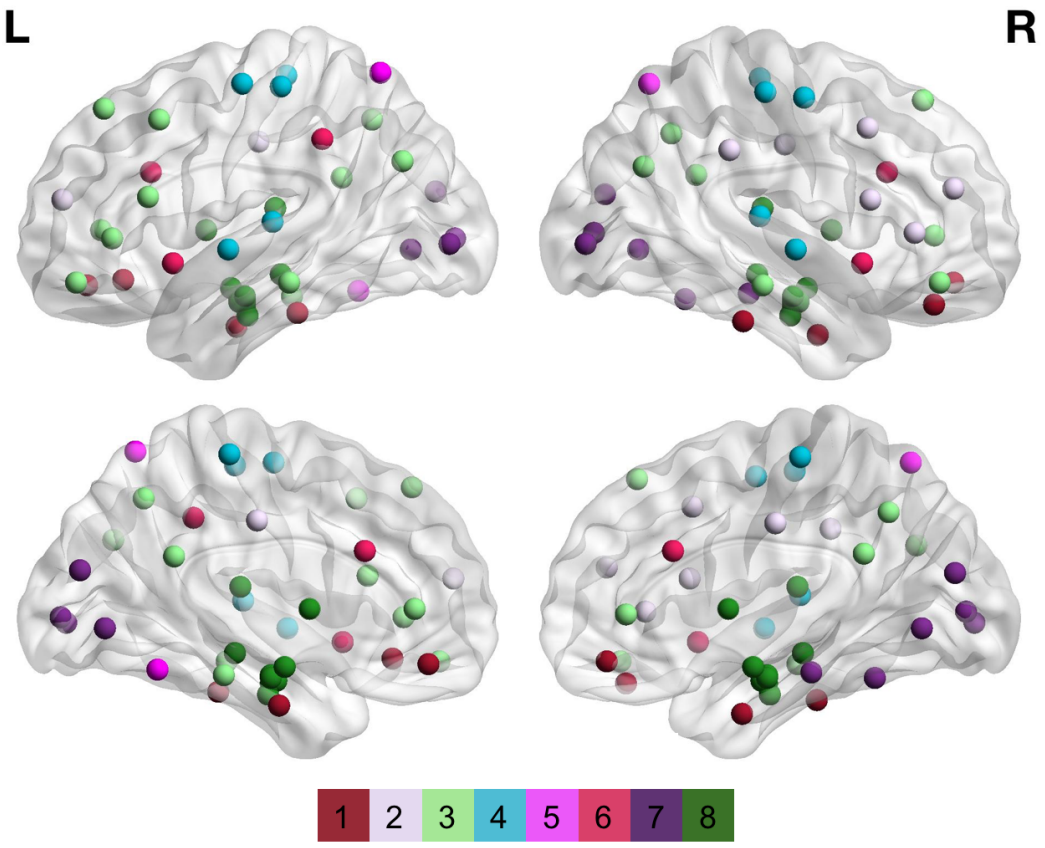

Figure 8.9. Assignment of individual regions of interest to 8 parcels.
Individual nodes reflect the approximate centre coordinate of the 62 DKT cortical regions and 18 hippocampal-white matter circuit regions. DKT regions were assigned to seven different parcels based on the functional networks presented in Yeo et al (2011)**.** The hippocampal-white matter circuit formed its own parcel (8). Visualization was done with BrainNet Viewer (Xia et al. 2013).

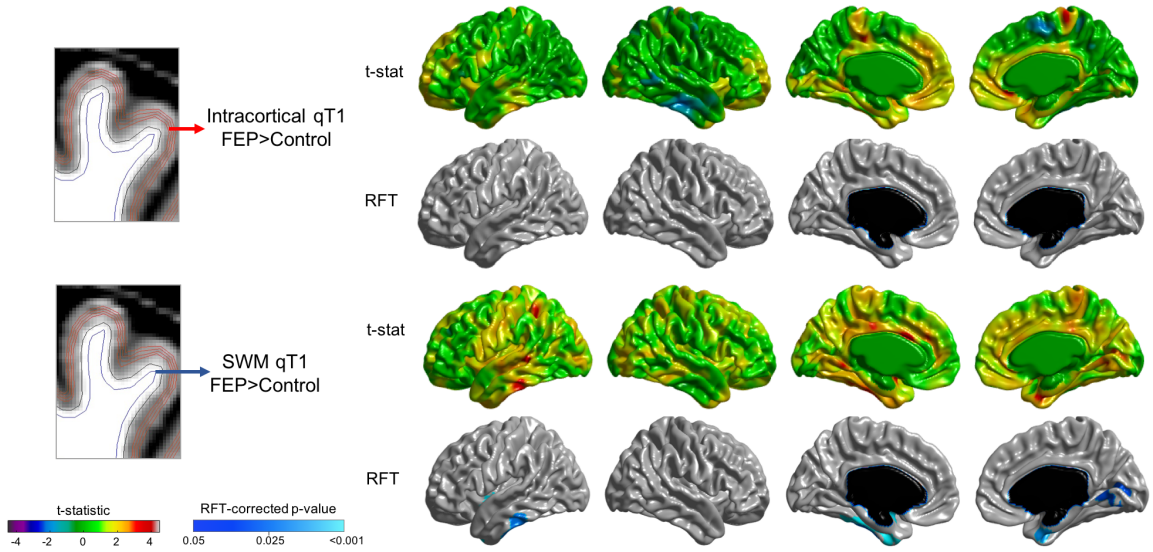

Figure 8.10. Group differences in IC and SWM qT1.
FEP patients have greater qT1 in superficial white matter (SWM) underlying bilateral temporal cortices, left insula, and right cuneus compared to healthy controls. No regions survived correction for multiple comparisons when examining qT1 intracortically (IC), although the t-statistic map shows regions of bilateral medial frontal and temporal, and paracentral regions that show trends of increased qT1 in FEP compared to controls. Brain views from left to right: left lateral, right lateral, left medial, right medial.

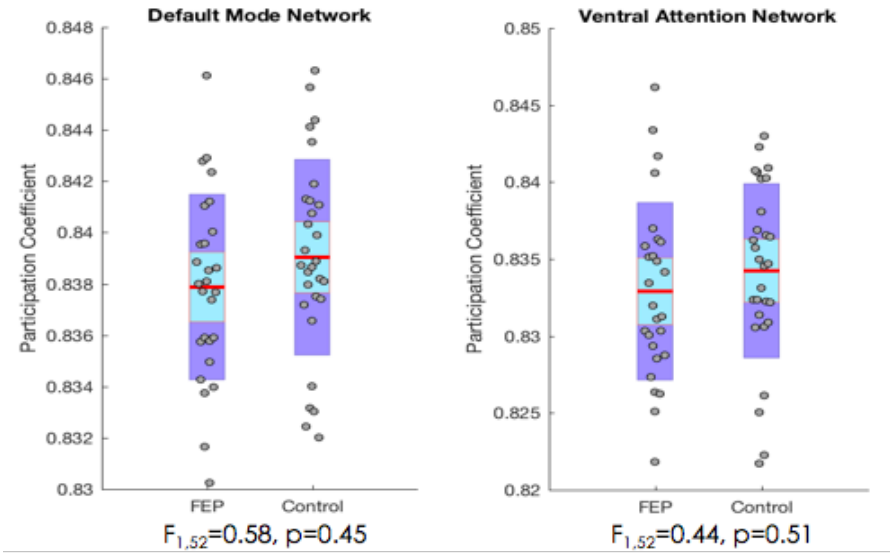

Figure 8.11. No group differences in PC of default mode and ventral attention networks.
For the boxplots, the red line denotes the mean, light blue boxes are the 95% confidence intervals, dark blue boxes represent 1 standard deviation, and gray dots are individual data points.

Bibliography

Abi-Dargham A, Meyer JM. 2014. Schizophrenia: The role of dopamine and glutamate. J Clin Psychiatry. 75:274–275.

Abramovic L, Boks MPM, Vreeker A, Bouter DC, Kruiper C, Verkooijen S, Van Bergen AH, Ophoff RA, Kahn RS, Van Haren NEM. 2016. The association of antipsychotic medication and lithium with brain measures in patients with bipolar disorder. Eur Neuropsychopharmacol. 26:1741–1751.

Ad-Dab'bagh Y, Einarson D, Lyttelton O, Muehlboeck J-S, Mok K, Ivanov O, Vincent RD, Lepage C, Lerch J, Fombonne E, Evans AC. 2006. The CIVET Image-Processing Environment: A Fully Automated Comprehensive Pipeline for Anatomical Neuroimaging Research. Proc 12th Annu Meet Organ Hum Brain Mapp. Florence.

Addington D, Addington J, Schissel B. 1990. A depression rating scale for schizophrenics. Schizophr Res. 3:247–251.

Addington J, Addington D. 2008. Social and cognitive functioning in psychosis. Schizophr Res. 99:176–181.

Addington J, Cadenhead KS, Cornblatt BA, Mathalon DH, McGlashan TH, Perkins DO, Seidman LJ, Tsuang MT, Walker EF, Woods SW, Addington JA, Cannon TD. 2012. North American Prodrome Longitudinal Study (NAPLS 2): Overview and recruitment. Schizophr Res. 142:77–82.

Akaike H. 1998. Information theory and an extension of the maximum likelihood principle. In: Selected Papers of Hirotugu Akaike, Springer Series in Statistics. New York, NY: Springer New York. p. 199–213.

Albert N, Bertelsen M, Thorup A, Petersen L, Jeppesen P, Le Quack P, Krarup G, Jørgensen P, Nordentoft M. 2011. Predictors of recovery from psychosis: Analyses of clinical and social factors associated with recovery among patients with first-episode psychosis after 5 years. Schizophr Res. 125:257–266.

Aleman A, Hijman R, de Haan EH, Kahn RS. 1999. Memory impairment in schizophrenia: a meta-analysis. Am J Psychiatry. 156:1358–1366.

Alexander-Bloch A, Clasen L, Stockman M, Ronan L, Lalonde F, Giedd J, Raznahan A. 2016. Subtle in-scanner motion biases automated measurement of brain anatomy from in vivo MRI. Hum Brain Mapp. 00:1–13.

Alexander-Bloch A, Giedd JN, Bullmore E. 2013. Imaging structural co-variance between human brain regions. 1–15.

Alexander MP, Stuss DT, Fansabedian N. 2003. California Verbal Learning Test: performance by patients with focal frontal and non-frontal lesions. Brain. 126:1493–1503.

Alfaro-Almagro F, Jenkinson M, Bangerter NK, Andersson JLR, Griffanti L, Douaud G, Sotiropoulos SN, Jbabdi S, Hernandez-Fernandez M, Vallee E, Vidaurre D, Webster M, McCarthy P, Rorden C, Daducci A, Alexander DC, Zhang H, Dragonu I, Matthews PM, Miller KL, Smith SM. 2018. Image processing and Quality Control for the first 10,000 brain imaging datasets from UK Biobank. Neuroimage. 166:400–424.

Amaral DG, Witter MP. 1989. The three-dimensional organization of the hippocampal formation: a review of anatomical data. Neuroscience. 31:571–591.

Amaral RSC, Park MTM, Devenyi GA, Lynn V, Pipitone J, Winterburn J, Chavez S, Schira M,

Lobaugh NJ, Voineskos AN, Pruessner JC, Chakravarty MM, Alzheimer's Disease Neuroimaging Initiative. 2018. Manual segmentation of the fornix, fimbria, and alveus on high-resolution 3T MRI: Application via fully-automated mapping of the human memory circuit white and grey matter in healthy and pathological aging. Neuroimage. 170:132–150.
Amlien IK, Fjell AM, Tamnes CK, Grydeland H, Krogsrud SK, Chaplin TA, Rosa MGP, Walhovd KB. 2016. Organizing Principles of Human Cortical Development - Thickness and Area from 4 to 30 Years: Insights from Comparative Primate Neuroanatomy. Cereb Cortex. 26:257–267.
Andreasen N. 1984a. Scale for the Assessment of Negative Symptoms (SANS). Iowa City: University of Iowa.
Andreasen N. 1984b. Scale for the Assessment of Positive Symptoms (SAPS). Iowa City: University of Iowa.
Andreasen N, Nasrallah HA, Dunn V, Olson SC, Grove WM, Ehrhardt JC, Coffman JA, Crossett JH. 1986. Structural abnormalities in the frontal system in schizophrenia. A magnetic resonance imaging study. Arch Gen Psychiatry. 43:136–144.
Andreasen NC. 1982. Negative symptoms in schizophrenia. Definition and reliability. Arch Gen Psychiatry. 39:784–788.
Andreasen NC, Ehrhardt JC, Swayze VW, Tyrrell G, Cohen G, Ku JS, Arndt S. 1991. T1 and T2 relaxation times in schizophrenia as measured with magnetic resonance imaging. Schizophr Res. 5:223–232.
Andreasen NC, Nopoulos P, Magnotta V, Pierson R, Ziebell S, Ho B-C. 2011. Progressive Brain Change in Schizophrenia: A Prospective Longitudinal Study of First-Episode Schizophrenia. Biol Psychiatry. 70:672–679.
Andrews DS, Avino TA, Gudbrandsen M, Daly E, Marquand A, Murphy CM, Lai M-C, Lombardo M V., Ruigrok ANV, Williams SC, Bullmore ET, The MRC AIMS Consortium TMA, Suckling J, Baron-Cohen S, Craig MC, Murphy DGM, Ecker C. 2017. In Vivo Evidence of Reduced Integrity of the Gray–White Matter Boundary in Autism Spectrum Disorder. Cereb Cortex. 69:63–70.
Ansell BRE, Dwyer DB, Wood SJ, Bora E, Brewer WJ, Proffitt TM, Velakoulis D, McGorry PD, Pantelis C. 2015. Divergent effects of first-generation and second-generation antipsychotics on cortical thickness in first-episode psychosis. Psychol Med. 45:515–527.
Arango C, Buchanan RW, Kirkpatrick B, Carpenter WT. 2004. The deficit syndrome in schizophrenia: implications for the treatment of negative symptoms. Eur Psychiatry. 19:21–26.
Ariëns-Kappers CU. 1909. The phylogenesis of the paleocortex and archicortex compared with the evolution of the visual neocortex. Arch Neurol Psychiatry. 4:161–173.
Arkesteijn GAM, Poot DHJ, de Groot M, Ikram MA, Niessen WJ, van Vliet LJ, Vernooij MW, Vos FM. 2017. CSF contamination-invariant statistics in conventional diffusion-weighted MRI of the fornix. Biomed Phys Eng Express. 3:065003.
Arnett JJ, Žukauskienė R, Sugimura K. 2014. The new life stage of emerging adulthood at ages 18-29 years: Implications for mental health. The Lancet Psychiatry. 1:569–576.
Asami T, Hyuk Lee S, Bouix S, Rathi Y, Whitford TJ, Niznikiewicz M, Nestor P, McCarley RW, Shenton ME, Kubicki M. 2014. Cerebral white matter abnormalities and their associations with negative but not positive symptoms of schizophrenia. Psychiatry Res. 222:52–59.
Aubert-Broche B, Fonov VS, García-Lorenzo D, Mouiha A, Guizard N, Coupé P, Eskildsen SF,

Collins DL. 2013. A new method for structural volume analysis of longitudinal brain MRI data and its application in studying the growth trajectories of anatomical brain structures in childhood. Neuroimage. 82:393–402.
Avery SN, Rogers BP, Heckers S. 2018. Hippocampal Network Modularity Is Associated With Relational Memory Dysfunction in Schizophrenia. Biol Psychiatry Cogn Neurosci Neuroimaging. 3:423–432.
Baglivo V, Cao B, Mwangi B, Bellani M, Perlini C, Lasalvia A, Dusi N, Bonetto C, Cristofalo D, Alessandrini F, Zoccatelli G, Ciceri E, Dario L, Enrico C, Francesca P, Mazzi F, Paolo S, Balestrieri M, Soares JC, Ruggeri M, Brambilla P. 2018. Hippocampal Subfield Volumes in Patients With First-Episode Psychosis. Schizophr Bull. 44:552–559.
Bajada CJ, Schreiber J, Caspers S. 2019. Fiber length profiling: A novel approach to structural brain organization. Neuroimage. 186:164–173.
Ballmaier M, Schlagenhauf F, Toga AW, Gallinat J, Koslowski M, Zoli M, Hojatkashani C, Narr KL, Heinz A. 2008. Regional patterns and clinical correlates of basal ganglia morphology in non-medicated schizophrenia. Schizophr Res. 106:140–147.
Barch DM, Sheffield JM. 2014. Cognitive impairments in psychotic disorders: common mechanisms and measurement. World Psychiatry. 13:224–232.
Baron RM, Kenny DA. 1986. The moderator-mediator variable distinction in social psychological research: conceptual, strategic, and statistical considerations. J Pers Soc Psychol. 51:1173–1182.
Barta PE, Pearlson GD, Powers RE, Richards SS, Tune LE. 1990. Auditory hallucinations and smaller superior temporal gyral volume in schizophrenia. Am J Psychiatry. 147:1457–1462.
Bartsch T, Wulff P. 2015. The hippocampus in aging and disease: From plasticity to vulnerability. Neuroscience. 309:1–16.
Bartzokis G. 2004. Quadratic trajectories of brain myelin content: unifying construct for neuropsychiatric disorders. Neurobiol Aging. 25:49–62.
Bartzokis G, Lu PH, Stewart SB, Oluwadara B, Lucas AJ, Pantages J, Pratt E, Sherin JE, Altshuler LL, Mintz J, Gitlin MJ, Subotnik KL, Nuechterlein KH. 2009. In vivo evidence of differential impact of typical and atypical antipsychotics on intracortical myelin in adults with schizophrenia. Schizophr Res. 113:322–331.
Battaglia FP, Benchenane K, Sirota A, Pennartz CMA, Wiener SI. 2011. The hippocampus: Hub of brain network communication for memory. Trends Cogn Sci. 15:310–318.
Baum GL, Ciric R, Roalf DR, Betzel RF, Moore TM, Shinohara RT, Kahn AE, Vandekar SN, Rupert PE, Quarmley M, Cook PA, Elliott MA, Ruparel K, Gur RE, Gur RC, Bassett DS, Satterthwaite TD. 2017. Modular Segregation of Structural Brain Networks Supports the Development of Executive Function in Youth. Curr Biol. 27:1561–1572.e8.
Baumann PS, Griffa A, Fournier M, Golay P, Ferrari C, Alameda L, Cuenod M, Thiran J-P, Hagmann P, Do KQ, Conus P. 2016. Impaired fornix–hippocampus integrity is linked to peripheral glutathione peroxidase in early psychosis. Transl Psychiatry. 6:e859–e859.
Benes FM, Turtle M, Khan Y, Farol P. 1994. Myelination of a Key Relay Zone in the Hippocampal Formation Occurs in the Human Brain during Childhood, Adolescence, and Adulthood. Arch Gen Psychiatry. 51:477–484.
Benjamini Y, Hochberg Y. 1995. Controlling the false discovery rate: a practical and powerful approach to multiple testing. J R Stat Soc B. 57:289–300.
Benjamini Y, Krieger AM, Yekutieli D. 2006. Adaptive linear step-up procedures that control the false discovery rate. Biometrika. 93:491–507.

Benoit A, Bodnar M, Malla AK, Joober R, Lepage M. 2012. The structural neural substrates of persistent negative symptoms in first-episode of non-affective psychosis: a voxel-based morphometry study. Front psychiatry. 3:42.
Benoit A, Malla AK, Iyer SN, Joober R, Bherer L, Lepage M. 2015. Cognitive deficits characterization using the CogState Research Battery in first-episode psychosis patients. Schizophr Res Cogn. 2:140–145.
Bernasconi R, Smieskova R, Schmidt A, Harrisberger F, Raschle NM, Lenz C, Walter A, Simon A, Riecher-Rössler A, Radue E-W, Lang UE, Fusar-Poli P, Borgwardt SJ. 2015. Hippocampal volume correlates with attenuated negative psychotic symptoms irrespective of antidepressant medication. NeuroImage Clin. 8:230–237.
Bervoets C, Morrens M, Vansteelandt K, Kok F, De Patoul A, Halkin V, Pitsi D, Constant E, Peuskens J, Sabbe B. 2012. Effect of aripiprazole on verbal memory and fluency in schizophrenic patients: Results from the ESCAPE study. CNS Drugs. 26:975–982.
Bezgin G, Lewis JD, Evans AC. 2018. Developmental changes of cortical white-gray contrast as predictors of autism diagnosis and severity. Transl Psychiatry. 8.
Bird CM, Burgess N. 2008. The hippocampus and memory: insights from spatial processing. Nat Rev Neurosci. 9:182–194.
Birur B, Kraguljac NV, Shelton RC, Lahti AC. 2017. Brain structure, function, and neurochemistry in schizophrenia and bipolar disorder-a systematic review of the magnetic resonance neuroimaging literature. NPJ Schizophr. 3:15.
Blanchard JJ, Cohen AS. 2006. The Structure of Negative Symptoms Within Schizophrenia: Implications for Assessment. Schizophr Bull. 32:238–245.
Bleuler E. 1911. Dementia Praecox or the Group of Schizophrenias (In German). New York, NY: International Universities Press.
Bluhm RL, Miller J, Lanius RA, Osuch EA, Boksman K, Neufeld R, Theberge J, Schaefer B, Williamson P. 2007. Spontaneous Low-Frequency Fluctuations in the BOLD Signal in Schizophrenic Patients: Anomalies in the Default Network. Schizophr Bull. 33:1004–1012.
Bodnar M, Hovington CL, Buchy L, Malla AK, Joober R, Lepage M. 2014. Cortical Thinning in Temporo-Parietal Junction (TPJ) in Non-Affective First-Episode of Psychosis Patients with Persistent Negative Symptoms. PLoS One. 9:e101372.
Bodnar M, Joober R, Lepage M. 2016. Insight and Adherence in Primary and Secondary Persistent Negative Symptoms: A Longitudinal Investigation of First-Episode Schizophrenia. In: The 5th Biennial Meeting of the Schizophrenia International Research Society. Florence, Italy.
Bodnar M, Malla AK, Czechowska Y, Benoit A, Fathalli F, Joober R, Pruessner M, Pruessner J, Lepage M. 2010. Neural markers of remission in first-episode schizophrenia: A volumetric neuroimaging study of the hippocampus and amygdala. Schizophr Res. 122:72–80.
Bodnar M, Malla AK, Makowski C, Chakravarty MM, Joober R, Lepage M. 2016. The effect of second-generation antipsychotics on hippocampal volume in first episode of psychosis: longitudinal study. Br J Psychiatry Open. 2:139–146.
Bogerts B, Ashtari M, Degreef G, Alvir JMJ, Bilder RM, Lieberman JA. 1990. Reduced temporal limbic structure volumes on magnetic resonance images in first episode schizophrenia. Psychiatry Res Neuroimaging. 35:1–13.
Bois C, Levita L, Ripp I, Owens DCG, Johnstone EC, Whalley HC, Lawrie SM. 2015. Hippocampal, amygdala and nucleus accumbens volume in first-episode schizophrenia patients and individuals at high familial risk: A cross-sectional comparison. Schizophr Res.

165:45–51.
Bonnín CM, Sánchez-Moreno J, Martínez-Arán A, Solé B, Reinares M, Rosa AR, Goikolea JM, Benabarre A, Ayuso-Mateos JL, Ferrer M, Vieta E, Torrent C. 2012. Subthreshold symptoms in bipolar disorder: Impact on neurocognition, quality of life and disability. J Affect Disord. 136:650–659.
Boonstra N, Klaassen R, Sytema S, Marshall M, De Haan L, Wunderink L, Wiersma D. 2012. Duration of untreated psychosis and negative symptoms - A systematic review and meta-analysis of individual patient data. Schizophr Res. 142:12–19.
Borghammer P, Østergaard K, Cumming P, Gjedde A, Rodell A, Hall N, Chakravarty MM. 2010. A deformation-based morphometry study of patients with early-stage Parkinson's disease. Eur J Neurol. 17:314–320.
Boucher M, Whitesides S, Evans A. 2009. Depth potential function for folding pattern representation, registration and analysis. Med Image Anal. 13:203–214.
Brandon NJ, Sawa A. 2011. Linking neurodevelopmental and synaptic theories of mental illness through DISC1. Nat Rev Neurosci. 12:707–722.
Brewer WJ, Francey SM, Wood SJ, Jackson HJ, Pantelis C, Phillips LJ, Yung AR, Anderson VA, McGorry PD. 2005a. Memory Impairments Identified in People at Ultra-High Risk for Psychosis Who Later Develop First-Episode Psychosis. Am J Psychiatry. 162:71–78.
Brewer WJ, Francey SM, Wood SJ, Jackson HJ, Pantelis C, Phillips LJ, Yung AR, Anderson VA, McGorry PD. 2005b. Memory Impairments Identified in People at Ultra-High Risk for Psychosis Who Later Develop First-Episode Psychosis. Am J Psychiatry. 162:71–78.
Brown RG, Pluck G. 2000. Negative symptoms: the "pathology" of motivation and goal-directed behaviour. Trends Neurosci. 23:412–417.
Buchanan RW. 2007. Persistent negative symptoms in schizophrenia: An overview. Schizophr Bull. 33:1013–1022.
Buchanan RW, Breier A, Kirkpatrick B, Elkashef A, Munson RC, Gellad F, Carpenter WT. 1993. Structural abnormalities in deficit and nondeficit schizophrenia. Am J Psychiatry. 150:59–65.
Bullmore E, Sporns O. 2009. Complex brain networks: graph theoretical analysis of structural and functional systems. Nat Rev Neurosci. 10:186–198.
Caligiuri ME, Nisticò R, Arabia G, Morelli M, Novellino F, Salsone M, Barbagallo G, Lupo A, Cascini GL, Galea D, Cherubini A, Quattrone A. 2016. Alterations of putaminal shape in de novo Parkinson's disease. Mov Disord. 00:1–8.
Cannon M, Jones P, Gilvarry C, Rifkin L, McKenzie K, Foerster A, Murray RM. 1997. Premorbid social functioning in schizophrenia and bipolar disorder: similarities and differences. Am J Psychiatry. 154:1544–1550.
Cannon TD, Chung Y, He G, Sun D, Jacobson A, Van Erp TGM, McEwen S, Addington J, Bearden CE, Cadenhead K, Cornblatt B, Mathalon DH, McGlashan T, Perkins D, Jeffries C, Seidman LJ, Tsuang M, Walker E, Woods SW, Heinssen R. 2015. Progressive reduction in cortical thickness as psychosis develops: A multisite longitudinal neuroimaging study of youth at elevated clinical risk. Biol Psychiatry. 77:147–157.
Cannon TD, Yu C, Addington J, Bearden CE, Cadenhead KS, Cornblatt BA, Heinssen R, Jeffries CD, Mathalon DH, McGlashan TH, Perkins DO, Seidman LJ, Tsuang MT, Walker EF, Woods SW, Kattan MW. 2016. An Individualized Risk Calculator for Research in Prodromal Psychosis. Am J Psychiatry. 173:980–988.
Cantor-Graae E, Warkentin S, Nilsson A. 1995. Neuropsychological assessment of schizophrenic

patients during a psychotic episode: persistent cognitive deficit? Acta Psychiatr Scand. 91:283–288.
Cao M, Wang J-H, Dai Z-J, Cao X-Y, Jiang L-L, Fan F-M, Song X-W, Xia M-R, Shu N, Dong Q, Milham MP, Castellanos FX, Zuo X-N, He Y. 2014. Topological organization of the human brain functional connectome across the lifespan. Dev Cogn Neurosci. 7:76–93.
Cardinal RN, Parkinson JA, Hall J, Everitt BJ. 2002. Emotion and motivation: the role of the amygdala, ventral striatum, and prefrontal cortex. Neurosci Biobehav Rev. 26:321–352.
Carletti F, Woolley JB, Bhattacharyya S, Perez-Iglesias R, Fusar Poli P, Valmaggia L, Broome MR, Bramon E, Johns L, Giampietro V, Williams SCR, Barker GJ, McGuire PK. 2012. Alterations in white matter evident before the onset of psychosis. Schizophr Bull. 38:1170–1179.
Carrión RE, McLaughlin D, Auther AM, Olsen R, Correll CU, Cornblatt BA. 2015. The impact of psychosis on the course of cognition: a prospective, nested case-control study in individuals at clinical high-risk for psychosis. Psychol Med. 45:3341–3354.
Cassidy CM, Rabinovitch M, Schmitz N, Joober R, Malla A. 2010. A comparison study of multiple measures of adherence to antipsychotic medication in first-episode psychosis. J Clin Psychopharmacol. 30:64–67.
Chakravarty MM, Rapoport JL, Giedd JN, Raznahan A, Shaw P, Collins DL, Lerch JP, Gogtay N. 2015. Striatal shape abnormalities as novel neurodevelopmental endophenotypes in schizophrenia: A longitudinal study. Hum Brain Mapp. 36:1458–1469.
Chakravarty MM, Steadman P, van Eede MC, Calcott RD, Gu V, Shaw P, Raznahan A, Collins DL, Lerch JP. 2013. Performing label-fusion-based segmentation using multiple automatically generated templates. Hum Brain Mapp. 34:2635–2654.
Chang WC, Ming Hui CL, Yan Wong GH, Wa Chan SK, Ming Lee EH, Hai Chen EY. 2013. Symptomatic remission and cognitive impairment in first-episode schizophrenia: a prospective 3-year follow-up study. J Clin Psychiatry. 74:e1046-53.
Charlton RA, Barrick TR, Markus HS, Morris RG. 2013. Verbal working and long-term episodic memory associations with white matter microstructure in normal aging investigated using tract-based spatial statistics. Psychol Aging. 28:768–777.
Chen C-H, Fiecas M, Gutiérrez ED, Panizzon MS, Eyler LT, Vuoksimaa E, Thompson WK, Fennema-Notestine C, Hagler DJ, Jernigan TL, Neale MC, Franz CE, Lyons MJ, Fischl B, Tsuang MT, Dale AM, Kremen WS. 2013. Genetic topography of brain morphology. Proc Natl Acad Sci U S A. 110:17089–17094.
Chung MK, Worsley KJ, Nacewicz BM, Dalton KM, Davidson RJ. 2010. General multivariate linear modeling of surface shapes using SurfStat. Neuroimage. 53:491–505.
Cirillo MA, Seidman LJ. 2003. Verbal declarative memory dysfunction in schizophrenia: from clinical assessment to genetics and brain mechanisms. Neuropsychol Rev. 13:43–77.
Clark RE, Squire LR. 2013. Similarity in form and function of the hippocampus in rodents, monkeys, and humans. Proc Natl Acad Sci. 110:10365–10370.
Cobia DJ, Smith MJ, Wang L, Csernansky JG. 2012. Longitudinal progression of frontal and temporal lobe changes in schizophrenia. Schizophr Res. 139:1–6.
Cohen AS, Elvevåg B. 2014. Automated computerized analysis of speech in psychiatric disorders. Curr Opin Psychiatry. 27:203–209.
Cohen AS, Mitchell KR, Elvevåg B. 2014. What do we really know about blunted vocal affect and alogia? A meta-analysis of objective assessments. Schizophr Res. 159:533–538.
Cohen JR, D'Esposito M. 2016. The Segregation and Integration of Distinct Brain Networks and

Their Relationship to Cognition. J Neurosci. 36:12083–12094.
Collin G, Keshavan MS. 2018. Connectome development and a novel extension to the neurodevelopmental model of schizophrenia. Dialogues Clin Neurosci. 20:101–111.
Collins DL, Holmes CJ, Peters TM, Evans a C. 1995. Automatic 3-D model-based neuroanatomical segmentation. Hum Brain Mapp. 3:190–208.
Collins DL, Neelin P, Peters TM, Evans AC. 1994. Automatic 3D intersubject Registration of MR Volumetric Data in Standardized Talairach Space. J Comput Assist Tomogr. 18:192–205.
Conlon P, Trimble MR. 1987. Magnetic Resonance Imaging in Psychiatry. Can J Psychiatry. 32:702–712.
Cornblatt B, Obuchowski M, Roberts S, Pollack S, Erlenmeyer-Kimling L. 1999. Cognitive and behavioral precursors of schizophrenia. Dev Psychopathol. 11:487–508.
Cotton SM, Lambert M, Schimmelmann BG, Foley DL, Morley KI, McGorry PD, Conus P. 2009. Gender differences in premorbid, entry, treatment, and outcome characteristics in a treated epidemiological sample of 661 patients with first episode psychosis. Schizophr Res. 114:17–24.
Craig TJ, Bromet EJ, Fennig S, Tanenberg-Karant M, Lavelle J, Galambos N. 2000. Is there an association between duration of untreated psychosis and 24-month clinical outcome in a first-admission series? Am J Psychiatry. 157:60–66.
Crews F, He J, Hodge C. 2007. Adolescent cortical development: A critical period of vulnerability for addiction. Pharmacol Biochem Behav. 86:189–199.
Cropley VL, Klauser P, Lenroot RK, Bruggemann J, Sundram S, Bousman C, Pereira A, Di Biase MA, Weickert TW, Weickert CS, Pantelis C, Zalesky A. 2017. Accelerated Gray and White Matter Deterioration With Age in Schizophrenia. Am J Psychiatry. 174:286–295.
Cropley VL, Pantelis C. 2014. Using longitudinal imaging to map the “relapse signature” of schizophrenia and other psychoses. Epidemiol Psychiatr Sci. 23:219–225.
Cross-Disorder Group of the Psychiatric Genomics Consortium. 2013. Identification of risk loci with shared effects on five major psychiatric disorders: a genome-wide analysis. Lancet (London, England). 381:1371–1379.
Crossley NA, Mechelli A, Fusar-Poli P, Broome MR, Matthiasson P, Johns LC, Bramon E, Valmaggia L, Williams SCR, McGuire PK. 2009. Superior temporal lobe dysfunction and frontotemporal dysconnectivity in subjects at risk of psychosis and in first-episode psychosis. Hum Brain Mapp. 30:4129–4137.
Crossley NA, Mechelli A, Scott J, Carletti F, Fox PT, MCGUIRE P, Bullmore ET. 2014. The hubs of the human connectome are generally implicated in the anatomy of brain disorders. Brain. 137:2382–2395.
Crow TJ. 1980. Molecular pathology of schizophrenia: more than one disease process? Br Med J. 280:66–68.
Das T, Borgwardt S, Hauke DJ, Harrisberger F, Lang UE, Riecher-Rössler A, Palaniyappan L, Schmidt A. 2018. Disorganized Gyrification Network Properties During the Transition to Psychosis. JAMA Psychiatry. 75:613.
Dazzan P, Arango C, Fleischacker W, Galderisi S, Glenthoj B, Leucht S, Meyer-Lindenberg A, Kahn R, Rujescu D, Sommer I, Winter I, McGuire P. 2015. Magnetic Resonance Imaging and the Prediction of Outcome in First-Episode Schizophrenia: A Review of Current Evidence and Directions for Future Research. Schizophr Bull. 41:574–583.
de Flores R, La Joie R, Chételat G. 2015. Structural imaging of hippocampal subfields in healthy

aging and Alzheimer's disease. Neuroscience. 309:29–50.
Dean DJ, Orr JM, Bernard JA, Gupta T, Pelletier-Baldelli A, Carol EE, Mittal VA. 2016. Hippocampal Shape Abnormalities Predict Symptom Progression in Neuroleptic-Free Youth at Ultrahigh Risk for Psychosis. Schizophr Bull. 42:161–169.
DeLisi LE. 2008. The concept of progressive brain change in schizophrenia: Implications for understanding schizophrenia. Schizophr Bull. 34:312–321.
DeLisi LE, Sakuma M, Tew W, Kushner M, Hoff AL, Grimson R. 1997. Schizophrenia as a chronic active brain process: a study of progressive brain structural change subsequent to the onset of schizophrenia. Psychiatry Res Neuroimaging. 74:129–140.
DeLisi LE, Tew W, Xie S, Hoff AL, Sakuma M, Kushner M, Lee G, Shedlack K, Smith AM, Grimson R. 1995. A prospective follow-up study of brain morphology and cognition in first-episode schizophrenic patients: Preliminary findings. Biol Psychiatry. 38:349–360.
Deoni SCL. 2010. Quantitative relaxometry of the brain. Top Magn Reson Imaging. 21:101–113.
Díaz-Caneja CM, Pina-Camacho L, Rodríguez-Quiroga A, Fraguas D, Parellada M, Arango C. 2015. Predictors of outcome in early-onset psychosis: a systematic review. npj Schizophr. 1:14005.
Dickinson D, Pratt DN, Giangrande EJ, Grunnagle M, Orel J, Weinberger DR, Callicott JH, Berman KF. 2017. Attacking Heterogeneity in Schizophrenia by Deriving Clinical Subgroups From Widely Available Symptom Data. Schizophr Bull. 56:921–926.
Dinse J, Härtwich N, Waehnert MD, Tardif CL, Schäfer A, Geyer S, Preim B, Turner R, Bazin P-L. 2015. A cytoarchitecture-driven myelin model reveals area-specific signatures in human primary and secondary areas using ultra-high resolution in-vivo brain MRI. Neuroimage. 114:71–87.
Duan X, Chang JH, Ge S, Faulkner RL, Kim JY, Kitabatake Y, Liu X, Yang C-H, Jordan JD, Ma DK, Liu CY, Ganesan S, Cheng H-J, Ming G, Lu B, Song H. 2007. Disrupted-In-Schizophrenia 1 Regulates Integration of Newly Generated Neurons in the Adult Brain. Cell. 130:1146–1158.
Ducharme S, Albaugh MD, Nguyen TV, Hudziak JJ, Mateos-Pérez JM, Labbe A, Evans AC, Karama S, Ball WS, Byars AW, Schapiro M, Bommer W, Carr A, German A, Dunn S, Rivkin MJ, Waber D, Mulkern R, Vajapeyam S, Chiverton A, Davis P, Koo J, Marmor J, Mrakotsky C, Robertson R, McAnulty G, Brandt ME, Fletcher JM, Kramer LA, Yang G, McCormack C, Hebert KM, Volero H, Botteron K, McKinstry RC, Warren W, Nishino T, Almli CR, Todd R, Constantino J, McCracken JT, Levitt J, Alger J, O'Neil J, Toga A, Asarnow R, Fadale D, Heinichen L, Ireland C, Wang DJ, Moss E, Zimmerman RA, Bintliff B, Bradford R, Newman J, Arnaoutelis R, Pike GB, Collins DL, Leonard G, Paus T, Zijdenbos A, Das S, Fonov V, Fu L, Harlap J, Leppert I, Milovan D, Vins D, Zeffiro T, Van Meter J, Lange N, Froimowitz MP, Rainey C, Henderson S, Edwards JL, Dubois D, Smith K, Singer T, Wilber AA, Pierpaoli C, Basser PJ, Chang LC, Koay CG, Walker L, Freund L, Rumsey J, Baskir L, Stanford L, Sirocco K, Gwinn-Hardy K, Spinella G, Alger JR, O'Neill J. 2016. Trajectories of cortical thickness maturation in normal brain development - The importance of quality control procedures. Neuroimage. 125:267–279.
Eaton WW, Thara R, Federman B, Melton B, Liang KY. 1995. Structure and course of positive and negative symptoms in schizophrenia. Arch Gen Psychiatry. 52:127–134.
Ebert A, Bär K-J. 2010. Emil Kraepelin: A pioneer of scientific understanding of psychiatry and psychopharmacology. Indian J Psychiatry. 52:191–192.
Ecker C, Shahidiani a., Feng Y, Daly E, Murphy C, D'Almeida V, Deoni S, Williams SC, Gillan

N, Gudbrandsen M, Wichers R, Andrews D, Van Hemert L, Murphy DGM. 2014. The effect of age, diagnosis, and their interaction on vertex-based measures of cortical thickness and surface area in autism spectrum disorder. J Neural Transm. 121:1157–1170.
Ehrlich I, Humeau Y, Grenier F, Ciocchi S, Herry C, Lüthi A. 2009. Amygdala Inhibitory Circuits and the Control of Fear Memory. Neuron. 62:757–771.
Eichenbaum H. 2000. A cortical-hippocampal system for declarative memory. Nat Rev Neurosci. 1:41–50.
Ellison-Wright I, Bullmore E. 2010. Anatomy of bipolar disorder and schizophrenia: A meta-analysis. Schizophr Res. 117:1–12.
Erickson KI, Voss MW, Prakash RS, Basak C, Szabo A, Chaddock L, Kim JS, Heo S, Alves H, White SM, Wojcicki TR, Mailey E, Vieira VJ, Martin SA, Pence BD, Woods JA, McAuley E, Kramer AF. 2011. Exercise training increases size of hippocampus and improves memory. Proc Natl Acad Sci U S A. 108:3017–3022.
Eriksson PS, Perfilieva E, Björk-Eriksson T, Alborn a M, Nordborg C, Peterson D a, Gage FH. 1998. Neurogenesis in the adult human hippocampus. Nat Med. 4:1313–1317.
Evans AC. 2013. Networks of anatomical covariance. Neuroimage. 80:489–504.
Fair DA, Cohen AL, Power JD, Dosenbach NUF, Church JA, Miezin FM, Schlaggar BL, Petersen SE. 2009. Functional Brain Networks Develop from a "Local to Distributed" Organization. PLoS Comput Biol. 5:e1000381.
Faludi G, Mirnics K. 2011. Synaptic changes in the brain of subjects with schizophrenia. Int J Dev Neurosci. 29:305–309.
Feinberg I. 1982. Schizophrenia: Caused by a fault in programmed synaptic elimination during adolescence? J Psychiatr Res. 17:319–334.
Fernando ABP, Murray JE, Milton AL. 2013. The amygdala: securing pleasure and avoiding pain. Front Behav Neurosci. 7:190.
Ferro A, Roiz-Santiáñez R, de la Foz VO-G, Tordesillas-Gutiérrez D, Ayesa-Arriola R, de La Fuente-González N, Fañanás L, Brambilla P, Crespo-Facorro B. 2015. A cross-sectional and longitudinal structural magnetic resonance imaging study of the post-central gyrus in first-episode schizophrenia patients. Psychiatry Res Neuroimaging. 231:42–49.
First M, Spitzer R, Gibbon M, JBW W. 1998. Structured clinical interview for DSM-IV patient edition (SCID-I/P V and SCID-I/NP Version 2.0). New York: Biometric Research Department.
Fischer M. 1971. Psychoses in the offspring of schizophrenic monozygotic twins and their normal co-twins. Br J Psychiatry. 118:43–52.
Fischl B, Salat DH, Busa E, Albert M, Dieterich M, Haselgrove C, Van Der Kouwe A, Killiany R, Kennedy D, Klaveness S, Montillo A, Makris N, Rosen B, Dale AM. 2002. Whole brain segmentation: Automated labeling of neuroanatomical structures in the human brain. Neuron. 33:341–355.
Foussias G, Agid O, Fervaha G, Remington G. 2014. Negative symptoms of schizophrenia: Clinical features, relevance to real world functioning and specificity versus other CNS disorders. Eur Neuropsychopharmacol. 24:693–709.
Frank E, Nimgaonkar VL, Phillips ML, Kupfer DJ. 2015. All the world's a (clinical) stage: rethinking bipolar disorder from a longitudinal perspective. Mol Psychiatry. 20:23–31.
Friederici AD. 2011. The brain basis of language processing: from structure to function. Physiol Rev. 91:1357–1392.
Friston K, Brown HR, Siemerkus J, Stephan KE. 2016. The dysconnection hypothesis (2016).

Schizophr Res. 176:83–94.
Friston K, Frith C. 1995. Schizophrenia: a disconnection syndrome? J Clin Neurosci. 3:89–97.
Friston KJ. 1998. The disconnection hypothesis. Schizophr Res. 30:115–125.
Fusar-Poli P, Papanastasiou E, Stahl D, Rocchetti M, Carpenter W, Shergill S, McGuire P. 2015. Treatments of Negative Symptoms in Schizophrenia: Meta-Analysis of 168 Randomized Placebo-Controlled Trials. Schizophr Bull. 41:892–899.
Fusar-Poli P, Smieskova R, Kempton MJ, Ho BC, Andreasen NC, Borgwardt S. 2013. Progressive brain changes in schizophrenia related to antipsychotic treatment? A meta-analysis of longitudinal MRI studies. Neurosci Biobehav Rev. 37:1680–1691.
Galderisi S, Merlotti E, Mucci A. 2015. Neurobiological background of negative symptoms. Eur Arch Psychiatry Clin Neurosci. 265:543–558.
Galderisi S, Mucci A, Bitter I, Libiger J, Bucci P, Fleischhacker WW, Kahn RS, Group for the ES. 2013. Persistent negative symptoms in first episode patients with schizophrenia Results from the European First Episode Schizophrenia Trial. Eur Neuropsychopharmacol. 23:196–204.
Galderisi S, Rucci P, Kirkpatrick B, Mucci A, Gibertoni D, Rocca P, Rossi A, Bertolino A, Strauss GP, Aguglia E, Bellomo A, Murri MB, Bucci P, Carpiniello B, Comparelli A, Cuomo A, De Berardis D, Dell'Osso L, Di Fabio F, Gelao B, Marchesi C, Monteleone P, Montemagni C, Orsenigo G, Pacitti F, Roncone R, Santonastaso P, Siracusano A, Vignapiano A, Vita A, Zeppegno P, Maj M. 2018. Interplay Among Psychopathologic Variables, Personal Resources, Context-Related Factors, and Real-life Functioning in Individuals With Schizophrenia. JAMA Psychiatry.
Ganzetti M, Wenderoth N, Mantini D. 2015. Mapping pathological changes in brain structure by combining T1- and T2-weighted MR imaging data. Neuroradiology. 57:917–928.
Gard DE, Fisher M, Garrett C, Genevsky A, Vinogradov S. 2009. Motivation and its Relationship to Neurocognition, Social Cognition, and Functional Outcome in Schizophrenia. Schizophr Res. 115:74–81.
Glasser MF, Van Essen DC. 2011. Mapping human cortical areas in vivo based on myelin content as revealed by T1- and T2-weighted MRI. J Neurosci. 31:11597–11616.
Godsil BP, Kiss JP, Spedding M, Jay TM. 2013. The hippocampal–prefrontal pathway: The weak link in psychiatric disorders? Eur Neuropsychopharmacol. 23:1165–1181.
Goeree R, Farahati F, Burke N, Blackhouse G, O'Reilly D, Pyne J, Tarride J -E. 2005. The economic burden of schizophrenia in Canada in 2004. Curr Med Res Opin. 21:2017–2028.
Gogtay N, Giedd JN, Lusk L, Hayashi KM, Greenstein D, Vaituzis AC, Nugent Tom F III, Herman DH, Clasen LS, Toga AW, Rapoport JL, Thompson PM. 2004. Dynamic mapping of human cortical development during childhood through early adulthood. PNAS. 101:8174–8179.
Goldberg TE, Torrey EF, Gold JM, Ragland JD, Bigelow LB, Weinberger DR. 1993. Learning and memory in monozygotic twins discordant for schizophrenia. Psychol Med. 23:71–85.
Goldman AL, Pezawas L, Mattay VS, Fischl B, Verchinski BA, Chen Q, Weinberger DR, Meyer-Lindenberg A, Meyer-Lindenberg A. 2009. Widespread reductions of cortical thickness in schizophrenia and spectrum disorders and evidence of heritability. Arch Gen Psychiatry. 66:467–477.
Gonçalves JT, Schafer ST, Gage FH. 2016. Adult Neurogenesis in the Hippocampus: From Stem Cells to Behavior. Cell. 167:897–914.
Gong Q, Lui S, Sweeney JA. 2016. A selective review of cerebral abnormalities in patients with

first-episode schizophrenia before and after treatment. Am J Psychiatry. 173:232–243.
Good CD, Johnsrude I, Ashburner J, Henson RN, Friston KJ, Frackowiak RS. 2001. Cerebral asymmetry and the effects of sex and handedness on brain structure: a voxel-based morphometric analysis of 465 normal adult human brains. Neuroimage. 14:685–700.
Goodkind M, Eickhoff SB, Oathes DJ, Jiang Y, Chang A, Jones-Hagata LB, Ortega BN, Zaiko Y V., Roach EL, Korgaonkar MS, Grieve SM, Galatzer-Levy I, Fox PT, Etkin A. 2015. Identification of a Common Neurobiological Substrate for Mental Illness. JAMA Psychiatry. 72:305.
Gousias IS, Edwards AD, Rutherford MA, Counsell SJ, Hajnal J V, Rueckert D, Hammers A. 2012. Magnetic resonance imaging of the newborn brain: Manual segmentation of labelled atlases in term-born and preterm infants. Neuroimage. 62:1499–1509.
Gradin VB, Waiter G, O'Connor A, Romaniuk L, Stickle C, Matthews K, Hall J, Douglas Steele J. 2013. Salience network-midbrain dysconnectivity and blunted reward signals in schizophrenia. Psychiatry Res Neuroimaging. 211:104–111.
Green MF, Harvey PD. 2014. Cognition in schizophrenia: Past, present, and future. Schizophr Res Cogn. 1:1–21.
Green MF, Hellemann G, Horan WP, Lee J, Wynn JK. 2012. From perception to functional outcome in schizophrenia: modeling the role of ability and motivation. Arch Gen Psychiatry. 69:1216–1224.
Green MF, Nuechterlein KH. 1999. Should Schizophrenia Be Treated as a Neurocognitive Disorder? Schizophr Bull. 25:309–3019.
Greene DJ, Black KJ, Schlaggar BL. 2016. Considerations for MRI study design and implementation in pediatric and clinical populations. Dev Cogn Neurosci. 18:101–112.
Grimm O, Pohlack S, Cacciaglia R, Plichta M, Demirakca T, Flor H. 2015. Amygdala and hippocampal volume: A comparison between manual segmentation, Freesurfer and VBM. J Neurosci Methods. 253:254–261.
Grydeland H, Vértes PE, Váša F, Romero-Garcia R, Whitaker K, Alexander-Bloch AF, Bjørnerud A, Patel AX, Sederevičius D, Tamnes CK, Westlye LT, White SR, Walhovd KB, Fjell AM, Bullmore ET. 2019. Waves of Maturation and Senescence in Micro-structural MRI Markers of Human Cortical Myelination over the Lifespan. Cereb Cortex. 29:1369–1381.
Gu S, Satterthwaite TD, Medaglia JD, Yang M, Gur RE, Gur RC, Bassett DS. 2015. Emergence of system roles in normative neurodevelopment. Proc Natl Acad Sci U S A. 112:13681–13686.
Guadalupe T, Willems RM, Zwiers MP, Arias Vasquez A, Hoogman M, Hagoort P, Fernandez G, Buitelaar J, Franke B, Fisher SE, Francks C. 2014. Differences in cerebral cortical anatomy of left- and right-handers. Front Psychol. 5:261.
Guimond S, Chakravarty MM, Bergeron-Gagnon L, Patel R, Lepage M. 2016. Verbal memory impairments in schizophrenia associated with cortical thinning. NeuroImage Clin. 11:20–29.
Gunstad J, Paul RH, Cohen RA, Tate DF, Gordon E. 2006. Obesity is associated with memory deficits in young and middle-aged adults. Eat Weight Disord. 11:e15-9.
Guo S, Palaniyappan L, Liddle PF, Feng J. 2016. Dynamic cerebral reorganization in the pathophysiology of schizophrenia: a MRI-derived cortical thickness study. Psychol Med. 1–14.
Gur RE, Loughead J, Kohler CG, Elliott MA, Lesko K, Ruparel K, Wolf DH, Bilker WB, Gur

RC. 2007. Limbic Activation Associated With Misidentification of Fearful Faces and Flat Affect in Schizophrenia. Arch Gen Psychiatry. 64:1356.
Haber SN. 2016. Corticostriatal circuitry. Dialogues Clin Neurosci. 18:7–21.
Hagler DJ, Hatton SN, Makowski C, Cornejo MD, Fair DA, Dick AS, Sutherland MT, Casey BJ, Barch DM, Harms MP, Watts R, Bjork JM, Garavan HP, Hilmer L, Pung CJ, Sicat CS, Kuperman J, Bartsch H, Xue F, Heitzeg MM, Laird AR, Trinh TT, Gonzalez R, Tapert SF, Riedel MC, Squeglia LM, Hyde LW, Rosenberg MD, Earl EA, Howlett KD, Baker FC, Soules M, Diaz J, Ruiz de Leon O, Thompson WK, Neale MC, Herting M, Sowell ER, Alvarez RP, Hawes SW, Sanchez M, Bodurka J, Breslin FJ, Morris AS, Paulus MP, Simmons WK, Polimeni JR, van der Kouwe A, Nencka AS, Gray KM, Pierpaoli C, Matochik JA, Noronha A, Aklin WM, Conway K, Glantz M, Hoffman E, Little R, Lopez M, Pariyadath V, Weiss SRB, Wolff-Hughes DL, DelCarmen-Wiggins R, Feldstein Ewing SW, Miranda-Dominguez O, Nagel BJ, Perrone AJ, Sturgeon DT, Goldstone A, Pfefferbaum A, Pohl KM, Prouty D, Uban K, Bookheimer SY, Dapretto M, Galvan A, Bagot K, Giedd J, Infante MA, Jacobus J, Patrick K, Shilling PD, Desikan R, Li Y, Sugrue L, Banich MT, Friedman N, Hewitt JK, Hopfer C, Sakai J, Tanabe J, Cottler LB, Nixon SJ, Chang L, Cloak C, Ernst T, Reeves G, Kennedy DN, Heeringa S, Peltier S, Schulenberg J, Sripada C, Zucker RA, Iacono WG, Luciana M, Calabro FJ, Clark DB, Lewis DA, Luna B, Schirda C, Brima T, Foxe JJ, Freedman EG, Mruzek DW, Mason MJ, Huber R, McGlade E, Prescot A, Renshaw PF, Yurgelun-Todd DA, Allgaier NA, Dumas JA, Ivanova M, Potter A, Florsheim P, Larson C, Lisdahl K, Charness ME, Fuemmeler B, Hettema JM, Steinberg J, Anokhin AP, Glaser P, Heath AC, Madden PA, Baskin-Sommers A, Constable RT, Grant SJ, Dowling GJ, Brown SA, Jernigan TL, Dale AM. 2018. Image processing and analysis methods for the Adolescent Brain Cognitive Development Study. bioRxiv.
Hajek T, Kopecek M, Kozeny J, Gunde E, Alda M, Höschl C. 2009. Amygdala volumes in mood disorders - Meta-analysis of magnetic resonance volumetry studies. J Affect Disord. 115:395–410.
Hamilton M. 1959. The assessment of anxiety states by rating. Br J Med Psychol. 32.
Hammers A, Allom R, Koepp MJ, Free SL, Myers R, Lemieux L, Mitchell TN, Brooks DJ, Duncan JS. 2003. Three-dimensional maximum probability atlas of the human brain, with particular reference to the temporal lobe. Hum Brain Mapp. 19:224–247.
Hamparsum B. 1987. Model selection and Akaike's Information Criterion (AIC): The general theory and its analytical extensions. Psychometrika. 52:345–370.
Hao Y, Yan Q, Liu H, Xu L, Xue Z, Song X, Kaneko Y, Jiang T, Liu Z, Shan B. 2009. Schizophrenia patients and their healthy siblings share disruption of white matter integrity in the left prefrontal cortex and the hippocampus but not the anterior cingulate cortex.
Haroutunian V, Katsel P, Roussos P, Davis KL, Altshuler LL, Bartzokis G. 2014. Myelination, oligodendrocytes, and serious mental illness. Glia. 62:1856–1877.
Harrison PJ. 2004. The hippocampus in schizophrenia: a review of the neuropathological evidence and its pathophysiological implications. Psychopharmacology (Berl). 174:151–162.
Harrison PJ, Law AJ. 2006. Neuregulin 1 and Schizophrenia: Genetics, Gene Expression, and Neurobiology. Biol Psychiatry. 60:132–140.
Hartmann-Riemer MN, Hager OM, Kirschner M, Bischof M, Kluge A, Seifritz E, Kaiser S. 2015. The association of neurocognitive impairment with diminished expression and apathy in schizophrenia. Schizophr Res. 169:427–432.

Haukvik UK, Hartberg CB, Nerland S, Jørgensen KN, Lange EH, Simonsen C, Nesvåg R, Dale AM, Andreassen OA, Melle I, Agartz I. 2016. No progressive brain changes during a 1-year follow-up of patients with first-episode psychosis. Psychol Med. 46:589–598.
Haukvik UK, Westlye LT, Mørch-Johnsen L, Jørgensen KN, Lange EH, Dale AM, Melle I, Andreassen OA, Agartz I. 2015. In vivo hippocampal subfield volumes in schizophrenia and bipolar disorder. Biol Psychiatry. 77:581–588.
Havsteen I, Ohlhues A, Madsen KH, Nybing JD, Christensen H, Christensen A. 2017. Are Movement Artifacts in Magnetic Resonance Imaging a Real Problem?-A Narrative Review. Front Neurol. 8:232.
Hibar DP, Westlye LT, Doan NT, Jahanshad N, Cheung JW, Ching CRK, Versace A, Bilderbeck AC, Uhlmann A, Mwangi B, Krämer B, Overs B, Hartberg CB, Abé C, Dima D, Grotegerd D, Sprooten E, Bøen E, Jimenez E, Howells FM, Delvecchio G, Temmingh H, Starke J, Almeida JRC, Goikolea JM, Houenou J, Beard LM, Rauer L, Abramovic L, Bonnin M, Ponteduro MF, Keil M, Rive MM, Yao N, Yalin N, Najt P, Rosa PG, Redlich R, Trost S, Hagenaars S, Fears SC, Alonso-Lana S, van Erp TGM, Nickson T, Chaim-Avancini TM, Meier TB, Elvsåshagen T, Haukvik UK, Lee WH, Schene AH, Lloyd AJ, Young AH, Nugent A, Dale AM, Pfennig A, McIntosh AM, Lafer B, Baune BT, Ekman CJ, Zarate CA, Bearden CE, Henry C, Simhandl C, McDonald C, Bourne C, Stein DJ, Wolf DH, Cannon DM, Glahn DC, Veltman DJ, Pomarol-Clotet E, Vieta E, Canales-Rodriguez EJ, Nery FG, Duran FLS, Busatto GF, Roberts G, Pearlson GD, Goodwin GM, Kugel H, Whalley HC, Ruhe HG, Soares JC, Fullerton JM, Rybakowski JK, Savitz J, Chaim KT, Fatjó-Vilas M, Soeiro-de-Souza MG, Boks MP, Zanetti M V, Otaduy MCG, Schaufelberger MS, Alda M, Ingvar M, Phillips ML, Kempton MJ, Bauer M, Landén M, Lawrence NS, van Haren NEM, Horn NR, Freimer NB, Gruber O, Schofield PR, Mitchell PB, Kahn RS, Lenroot R, Machado-Vieira R, Ophoff RA, Sarró S, Frangou S, Satterthwaite TD, Hajek T, Dannlowski U, Malt UF, Arolt V, Gattaz WF, Drevets WC, Caseras X, Agartz I, Thompson PM, Andreassen OA. 2018. Cortical abnormalities in bipolar disorder: an MRI analysis of 6503 individuals from the ENIGMA Bipolar Disorder Working Group. Mol Psychiatry. 23:932–942.
Hibar DP, Westlye LT, van Erp TGM, Rasmussen J, Leonardo CD, Faskowitz J, Haukvik UK, Hartberg CB, Doan NT, Agartz I, Dale AM, Gruber O, Krämer B, Trost S, Liberg B, Abé C, Ekman CJ, Ingvar M, Landén M, Fears SC, Freimer NB, Bearden CE, Costa Rica/Colombia Consortium for Genetic Investigation of Bipolar Endophenotypes the CRC for GI of B, Sprooten E, Glahn DC, Pearlson GD, Emsell L, Kenney J, Scanlon C, McDonald C, Cannon DM, Almeida J, Versace A, Caseras X, Lawrence NS, Phillips ML, Dima D, Delvecchio G, Frangou S, Satterthwaite TD, Wolf D, Houenou J, Henry C, Malt UF, Bøen E, Elvsåshagen T, Young AH, Lloyd AJ, Goodwin GM, Mackay CE, Bourne C, Bilderbeck A, Abramovic L, Boks MP, van Haren NEM, Ophoff RA, Kahn RS, Bauer M, Pfennig A, Alda M, Hajek T, Mwangi B, Soares JC, Nickson T, Dimitrova R, Sussmann JE, Hagenaars S, Whalley HC, McIntosh AM, Thompson PM, Andreassen OA. 2016. Subcortical volumetric abnormalities in bipolar disorder. Mol Psychiatry. 21:1710–1716.
Ho B-C, Andreasen NC, Nopoulos P, Arndt S, Magnotta V, Flaum M. 2003. Progressive Structural Brain Abnormalities and Their Relationship to Clinical Outcome. Arch Gen Psychiatry. 1–10.
Ho B-C, Andreasen NC, Ziebell S, Pierson R, Magnotta V. 2011. Long-term Antipsychotic Treatment and Brain Volumes. Arch Gen Psychiatry. 68:128.

Ho NF, Holt DJ, Cheung M, Iglesias JE, Goh A, Wang M, Lim JK, De Souza J, Poh JS, See YM, Adcock AR, Wood SJ, Chee MW, Lee J, Zhou J. 2017. Progressive Decline in Hippocampal CA1 Volume in Individuals at Ultra-High-Risk for Psychosis Who Do Not Remit: Findings from the Longitudinal Youth at Risk Study. Neuropsychopharmacology. 42.
Ho NF, Iglesias JE, Sum MY, Kuswanto CN, Sitoh YY, De Souza J, Hong Z, Fischl B, Roffman JL, Zhou J, Sim K, Holt DJ. 2017. Progression from selective to general involvement of hippocampal subfields in schizophrenia. Mol Psychiatry. 22:142–152.
Hoff AL, Sakuma M, Wieneke M, Horon R, Kushner M, DeLisi LE. 1999. Longitudinal neuropsychological follow-up study of patients with first-episode schizophrenia. Am J Psychiatry. 156:1336–1341.
Holdnack JA, Drozdick LW, Iverson GL, Chelune GJ. 2013. Serial Assessment with WAIS–IV and WMS–IV. WAIS-IV, WMS-IV, ACS. 279–329.
Hollingshead A. 1965. A Two-Factor Index of Social Position. New Haven, CN: Yale University Press.
Hollis C, Palaniyappan L. 2015. Schizophrenia and psychosis. In: Rutter's Child and Adolescent Psychiatry. Chichester, UK: John Wiley & Sons, Ltd. p. 774–792.
Hovington CL, Bodnar M, Chakravarty MM, Joober R, Malla AK, Lepage M. 2015. Investigation of white matter abnormalities in first episode psychosis patients with persistent negative symptoms. Psychiatry Res - Neuroimaging. 233:402–408.
Hovington CL, Bodnar M, Joober R, Malla AK, Lepage M. 2012. Identifying persistent negative symptoms in first episode psychosis. BMC Psychiatry. 12:1–11.
Hovington CL, Bodnar M, Joober R, Malla AK, Lepage M. 2013. Impairment in verbal memory observed in first episode psychosis patients with persistent negative symptoms. Schizophr Res. 147:223–229.
Howes OD, Kapur S. 2009. The dopamine hypothesis of schizophrenia: Version III - The final common pathway. Schizophr Bull. 35:549–562.
Hu M-L, Zong X-F, Mann JJ, Zheng J-J, Liao Y-H, Li Z-C, He Y, Chen X-G, Tang J-S. 2017. A Review of the Functional and Anatomical Default Mode Network in Schizophrenia. Neurosci Bull. 33:73–84.
Huntenburg JM, Bazin P-L, Goulas A, Tardif CL, Villringer A, Margulies DS. 2017. A Systematic Relationship Between Functional Connectivity and Intracortical Myelin in the Human Cerebral Cortex. Cereb Cortex. 27:981–997.
Insel T, Cuthbert B, Garvey M, Heinssen R, Pine DS, Quinn K, Sanislow C, Wang P. 2010. Research Domain Criteria (RDoC): Toward a New Classification Framework for Research on Mental Disorders. Am J Psychiatry. 167:748–751.
Insel TR. 2014. The NIMH Research Domain Criteria (RDoC) Project: Precision Medicine for Psychiatry. Am J Psychiatry. 171:395–397.
Isıklı S, Ugurlu O, Durmusoglu E, Kizilates G, Kitis O, Ozan E, Eker C, Coburn K, Gonul AS. 2013. Altered hippocampal formation shape in first-episode depressed patients at 5-year follow-up. J Psychiatr Res. 47:50–55.
Ivanov I, Bansal R, Hao X, Zhu H, Kellendonk C, Miller L, Sanchez-Pena J, Miller AM, Chakravarty MM, Klahr K, Durkin K, Greenhill LL, Peterson BS. 2010. Morphological abnormalities of the thalamus in youths with attention deficit hyperactivity disorder. Am J Psychiatry. 167:397–408.
Iwatani J, Ishida T, Donishi T, Ukai S, Shinosaki K, Terada M, Kaneoke Y. 2015. Use of T1-

weighted/T2-weighted magnetic resonance ratio images to elucidate changes in the schizophrenic brain. Brain Behav. 5:e00399.
Iyer S, Jordan G, MacDonald K, Joober R, Malla A. 2015. Early intervention for psychosis: a Canadian perspective. J Nerv Ment Dis. 203:356–364.
Jang S-K, Choi H-I, Park S, Jaekal E, Lee G-Y, Cho Y Il, Choi K-H. 2016. A Two-Factor Model Better Explains Heterogeneity in Negative Symptoms: Evidence from the Positive and Negative Syndrome Scale. Front Psychol. 7:707.
Ji E, Guevara P, Guevara M, Grigis A, Labra N, Sarrazin S, Hamdani N, Bellivier F, Delavest M, Leboyer M, Tamouza R, Poupon C, Mangin J-F, Houenou J. 2018. Increased and decreased superficial white matter structural connectivity in schizophrenia and bipolar disorder. bioRxiv. 473686.
Jones SE, Buchbinder BR, Aharon I. 2000. Three-dimensional mapping of cortical thickness using Laplace's equation. Hum Brain Mapp. 11:12–32.
Jordan G, Lutgens D, Joober R, Lepage M, Iyer SN, Malla A. 2014. The Relative Contribution of Cognition and Symptomatic Remission to Functional Outcome Following Treatment of a First Episode of Psychosis. J Clin Psychiatry. 75:e566–e572.
Jordan G, Veru F, Lepage M, Joober R, Malla A, Iyer SN. 2018. Pathways to functional outcomes following a first episode of psychosis: The roles of premorbid adjustment, verbal memory and symptom remission. Aust New Zeal J Psychiatry. 52:793–803.
Jorgensen KN, Nerland S, Norbom LB, Doan NT, Nesvag R, Morch-Johnsen L, Haukvik UK, Melle I, Andreassen OA, Westlye LT, Agartz I. 2016. Increased MRI-based cortical grey/white-matter contrast in sensory and motor regions in schizophrenia and bipolar disorder. Psychol Med. 1–15.
June SK, Singh V, Jun KL, Lerch J, Ad-Dab'bagh Y, MacDonald D, Jong ML, Kim SI, Evans AC. 2005. Automated 3-D extraction and evaluation of the inner and outer cortical surfaces using a Laplacian map and partial volume effect classification. Neuroimage. 27:210–221.
Kalmady SV, Venkatasubramanian G, Shivakumar V, Gautham S, Subramaniam A, Jose DA, Maitra A, Ravi V, Gangadhar BN. 2014. Relationship between Interleukin-6 Gene Polymorphism and Hippocampal Volume in Antipsychotic-Naïve Schizophrenia: Evidence for Differential Susceptibility? PLoS One. 9:e96021.
Karama S, Colom R, Johnson W, Deary IJ, Haier R, Waber DP, Lepage C, Ganjavi H, Jung R, Evans AC. 2011. Cortical thickness correlates of specific cognitive performance accounted for by the general factor of intelligence in healthy children aged 6 to 18. Neuroimage. 55:1443–1453.
Karbasforoushan H, Woodward ND. 2012. Resting-state networks in schizophrenia. Curr Top Med Chem. 12:2404–2414.
Kavanaugh BC, Gaudet CE, Dupont-Frechette JA, Tellock PP, Maher ID, Haisley LD, Holler KA. 2016. Verbal Memory Abilities in Severe Childhood Psychiatric Disorders and the Influence of Attention and Executive Functions. Arch Clin Neuropsychol. acw020.
Kawano M, Sawada K, Shimodera S, Ogawa Y, Kariya S, Lang DJ, Inoue S, Honer WG. 2015. Hippocampal subfield volumes in first episode and chronic schizophrenia. PLoS One. 10:1–14.
Kay SR, Fiszbein A, Opler LA. 1987. The Positive and Negative Syndrome Scale (PANSS) for Schizophrenia. Schizophr Bull. 13:261–276.
Kelleher I, Connor D, Clarke MC, Devlin N, Harley M, Cannon M. 2012. Prevalence of psychotic symptoms in childhood and adolescence: a systematic review and meta-analysis

of population-based studies. Psychol Med. 42:1857–1863.
Keller J, Shen L, Gomez RG, Garrett A, Solvason HB, Reiss A, Schatzberg AF. 2008. Hippocampal and amygdalar volumes in psychotic and nonpsychotic unipolar depression. Am J Psychiatry. 165:872–880.
Kelly S, Jahanshad N, Zalesky A, Kochunov P, Agartz I, Alloza C, Andreassen OA, Arango C, Banaj N, Bouix S, Bousman CA, Brouwer RM, Bruggemann J, Bustillo J, Cahn W, Calhoun V, Cannon D, Carr V, Catts S, Chen J, Chen J, Chen X, Chiapponi C, Cho KK, Ciullo V, Corvin AS, Crespo-Facorro B, Cropley V, De Rossi P, Diaz-Caneja CM, Dickie EW, Ehrlich S, Fan F, Faskowitz J, Fatouros-Bergman H, Flyckt L, Ford JM, Fouche J-P, Fukunaga M, Gill M, Glahn DC, Gollub R, Goudzwaard ED, Guo H, Gur RE, Gur RC, Gurholt TP, Hashimoto R, Hatton SN, Henskens FA, Hibar DP, Hickie IB, Hong LE, Horacek J, Howells FM, Hulshoff Pol HE, Hyde CL, Isaev D, Jablensky A, Jansen PR, Janssen J, Jönsson EG, Jung LA, Kahn RS, Kikinis Z, Liu K, Klauser P, Knöchel C, Kubicki M, Lagopoulos J, Langen C, Lawrie S, Lenroot RK, Lim KO, Lopez-Jaramillo C, Lyall A, Magnotta V, Mandl RCW, Mathalon DH, McCarley RW, McCarthy-Jones S, McDonald C, McEwen S, McIntosh A, Melicher T, Mesholam-Gately RI, Michie PT, Mowry B, Mueller BA, Newell DT, O'Donnell P, Oertel-Knöchel V, Oestreich L, Paciga SA, Pantelis C, Pasternak O, Pearlson G, Pellicano GR, Pereira A, Pineda Zapata J, Piras F, Potkin SG, Preda A, Rasser PE, Roalf DR, Roiz R, Roos A, Rotenberg D, Satterthwaite TD, Savadjiev P, Schall U, Scott RJ, Seal ML, Seidman LJ, Shannon Weickert C, Whelan CD, Shenton ME, Kwon JS, Spalletta G, Spaniel F, Sprooten E, Stäblein M, Stein DJ, Sundram S, Tan Y, Tan S, Tang S, Temmingh HS, Westlye LT, Tønnesen S, Tordesillas-Gutierrez D, Doan NT, Vaidya J, van Haren NEM, Vargas CD, Vecchio D, Velakoulis D, Voineskos A, Voyvodic JQ, Wang Z, Wan P, Wei D, Weickert TW, Whalley H, White T, Whitford TJ, Wojcik JD, Xiang H, Xie Z, Yamamori H, Yang F, Yao N, Zhang G, Zhao J, van Erp TGM, Turner J, Thompson PM, Donohoe G. 2018. Widespread white matter microstructural differences in schizophrenia across 4322 individuals: results from the ENIGMA Schizophrenia DTI Working Group. Mol Psychiatry. 23:1261–1269.
Kensinger E. 2009. Remembering the Details: Effects of Emotion. Emot Rev. 1:99–113.
Kern RS, Green MF, Cornblatt BA, Owen JR, McQuade RD, Carson WH, Ali M, Marcus R. 2006. The neurocognitive effects of aripiprazole: An open-label comparison with olanzapine. Psychopharmacology (Berl). 187:312–320.
Keshavan MS, Anderson S, Pettergrew JW. 1994. Is Schizophrenia due to excessive synaptic pruning in the prefrontal cortex? The Feinberg hypothesis revisited. J Psychiatr Res. 28:239–265.
Keshavan MS, Hogarty GE. 1999. Brain maturational processes and delayed onset in schizophrenia. Dev Psychopathol. 11:525–543.
Keshavan MS, Nasrallah HA, Tandon R. 2011. Schizophrenia, "Just the Facts", 6. Moving ahead with the schizophrenia concept: from the elephant to the mouse. Schizophr Res. 127:3–13.
Khundrakpam BS, Lewis JD, Jeon S, Kostopoulos P, Itturia Medina Y, Chouinard-Decorte F, Evans AC. 2017. Exploring Individual Brain Variability during Development based on Patterns of Maturational Coupling of Cortical Thickness: A Longitudinal MRI Study. Cereb Cortex.
Kikul J, Van Allen TS, Exner C. 2012. Underlying mechanisms of verbal memory deficits in obsessive-compulsive disorder and major depression – The role of cognitive self-consciousness. J Behav Ther Exp Psychiatry. 43:863–870.

Kim JS, Singh V, Lee JK, Lerch J, Ad-Dab'bagh Y, MacDonald D, Lee JM, Kim SI, Evans AC. 2005. Automated 3-D extraction and evaluation of the inner and outer cortical surfaces using a Laplacian map and partial volume effect classification. Neuroimage. 27:210–221.
Kim MJ, Loucks RA, Palmer AL, Brown AC, Solomon KM, Marchante AN, Whalen PJ. 2011. The structural and functional connectivity of the amygdala: From normal emotion to pathological anxiety. Behav Brain Res. 223:403–410.
Kirkpatrick B, Fenton WS, Carpenter WT, Marder SR. 2006. The NIMH-MATRICS consensus statement on negative symptoms. Schizophr Bull. 32:214–219.
Klauser P, Baker ST, Cropley VL, Bousman C, Fornito A, Cocchi L, Fullerton JM, Rasser P, Schall U, Henskens F, Michie PT, Loughland C, Catts S V, Mowry B, Weickert TW, Shannon Weickert C, Carr V, Lenroot R, Pantelis C, Zalesky A. 2017. White Matter Disruptions in Schizophrenia Are Spatially Widespread and Topologically Converge on Brain Network Hubs. Schizophr Bull. 43:425–435.
Klein A, Tourville J. 2012. 101 Labeled Brain Images and a Consistent Human Cortical Labeling Protocol. Front Neurosci. 6:171.
Knöchel C, Schmied C, Linden DEJ, Stäblein M, Prvulovic D, de A. de Carvalho L, Harrison O, Barros PO, Carvalho AF, Reif A, Alves GS, Oertel-Knöchel V. 2016. White matter abnormalities in the fornix are linked to cognitive performance in SZ but not in BD disorder: An exploratory analysis with DTI deterministic tractography. J Affect Disord. 201:64–78.
Knoll JL, Garver DL, Ramberg JE, Kingsbury SJ, Croissant D, McDermott B. 1998. Heterogeneity of the psychoses: is there a neurodegenerative psychosis? Schizophr Bull. 24:365–379.
Kochunov P, Ganjgahi H, Winkler A, Kelly S, Shukla DK, Du X, Jahanshad N, Rowland L, Sampath H, Patel B, O'Donnell P, Xie Z, Paciga SA, Schubert CR, Chen J, Zhang G, Thompson PM, Nichols TE, Hong LE. 2016. Heterochronicity of white matter development and aging explains regional patient control differences in schizophrenia. Hum Brain Mapp. 37:4673–4688.
Kraepelin E. 1899. Psychiatrie: ein lehrbuch fur studierende und aerzte. Leipzig, Germany: JA Barth.
Kring AM, Gur RE, Blanchard JJ, Horan WP, Reise SP. 2013. The Clinical Assessment Interview for Negative Symptoms (CAINS): Final Development and Validation. Am J Psychiatry. 170:165–172.
Kubicki M, Park H, Westin CF, Nestor PG, Mulkern R V, Maier SE, Niznikiewicz M, Connor EE, Levitt JJ, Frumin M, Kikinis R, Jolesz FA, McCarley RW, Shenton ME. 2005. DTI and MTR abnormalities in schizophrenia: analysis of white matter integrity. Neuroimage. 26:1109–1118.
Lake EMR, Steffler EA, Rowley CD, Sehmbi M, Minuzzi L, Frey BN, Bock NA. 2017. Altered intracortical myelin staining in the dorsolateral prefrontal cortex in severe mental illness. Eur Arch Psychiatry Clin Neurosci. 267:369–376.
Lang DJM, Yip E, MacKay AL, Thornton AE, Vila-Rodriguez F, MacEwan GW, Kopala LC, Smith GN, Laule C, MacRae CB, Honer WG. 2014. 48 echo T_2 myelin imaging of white matter in first-episode schizophrenia: evidence for aberrant myelination. NeuroImage Clin. 6:408–414.
Lange SC de, Scholtens LH, Berg LH van den, Boks MP, Bozzali M, Cahn W, Dannlowski U, Durston S, Geuze E, Haren NEM van, Hillegers MHJ, Koch K, Jurado MÁ, Mancini M,

Marqués-Iturria I, Meinert S, Ophoff RA, Reess TJ, Repple J, Kahn RS, Heuvel MP van den, (ADNI) the ADNI. 2018. Shared vulnerability for connectome alterations across psychiatric and neurological brain disorders. bioRxiv. 360586.
Laskaris LE, Di Biase MA, Everall I, Chana G, Christopoulos A, Skafidas E, Cropley VL, Pantelis C. 2016. Microglial activation and progressive brain changes in schizophrenia. Br J Pharmacol. 173:666–680.
Laule C, Vavasour IM, Kolind SH, Li DKB, Traboulsee TL, Moore GRW, MacKay AL. 2007. Magnetic resonance imaging of myelin. Neurotherapeutics. 4:460–484.
Lebel C, Beaulieu C. 2011. Longitudinal development of human brain wiring continues from childhood into adulthood. J Neurosci. 31:10937–10947.
Lee S-H, Kubicki M, Asami T, Seidman LJ, Goldstein JM, Mesholam-Gately RI, McCarley RW, Shenton ME. 2013. Extensive white matter abnormalities in patients with first-episode schizophrenia: a Diffusion Tensor Imaging (DTI) study. Schizophr Res. 143:231–238.
Lee S, Kim S-J, Kwon O-B, Lee JH, Kim J-H. 2013. Inhibitory networks of the amygdala for emotional memory. Front Neural Circuits. 7.
Leeson VC, Robbins TW, Franklin C, Harrison M, Harrison I, Ron MA, Barnes TRE, Joyce EM. 2009. Dissociation of long-term verbal memory and fronto-executive impairment in first-episode psychosis. Psychol Med. 39:1799.
Lehmann HE, Ban TA. 1997. The History of the Psychopharmacology of Schizophrenia. Can J Psychiatry. 42:152–162.
Lepage M, Bodnar M, Bowie CR. 2014. Neurocognition: clinical and functional outcomes in schizophrenia. Can J Psychiatry. 59:5–12.
Lepage M, Buchy L, Bodnar M, Bertrand M-C, Joober R, Malla A. 2008. Cognitive insight and verbal memory in first episode of psychosis. Eur Psychiatry. 23:368–374.
Lepage M, Sergerie K, Benoit a, Czechowska Y, Dickie E, Armony JL. 2011. Emotional face processing and flat affect in schizophrenia: functional and structural neural correlates. Psychol Med. 41:1833–1844.
Lerch JP, Evans AC. 2005. Cortical thickness analysis examined through power analysis and a population simulation. Neuroimage. 24:163–173.
Lerch JP, Worsley K, Shaw WP, Greenstein DK, Lenroot RK, Giedd J, Evans AC. 2006. Mapping anatomical correlations across cerebral cortex (MACACC) using cortical thickness from MRI. Neuroimage. 31:993–1003.
Leucht S, Cipriani A, Spineli L, Mavridis D, Örey D, Richter F, Samara M, Barbui C, Engel RR, Geddes JR, Kissling W, Stapf MP, Lässig B, Salanti G, Davis JM. 2013. Comparative efficacy and tolerability of 15 antipsychotic drugs in schizophrenia: a multiple-treatments meta-analysis. Lancet. 382:951–962.
Leucht S, Samara M, Heres S, Patel MX, Furukawa T, Cipriani A, Geddes J, Davis JM. 2015. Dose Equivalents for Second-Generation Antipsychotic Drugs: The Classical Mean Dose Method. Schizophr Bull. 41:1397–1402.
Lewis JD, Evans AC, Tohka J. 2018. T1 white/gray contrast as a predictor of chronological age, and an index of cognitive performance. Neuroimage. 173:341–450.
Li B, Woo R-S, Mei L, Malinow R. 2007. The Neuregulin-1 Receptor ErbB4 Controls Glutamatergic Synapse Maturation and Plasticity. Neuron. 54:583–597.
Li W, van Tol M-J, Li M, Miao W, Jiao Y, Heinze H-J, Bogerts B, He H, Walter M. 2014. Regional specificity of sex effects on subcortical volumes across the lifespan in healthy aging. Hum Brain Mapp. 35:238–247.

Lieberman JA. 1999. Is schizophrenia a neurodegenerative disorder? a clinical and neurobiological perspective. Biol Psychiatry. 46:729–739.
Lieberman JA, Girgis RR, Brucato G, Moore H, Provenzano F, Kegeles L, Javitt D, Kantrowitz J, Wall MM, Corcoran CM, Schobel SA, Small SA. 2018. Hippocampal dysfunction in the pathophysiology of schizophrenia: a selective review and hypothesis for early detection and intervention. Mol Psychiatry. 23:1764–1772.
Lin C-Y, Tsai GE, Lane H-Y. 2014. Assessing and treating cognitive impairment in schizophrenia: current and future. Curr Pharm Des. 20:5127–5138.
Lindgren M, Manninen M, Kalska H, Mustonen U, Laajasalo T, Moilanen K, Huttunen MO, Cannon TD, Therman S, Suvisaari J. 2017. Evaluation of verbal list learning as a predictor of psychosis. Early Interv Psychiatry. 11:171–176.
Lockhart S, Sawa A, Niwa M. 2018. Developmental trajectories of brain maturation and behavior: Relevance to major mental illnesses. J Pharmacol Sci. 137:1–4.
López-Muñoz F, Alamo C, Cuenca E, Shen WW, Clervoy P, Rubio G. 2005. History of the discovery and clinical introduction of chlorpromazine. Ann Clin Psychiatry. 17:113–135.
Lorensen WE, Cline HE. 1987. Marching cubes: A high resolution 3D surface construction algorithm. Proc 14th Annu Conf Comput Graph Interact Tech - SIGGRAPH '87. 21:163–169.
Luck D, Buchy L, Czechowska Y, Bodnar M, Pike GB, Campbell JSW, Achim A, Malla A, Joober R, Lepage M. 2011. Fronto-temporal disconnectivity and clinical short-term outcome in first episode psychosis: A DTI-tractography study. J Psychiatr Res. 45:369–377.
Lutgens D, Iyer S, Joober R, Schmitz N, Lepage M, Mustafa S, Malla A. 2019. Progress of Negative Symptoms during the Critical Period of the First Five Years of a First Episode of Psychosis. Psychol Med. 49:66–74.
Lutgens D, Lepage M, Iyer S, Malla A. 2014. Predictors of cognition in first episode psychosis. Schizophr Res. 152:164–169.
Lysaker PH, Carcione A, Dimaggio G, Johannesen JK, Nicolo G, Procacci M, Semerari A. 2005. Metacognition amidst narratives of self and illness in schizophrenia: associations with neurocognition, symptoms, insight and quality of life. Acta Psychiatr Scand. 112:64–71.
Lyttelton O, Boucher M, Robbins S, Evans A. 2007. An unbiased iterative group registration template for cortical surface analysis. Neuroimage. 34:1535–1544.
Lyttelton OC, Karama S, Ad-Dab'bagh Y, Zatorre RJ, Carbonell F, Worsley K, Evans AC. 2009. Positional and surface area asymmetry of the human cerebral cortex. Neuroimage. 46:895–903.
MacDonald K, Malla A, Joober R, Shah JL, Goldberg K, Abadi S, Doyle M, Iyer SN. 2018. Description, evaluation and scale-up potential of a model for rapid access to early intervention for psychosis. Early Interv Psychiatry. 12:1222–1228.
Magon S, Chakravarty MM, Amann M, Weier K, Naegelin Y, Andelova M, Radue E-W, Stippich C, Lerch JP, Kappos L, Sprenger T. 2014. Label-fusion-segmentation and deformation-based shape analysis of deep gray matter in multiple sclerosis: The impact of thalamic subnuclei on disability. Hum Brain Mapp. 35:4193–4203.
Makowski C, Béland S, Kostopoulos P, Bhagwat N, Devenyi GA, Malla AK, Joober R, Lepage M, Chakravarty MM. 2018. Evaluating accuracy of striatal, pallidal, and thalamic segmentation methods: Comparing automated approaches to manual delineation. Neuroimage. 170:182–198.
Makowski C, Bodnar M, Malla AK, Joober R, Lepage M. 2016. Age-related cortical thickness

trajectories in first episode psychosis patients presenting with early persistent negative symptoms. npj Schizophr. 2:16029.
Makowski C, Bodnar M, Shenker JJ, Malla AK, Joober R, Chakravarty MM, Lepage M. 2017. Linking persistent negative symptoms to amygdala–hippocampus structure in first-episode psychosis. Transl Psychiatry. 7:e1195.
Makowski C, Lepage M, Evans AC. 2019. Head motion: the dirty little secret of neuroimaging in psychiatry. J Psychiatry Neurosci. 44:62–68.
Makowski C, Lewis JD, Lepage C, Malla AK, Joober R, Evans AC, Lepage M. 2019a. Intersection of Verbal Memory and Expressivity on Cortical Contrast and Thickness in First Episode Psychosis. Under Rev Psychol Med.
Makowski C, Lewis JD, Lepage C, Malla AK, Joober R, Lepage M, Evans AC. 2019b. Structural Associations in First Episode Psychosis Using Cortical Contrast and Cortical Thickness. Cereb Cortex. In Press.
Malla A, Payne J. 2005. First-Episode Psychosis: Psychopathology, Quality of Life, and Functional Outcome. Schizophr Bull. 31:650–671.
Malla AK, Norman RMG, Manchanda R, Townsend L. 2002. Symptoms, cognition, treatment adherence and functional outcome in first-episode psychosis. Psychol Med. 32:1109–1119.
Malla AK, Takhar JJ, Norman RMG, Manchanda R, Cortese L, Haricharan R, Verdi M, Ahmed R. 2002a. Negative symptoms in first episode non-affective psychosis. Acta Psychiatr Scand. 105:431–439.
Malla AK, Takhar JJ, Norman RMG, Manchanda R, Cortese L, Haricharan R, Verdi M, Ahmed R. 2002b. Negative symptoms in first episode non-affective psychosis. Acta Psychiatr Scand. 105:431–439.
Mamah D, Alpert KI, Barch DM, Csernansky JG, Wang L. 2016. Subcortical neuromorphometry in schizophrenia spectrum and bipolar disorders. NeuroImage Clin. 11:276–286.
Mamah D, Harms MP, Barch D, Styner M, Lieberman JA, Wang L. 2012. Hippocampal shape and volume changes with antipsychotics in early stage psychotic illness. Front Psychiatry. 3.
Marder E. 2015. Understanding brains: details, intuition, and big data. PLoS Biol. 13:e1002147.
Marder SR, Galderisi S. 2017. The current conceptualization of negative symptoms in schizophrenia. World Psychiatry. 16:14–24.
Marín O. 2016. Developmental timing and critical windows for the treatment of psychiatric disorders. Nat Med. 22:1229–1238.
Marques JP, Kober T, Krueger G, van der Zwaag W, Van de Moortele P-F, Gruetter R. 2010. MP2RAGE, a self bias-field corrected sequence for improved segmentation and T1-mapping at high field. Neuroimage. 49:1271–1281.
Martin JH. 1996. Neuroanatomy: Text and Atlas. 2nd editio. ed. Stamford, Connecticut: Appleton & Lange.
Mathew I, Gardin TM, Tandon N, Eack S, Francis AN, Seidman LJ, Clementz B, Pearlson GD, Sweeney J a, Tamminga C a, Keshavan MS. 2014. Medial Temporal Lobe Structures and Hippocampal Subfields in Psychotic Disorders: Findings From the Bipolar-Schizophrenia Network on Intermediate Phenotypes (B-SNIP) Study. JAMA psychiatry. 71:769–777.
Messinger JW, Trémeau F, Antonius D, Mendelsohn E, Prudent V, Stanford AD, Malaspina D. 2011. Avolition and expressive deficits capture negative symptom phenomenology: Implications for DSM-5 and schizophrenia research. Clin Psychol Rev. 31:161–168.
Meyer-Lindenberg AS, Olsen RK, Kohn PD, Brown T, Egan MF, Weinberger DR, Berman KF.

2005. Regionally Specific Disturbance of Dorsolateral Prefrontal–Hippocampal Functional Connectivity in Schizophrenia. Arch Gen Psychiatry. 62:379.
Millan MJ, Fone K, Steckler T, Horan WP. 2014. Negative symptoms of schizophrenia: clinical characteristics, pathophysiological substrates, experimental models and prospects for improved treatment. Eur Neuropsychopharmacol. 24:645–692.
Miller AM, Bansal R, Hao X, Sanchez-Pena JP, Sobel LJ, Liu J, Xu D, Zhu H, Chakravarty MM, Durkin K, Ivanov I, Plessen KJ, Kellendonk CB, Peterson BS. 2010. Enlargement of thalamic nuclei in Tourette syndrome. Arch Gen Psychiatry. 67:955–964.
Mills KL, Tamnes CK. 2014. Methods and considerations for longitudinal structural brain imaging analysis across development. Dev Cogn Neurosci. 9:172–190.
Mišić B, Goñi J, Betzel RF, Sporns O, McIntosh AR. 2014. A network convergence zone in the hippocampus. PLoS Comput Biol. 10:e1003982.
Mitelman SA, Shihabuddin L, Brickman AM, Hazlett EA, Buchsbaum MS. 2005. Volume of the cingulate and outcome in schizophrenia. Schizophr Res. 72:91–108.
Mørch-Johnsen L, Agartz I, Jensen J. 2018. The Neural Correlates of Negative Symptoms in Schizophrenia: Examples From MRI Literature. Clin EEG Neurosci. 49:12–17.
Mørch-Johnsen L, Nesvåg R, Faerden A, Haukvik UK, Jørgensen KN, Lange EH, Andreassen OA, Melle I, Agartz I. 2015. Brain structure abnormalities in first-episode psychosis patients with persistent apathy. Schizophr Res. 164:59–64.
Moreno-Küstner B, Martín C, Pastor L. 2018. Prevalence of psychotic disorders and its association with methodological issues. A systematic review and meta-analyses. PLoS One. 13:e0195687.
Morgan KD, Dazzan P, Orr KG, Hutchinson G, Chitnis X, Suckling J, Lythgoe D, Pollock S-J, Rossell S, Shapleske J, Fearon P, Morgan C, David A, McGuire PK, Jones PB, Leff J, Murray RM. 2007. Grey matter abnormalities in first-episode schizophrenia and affective psychosis. Br J Psychiatry Suppl. 51:s111-6.
Moscovitch M, Cabeza R, Winocur G, Nadel L. 2016. Episodic Memory and Beyond: The Hippocampus and Neocortex in Transformation. Annu Rev Psychol. 67:105–134.
Mucci A, Merlotti E, Üçok A, Aleman A. 2017. Primary and persistent negative symptoms: Concepts, assessments and neurobiological bases. Schizophr Res. 186:19–28.
Mucci A, Piegari G, Galderisi S. 2008. Cognitive-enhancing effects of aripiprazole: a case report. Clin Pract Epidemiol Ment Health. 4:24.
Mueller S, Keeser D, Reiser MF, Teipel S. 2012. Functional and Structural MR Imaging in Neuropsychiatric Disorders, Part 2 : Application in Schizophrenia and Autism. Am J Neuroradiol. 33:2033–2037.
Murray RM, Sideli L, LA Cascia C, LA Barbera D. 2015. Bridging the gap between research into biological and psychosocial models of psychosis. Shanghai Arch psychiatry. 27:139–143.
Nacewicz BM, Dalton KM, Johnstone T, Long MT, McAuliff EM, Oakes TR, Alexander AL, Davidson RJ. 2006. Amygdala volume and nonverbal social impairment in adolescent and adult males with autism. Arch Gen Psychiatry. 63:1417–1428.
Nagai T, Murai R, Matsui K, Kamei H, Noda Y, Furukawa H, Nabeshima T. 2009. Aripiprazole ameliorates phencyclidine-induced impairment of recognition memory through dopamine D1 and serotonin 5-HT1A receptors. Psychopharmacology (Berl). 202:315–328.
Nakagami E, Xie B, Hoe M, Brekke JS. 2008. Intrinsic motivation, neurocognition and psychosocial functioning in schizophrenia: Testing mediator and moderator effects.

Schizophr Res. 105:95–104.
Nakagawa Y, Chiba K. 2016. Involvement of Neuroinflammation during Brain Development in Social Cognitive Deficits in Autism Spectrum Disorder and Schizophrenia. J Pharmacol Exp Ther. 358:504–515.
Nakahara S, Matsumoto M, van Erp TGM. 2018. Hippocampal subregion abnormalities in schizophrenia: A systematic review of structural and physiological imaging studies. Neuropsychopharmacol Reports. 38:156–166.
Narr KL, Thompson PM, Szeszko P, Robinson D, Jang S, Woods RP, Kim S, Hayashi KM, Asunction D, Toga AW, Bilder RM. 2004. Regional specificity of hippocampal volume reductions in first-episode schizophrenia. Neuroimage. 21:1563–1575.
Natu VS, Gomez J, Barnett M, Jeska B, Kirilina E, Jaeger C, Zhen Z, Cox S, Weiner KS, Weiskopf N, Grill-Spector K. 2018. Apparent thinning of visual cortex during childhood is associated with myelination, not pruning. bioRxiv. 368274.
Nazeri A, Chakravarty MM, Felsky D, Lobaugh NJ, Rajji TK, Mulsant BH, Voineskos AN. 2013. Alterations of Superficial White Matter in Schizophrenia and Relationship to Cognitive Performance. 38:1954–1962.
Nenadic I, Yotter RA, Sauer H, Gaser C. 2015. Patterns of cortical thinning in different subgroups of schizophrenia. Br J Psychiatry. 206:479–483.
Nesvåg R, Bergmann Ø, Rimol LM, Lange EH, Haukvik UK, Hartberg CB, Fagerberg T, Söderman E, Jönsson EG, Agartz I. 2012. A 5-year follow-up study of brain cortical and subcortical abnormalities in a schizophrenia cohort. Schizophr Res. 142:209–216.
Nichols S, Jones W, Roman MJ, Wulfeck B, Delis DC, Reilly J, Bellugi U. 2004. Mechanisms of verbal memory impairment in four neurodevelopmental disorders. Brain Lang. 88:180–189.
Nopoulos P, Flashman L, Flaum M, Arndt S, Andreasen N. 1994. Stability of cognitive functioning early in the course of schizophrenia. Schizophr Res. 14:29–37.
Nowakowska E, Kus K, Ratajczak P, Cichocki M, Wo??niak A. 2014. The influence of aripiprazole, olanzapine and enriched environment on depressant-like behavior, spatial memory dysfunction and hippocampal level of BDNF in prenatally stressed rats. Pharmacol Reports. 66:404–411.
Nugent AC, Luckenbaugh D a., Wood SE, Bogers W, Zarate C a., Drevets WC. 2013. Automated subcortical segmentation using FIRST: Test-retest reliability, interscanner reliability, and comparison to manual segmentation. Hum Brain Mapp. 34:2313–2329.
Nürnberger L, Gracien R-M, Hok P, Hof S-M, Rüb U, Steinmetz H, Hilker R, Klein JC, Deichmann R, Baudrexel S. 2017. Longitudinal changes of cortical microstructure in Parkinson's disease assessed with T1 relaxometry. NeuroImage Clin. 13:405–414.
Ochoa S, Usall J, Cobo J, Labad X, Kulkarni J. 2012. Gender Differences in Schizophrenia and First-Episode Psychosis: A Comprehensive Literature Review. Schizophr Res Treatment. 2012:1–9.
Ohtani T, Bouix S, Hosokawa T, Saito Y, Eckbo R, Ballinger T, Rausch A, Melonakos E, Kubicki M. 2014. Abnormalities in white matter connections between orbitofrontal cortex and anterior cingulate cortex and their associations with negative symptoms in schizophrenia: A DTI study. Schizophr Res. 157:190–197.
Ohtani T, Bouix S, Lyall AE, Hosokawa T, Saito Y, Melonakos E, Westin CF, Seidman LJ, Goldstein J, Mesholam-Gately R, Petryshen T, Wojcik J, Kubicki M. 2015. Abnormal white matter connections between medial frontal regions predict symptoms in patients with first episode schizophrenia. Cortex. 71:264–276.

Olabi B, Ellison-Wright I, McIntosh AM, Wood SJ, Bullmore E, Lawrie SM. 2011. Are there progressive brain changes in schizophrenia? a meta-analysis of structural magnetic resonance imaging studies. Biol Psychiatry. 70:88–96.
Oldfield R. 1971. The assessment and analysis of handedness: the Edinburgh inventory. Neuropsychologia. 9:97–113.
Overall JE, Gorham DR. 1962. The Brief Psychiatric Rating Scale. Psychol Rep. 10:799–812.
Owen M. 2018. 9. Does Biology Read the DSM? Transdiagnostic Findings in Psychosis And Implications For Treatment. Schizophr Bull. 44:S12–S13.
Öztekin I, Davachi L, McElree B. 2010. Are Representations in Working Memory Distinct From Representations in Long-Term Memory? Psychol Sci. 21:1123–1133.
Pajonk F-G, Wobrock T, Gruber O, Scherk H, Berner D, Kaizl I, Kierer A, Müller S, Oest M, Meyer T, Backens M, Schneider-Axmann T, Thornton AE, Honer WG, Falkai P. 2010. Hippocampal Plasticity in Response to Exercise in Schizophrenia. Arch Gen Psychiatry. 67:133.
Palaniyappan L. 2017. Progressive cortical reorganisation: A framework for investigating structural changes in schizophrenia. Neurosci Biobehav Rev. 79:1–13.
Palaniyappan L, Hodgson O, Balain V, Iwabuchi SJ, Gowland PA, Liddle PF. 2018. Structural covariance and cortical reorganization in schizophrenia: A MRI-based morphometric study. Psychol Med. In Press.
Palaniyappan L, Marques TR, Taylor H, Handley R, Mondelli V, Bonaccorso S, Giordano A, McQueen G, DiForti M, Simmons A, David AS, Pariante CM, Murray RM, Dazzan P. 2013. Cortical Folding Defects as Markers of Poor Treatment Response in First-Episode Psychosis. JAMA Psychiatry. 70:1031.
Palaniyappan L, Marques TR, Taylor H, Mondelli V, Reinders AATS, Bonaccorso S, Giordano A, DiForti M, Simmons A, David AS, Pariante CM, Murray RM, Dazzan P. 2016. Globally Efficient Brain Organization and Treatment Response in Psychosis: A Connectomic Study of Gyrification. Schizophr Bull. 42:1446–1456.
Palaniyappan L, Simmonite M, White TP, Liddle EB, Liddle PF. 2013. Neural Primacy of the Salience Processing System in Schizophrenia. Neuron. 79:814–828.
Panizzon MS, Fennema-Notestine C, Eyler LT, Jernigan TL, Prom-Wormley E, Neale M, Jacobson K, Lyons MJ, Grant MD, Franz CE, Xian H, Tsuang M, Fischl B, Seidman L, Dale A, Kremen WS. 2009. Distinct genetic influences on cortical surface area and cortical thickness. Cereb Cortex. 19:2728–2735.
Panizzon MS, Fennema-Notestine C, Kubarych TS, Chen CH, Eyler LT, Fischl B, Franz CE, Grant MD, Hamza S, Jak A, Jernigan TL, Lyons MJ, Neale MC, Prom-Wormley EC, Seidman L, Tsuang MT, Wu H, Xian H, Dale AM, Kremen WS. 2012. Genetic and environmental influences of white and gray matter signal contrast: A new phenotype for imaging genetics? Neuroimage. 60:1686–1695.
Pantelis C. 2005. Structural Brain Imaging Evidence for Multiple Pathological Processes at Different Stages of Brain Development in Schizophrenia. Schizophr Bull. 31:672–696.
Papez J. 1937. A proposed mechanism of emotion. Arch Neurol Psychiatry. 38:725–743.
Pardoe HR, Kucharsky Hiess R, Kuzniecky R. 2016. Motion and morphometry in clinical and nonclinical populations. Neuroimage. 135:177–185.
Park SW, Lee JG, Ha EK, Choi SM, Cho HY, Seo MK, Kim YH. 2009. Differential effects of aripiprazole and haloperidol on BDNF-mediated signal changes in SH-SY5Y cells. Eur Neuropsychopharmacol. 19:356–362.

Patel S, Park MTM, Devenyi GA, Patel R, Masellis M, Knight J, Chakravarty MM. 2017. Heritability of hippocampal subfield volumes using a twin and non-twin siblings design. Hum Brain Mapp. 38:4337–4352.
Patenaude B, Smith SM, Kennedy DN, Jenkinson M. 2011. A Bayesian model of shape and appearance for subcortical brain segmentation. Neuroimage. 56:907–922.
Pearlson GD, Clementz BA, Sweeney JA, Keshavan MS, Tamminga CA. 2016. Does Biology Transcend the Symptom-based Boundaries of Psychosis? Psychiatr Clin North Am. 1–10.
Perälä J, Suvisaari J, Saarni SI, Kuoppasalmi K, Isometsä E, Pirkola S, Partonen T, Tuulio-Henriksson A, Hintikka J, Kieseppä T, Härkänen T, Koskinen S, Lönnqvist J. 2007. Lifetime Prevalence of Psychotic and Bipolar I Disorders in a General Population. Arch Gen Psychiatry. 64:19.
Peralta V, Cuesta MJ. 1999. Dimensional structure of psychotic symptoms: an item-level analysis of SAPS and SANS symptoms in psychotic disorders. Schizophr Res. 38:13–26.
Pérez-Iglesias R, Tordesillas-Gutiérrez D, McGuire PK, Barker GJ, Roiz-Santiañez R, Mata I, de Lucas EM, Rodríguez-Sánchez JM, Ayesa-Arriola R, Vazquez-Barquero JL, Crespo-Facorro B. 2010. White matter integrity and cognitive impairment in first-episode psychosis. Am J Psychiatry. 167:451–458.
Perkins DO, Gu H, Boteva K, Lieberman JA. 2005. Relationship between duration of untreated psychosis and outcome in first-episode schizophrenia: a critical review and meta-analysis. Am J Psychiatry. 162:1785–1804.
Phelps EA. 2004. Human emotion and memory: Interactions of the amygdala and hippocampal complex. Curr Opin Neurobiol. 14:198–202.
Phillips OR, Nuechterlein KH, Asarnow RF, Clark KA, Cabeen R, Yang Y, Woods RP, Toga AW, Narr KL. 2011. Mapping Corticocortical Structural Integrity in Schizophrenia and Effects of Genetic Liability. Biol Psychiatry. 70:680–689.
Pier KS, Marin LK, Wilsnack J, Goodman M. 2016. The Neurobiology of Borderline Personality Disorder. Psychiatr Times. 33.
Pietrzak RH, Olver J, Norman T, Piskulic D, Maruff P, Snyder PJ. 2009. A comparison of the CogState Schizophrenia Battery and the Measurement and Treatment Research to Improve Cognition in Schizophrenia (MATRICS) Battery in assessing cognitive impairment in chronic schizophrenia. J Clin Exp Neuropsychol. 31:848–859.
Pina-Camacho L, Del Rey-Mejías Á, Janssen J, Bioque M, González-Pinto A, Arango C, Lobo A, Sarró S, Desco M, Sanjuan J, Lacalle-Aurioles M, Cuesta MJ, Saiz-Ruiz J, Bernardo M, Parellada M, Group Pep. 2015. Age at First Episode Modulates Diagnosis-Related Structural Brain Abnormalities in Psychosis. Schizophr Bull. 42:5–7.
Pipitone J, Park MTM, Winterburn J, Lett TA, Lerch JP, Pruessner JC, Lepage M, Voineskos AN, Chakravarty MM, Initiative the ADN. 2014. Multi-atlas segmentation of the whole hippocampus and subfields using multiple automatically generated templates. Neuroimage. 101:494–512.
Prabhakaran V, Nair VA, Austin BP, La C, Gallagher TA, Wu Y, McLaren DG, Xu G, Turski P, Rowley H. 2012. Current status and future perspectives of magnetic resonance high-field imaging: a summary. Neuroimaging Clin N Am. 22:373–97, xii.
Prastawa M, Gilmore JH, Lin W, Gerig G. 2005. Automatic segmentation of MR images of the developing newborn brain. Med Image Anal. 9:457–466.
Preacher KJ, Hayes AF. 2008. Asymptotic and resampling strategies for assessing and comparing indirect effects in multiple mediator models. Behav Res Methods. 40:879–891.

Pruessner JC, Collins DL, Pruessner M, Evans AC. 2001. Age and gender predict volume decline in the anterior and posterior hippocampus in early adulthood. J Neurosci. 21:194–200.
Pruessner M, Lepage M, Collins DL, Pruessner JC, Joober R, Malla AK. 2015. Reduced hippocampal volume and hypothalamus-pituitary-adrenal axis function in first episode psychosis: evidence for sex differences. NeuroImage Clin. 7:195–202.
Purves D, Brannon E, Cabeza R. 2008. Principles of Cognitive Neuroscience. Sunderland, MA: Sinauer Associates.
Qiu a, Gan SC, Wang Y, Sim K. 2013. Amygdala-hippocampal shape and cortical thickness abnormalities in first-episode schizophrenia and mania. Psychol Med. 43:1353–1363.
Quigley SJ, Scanlon C, Kilmartin L, Emsell L, Langan C, Hallahan B, Murray M, Waters C, Waldron M, Hehir S, Casey H, McDermott E, Ridge J, Kenney J, O'Donoghue S, Nannery R, Ambati S, McCarthy P, Barker GJ, Cannon DM, McDonald C. 2015. Volume and shape analysis of subcortical brain structures and ventricles in euthymic bipolar I disorder. Psychiatry Res. 233:324–330.
Radua J, Borgwardt S, Crescini A, Mataix-Cols D, Meyer-Lindenberg A, McGuire PK, Fusar-Poli P. 2012. Multimodal meta-analysis of structural and functional brain changes in first episode psychosis and the effects of antipsychotic medication. Neurosci Biobehav Rev. 36:2325–2333.
Rais M, van Haren NEM, Cahn W, Schnack HG, Lepage C, Collins L, Evans AC, Hulshoff Pol HE, Kahn RS. 2010. Cannabis use and progressive cortical thickness loss in areas rich in CB1 receptors during the first five years of schizophrenia. Eur Neuropsychopharmacol. 20:855–865.
Rapoport JL, Gogtay N. 2011. Childhood onset schizophrenia: support for a progressive neurodevelopmental disorder. Int J Dev Neurosci. 29:251–258.
Raslau FD, Mark IT, Klein AP, Ulmer JL, Mathews V, Mark LP. 2015. Memory part 2: the role of the medial temporal lobe. AJNR Am J Neuroradiol. 36:846–849.
Raznahan A, Lerch JP, Lee N, Greenstein D, Wallace GL, Stockman M, Clasen L, Shaw PW, Giedd JN. 2011. Patterns of coordinated anatomical change in human cortical development: A longitudinal neuroimaging study of maturational coupling. Neuron. 72:873–884.
Raznahan A, Shaw P, Lalonde F, Stockman M, Wallace GL, Greenstein D, Clasen L, Gogtay N, Giedd JN. 2011. How does your cortex grow? J Neurosci. 31:7174–7177.
Raznahan A, Shaw PW, Lerch JP, Clasen LS, Greenstein D, Berman R, Pipitone J, Chakravarty MM, Giedd JN. 2014. Longitudinal four-dimensional mapping of subcortical anatomy in human development. Proc Natl Acad Sci U S A. 111:1592–1597.
Remington G, Foussias G, Fervaha G, Agid O, Takeuchi H, Lee J, Hahn M. 2016. Treating Negative Symptoms in Schizophrenia: an Update. Curr Treat options psychiatry. 3:133–150.
Reuter M, Tisdall MD, Qureshi A, Buckner RL, van der Kouwe AJW, Fischl B. 2015. Head motion during MRI acquisition reduces gray matter volume and thickness estimates. Neuroimage. 107:107–115.
Riedel M, Spellmann I, Schennach-Wolff R, Musil R, Dehning S, Cerovecki A, Opgen-Rhein M, Matz J, Seemüller F, Obermeier M, Severus E, Engel RR, Müller N, Möller HJ. 2010. Effect of aripiprazole on cognition in the treatment of patients with schizophrenia. Pharmacopsychiatry. 43:50–57.
Rimol LM, Panizzon MS, Fennema-Notestine C, Eyler LT, Fischl B, Franz CE, Hagler DJ,

Lyons MJ, Neale MC, Pacheco J, Perry ME, Schmitt JE, Grant MD, Seidman LJ, Thermenos HW, Tsuang MT, Eisen SA, Kremen WS, Dale AM. 2010. Cortical thickness is influenced by regionally specific genetic factors. Biol Psychiatry. 67:493–499.

Ripke S, Neale BM, Corvin A, Walters JTR, Farh K-H, Holmans PA, Lee P, Bulik-Sullivan B, Collier DA, Huang H, Pers TH, Agartz I, Agerbo E, Albus M, Alexander M, Amin F, Bacanu SA, Begemann M, Belliveau Jr RA, Bene J, Bergen SE, Bevilacqua E, Bigdeli TB, Black DW, Bruggeman R, Buccola NG, Buckner RL, Byerley W, Cahn W, Cai G, Campion D, Cantor RM, Carr VJ, Carrera N, Catts S V, Chambert KD, Chan RCK, Chen RYL, Chen EYH, Cheng W, Cheung EFC, Ann Chong S, Robert Cloninger C, Cohen D, Cohen N, Cormican P, Craddock N, Crowley JJ, Curtis D, Davidson M, Davis KL, Degenhardt F, Del Favero J, Demontis D, Dikeos D, Dinan T, Djurovic S, Donohoe G, Drapeau E, Duan J, Dudbridge F, Durmishi N, Eichhammer P, Eriksson J, Escott-Price V, Essioux L, Fanous AH, Farrell MS, Frank J, Franke L, Freedman R, Freimer NB, Friedl M, Friedman JI, Fromer M, Genovese G, Georgieva L, Giegling I, Giusti-Rodríguez P, Godard S, Goldstein JI, Golimbet V, Gopal S, Gratten J, de Haan L, Hammer C, Hamshere ML, Hansen M, Hansen T, Haroutunian V, Hartmann AM, Henskens FA, Herms S, Hirschhorn JN, Hoffmann P, Hofman A, Hollegaard M V, Hougaard DM, Ikeda M, Joa I, Julià A, Kahn RS, Kalaydjieva L, Karachanak-Yankova S, Karjalainen J, Kavanagh D, Keller MC, Kennedy JL, Khrunin A, Kim Y, Klovins J, Knowles JA, Konte B, Kucinskas V, Ausrele Kucinskiene Z, Kuzelova-Ptackova H, Kähler AK, Laurent C, Lee Chee Keong J, Hong Lee S, Legge SE, Lerer B, Li M, Li T, Liang K-Y, Lieberman J, Limborska S, Loughland CM, Lubinski J, Lönnqvist J, Macek Jr M, Magnusson PKE, Maher BS, Maier W, Mallet J, Marsal S, Mattheisen M, Mattingsdal M, McCarley RW, McDonald C, McIntosh AM, Meier S, Meijer CJ, Melegh B, Melle I, Mesholam-Gately RI, Metspalu A, Michie PT, Milani L, Milanova V, Mokrab Y, Morris DW, Mors O, Murphy KC, Murray RM, Myin-Germeys I, Müller-Myhsok B, Nelis M, Nenadic I, Nertney DA, Nestadt G, Nicodemus KK, Nikitina-Zake L, Nisenbaum L, Nordin A, O'Callaghan E, O'Dushlaine C, O'Neill FA, Oh S-Y, Olincy A, Olsen L, Van Os J, Pantelis C, Papadimitriou GN, Papiol S, Parkhomenko E, Pato MT, Paunio T, Pejovic-Milovancevic M, Perkins DO, Pietiläinen O, Pimm J, Pocklington AJ, Powell J, Price A, Pulver AE, Purcell SM, Quested D, Rasmussen HB, Reichenberg A, Reimers MA, Richards AL, Roffman JL, Roussos P, Ruderfer DM, Salomaa V, Sanders AR, Schall U, Schubert CR, Schulze TG, Schwab SG, Scolnick EM, Scott RJ, Seidman LJ, Shi J, Sigurdsson E, Silagadze T, Silverman JM, Sim K, Slominsky P, Smoller JW, So H-C, Spencer CA, Stahl EA, Stefansson H, Steinberg S, Stogmann E, Straub RE, Strengman E, Strohmaier J, Scott Stroup T, Subramaniam M, Suvisaari J, Svrakic DM, Szatkiewicz JP, Söderman E, Thirumalai S, Toncheva D, Tosato S, Veijola J, Waddington J, Walsh D, Wang D, Wang Q, Webb BT, Weiser M, Wildenauer DB, Williams NM, Williams S, Witt SH, Wolen AR, Wong EHM, Wormley BK, Simon Xi H, Zai CC, Zheng X, Zimprich F, Wray NR, Stefansson K, Visscher PM, Trust Case-Control Consortium W, Adolfsson R, Andreassen OA, Blackwood DHR, Bramon E, Buxbaum JD, Børglum AD, Cichon S, Darvasi A, Domenici E, Ehrenreich H, Esko T, Gejman P V, Gill M, Gurling H, Hultman CM, Iwata N, Jablensky A V, Jönsson EG, Kendler KS, Kirov G, Knight J, Lencz T, Levinson DF, Li QS, Liu J, Malhotra AK, McCarroll SA, McQuillin A, Moran JL, Mortensen PB, Mowry BJ, Nöthen MM, Ophoff RA, Owen MJ, Palotie A, Pato CN, Petryshen TL, Posthuma D, Rietschel M, Riley BP, Rujescu D, Sham PC, Sklar P, St Clair D, Weinberger DR, Wendland JR, Werge T, Daly MJ, Sullivan PF, O'Donovan MC,

Consortium SWG of the PG. 2014. Biological insights from 108 schizophrenia-associated genetic loci. Nature. 511:421.
Roddy DW, Farrell C, Doolin K, Roman E, Tozzi L, Frodl T, O'Keane V, O'Hanlon E. 2019. The Hippocampus in Depression: More Than the Sum of Its Parts? Advanced Hippocampal Substructure Segmentation in Depression. Biol Psychiatry. 85:487–497.
Roiz-Santiáñez R, Ortiz-García de la Foz V, Ayesa-Arriola R, Tordesillas-Gutiérrez D, Jorge R, Varela-Gómez N, Suárez-Pinilla P, Córdova-Palomera A, Navasa-Melado JM, Crespo-Facorro B. 2015. No progression of the alterations in the cortical thickness of individuals with schizophrenia-spectrum disorder: a three-year longitudinal magnetic resonance imaging study of first-episode patients. Psychol Med. 45:2861–2871.
Roiz-Santiáñez R, Tordesillas-Gutiérrez D, Ortíz-García de la Foz V, Ayesa-Arriola R, Gutiérrez A, Tabarés-Seisdedos R, Vázquez-Barquero JL, Crespo-Facorro B. 2012. Effect of antipsychotic drugs on cortical thickness. A randomized controlled one-year follow-up study of haloperidol, risperidone and olanzapine. Schizophr Res. 141:22–28.
Rowley CD, Bazin PL, Tardif CL, Sehmbi M, Hashim E, Zaharieva N, Minuzzi L, Frey BN, Bock N a. 2015. Assessing intracortical myelin in the living human brain using myelinated cortical thickness. Front Neurosci. 9.
Rubinov M, Bullmore E. 2013. Schizophrenia and abnormal brain network hubs. Dialogues Clin Neurosci. 15:339–349.
Rubinov M, Sporns O. 2010. Complex network measures of brain connectivity: Uses and interpretations. Neuroimage. 52:1059–1069.
Salat DH, Lee SY, van der Kouwe AJ, Greve DN, Fischl B, Rosas HD. 2009. Age-associated alterations in cortical gray and white matter signal intensity and gray to white matter contrast. Neuroimage. 48:21–28.
Saling MM. 2009. Verbal memory in mesial temporal lobe epilepsy: beyond material specificity. Brain. 132:570–582.
Samudra N, Ivleva EI, Hubbard NA, Rypma B, Sweeney JA, Clementz BA, Keshavan MS, Pearlson GD, Tamminga CA. 2015. Alterations in hippocampal connectivity across the psychosis dimension. Psychiatry Res Neuroimaging. 233:148–157.
Sánchez-Benavides G, Gómez-Ansón B, Sainz A, Vives Y, Delfino M, Peña-Casanova J. 2010. Manual validation of FreeSurfer's automated hippocampal segmentation in normal aging, mild cognitive impairment, and Alzheimer Disease subjects. Psychiatry Res. 181:219–225.
Sandman CA, Head K, Muftuler LT, Su L, Buss C, Davis EP. 2014. Shape of the basal ganglia in preadolescent children is associated with cognitive performance. Neuroimage. 99:93–102.
Saur D, Kreher BW, Schnell S, Kümmerer D, Kellmeyer P, Vry M-S, Umarova R, Musso M, Glauche V, Abel S, Huber W, Rijntjes M, Hennig J, Weiller C. 2008. Ventral and dorsal pathways for language. Proc Natl Acad Sci U S A. 105:18035–18040.
Savalia NK, Agres PF, Chan MY, Feczko EJ, Kennedy KM, Wig GS. 2017. Motion-related artifacts in structural brain images revealed with independent estimates of in-scanner head motion. Hum Brain Mapp. 38:472–492.
Saykin AJ, Shtasel DL, Gur RE, Kester DB, Mozley LH, Stafiniak P, Gur RC. 1994. Neuropsychological deficits in neuroleptic naive patients with first-episode schizophrenia. Arch Gen Psychiatry. 51:124–131.
Schmitz N, Malla A, Norman R, Archie S, Zipursky R. 2007. Inconsistency in the relationship between duration of untreated psychosis (DUP) and negative symptoms: Sorting out the

problem of heterogeneity. Schizophr Res. 93:152–159.
Schneider M, Walter H, Moessnang C, Schäfer A, Erk S, Mohnke S, Romund L, Garbusow M, Dixson L, Heinz A, Romanczuk-Seiferth N, Meyer-Lindenberg A, Tost H. 2017. Altered DLPFC-Hippocampus Connectivity During Working Memory: Independent Replication and Disorder Specificity of a Putative Genetic Risk Phenotype for Schizophrenia. Schizophr Bull. 43:1114–1122.
Schoemaker D, Buss C, Head K, Sandman C a., Davis EP, Chakravarty MM, Gauthier S, Pruessner JC. 2016. Hippocampus and amygdala volumes from magnetic resonance images in children: Assessing accuracy of FreeSurfer and FSL against manual segmentation. Neuroimage. 129:1–14.
Schulze L, Schmahl C, Niedtfeld I. 2016. Neural Correlates of Disturbed Emotion Processing in Borderline Personality Disorder: A Multimodal Meta-Analysis. Biol Psychiatry. 79:97–106.
Schumann G, Loth E, Banaschewski T, Barbot A, Barker G, Büchel C, Conrod PJ, Dalley JW, Flor H, Gallinat J, Garavan H, Heinz A, Itterman B, Lathrop M, Mallik C, Mann K, Martinot J-L, Paus T, Poline J-B, Robbins TW, Rietschel M, Reed L, Smolka M, Spanagel R, Speiser C, Stephens DN, Ströhle A, Struve M, IMAGEN consortium. 2010. The IMAGEN study: reinforcement-related behaviour in normal brain function and psychopathology. Mol Psychiatry. 15:1128–1139.
Schüz A, Braitenburg V. 2002. The Human Cortical White Matter: Quantitative Aspects of Cortico-Cortical Long-Range Connectivity. In: Schüz A,, Miller R, editors. Cortical Areas: Unity and Diversity. Taylor & Francis.
Scoville WB. 1954. The Limbic Lobe in Man. J Neurosurg. 11:64–66.
Scoville WB, Milner B. 1957. Loss of Recent Memory After Bilateral Hippocampal Lesions. J Neurol Neurosurg Psychiatry. 20:11–21.
Seidman LJ, Faraone S V, Goldstein JM, Kremen WS, Horton NJ, Makris N, Toomey R, Kennedy D, Caviness VS, Tsuang MT. 2002. Left hippocampal volume as a vulnerability indicator for schizophrenia: a magnetic resonance imaging morphometric study of nonpsychotic first-degree relatives. Arch Gen Psychiatry. 59:839–849.
Seidman LJ, Shapiro DI, Stone WS, Woodberry KA, Ronzio A, Cornblatt BA, Addington J, Bearden CE, Cadenhead KS, Cannon TD, Mathalon DH, McGlashan TH, Perkins DO, Tsuang MT, Walker EF, Woods SW. 2016. Association of Neurocognition With Transition to Psychosis. JAMA Psychiatry. 73:1239.
Shah JL, Chakravarty MM, Joober R, Lepage M. 2016. Dynamic endophenotypes and longitudinal trajectories: capturing changing aspects of development in early psychosis. J Psychiatry Neurosci. 41:148–151.
Shaw P, De Rossi P, Watson B, Wharton A, Greenstein D, Raznahan A, Sharp W, Lerch JP, Chakravarty MM. 2014. Mapping the development of the basal ganglia in children with attention-deficit/hyperactivity disorder. J Am Acad Child Adolesc Psychiatry. 53:780–9.e11.
Shaw P, Kabani NJ, Lerch JP, Eckstrand K, Lenroot R, Gogtay N, Greenstein D, Clasen L, Evans A, Rapoport JL, Giedd JN, Wise SP. 2008. Neurodevelopmental Trajectories of the Human Cerebral Cortex. J Neurosci. 28.
Shaw P, Sharp W, Sudre G, Wharton a, Greenstein D, Raznahan a, Evans a, Chakravarty MM, Lerch JP, Rapoport J. 2014. Subcortical and cortical morphological anomalies as an endophenotype in obsessive-compulsive disorder. Mol Psychiatry. 20:1–8.
Sheffield JM, Kandala S, Tamminga CA, Pearlson GD, Keshavan MS, Sweeney JA, Clementz

BA, Lerman-Sinkoff DB, Hill SK, Barch DM. 2017. Transdiagnostic Associations Between Functional Brain Network Integrity and Cognition. JAMA Psychiatry. 64:633–647.
Sheffield JM, Karcher NR, Barch DM. 2018. Cognitive Deficits in Psychotic Disorders: A Lifespan Perspective. Neuropsychol Rev. 28:509–533.
Sheline YI, Liston C, McEwen BS. 2019. Parsing the Hippocampus in Depression: Chronic Stress, Hippocampal Volume, and Major Depressive Disorder. Biol Psychiatry. 85:436–438.
Sherif T, Rioux P, Rousseau M-E, Kassis N, Beck N, Adalat R, Das S, Glatard T, Evans AC. 2014. CBRAIN: a web-based, distributed computing platform for collaborative neuroimaging research. Front Neuroinform. 8:54.
Sigmundsson T, Suckling J, Maier M, Williams SCR, Bullmore ET, Greenwood KE, Fukuda R, Ron MA, Toone BK. 2001. Structural Abnormalities in Frontal, Temporal, and Limbic Regions and Interconnecting White Matter Tracts in Schizophrenic Patients With Prominent Negative Symptoms. Am J Psychiatry. 158:234–243.
Simons JS, Spiers HJ. 2003. Prefrontal and medial temporal lobe interactions in long-term memory. Nat Rev Neurosci. 4:637–648.
Sled JG, Zijdenbos AP, Evans AC. 1998. A nonparametric method for automatic correction of intensity nonuniformity in MRI data. IEEE Trans Med Imaging. 17:87–97.
Small SA, Schobel SA, Buxton RB, Witter MP, Barnes CA. 2011. A pathophysiological framework of hippocampal dysfunction in ageing and disease. Nat Rev Neurosci. 12:585–601.
Smieskova R, Fusar-Poli P, Allen P, Bendfeldt K, Stieglitz RD, Drewe J, Radue EW, McGuire PK, Riecher-Rössler A, Borgwardt SJ. 2010. Neuroimaging predictors of transition to psychosis—A systematic review and meta-analysis. Neurosci Biobehav Rev. 34:1207–1222.
Smith DM, Barredo J, Mizumori SJY. 2012. Complimentary roles of the hippocampus and retrosplenial cortex in behavioral context discrimination. Hippocampus. 22:1121–1133.
Smith DM, Miller AMP, Vedder LC. 2018. The retrosplenial cortical role in encoding behaviorally significant cues. Behav Neurosci. 132:356–365.
Smith EE, Jonides J. 1999. Storage and executive processes in the frontal lobes. Science (80-). 283:1657–1661.
Song D, Harway M, Marmarelis VZ, Hampson RE, Deadwyler SA, Berger TW. 2014. Extraction and restoration of hippocampal spatial memories with non-linear dynamical modeling. Front Syst Neurosci. 8:97.
Sponheim SR, Steele VR, McGuire KA. 2004. Verbal memory processes in schizophrenia patients and biological relatives of schizophrenia patients: intact implicit memory, impaired explicit recollection. Schizophr Res. 71:339–348.
Sporns O, Tononi G, Kötter R. 2005. The human connectome: A structural description of the human brain. PLoS Comput Biol. 1:0245–0251.
Squire LR, Stark CEL, Clark RE. 2004. THE MEDIAL TEMPORAL LOBE. Annu Rev Neurosci. 27:279–306.
Stahl E, Forstner A, McQuillin A, Ripke S, PGC BDWG of the, Ophoff R, Scott L, Cichon S, Andreassen OA, Sklar P, Kelsoe J, Breen G. 2017. Genomewide association study identifies 30 loci associated with bipolar disorder. bioRxiv. 173062.
Steen RG, Mull C, Mcclure R, Hamer RM, Lieberman JA. 2006. Brain volume in first-episode schizophrenia. Br J Psychiatry. 188:510–518.

Stein JL, Wiedholz LM, Bassett DS, Weinberger DR, Zink CF, Mattay VS, Meyer-Lindenberg A. 2007. A validated network of effective amygdala connectivity. Neuroimage. 36:736–745.
Stephan KE, Friston KJ, Frith CD. 2009. Dysconnection in Schizophrenia: From Abnormal Synaptic Plasticity to Failures of Self-monitoring. Schizophr Bull. 35:509–527.
Storsve AB, Fjell AM, Tamnes CK, Westlye LT, Overbye K, Aasland HW, Walhovd KB. 2014. Differential Longitudinal Changes in Cortical Thickness, Surface Area and Volume across the Adult Life Span: Regions of Accelerating and Decelerating Change. J Neurosci. 34:8488–8498.
Strasser HC, Lilyestrom J, Ashby ER, Honeycutt NA, Schretlen DJ, Pulver AE, Hopkins RO, Depaulo JR, Potash JB, Schweizer B, Yates KO, Kurian E, Barta PE, Pearlson GD. 2005. Hippocampal and ventricular volumes in psychotic and nonpsychotic bipolar patients compared with schizophrenia patients and community control subjects: A pilot study. Biol Psychiatry. 57:633–639.
Strauss GP, Nuñez A, Ahmed AO, Barchard KA, Granholm E, Kirkpatrick B, Gold JM, Allen DN. 2018. The Latent Structure of Negative Symptoms in Schizophrenia. JAMA Psychiatry.
Suddath RL, Casanova MF, Goldberg TE, Daniel DG, Kelsoe JR, Weinberger DR. 1989. Temporal lobe pathology in schizophrenia: a quantitative magnetic resonance imaging study. Am J Psychiatry. 146:464–472.
Sussman D, Leung RC, Chakravarty MM, Lerch JP, Taylor MJ. 2016. Developing human brain: Age-related changes in cortical, subcortical, and cerebellar anatomy. Brain Behav. 457:1–15.
Szeszko PR, Robinson DG, Ikuta T, Peters BD, Gallego JA, Kane J, Malhotra AK. 2014. White matter changes associated with antipsychotic treatment in first-episode psychosis. Neuropsychopharmacology. 39:1324–1331.
Takayanagi Y, Gerner G, Takayanagi M, Rao V, Vannorsdall TD, Sawa A, Schretlen DJ, Cascella NG. 2013. Hippocampal Volume Reduction Correlates With Apathy in Traumatic Brain Injury, But Not Schizophrenia. J Neuropsychiatry Clin Neurosci. 25:292–301.
Tamminga CA, Southcott S, Sacco C, Wagner AD, Ghose S. 2012. Glutamate Dysfunction in Hippocampus: Relevance of Dentate Gyrus and CA3 Signaling. Schizophr Bull. 38:927–935.
Tamminga CA, Stan AD, Wagner AD. 2010. The Hippocampal Formation in Schizophrenia. Am J Psychiatry. 167:1178–1193.
Tamnes CK, Østby Y, Fjell AM, Westlye LT, Due-Tønnessen P, Walhovd KB. 2010. Brain Maturation in Adolescence and Young Adulthood: Regional Age-Related Changes in Cortical Thickness and White Matter Volume and Microstructure. Cereb Cortex. 20:534–548.
Tamnes CK, Walhovd KB, Dale AM, Østby Y, Grydeland H, Richardson G, Westlye LT, Roddey JC, Hagler DJ, Due-Tønnessen P, Holland D, Fjell AM. 2013. Brain development and aging: Overlapping and unique patterns of change. Neuroimage. 68:63–74.
Tandon R, Gaebel W, Barch DM, Bustillo J, Gur RE, Heckers S, Malaspina D, Owen MJ, Schultz S, Tsuang M, Van Os J, Carpenter W. 2013. Definition and description of schizophrenia in the DSM-5. Schizophr Res. 150:3–10.
Tardif CL, Devenyi GA, Amaral RSC, Pelleieux S, Poirier J, Rosa-Neto P, Breitner J, Chakravarty | M Mallar, Brain M, Chakravarty MM. 2018. Regionally specific changes in

the hippocampal circuitry accompany progression of cerebrospinal fluid biomarkers in preclinical Alzheimer's disease. Hum Brain Mapp. 39:971–984.
Thompson PM, Stein JL, Medland SE, Hibar DP, Vasquez AA, Renteria ME, Toro R, Jahanshad N, Schumann G, Franke B, Wright MJ, Martin NG, Agartz I, Alda M, Alhusaini S, Almasy L, Almeida J, Alpert K, Andreasen NC, Andreassen OA, Apostolova LG, Appel K, Armstrong NJ, Aribisala B, Bastin ME, Bauer M, Bearden CE, Bergmann Ø, Binder EB, Blangero J, Bockholt HJ, Bøen E, Bois C, Boomsma DI, Booth T, Bowman IJ, Bralten J, Brouwer RM, Brunner HG, Brohawn DG, Buckner RL, Buitelaar J, Bulayeva K, Bustillo JR, Calhoun VD, Cannon DM, Cantor RM, Carless MA, Caseras X, Cavalleri GL, Chakravarty MM, Chang KD, Ching CRK, Christoforou A, Cichon S, Clark VP, Conrod P, Coppola G, Crespo-Facorro B, Curran JE, Czisch M, Deary IJ, de Geus EJC, den Braber A, Delvecchio G, Depondt C, de Haan L, de Zubicaray GI, Dima D, Dimitrova R, Djurovic S, Dong H, Donohoe G, Duggirala R, Dyer TD, Ehrlich S, Ekman CJ, Elvsåshagen T, Emsell L, Erk S, Espeseth T, Fagerness J, Fears S, Fedko I, Fernández G, Fisher SE, Foroud T, Fox PT, Francks C, Frangou S, Frey EM, Frodl T, Frouin V, Garavan H, Giddaluru S, Glahn DC, Godlewska B, Goldstein RZ, Gollub RL, Grabe HJ, Grimm O, Gruber O, Guadalupe T, Gur RE, Gur RC, Göring HHH, Hagenaars S, Hajek T, Hall GB, Hall J, Hardy J, Hartman CA, Hass J, Hatton SN, Haukvik UK, Hegenscheid K, Heinz A, Hickie IB, Ho B-C, Hoehn D, Hoekstra PJ, Hollinshead M, Holmes AJ, Homuth G, Hoogman M, Hong LE, Hosten N, Hottenga J-J, Hulshoff Pol HE, Hwang KS, Jack CR, Jenkinson M, Johnston C, Jönsson EG, Kahn RS, Kasperaviciute D, Kelly S, Kim S, Kochunov P, Koenders L, Krämer B, Kwok JBJ, Lagopoulos J, Laje G, Landen M, Landman BA, Lauriello J, Lawrie SM, Lee PH, Le Hellard S, Lemaître H, Leonardo CD, Li C, Liberg B, Liewald DC, Liu X, Lopez LM, Loth E, Lourdusamy A, Luciano M, Macciardi F, Machielsen MWJ, MacQueen GM, Malt UF, Mandl R, Manoach DS, Martinot J-L, Matarin M, Mather KA, Mattheisen M, Mattingsdal M, Meyer-Lindenberg A, McDonald C, McIntosh AM, McMahon FJ, McMahon KL, Meisenzahl E, Melle I, Milaneschi Y, Mohnke S, Montgomery GW, Morris DW, Moses EK, Mueller BA, Muñoz Maniega S, Mühleisen TW, Müller-Myhsok B, Mwangi B, Nauck M, Nho K, Nichols TE, Nilsson L-G, Nugent AC, Nyberg L, Olvera RL, Oosterlaan J, Ophoff RA, Pandolfo M, Papalampropoulou-Tsiridou M, Papmeyer M, Paus T, Pausova Z, Pearlson GD, Penninx BW, Peterson CP, Pfennig A, Phillips M, Pike GB, Poline J-B, Potkin SG, Pütz B, Ramasamy A, Rasmussen J, Rietschel M, Rijpkema M, Risacher SL, Roffman JL, Roiz-Santiañez R, Romanczuk-Seiferth N, Rose EJ, Royle NA, Rujescu D, Ryten M, Sachdev PS, Salami A, Satterthwaite TD, Savitz J, Saykin AJ, Scanlon C, Schmaal L, Schnack HG, Schork AJ, Schulz SC, Schür R, Seidman L, Shen L, Shoemaker JM, Simmons A, Sisodiya SM, Smith C, Smoller JW, Soares JC, Sponheim SR, Sprooten E, Starr JM, Steen VM, Strakowski S, Strike L, Sussmann J, Sämann PG, Teumer A, Toga AW, Tordesillas-Gutierrez D, Trabzuni D, Trost S, Turner J, Van den Heuvel M, van der Wee NJ, van Eijk K, van Erp TGM, van Haren NEM, van 't Ent D, van Tol M-J, Valdés Hernández MC, Veltman DJ, Versace A, Völzke H, Walker R, Walter H, Wang L, Wardlaw JM, Weale ME, Weiner MW, Wen W, Westlye LT, Whalley HC, Whelan CD, White T, Winkler AM, Wittfeld K, Woldehawariat G, Wolf C, Zilles D, Zwiers MP, Thalamuthu A, Schofield PR, Freimer NB, Lawrence NS, Drevets W, the Alzheimer's Disease Neuroimaging Initiative ECICSYS (SYS) G. 2014. The ENIGMA Consortium: large-scale collaborative analyses of neuroimaging and genetic data. Brain Imaging Behav. 8:153–182.

Tishler TA, Bartzokis G, Lu PH, Raven EP, Khanoyan M, Kirkpatrick CJ, Pyle MH, Villablanca JP, Altshuler LL, Mintz J, Ventura J, Casaus LR, Subotnik KL, Nuechterlein KH, Ellingson BM. 2018. Abnormal Trajectory of Intracortical Myelination in Schizophrenia Implicates White Matter in Disease Pathophysiology and the Therapeutic Mechanism of Action of Antipsychotics. Biol Psychiatry Cogn Neurosci Neuroimaging. 3:454–462.
Tohka J, Zijdenbos A, Evans A. 2004. Fast and robust parameter estimation for statistical partial volume models in brain MRI. Neuroimage. 23:84–97.
Townsend LA, Norman RMG. 2004. Course of cognitive functioning in first episode schizophrenia spectrum disorders. Expert Rev Neurother. 4:61–68.
Treadway MT, Waskom ML, Dillon DG, Holmes AJ, Park MTM, Chakravarty MM, Dutra SJ, Polli FE, Iosifescu D V., Fava M, Gabrieli JDE, Pizzagalli DA. 2015. Illness progression, recent stress, and morphometry of hippocampal subfields and medial prefrontal cortex in major depression. Biol Psychiatry. 77:285–294.
Turetsky B, Cowell PE, Gur RC, Grossman RI, Shtasel DL, Gur RE. 1995. Frontal and Temporal Lobe Brain Volumes in Schizophrenia. Arch Gen Psychiatry. 52:1061.
Tustison NJ, Avants BB, Cook PA, Zheng Y, Egan A, Yushkevich PA, Gee JC. 2010. N4ITK: improved N3 bias correction. IEEE Trans Med Imaging. 29:1310–1320.
Umene-Nakano W, Yoshimura R, Okamoto T, Hori H, Nakamura J. 2013. Aripiprazole improves various cognitive and behavioral impairments after traumatic brain injury: A case report. Gen Hosp Psychiatry. 35:103.e7-103.e9.
Uranova NA, Vikhreva O V., Rachmanova VI, Orlovskaya DD. 2011. Ultrastructural Alterations of Myelinated Fibers and Oligodendrocytes in the Prefrontal Cortex in Schizophrenia: A Postmortem Morphometric Study. Schizophr Res Treatment. 2011:1–13.
Uranova NA, Vostrikov VM, Vikhreva O V., Zimina IS, Kolomeets NS, Orlovskaya DD. 2007. The role of oligodendrocyte pathology in schizophrenia. Int J Neuropsychopharmacol. 10:537.
van den Heuvel MP, Mandl RCW, Stam CJ, Kahn RS, Hulshoff Pol HE. 2010. Aberrant frontal and temporal complex network structure in schizophrenia: a graph theoretical analysis. J Neurosci. 30:15915–15926.
van den Heuvel MP, Sporns O, Collin G, Scheewe T, Mandl RCW, Cahn W, Goñi J, Hulshoff Pol HE, Kahn RS. 2013. Abnormal Rich Club Organization and Functional Brain Dynamics in Schizophrenia. JAMA Psychiatry. 70:783.
van der Meer D, Rokicki J, Kaufmann T, Córdova-Palomera A, Moberget T, Alnæs D, Bettella F, Frei O, Doan NT, Sønderby IE, Smeland OB, Agartz I, Bertolino A, Bralten J, Brandt CL, Buitelaar JK, Djurovic S, van Donkelaar M, Dørum ES, Espeseth T, Faraone S V., Fernández G, Fisher SE, Franke B, Haatveit B, Hartman CA, Hoekstra PJ, Håberg AK, Jönsson EG, Kolskår KK, Le Hellard S, Lund MJ, Lundervold AJ, Lundervold A, Melle I, Monereo Sánchez J, Norbom LC, Nordvik JE, Nyberg L, Oosterlaan J, Papalino M, Papassotiropoulos A, Pergola G, de Quervain DJF, Richard G, Sanders A-M, Selvaggi P, Shumskaya E, Steen VM, Tønnesen S, Ulrichsen KM, Zwiers MP, Andreassen OA, Westlye LT. 2018. Brain scans from 21,297 individuals reveal the genetic architecture of hippocampal subfield volumes. Mol Psychiatry. 1.
van Erp TGM, Hibar DP, Rasmussen JM, Glahn DC, Pearlson GD, Andreassen OA, Agartz I, Westlye LT, Haukvik UK, Dale AM, Melle I, Hartberg CB, Gruber O, Kraemer B, Zilles D, Donohoe G, Kelly S, McDonald C, Morris DW, Cannon DM, Corvin A, Machielsen MWJ, Koenders L, de Haan L, Veltman DJ, Satterthwaite TD, Wolf DH, Gur RC, Gur RE, Potkin

SG, Mathalon DH, Mueller BA, Preda A, Macciardi F, Ehrlich S, Walton E, Hass J, Calhoun VD, Bockholt HJ, Sponheim SR, Shoemaker JM, van Haren NEM, Hulshoff Pol HE, Pol HEH, Ophoff RA, Kahn RS, Roiz-Santiañez R, Crespo-Facorro B, Wang L, Alpert KI, Jönsson EG, Dimitrova R, Bois C, Whalley HC, McIntosh AM, Lawrie SM, Hashimoto R, Thompson PM, Turner JA. 2016. Subcortical brain volume abnormalities in 2028 individuals with schizophrenia and 2540 healthy controls via the ENIGMA consortium. Mol Psychiatry. 21:547–553.

van Erp TGM, Walton E, Hibar DP, Schmaal L, Jiang W, Glahn DC, Pearlson GD, Yao N, Fukunaga M, Hashimoto R, Okada N, Yamamori H, Bustillo JR, Clark VP, Agartz I, Mueller BA, Cahn W, de Zwarte SMC, Hulshoff Pol HE, Kahn RS, Ophoff RA, van Haren NEM, Andreassen OA, Dale AM, Doan NT, Gurholt TP, Hartberg CB, Haukvik UK, Jørgensen KN, Lagerberg T V., Melle I, Westlye LT, Gruber O, Kraemer B, Richter A, Zilles D, Calhoun VD, Crespo-Facorro B, Roiz-Santiañez R, Tordesillas-Gutiérrez D, Loughland C, Carr VJ, Catts S, Cropley VL, Fullerton JM, Green MJ, Henskens FA, Jablensky A, Lenroot RK, Mowry BJ, Michie PT, Pantelis C, Quidé Y, Schall U, Scott RJ, Cairns MJ, Seal M, Tooney PA, Rasser PE, Cooper G, Shannon Weickert C, Weickert TW, Morris DW, Hong E, Kochunov P, Beard LM, Gur RE, Gur RC, Satterthwaite TD, Wolf DH, Belger A, Brown GG, Ford JM, Macciardi F, Mathalon DH, O'Leary DS, Potkin SG, Preda A, Voyvodic J, Lim KO, McEwen S, Yang F, Tan Y, Tan S, Wang Z, Fan F, Chen J, Xiang H, Tang S, Guo H, Wan P, Wei D, Bockholt HJ, Ehrlich S, Wolthusen RPF, King MD, Shoemaker JM, Sponheim SR, De Haan L, Koenders L, Machielsen MW, van Amelsvoort T, Veltman DJ, Assogna F, Banaj N, de Rossi P, Iorio M, Piras F, Spalletta G, McKenna PJ, Pomarol-Clotet E, Salvador R, Corvin A, Donohoe G, Kelly S, Whelan CD, Dickie EW, Rotenberg D, Voineskos AN, Ciufolini S, Radua J, Dazzan P, Murray R, Reis Marques T, Simmons A, Borgwardt S, Egloff L, Harrisberger F, Riecher-Rössler A, Smieskova R, Alpert KI, Wang L, Jönsson EG, Koops S, Sommer IEC, Bertolino A, Bonvino A, Di Giorgio A, Neilson E, Mayer AR, Stephen JM, Kwon JS, Yun J-Y, Cannon DM, McDonald C, Lebedeva I, Tomyshev AS, Akhadov T, Kaleda V, Fatouros-Bergman H, Flyckt L, Farde L, Flyckt L, Engberg G, Erhardt S, Fatouros-Bergman H, Cervenka S, Schwieler L, Piehl F, Agartz I, Collste K, Victorsson P, Malmqvist A, Hedberg M, Orhan F, Busatto GF, Rosa PGP, Serpa MH, Zanetti M V., Hoschl C, Skoch A, Spaniel F, Tomecek D, Hagenaars SP, McIntosh AM, Whalley HC, Lawrie SM, Knöchel C, Oertel-Knöchel V, Stäblein M, Howells FM, Stein DJ, Temmingh HS, Uhlmann A, Lopez-Jaramillo C, Dima D, McMahon A, Faskowitz JI, Gutman BA, Jahanshad N, Thompson PM, Turner JA. 2018. Cortical Brain Abnormalities in 4474 Individuals With Schizophrenia and 5098 Control Subjects via the Enhancing Neuro Imaging Genetics Through Meta Analysis (ENIGMA) Consortium. Biol Psychiatry. 84:644–654.

van Haren NEM, Schnack HG, Cahn W, van den Heuvel MP, Lepage C, Collins L, Evans AC, Hulshoff Pol HE, Kahn RS. 2011. Changes in cortical thickness during the course of illness in schizophrenia. Arch Gen Psychiatry. 68:871–880.

van Os J. 2016. "Schizophrenia" does not exist. BMJ. 352:375.

Vann SD, Aggleton JP, Maguire EA. 2009. What does the retrosplenial cortex do? Nat Rev Neurosci. 10:792–802.

Velakoulis D, Wood SJ, Wong MTH, McGorry PD, Yung A, Phillips L, Brewer W, Proffitt T, Desmond P, Pantelis C. 2006. Hippocampal and Amygdala Volumes According to Psychosis Stage and Diagnosis. Arch Gen Psychiatry. 63:139–149.

Vita A, De Peri L, Deste G, Barlati S, Sacchetti E. 2015. The Effect of Antipsychotic Treatment on Cortical Gray Matter Changes in Schizophrenia: Does the Class Matter? A Meta-analysis and Meta-regression of Longitudinal Magnetic Resonance Imaging Studies. Biol Psychiatry. 78.

Vita A, De Peri L, Deste G, Sacchetti E. 2012. Progressive loss of cortical gray matter in schizophrenia: a meta-analysis and meta-regression of longitudinal MRI studies. Transl Psychiatry. 2:e190.

Voineskos AN, Winterburn JL, Felsky D, Pipitone J, Rajji TK, Mulsant BH, Chakravarty MM. 2015. Hippocampal (subfield) volume and shape in relation to cognitive performance across the adult lifespan. Hum Brain Mapp. 00.

Volkow ND, Koob GF, Croyle RT, Bianchi DW, Gordon JA, Koroshetz WJ, Pérez-Stable EJ, Riley WT, Bloch MH, Conway K, Deeds BG, Dowling GJ, Grant S, Howlett KD, Matochik JA, Morgan GD, Murray MM, Noronha A, Spong CY, Wargo EM, Warren KR, Weiss SRB. 2017. The conception of the ABCD study: From substance use to a broad NIH collaboration. Dev Cogn Neurosci.

Wagstyl K, Ronan L, Whitaker KJ, Goodyer IM, Roberts N, Crow TJ, Fletcher PC. 2016. Multiple markers of cortical morphology reveal evidence of supragranular thinning in schizophrenia. Transl Psychiatry. 6:e780.

Walhovd KB, Fjell AM, Giedd J, Dale AM, Brown TT. 2016. Through Thick and Thin: a Need to Reconcile Contradictory Results on Trajectories in Human Cortical Development. Cereb Cortex. 1989:bhv301.

Walhovd KB, Westerhausen R, de Lange A-MG, Bråthen ACS, Grydeland H, Engvig A, Fjell AM. 2016. Premises of plasticity — And the loneliness of the medial temporal lobe. Neuroimage. 131:48–54.

Walton E, Hibar DP, van Erp TGM, Potkin SG, Roiz-Santiañez R, Crespo-Facorro B, Suarez-Pinilla P, van Haren NEM, de Zwarte SMC, Kahn RS, Cahn W, Doan NT, Jørgensen KN, Gurholt TP, Agartz I, Andreassen OA, Westlye LT, Melle I, Berg AO, Morch-Johnsen L, Færden A, Flyckt L, Fatouros-Bergman H, Jönsson EG, Hashimoto R, Yamamori H, Fukunaga M, Jahanshad N, De Rossi P, Piras F, Banaj N, Spalletta G, Gur RE, Gur RC, Wolf DH, Satterthwaite TD, Beard LM, Sommer IE, Koops S, Gruber O, Richter A, Krämer B, Kelly S, Donohoe G, McDonald C, Cannon DM, Corvin A, Gill M, Di Giorgio A, Bertolino A, Lawrie S, Nickson T, Whalley HC, Neilson E, Calhoun VD, Thompson PM, Turner JA, Ehrlich S, Ehrlich S, Karolinska Schizophrenia Project consortium (KaSP). 2017. Prefrontal cortical thinning links to negative symptoms in schizophrenia via the ENIGMA consortium. Psychol Med. 1–13.

Wang Y, Tang W, Fan X, Zhang J, Geng D, Jiang K, Zhu D, Song Z, Xiao Z, Liu D. 2017. Resting-state functional connectivity changes within the default mode network and the salience network after antipsychotic treatment in early-phase schizophrenia. Neuropsychiatr Dis Treat. 13:397–406.

Wang Z, Neylan TC, Mueller SG, Lenoci M, Truran D, Marmar CR, Weiner MW, Schuff N. 2010. Magnetic Resonance Imaging of Hippocampal Subfields in Posttraumatic Stress Disorder. Arch Gen Psychiatry. 67:296.

Wannan CMJ, Cropley VL, Chakravarty MM, Van Rheenen TE, Mancuso S, Bousman C, Everall I, McGorry PD, Pantelis C, Bartholomeusz CF. 2018. Hippocampal subfields and visuospatial associative memory across stages of schizophrenia-spectrum disorder. Psychol Med. 1–11.

Watson DR, Bai F, Barrett SL, Turkington A, Rushe TM, Mulholland CC, Cooper SJ. 2012. Structural changes in the hippocampus and amygdala at first episode of psychosis. Brain Imaging Behav. 6:49–60.
Wechsler D. 1997. Weschler Memory Scale (3rd ed). New York: The Psychological Corporation.
Wei Y, Collin G, Mandl RCW, Cahn W, Keunen K, Schmidt R, Kahn RS, van den Heuvel MP. 2017. Cortical magnetization transfer abnormalities and connectome dysconnectivity in schizophrenia. Schizophr Res.
Weinberger DR. 1986. The pathogenesis of schizophrenia: a neurodevelopmental theory. In: Weinberger R,, Nasrallah D, editors. The Neurology of Schizophrenia. Elsevier. p. 387–405.
Weinberger DR, Berman KF, Suddath R, Torrey EF. 1992. Evidence of dysfunction of a prefrontal-limbic network in schizophrenia: a magnetic resonance imaging and regional cerebral blood flow study of discordant monozygotic twins. Am J Psychiatry. 149:890–897.
Weinberger DR, Radulescu E. 2016. Finding the Elusive Psychiatric "Lesion" With 21st-Century Neuroanatomy: A Note of Caution. Am J Psychiatry. 173:27–33.
Wenger E, Brozzoli C, Lindenberger U, Lövdén M. 2017. Expansion and Renormalization of Human Brain Structure During Skill Acquisition. Trends Cogn Sci. 21:930–939.
Wernicke C. 1906. Grundriss der Psychiatrie in klinischen Vorlesungen. Leipzig, Germany: Thieme.
Weschler D. 1997. Weschler Adult Intelligence Scale - 3rd Edition. San Antonio, TX: The Psychological Corporation.
Weschler D. 1999. Weschler Abbreviated Scale of Intelligence. San Antonio, TX: The Psychological Corporation.
Weschler D. 2009. Wechsler Memory Scale—Fourth Edition (WMS–IV) technical and interpretive manual. San Antonia, TX: Pearson.
Westlye LT, Walhovd KB, Dale AM, Espeseth T, Reinvang I, Raz N, Agartz I, Greve DN, Fischl B, Fjell AM. 2009. Increased sensitivity to effects of normal aging and Alzheimer's disease on cortical thickness by adjustment for local variability in gray/white contrast: A multi-sample MRI study. Neuroimage. 47:1545–1557.
Wheeler AL, Voineskos AN. 2014. A review of structural neuroimaging in schizophrenia: from connectivity to connectomics. Front Hum Neurosci. 8:653.
Whitaker KJ, Vértes PE, Romero-Garcia R, Váša F, Moutoussis M, Prabhu G, Weiskopf N, Callaghan MF, Wagstyl K, Rittman T, Tait R, Ooi C, Suckling J, Inkster B, Fonagy P, Dolan RJ, Jones PB, Goodyer IM, NSPN Consortium the N, Bullmore ET. 2016. Adolescence is associated with genomically patterned consolidation of the hubs of the human brain connectome. Proc Natl Acad Sci U S A. 113:9105–9110.
White N, Roddey C, Shankaranarayanan A, Han E, Rettmann D, Santos J, Kuperman J, Dale A. 2010. PROMO: Real-time prospective motion correction in MRI using image-based tracking. Magn Reson Med. 63:91–105.
Whitford TJ, Ford JM, Mathalon DH, Kubicki M, Shenton ME. 2012. Schizophrenia, myelination, and delayed corollary discharges: a hypothesis. Schizophr Bull. 38:486–494.
Whitford TJ, Grieve SM, Farrow TFD, Gomes L, Brennan J, Harris AWF, Gordon E, Williams LM. 2007. Volumetric White Matter Abnormalities in First-Episode Schizophrenia: A Longitudinal, Tensor-Based Morphometry Study. Am J Psychiatry. 164:1082–1089.
Wible CG, Anderson J, Shenton ME, Kricun A, Hirayasu Y, Tanaka S, Levitt JJ, O'Donnell BF,

Kikinis R, Jolesz FA, McCarley RW. 2001. Prefrontal cortex, negative symptoms, and schizophrenia: an MRI study. Psychiatry Res. 108:65–78.
Wierenga LM, Langen M, Oranje B, Durston S. 2014. Unique developmental trajectories of cortical thickness and surface area. Neuroimage. 87:120–126.
Wild J, Gur RC. 2008. Verbal memory and treatment response in post-traumatic stress disorder. Br J Psychiatry. 193:254–255.
Willems RM, Van der Haegen L, Fisher SE, Francks C. 2014. On the other hand: including left-handers in cognitive neuroscience and neurogenetics. Nat Rev Neurosci. 15:193–201.
Williamson P. 1987. Hypofrontality in schizophrenia: a review of the evidence. Can J Psychiatry. 32:399–404.
Winterburn JL, Pruessner JC, Chavez S, Schira MM, Lobaugh NJ, Voineskos AN, Chakravarty MM. 2013. A novel in vivo atlas of human hippocampal subfields using high-resolution 3T magnetic resonance imaging. Neuroimage. 74:254–265.
Witthaus H, Mendes U, Brüne M, Özgürdal S, Bohner G, Gudlowski Y, Kalus P, Andreasen N, Heinz A, Klingebiel R, Juckel G. 2010. Hippocampal subdivision and amygdalar volumes in patients in an at-risk mental state for schizophrenia. J Psychiatry Neurosci. 35:33–40.
Wolf RC, Vasic N, Sambataro F, Höse A, Frasch K, Schmid M, Walter H. 2009. Temporally anticorrelated brain networks during working memory performance reveal aberrant prefrontal and hippocampal connectivity in patients with schizophrenia. Prog Neuro-Psychopharmacology Biol Psychiatry. 33:1464–1473.
Wolfers T, Doan NT, Kaufmann T, Alnæs D, Moberget T, Agartz I, Buitelaar JK, Ueland T, Melle I, Franke B, Andreassen OA, Beckmann CF, Westlye LT, Marquand AF. 2018. Mapping the Heterogeneous Phenotype of Schizophrenia and Bipolar Disorder Using Normative Models. JAMA Psychiatry.
Wood SJ, Velakoulis D, Smith DJ, Bond D, Stuart GW, McGorry PD, Brewer WJ, Bridle N, Eritaia J, Desmond P, Singh B, Copolov D, Pantelis C. 2001. A longitudinal study of hippocampal volume in first episode psychosis and chronic schizophrenia. Schizophr Res. 52:37–46.
Worsley KJ, Taylor JE, Tomaiuolo F, Lerch J. 2004. Unified univariate and multivariate random field theory. Neuroimage. 23:S189–S195.
Wu M, Kujawa A, Lu LH, Fitzgerald DA, Klumpp H, Fitzgerald KD, Monk CS, Phan KL. 2016. Age-related changes in amygdala-frontal connectivity during emotional face processing from childhood into young adulthood. Hum Brain Mapp. 37:1684–1695.
Xia CH, Ma Z, Ciric R, Gu S, Betzel RF, Kaczkurkin AN, Calkins ME, Cook PA, García de la Garza A, Vandekar SN, Cui Z, Moore TM, Roalf DR, Ruparel K, Wolf DH, Davatzikos C, Gur RC, Gur RE, Shinohara RT, Bassett DS, Satterthwaite TD. 2018. Linked dimensions of psychopathology and connectivity in functional brain networks. Nat Commun. 9:3003.
Xia M, Wang J, He Y. 2013. BrainNet Viewer: A Network Visualization Tool for Human Brain Connectomics. PLoS One. 8:e68910.
Yao N, Winkler AM, Barrett J, Book GA, Beetham T, Horseman R, Leach O, Hodgson K, Knowles EE, Mathias S, Stevens MC, Assaf M, van Erp TGM, Pearlson GD, Glahn DC. 2017. Inferring pathobiology from structural MRI in schizophrenia and bipolar disorder: Modeling head motion and neuroanatomical specificity. Hum Brain Mapp. 38:3757–3770.
Yeo BTT, Krienen FM, Sepulcre J, Sabuncu MR, Lashkari D, Hollinshead M, Roffman JL, Smoller JW, Zöllei L, Polimeni JR, Fischl B, Liu H, Buckner RL. 2011. The organization of the human cerebral cortex estimated by intrinsic functional connectivity. J Neurophysiol.

106:1125–1165.
Zhang JY, Kowal DM, Nawoschik SP, Lou Z, Dunlop J. 2006. Distinct functional profiles of aripiprazole and olanzapine at RNA edited human 5-HT2C receptor isoforms. Biochem Pharmacol. 71:521–529.
Zhao G, Denisova K, Sehatpour P, Long J, Gui W, Qiao J, Javitt DC, Wang Z. 2016. Fractal Dimension Analysis of Subcortical Gray Matter Structures in Schizophrenia. PLoS One. 11:e0155415.
Zhou Y, Shu N, Liu Y, Song M, Hao Y, Liu H, Yu C, Liu Z, Jiang T. 2008. Altered resting-state functional connectivity and anatomical connectivity of hippocampus in schizophrenia. Schizophr Res. 100:120–132.
Zijdenbos AP, Forghani R, Evans AC. 2002. Automatic "pipeline" analysis of 3-D MRI data for clinical trials: application to multiple sclerosis. IEEE Trans Med Imaging. 21:1280–1291.
Zipursky RB, Reilly TJ, Murray RM, Barlati S, Sacchetti E, van Dijk EJ, Norris DG, de Leeuw F-E, Gollub RL, Ehrlich S, Vázquez-Barquero JL, Crespo-Facorro B, Murray RM, Dazzan P. 2013. The Myth of Schizophrenia as a Progressive Brain Disease. Schizophr Bull. 39:1363–1372.
Zugman A, Assunção I, Vieira G, Gadelha A, White TP, Oliveira PPM, Noto C, Crossley N, Mcguire P, Cordeiro Q, Belangero SIO, Bressan RA, Jackowski AP, Sato JR. 2015. Structural covariance in schizophrenia and first-episode psychosis: An approach based on graph analysis. J Psychiatr Res. 71:89–96.